MINISTRY OF EDUCATION AND SCIENCE UKRAINE

Odesa I. I. Mechnikov National University

ФОТОЭЛЕКТРОНИКА

PHOTOELECTRONICS
INTER-UNIVERSITIES SCIENTIFIC ARTICLES

Founded in 1986

Number 29

Odesa
ONU
2020

«PHOTOELECTRONICS»
№ 29 – 2020

INTER-UNIVERSITIES SCIENTIFIC ARTICLES

Founded in 1986

Certificate of State Registration
KB № 15953

«ФОТОЭЛЕКТРОНИКА»
№ 29–2020

МЕЖВЕДОМСТВЕННЫЙ НАУЧНЫЙ СБОРНИК

Основан в 1986 г.

Свидетельство о Государственной регистрации КВ № 15953

UDC 621.315.592:621.383.51:537.221

The results of theoretical and experimental studies in problems of the semiconductor and micro-electronic devices physics, opto- and qantum electronics, quantum optics, spectroscopy and photophysics of nucleus, atoms, molecules and solids are presented in the issue. New directions in the photoelectronics, stimulated by problems of the super intense laser radiation interaction with nuclei, atomic systems and substance, are considered. Scientific articles «Photoelectronics» collection abstracted in ВИНИТИ and «Джерело».

Scientific articles «Photoelectronics» collection abstracted in: Scientific Periodicals in National Library of Ukraine Vernadsky, Ukrainian Abstract Journal, Україніка наукова, ВИНИТИ, Джерело, Українські наукові журнали: The issue is introduced to the List of special editions of the Ukrainian Higher Certification Com¬mission in physics-mathematics and technical sciences.

For lecturers, scientists, post-graduates and students.

У збірнику наведено результати теоретичних і експериментальних досліджень з питань фізики напівпровідників та мікроелектронних приладів, опто- та квантової електроніки, квантової оптики, спектроскопії та фотофізики ядра, атомів, молекул та твердих тіл. Розглянуто нові напрямки розвитку фотоелектроніки, пов'язані із задачами взаємодії надінтенсивного лазерного випромінювання з ядром, атомними системами, речовиною.

Збірник включено до Переліку спеціальних видань ВАК України з фізико-математичних та технічних наук.
Збірник реферується: Scientific Periodicals in National Library of Ukraine Vernadsky, Ukrainian Abstract Journal, Україніка наукова, ВИНИТИ, Джерело, Українські наукові журнали.

Для викладачів, наукових працівників, аспіранів, студентів.

В сборнике приведены результаты теоретических и экспериментальных исследований по вопросам физики полупроводников и микроэлектронных приборов, опто- и квантовой электроники, квантовой оптики, спектроскопии и фотофизики ядра, атомов, молекул и твердых тел. Рассмотрены новые направ¬ления развития фотоэлектроники, связанные с задачами взаимодействия сверхинтенсивного лазерного излучения с ядром, атомными системами, веществом.

Сборник включен в Список специальных изданий ВАК Украины по физико-математическим и тех¬ническим наукам.
Сборник «Photoelectronics» реферируется в Scientific Periodicals in National Library of Ukraine Vernadsky, Ukrainian Abstract Journal, Україніка наукова, ВИНИТИ, Джерело, Українські наукові журнали.

Для преподавателей, научных работников, аспирантов, студентов.

Address of editorial board:
Odesa I. I. Mechnikov National University 42, Paster str., Odesa, 65026, Ukraine
Information is on the site: http://phys.onu.edu.ua/journals/photoele/
http://experiment.onu.edu.ua/exp_ru/files/?
e-mail: photoelectronics@onu.edu.ua.

Table of contents:

PACS 73.61.Le, 73.63.Bd

Chebanenko AP, Filevska LM , Grinevych VS, Smyntyna VA, Negrutsa OS

Odesa Mechnikov National University, Odesa, Dvorianskaya str., 2,
Odesa 65082, Ukraine, e-mail: lfilevska@gmail.com

THE AMMONIA VAPORS INFLUENCE ON THE ELECTRICAL CHARACTERISTICS OF NANOSIZED TIN DIOXIDE FILMS OBTAINED USING A POLYMER

In the presented paper the effect of ammonia vapors on the electrical properties of nanosized tin dioxide films obtained using polymers was investigated to assess the possibility of their use as an ammonia sensor's sensitive element at room temperature. Ammonia vapor leads to a decrease in the conductivity of the studied SnO_2 films. This is due to the fact that the adsorbed ammonia molecules increase the height of the intergranular potential barriers, and the surface shut-off bend of the energy bands. The main role in this is played by the processes of physical adsorption of ammonia molecules. The sensitivity of the films to ammonia vapor is in the range of 0.35-0.63 and reaches a maximum at a voltage of 300 V. The processes of adsorption and desorption take place in two stages and are reversible, as evidenced by the calculated time constants of adsorption and desorption.

Introduction

Among gas-sensitive materials, tin dioxide occupies a leading position due to its physicochemical properties [1,2]. The main of these properties is stability in active chemical media and the ability to change their physical parameters, in particular, conductivity and optical properties, depending on the composition of the environment [3]. Such properties make it possible to use tin dioxide for other purposes, such as transparent electrodes, catalysts of chemical reactions, and the like. [4.5]. The need in just such materials is due to the needs in environmental monitoring in all potentially dangerous cases: in chemical, food, medical industries, energy enterprises, heavy industry, agriculture, everyday life, etc. [6]. Like many other chemicals harmful to health and the environment, ammonia is tightly controlled [7]. Ammonia sensors are created using various technological methods based on many materials [8-10], among them nanomaterials and nanocomposites occupy the main place [11, 12]. The main sensitive parameter for monitoring ammonia vapors is an electrical conductivity (or electrical resistance), which changes in response to environmental changes [13]. The reason for such change is the surface reactions of the detected molecules or ions with physically or, most often, chemically adsorbed oxygen molecules (ions) [14]. This leads to a change in the concentration of electrons in the conduction band of the sensitive material. Typically, such reactions of chemical adsorption with the separation of oxygen atoms into ions associated with a surface, takes place at an elevated temperature. As a rule, sensors to monitor any composition are kept for several hours or even days switched on at an operating temperature (from 160 to 350 C). The use of nanomaterials leads to a reduction in such forming time and to a decrease in the operating temperature of the sensor.

In the presented work the effect of ammonia vapors on the electrical properties of nanosized tin dioxide films obtained using polymers was investigated to assess the possibility of their use as an ammonia sensor's sensitive element at room temperature.

Samples and research methods

Samples of tin dioxide films were obtained by the sol-gel method using polymers for nanoscale structuring of the film. The prepared solutions of bis(acetylacetonato)-dichlorotin(IV) and polyvinyl acetate in acetone were mixed and applied to glass substrates. Sample blanks dried in a drying oven were annealed in a muffle furnace with a gradual temperature increase and holding them for an hour at a temperature of 500 °C, and gradual subsequent cooling to room temperature. The resulting films are smooth, transparent,

and the presence of a nanoscale structure is confirmed by AFM studies.

At a research procedure by standard methods, current-voltage characteristics, temperature dependences of dark current, kinetic dependences of current were measured. All characteristics were measured in dry air and in air with ammonia vapor.

Results and discussion

Fig. 1 shows the current-voltage characteristics (CVC) of a tin dioxide film measured in an atmosphere of dry air and ammonia vapor at room temperature.

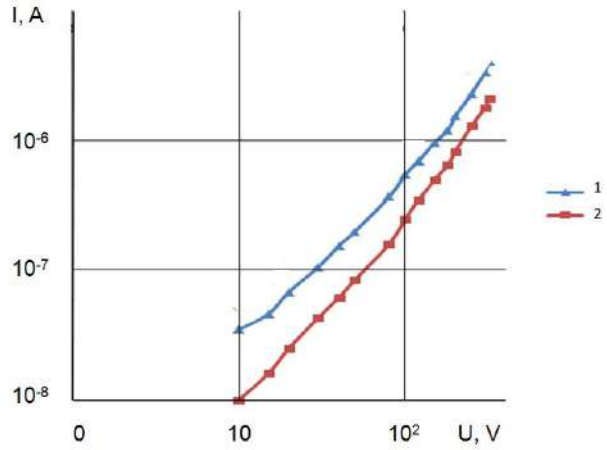

Fig. 1. Current-voltage characteristics of the SnO_2 film, measured in dry air (1), and in ammonia vapor (2), T = 292K.

It may be noted that the I - V characteristic measured in a dry air atmosphere (curve 1, Fig. 1) is superlinear and has a weak tendency to exponential current-voltage dependence. This dependence is typical for the barrier mechanisms of current flow. The latter suggests that, in the studied SnO_2 films, intercrystalline potential barriers are definitely present and noticeably affect the current flow.

In ammonia vapor, the resistance of the film is greater compared with the resistance in air; the superlinearity of its I–V characteristic also increases (Fig. 1, curve 2). It may be concluded, that the adsorption of ammonia molecules contributes to an increase of intercrystalline potential barriers heights and to an increase in the surface shut-off of energy bands bending. This usually occurs due to the interaction with chemisorbed oxygen ions on the surface of tin dioxide [15]. At the same time the chemisorption of oxygen on tin dioxide begins at a temperature of about 160-200 °C [14]. The nanosize of particles promotes reducing the temperature of chemisorption, so, that some of the oxygen can be chemisorbed at room temperature. As it is shown in [16], these can be only O^{2-} ions. The chemical reaction between oxygen adsorbed on the surface of a tin dioxide film and ammonia is possible if the temperature rises to 800 °C [17]. Tin dioxide is a catalyst for such reactions, it helps to lower the reaction temperature, but not to room temperature. In addition, the result of such a reaction should be a decrease in the resistance of the film and an increase in its conductivity. We have the opposite result - a decrease in the conductivity of the film when ammonia is injected. This fact indicates that the process of conductivity changing (decreasing) in our case has a different mechanism. The ammonia decomposition in VITRO is possible at an even higher temperature (1200-1300 °C), but in a catalyst presence - at 600 °C, although the process begins at 300 °C. But even during this process, which is similar to the dissociation of water molecules on the surface of the film, the conductivity should increase.

A number of chemical reactions on the surface of a tin dioxide film with a decrease of conductivity are described in [18]. However, as shown below, when calculating the adsorption and desorption constants, the processes occurring on the surface take place in two stages and are reversible. The reactions presented in [18], have the only one of reversible type.

To explain the resulting decrease in conductivity upon tin dioxide film contact with ammonia, it is advisable to consider the processes of physical adsorption of oxygen and ammonia, as well as the creation of ammonia complexes with surface atoms of tin or its oxides using Van-der-Waals interaction. These processes can take place at room temperature. There is no exchange of carriers (charges) between the adsorbate and the adsorbent at physical adsorption. However, the current flow may be influenced by the barriers growth due to physical adsorption and, as a consequence, to a decrease in the carrier's mobility in the

near-surface region, which also leads to a decrease in conductivity.

In Fig. 2 shows the temperature dependences of the dark current in the SnO2 film measured in dry air and in ammonia vapor at a constant voltage of U = 150 V.

It can be noted that both during heating and during cooling in ammonia vapor and in air, the current changes with temperature according to an exponential law. Conductivity has an activation character, and the conduction activation energy is approximately the same in all areas, regardless of the medium and temperature and is (0.39 - 0.46 eV).

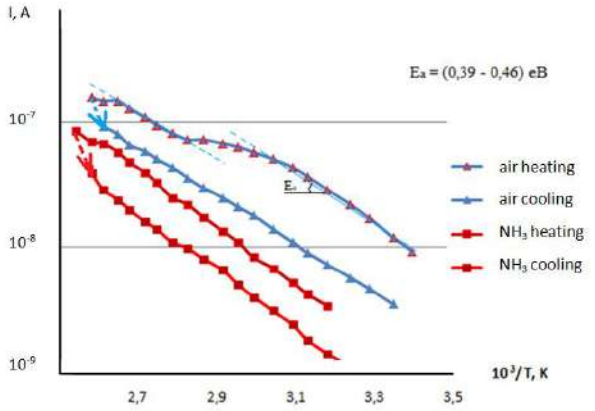

Fig. 2. Temperature dependences of the dark current measured in dry air and in ammonia vapor. (U = 150 V)

The obtained values of the activation energy can be explained on the basis of the model of an inhomogeneous semiconductor with large-scale potential fluctuations. In such a semiconductor, under the action of charged impurities potential (first of all, those adsorbed at intercrystalline boundaries), the energy bands are curved with the formation of a random potential relief [19]. The electrons' motion in a curved zone is possible if their energy exceeds a certain critical value E_{cr}, which is called the level of flow for electrons. The energy position of the percolation level is defined by the nature of the potential relief. An electron, which energy exceeds the level of percolation, can pass over the maximums of the potential relief or bypass them [20]. Therefore, the activation energy E_a = (0.39 - 0.46) eV determined from the temperature dependence is the activation energy of electrons from the Fermi level to the percolation level.

Study of nanostructured SnO_2 films' sensitivity to ammonia

In order to clarify the sensitivity of nanostructured films to ammonia vapors, the film was placed in a chamber where ammonia vapors and dry air were periodically admitted. The admission time of ammonia vapor or dry air was 90 seconds. The relaxation curve of the current flow in this case is shown in Fig. 3.

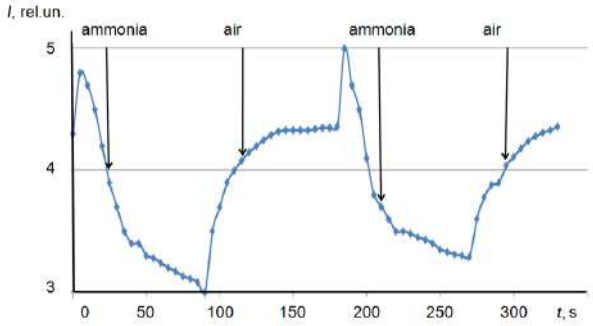

Fig. 3. Kinetics of the current changes in the film with periodic letting of ammonia vapors and dry air into the chamber (V = 300V).

It can be seen from Fig. 3 that when ammonia vapor is let into the chamber, the current rapidly decreases in about 30 s. For another 60 s., the current continues to decrease, but more slowly. Thus, adsorption of ammonia molecules on the surface of SnO_2 films leads to its electrical conductivity decrease. When the chamber is blown off by dry air, the conductivity of the SnO_2 film is restored to its original values. The shape of the current relaxation curve also indicates that the process of adsorption of ammonia is more inertial than the process of their desorption from the surface of the SnO_2 film. In addition, adsorption occurs in two stages: the first is fast (up to 30 s) and the second, which is much slower.

The current relaxation was measured in the range of applied voltages from 150 V to 320 V. For each voltage, the sensitivity S of the film to ammonia vapor was calculated using the formula:

$$S = \frac{I_0 - I}{I_0} \quad (1)$$

where is I_0 - the current in the film in dry air; I is the current in the film in an atmosphere of ammonia vapor.

The calculation results are presented in Table 3.

Table 3.
Dependence of the SnO_2 film sensitivity on the applied voltage

***V*, Volt**	**150**	**200**	**250**	**300**	**320**
S, rel.un.	0,34	0,39	0,55	0,63	0,57

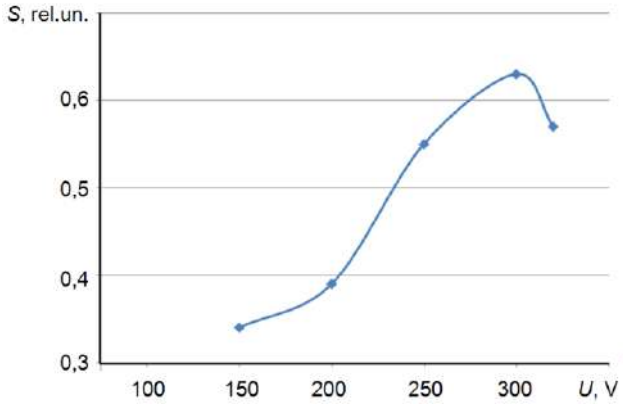

Fig. 4. The ammonia vapor sensitivity-voltage dependence of the SnO_2 film.

The dependence of the sensitivity of the SnO_2 film on the applied voltage is shown in Fig. 4; it can be seen that the sensitivity increases with an increase in the applied voltage and reaches a maximum value of 0.63 relative units at a voltage of 300 V.

The shape of the current relaxation curves (Fig. 3) suggests that the rise and fall of the current value with time occurs according to an exponential law. In particular, the current's decay (ammonia adsorption):

$$\mathbf{I = I_0 e^{-\frac{t}{\tau_a}}}. \qquad (2)$$

Current's rise (ammonia desorption):

$$\mathbf{I = I_0\left(1 - e^{t/\tau_d}\right)}. \qquad (3)$$

Here τ_a and τ_d are some constants characterizing the inertia of adsorption and desorption processes.

To confirm these assumptions, the current decay and rise curves were plotted in the relevant coordinates:

$$ln\left(\frac{I_0}{I}\right) \div t \quad \text{and} \quad ln\left(\frac{1}{1 - I/I_0}\right) \div t$$

(Fig. 5 and Fig. 6). Their satisfactory straightening in the above coordinates made it possible to calculate the time constants of adsorption and desorption. As can be seen from the given dependences, the processes of adsorption and desorption have two parts: a relatively fast adsorption with a time constant of 13.4 s and a relatively slow one with a time constant of 21.8 s. The values of desorption time constants are also close to these values. They are: 19.5 s for slow desorption and 13.2 s for fast desorption. The presence of two sections in the given dependences may indicate that the adsorption and desorption of ammonia occur in two stages. For adsorption, the first step is a fast one, but for desorption it is a slow step.

The processes of physical adsorption of both oxygen and ammonia in condition of the established dynamic equilibrium can proceed in parallel. That is, ammonia molecules are physically adsorbed on the film surface centers which are free at the moment of adsorption. Moreover, the presence of two time constants for adsorption and desorption also indicates a two-stage mechanism of this process. Usually, ammonia molecules easily join to metal atoms due to the unbalanced charge of the nitrogen atom. In some studies of tin dioxide films, the presence of under-oxidized forms of tin: Sn, SnO was shown [21]. As a rule, they are adsorption centers. Upon contact with ammonia, even without chemical interaction, a shift in the electron density of the surface tin atom (most likely associated with an oxygen vacancy) can occur. This leads to a change in the surface potential and, as a consequence, to a decrease in the mobility of charge carriers.

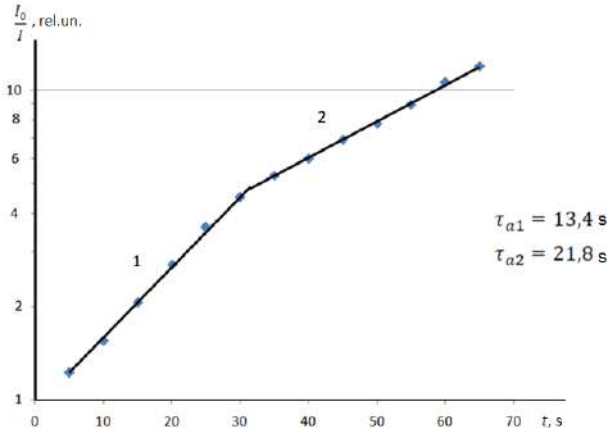

Fig. 5. Current relaxation when ammonia vapor is injected into the chamber (V = 300V).

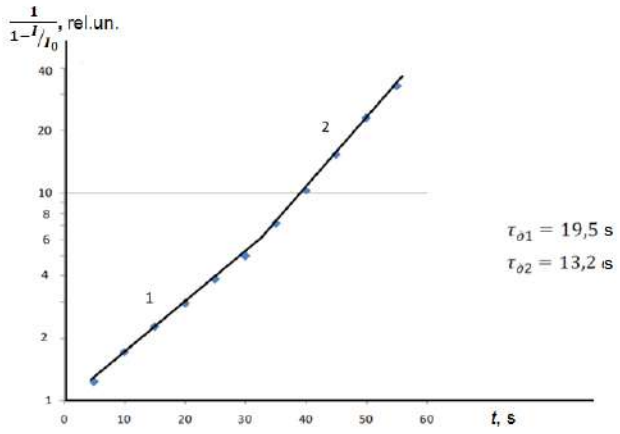

Fig. 6. Relaxation of the current at admitting dry air into the chamber. (V = 300V).

Two time constants of adsorption show that adsorption centers associated with atoms of metallic tin can be filled at first (fast adsorption with a time constant of 13.4, and then of tin oxide on the film surface – slow adsorption with a time constant of 21.8. Desorption is in the opposite direction Thus, the proximity of the values of adsorption and desorption constants and their behavior confirm the assumption about the role of physical adsorption processes in the sensitivity of the studied tin dioxide films at room temperature.

Conclusions

The studied nanostructured films of tin dioxide can be used as an elementary basis for gas sensors detecting the composition of the atmosphere and operating at room temperature.

Ammonia vapor leads to a decrease in the conductivity of the studied SnO_2 films. This is due to the fact that the adsorbed ammonia molecules increase the height of the intergranular potential barriers, and the surface shut-off bend of the energy bands. The main role in this is played by the processes of physical adsorption of ammonia molecules.

The sensitivity of the films to ammonia vapor is in the range of 0.35-0.63 rel and reaches a maximum at a voltage of 300 V. The processes of adsorption and desorption take place in two stages and are reversible, as evidenced by the calculated time constants of adsorption and desorption.

References:

1. Li B, Zhou Q, Peng S and Liao Y (2020) Recent Advances of SnO_2-Based Sensors for Detecting Volatile Organic Compounds. *Front. Chem.* 8:321. doi: 10.3389/fchem.2020.00321,
2. Wu Qi-Hui, Li Jing and Sun Shi-Gang Nano SnO_2 Gas Sensors, Current Nanoscience, 2010, 6, 525-538 525 1573-4137/10.
3. Das S., Jayaraman V., SnO_2: A comprehensive review on structures and gas sensors, Progress in Materials Science, 66, 2014, 112-255, ISSN 0079-6425, doi.org/10.1016/j.pmatsci.2014.06.003,
4. Ginley D.S., Hosono H., Paine D.C. Handbook of transparent conductors. Springer, New York, 2010.
5. Smyntyna V., Borshchak V. and Brytavskyi I.. Nonideal Heterojunctions for Image Sensors Nova Science Publishers, Inc. New York, 2018, 175.
6. Ho Cl. K., Robinson A., Miller D. R. and Davis M. J. Overview of Sensors and Needs for Environmental Monitoring Sensors 2005, 5, 4-37 http://www.mdpi.org/sensors
7. https://www.hse.gov.uk/pubns/priced/eh40.pdf, EH40/2005 Workplace exposure limits Containing the list of workplace exposure limits for use with the Control of Substances Hazardous to Health Regulations 2002 (as amended) London: TSO EH40/2005 (Fourth Edition 2020) London: TSO
8. Dongwook Kwak, Yu Lei, Radenka Maric, Ammonia gas sensors: A comprehensive review, Talanta, 204, 2019, 713-730, doi.org/10.1016/j.talanta.2019.06.034.
9. Doycho I.K., Gevelyuk S.A., Lepikh Ya.I., Rysiakiewicz-Pasek E.. Nature of gas sensitivity of dyes on the base of Sn(IV) complexes, Optica applicata, 49,3, 2019, 427-436.
10. Timmer B., Olthuis W., van den Berg A., Ammonia sensors and their applications – a review, Sensors and Actuators B: Chemical, 107, 2, 2005, 666-677, doi.org/10.1016/j.snb.2004.11.054.
11. Bandgar D.K., Navale S.T., Mane A.T., Gupta S.K., Aswal D.K., Patil V.B., Am-

monia sensing properties of polyaniline/α-Fe2O3 hybrid nanocomposites, Synthetic Metals, 204, 2015, 1-9, doi.org/10.1016/j.synthmet.2015.02.032.
12. Joulazadeh M., Navarchian A. H., Ammonia detection of one-dimensional nanostructured polypyrrole/metal oxide nanocomposites sensors, Synthetic Metals, 210 B, 2015, 404-411, doi.org/10.1016/j.synthmet.2015.10.026.
13. Karnati P., Akbar Sh., Morris P. A., Conduction mechanisms in one dimensional core-shell nanostructures for gas sensing: A review, Sensors and Actuators B: Chemical, 295, 2019, 127-143, doi.org/10.1016/j.snb.2019.05.049.
14. Batzill M. Surface Science Studies of Gas Sensing Materials: SnO_2. Sensors (Basel). 2006; 6(10):1345-1366.
15. Wang Ch., Yin L., Zhang L., Xiang D., Gao R., Review Metal Oxide Gas Sensors: Sensitivity and Influencing Factors Sensors 2010, 10, 2088-2106; doi:10.3390/s100302088.
16. Chang S.C. Oxygen chemisorption on tin oxide: Correlation between electrical conductivity and EPR measurements. J. Vac. Sci. Technol. 17, 1980, 366–369. https://doi.org/10.1116/1.570389
17. Inger M., Dobrzy´nska-Inger A., Rajewski J. and Wilk M., Optimization of Ammonia Oxidation Using Response Surface Methodology, Catalysts 2019, 9, 249, doi:10.3390/catal9030249
18. Hijazi M., Rieu M., Stambouli V., Tournier G., Viricelle J.-P., et al. Ambient temperature selective ammonia gas sensor based on SnO_2-APTES modifications. Sensors and Actuators B: Chemical, 256, 2018, 440-447. .1016/j.snb.2017.10.036.
19. Шейнкман М.К., Шик А.Я. Долговременные релаксации и остаточная проводимость в полупроводниках(обзор). ФТП, т.10(2), 1976, 209-233.
20. Бонч-Бруевич В.Л., Звягин И. П., Кайпер Р., Миронов А.Г., Эндерлайн Р., Эссер Б. Электронная теория неупорядоченных полупроводников, М., Наука, 1981, 383.
21. Рябцев С.В., Чувенкова О.А., Канныкин С.В., Попов А.Е., Рябцева Н.С., Воищев С.С., Турищев С.Ю., Домашевская Э.П.. Электрофизические и оптические свойства оксидных нанослоев, полученных термическим окислением металлического олова, ФТП, 50, 2, 2016,180-184.

PACS 73.61.Le, 73.63.Bd

Chebanenko A.P., Filevska L.M., Grinevych V.S., Smyntyna V.A., Negrutsa O.S.

THE AMMONIA VAPORS INFLUENCE ON THE ELECTRICAL CHARACTERISTICS OF NANOSIZED TIN DIOXIDE FILMS OBTAINED USING A POLYMER

Summary

In the presented paper the effect of ammonia vapors on the electrical properties of nanosized tin dioxide films obtained using polymers was investigated to assess the possibility of their use as an ammonia sensor's sensitive element at room temperature. Ammonia vapor leads to a decrease in the conductivity of the studied SnO_2 films. This is due to the fact that the adsorbed ammonia molecules increase the height of the intergranular potential barriers, and the surface shut-off bend of the energy bands. The main role in this is played by the processes of physical adsorption of ammonia molecules. The sensitivity of the films to ammonia vapor is in the range of 0.35-0.63 and reaches a maximum at a voltage of 300 V. The processes of adsorption and desorption take place in two stages and are reversible, as evidenced by the calculated time constants of adsorption and desorption.

Key words: tin dioxide, thin films, ammonia adsorption**.**

PACS 73.61.Le, 73.63.Bd

Чебаненко А.П., Филевская Л.М., Гриневич В.С., Сминтина В.А., Негруца О.С.

ВПЛИВ ПАРІВ АМІАКУ НА ЕЛЕКТРИЧНІ ХАРАКТЕРИСТИКИ НАНОРОЗМІРНИХ ПЛІВОК ДІОКСИДУ ОЛОВА, ОТРИМАНИХ З ВИКОРИСТАННЯМ ПОЛІМЕРУ

Резюме

У представленій роботі досліджено вплив аміаку на електричні властивості нанорозмірних плівок діоксиду олова, отриманих із використанням полімерів, з метою оцінки їх можливості використання в якості чутливого елемента датчика аміаку при кімнатній температурі. Пари аміаку призводять до зменшення провідності плівок SnO_2. Це пов'язано з тим, що адсорбовані молекули аміаку збільшують висоту міжзеренних потенційних бар'єрів та поверхневий вигин енергетичних зон. Основну роль у цьому відтворюють процеси фізичної адсорбції молекули аміаку. Чутливість плівок до пари аміаку знаходиться в діапазоні 0,35-0,63 і досягає максимуму при напрузі 300 В. Процеси адсорбції та десорбції протікають у дві стадії і є зворотними, про що свідчать розраховані сталі часу адсорбції та десорбції.

Ключові слова: діоксид олова, тонкі плівки, адсорбція аміаку.

PACS 73.61.Le, 73.63.Bd

Чебаненко А.П., Филевская Л.Н., Гриневич В.С., Смынтына В.А., Негруца О.С.

ВЛИЯНИЕ ПАРОВ АММИАКА НА ЭЛЕКТРИЧЕСКИЕ ХАРАКТЕРИСТИКИ НАНОРАЗМЕРНЫХ ПЛЕНОК ДИОКСИДА ОЛОВА, ПОЛУЧЕННЫХ С ИСПОЛЬЗОВАНИЕМ ПОЛИМЕРА

Резюме

В представленной работе исследовано влияние паров аммиака на электрические свойства наноразмерных пленок диоксида олова, полученных с использованием полимеров, с целью оценки возможности их использования в качестве чувствительного элемента датчика аммиака при комнатной температуре. Пары аммиака приводят к снижению проводимости исследованных пленок SnO_2. Это связано с тем, что адсорбированные молекулы аммиака увеличивают высоту межзеренных потенциальных барьеров и поверхностный запирающий изгиб энергетических зон. Основную роль в этом играют процессы физической адсорбции молекул аммиака. Чувствительность пленок к парам аммиака находится в диапазоне 0,35-0,63 и достигает максимума при напряжении 300 В. Процессы адсорбции и десорбции протекают в две стадии и являются обратимыми, о чем свидетельствуют рассчитанные постоянные времени адсорбции и десорбции.

Ключевые слова: диоксид олова, тонкие пленки, адсорбция аммиака.

This article has been received in September 2020.

PACS 538.9

R.M. Balabai, M.V. Naumenko

Kryvyi Rih State Pedagogical University 54, Gagarina Ave., Kryvyi Rih, 50086
E-mail: nikemar13@gmail.com

METHODOLOGY OF CONVERTING OF THE COORDINATES OF THE BASIS ATOMS IN A UNIT CELL OF CRYSTALLINE B-GA_2O_3, SPECIFIED IN A MONOCLINIC CRYSTALLOGRAPHIC SYSTEM, IN THE LABORATORY CARTESIAN COORDINATES FOR COMPUTER APPLICATIONS

One of the most important areas of modern technology is the creation of new structural materials with predetermined properties. Along with industrial methods for their preparation and technologies associated with the artificial growth of crystalline structures, various methods of computer modeling of new materials have recently become increasingly important. Such approaches can significantly reduce the number of full-scale experiments. Many applications of the computational materials science are related to the need to establish a relationship between structure and electronic characteristics, and other physical properties of crystals. This article on the example of crystalline β-Ga_2O_3 presents the algorithms used in the converting of the coordinates of the basis atoms in a unit cell of crystal, specified in a crystallographic system, in the Cartesian coordinates for the computational experiment.

1. Introduction

Gallium Oxide (β-Ga_2O_3) has recently attracted considerable interest for its unique combination of material properties, he has been recognized the perspective wide band gap semiconductor [1]. The perspectives for use of material β-Ga_2O_3 are conditioning systems, including pulsed power for avionics and electric ships, solid-state drivers for heavy electric motors, and advanced power management and control electronics. Certain classes of power electronics with capabilities beyond existing technologies due to its large bandgap, controllable doping, and the availability of large diameter, relatively inexpensive substrates In addition to having a lower electron mobility than binary alloys, high Al-AlGaN is difficult to dope controllably and selectively. The usual Si dopant ionization level becomes very deep in Al-rich AlGaN, and ion implantation activation efficiency is low. We will focus on whether Ga_2O_3 has a role in complementing SiC and GaN. Some of the key issues include the real application space of UWB semiconductors in power switching or RF power amplification, whether in realistic conditions they are capable of outperforming the mature SiC and GaN technology, and whether the material quality and cost, thermal problems, and reliability challenges will limit their application. The biggest difficulties in implementing Ga_2O_3 relate to its high thermal resistance and the absence of p-type conductivity through doping with acceptors. This limits the type of device structures that can be realized and requires effective thermal management approaches [2].

After an unprecedented development and application of classical and compound semiconductors, that started in mid of the XX century, wide bandgap materials were a natural step in the expansion of semiconducting materials that would offer an extended functionality of both electronic and optoelectronic devices. Wide bandgap materials, such as GaN, InGaN, and SiC have been successfully industrialized in the last decade with an impact on our daily life, in particular in the case of nitrides. Nowadays, the research is directed towards ultra-wide bandgap semiconducting materials with the energy gap exceeding 4 eV. There are several that materials that attract particular research attention, including AlGaN, AlN, diamond, and β-Ga_2O_3 belonging to the class of materials called transparent semiconducting oxides. Diamond is very difficult to fabricate in a large volume and of high structural quality.

Al-based nitrides also suffer from technological difficulties in obtaining a large volume of high quality crystals. Among ultra-wide bandgap semiconducting materials only β-Ga_2O_3 can be grown in the large volume. β-Ga_2O_3 with its unique optical and electrical properties is regarded as complementary to other ultra-wide bandgap semiconducting materials in new areas of applications, as solar-blind UV photodetectors, photocatalysts, gas sensors, solar cells, phosphors, and transparent conducting films for electrodes on a variety of optoelectronic devices [3-5].

The polymorphs (i.e., different forms or crystal structures) of $Ga_2O_3$and their regions of stability were identified more than 60 years ago [6]. There are five polymorphs of Ga_2O_3, labeled as corundum (α), monoclinic (β), defective spinel (γ), and orthorhombic (ε), with the δ phase commonly accepted as being a form of the orthorhombic phase [1, 6–10]. The β-phase (β-Ga_2O_3) is the most stable crystal structure and has been the subject of most studies [1, 6–16].

2. Methodology of converting of the coordinates of the basis atoms in a unit cell of crystal, specified in a crystallographic system, in the Cartesian coordinates

It is known that the centers of atoms of any ideal crystalline structure form, in simple cases, one or, in the general case, several regular point systems. By the correct system of points (a system of equivalent positions) we mean the set of points obtained by multiplying the starting point (nonequivalent) by all symmetry operations of a given space group [17]. Moreover, each regular point system contains only one point in an independent region.

In each spatial symmetry group, the regular point systems are subdivided into so-called Wyckoff positions. Wyckoff positions can be free (a region in three-dimensional space), or can be specified as a plane, or as a straight line, or as a point in three-dimensional space (point position). The basis atoms of the substance under study are located at specific Wyckoff positions within the framework of the topology defined by the spatial symmetry group. In total, in 230 spatial symmetry groups, there are 1731 Wyckoff positions [18-19].

The crystalline structure means the finite set of regular systems of atoms in a given Fedorov group. The crystalline structure is described by the following characteristics:

- spatial symmetry group;
- metric parameters of a unit cell (Bravais parallelepiped), to which are the constant lattices and angles between them;
- Wyckoff 's positions of the centers of the basis atoms that make up this structure, including their indices denoting the multiplicity of positions and the numerical values of the free coordinates of these positions in the unit cell.

The coordinates of all atoms of the crystalline structure can be calculated on the basis of these data and using Fedorov symmetry groups or international crystallographic tables.

Usually, when the crystal structures are modeled, the coordinates of the basis atoms are represented in relative coordinates in an oblique system: $x'_{1i} = \frac{x_{1i}}{a}, x'_{2i} = \frac{x_{2i}}{b}, x'_{3i} = \frac{x_{3i}}{c}$. If the origin is at the top of the unit cell, they are expressed in fractions of the elementary translations. These coordinates characterize the ratio of the lengths of the oblique projections of the radius vector coming from the origin to the lengths of the basis vectors *a*, *b*, *c* – elementary translations (parameters) of the Bravais lattice (unit cell). The relative coordinates of the *i*-th atom are positive numbers in the range from 0 to 1. Further, we will not use strokes, considering the coordinates of the atoms relative by the formula (1):

$$r_i = x_{1i}a + x_{2i}b + x_{3i}c \qquad (1)$$

The point that lies in an arbitrary cell of the crystal corresponds to the vector $r + ua + vb + wc$, where u, v and w are integer numbers of translations to which this cell is separated from the origin (depending on the direction of translations,

the numbers can be either positive, and negative).

Unit cell parameters and relative atomic coordinates completely determine the crystal structure. If we consider the orthogonal basis a, b, c, then the distance between the atoms i and j will be calculated by the formula (2):

$$\rho(r_i r_j) = \sqrt{\left(|a|(x_{1i} - x_{1j})\right)^2 + \left(|b|(x_{2i} - x_{2j})\right)^2 + (|c|(x_{3i} - x_{3j}))^2} \quad (2)$$

In the general case, the square of the distance between the centers of the atoms is calculated by the formula (3):

$$\begin{aligned}\rho(r_i r_j)^2 = &\left(|a|(x_{1i} - x_{1j})\right)^2 + \left(|b|(x_{2i} - x_{2j})\right)^2 + \left(|c|(x_{3i} - x_{3j})\right)^2 \\ &+ 2|b||c|(x_{2i} - x_{2j}) \cdot (x_{3i} - x_{3j})cos\alpha + |a||c|(x_{1i} - x_{1j}) \\ &\cdot (x_{3i} - x_{3j})cos\beta + |a||b|(x_{1i} - x_{1j}) \cdot (x_{2i} - x_{2j})cos\gamma\end{aligned} \quad (3)$$

where *α, β, γ* are the interplane angle. To construct the images of basis atoms, symmetry operations are applied for each Fedorov group. A symmetry operator, R, acts on a point *r* so that: *r′*=R·*r* , in which R represents a 3×3 matrix by the formula (4):

X, Y, and *Z* are converted into fractional crystallographic coordinates (*x,y,z*) in order to perform crystallographic operations, and inversely, geometric computations are more easily performed in Cartesian space. In orthonormal systems (cubic, tetragonal, and orthorhombic) the coordinate transformation reduces to a simple division of the coordinate values by the corresponding cell constants. For example,
x=X/a, and *X=ax*. In the case of a generic oblique crystallographic system, the transformation is described by a matrix operation: let the atomic positions be described by a Cartesian coordinate vector X by the formula(5):

$$X = \begin{pmatrix} X \\ Y \\ Z \end{pmatrix} \quad (5)$$

and the fractional coordinate vector in the crystallographic system be x by the formula (6):

$$x = \begin{pmatrix} x \\ y \\ z \end{pmatrix} \quad (6)$$

With the systems having the same origin the operation reduces to $x = MX$ and its

$$\begin{pmatrix} x' \\ y' \\ z' \end{pmatrix} = \begin{pmatrix} a_{11} & a_{12} & a_{13} \\ a_{21} & a_{22} & a_{23} \\ a_{31} & a_{32} & a_{33} \end{pmatrix} \begin{pmatrix} x \\ y \\ z \end{pmatrix} \quad (4)$$

inversion to $X = M^{-1}x$, with M the de-orthogonalization matrix, and its inverse M^{-1} the orthogonalization matrix. There are multiple choices of M depending on the order and selection of the axis rotations. The following convention is followed by most crystallographic programs:

- Cartesian axis A is collinear with crystallographic axis a;
- B is collinear with $(a \times b) \times A$;
- C is collinear with $(a \times b)$.

Using the above convention and we get the formula (7):

$$M^{-1} = \begin{pmatrix} a & ab\,cos\gamma & c\,cos\beta \\ 0 & b\,sin\gamma & \frac{c(cos\alpha - cos\beta\,cos\gamma)}{\sin\gamma} \\ 0 & 0 & \frac{V}{ab\,sin\gamma} \end{pmatrix} \quad (7)$$

with

$$V = \sqrt[2]{abc(1 - cos^2\alpha - cos^2\beta - cos^2\gamma + 2cos\alpha\, cos\beta\, cos\gamma)}$$

or

$$V = \det(M^{-1}) \qquad M = \frac{adj(M^{-1})}{det(M^{-1})} \tag{8}$$

The deorthogonalization matrix M, can be obtained by inversion of M^{-1} following Cramer's rule get by the formula (8):

and reduces to (9):

$$M^{-1} = \begin{pmatrix} a & b\,cos\gamma & \left(\frac{b\,cos\gamma c(cos\alpha - cos\beta\, cos\gamma)}{sin\gamma}\right)\frac{1}{V} \\ 0 & b\,sin\gamma & -\frac{ac(cos\alpha - cos\beta\, cos\gamma)}{V sin\gamma} \\ 0 & 0 & \frac{ab\,sin\gamma}{V} \end{pmatrix} \tag{9}$$

3. Converting of the coordinates of the basis atoms in a unit cell of crystalline β-Ga_2O_3, specified in a monoclinic crystallographic system, in the laboratory Cartesian coordinates

The above techniques will be applied to crystalline β-Ga_2O_3 for construction in the laboratory Cartesian coordinate system associated with a computer-generated author program of an atomic environment within a unit cell β-Ga_2O_3.

The monoclinic β-Ga_2O_3 [20] with space group C2/m has two nonequivalent Ga sites: Ga1 is the sixfold-coordinated site, while Ga2 is the fourfold. In addition, there are three nonequivalent O sites, which are threefold-coordinated O1 and O3 sites, while O2 is the four-fold. The lattice parameters at room temperature are measured to be $a = 12.23$ Å, $b = 3.04$ Å, $c = 5.80$ Å and the unique axis β=103.7° (angle between *a* and *c* axes) unit cell. The unit cell contains four formula units, eight Ga atoms and twelve O atoms are evenly distributed into two Ga and three O nonequivalent sites at positions 4*i*: $(000, \frac{1}{2}\frac{1}{2}0) \pm (x0z)$ [20-23] (Table 1).

Table 2 contains selected geometric parameters.

Table 1.

Nonequivalent atomic fractional positions of β-Ga_2O_3 [20]

Atom	*x*	*y*	*z*	Coordination
Ga1	0.09050 (2)	0	0.79460 (5)	fourfold
Ga2	0.15866 (2)	1/2	0.31402 (5)	sixfold
O1	0.1645 (2)	0	0.1098 (3)	threefold
O2	0.1733 (2)	0	0.5632 (4)	fourfold
O3	0.0041 (2)	1/2	0.2566 (3)	threefold

Table 2.

Selected geometric parametres (Å, °) [20]

Ga1-O1	1.835 (2)	Ga2-O1	1.937 (1)
Ga1-O2	1.863 (2)	Ga2-O2	2.074 (1)
Ga1-O3	1.833 (1)	Ga2-O2	2.005 (2)
O1-Ga1-O2	119.59 (9)	Ga2-O3	1.935 (2)

O1-Ga1-O3	106.79 (7)	O1-Ga2-O2	91.87 (7)
O2-Ga1-O3	105.92 (7)	O1-Ga2-O3	94.66 (7)
O3-Ga1-O3	111.9 (1)	O2-Ga2-O2	94.14 (6)
O1-Ga2-O1	103.22 (9)	O2-Ga2-O2	80.91 (6)
O1-Ga2-O2	80.91 (6)	O2-Ga2-O3	91.95 (7)

The fractional crystallographic coordinates of the atoms shown in Table 1 were converted to Cartesian coordinates using the algorithm described in paragraph 2. Their values are shown in Fig. 1, which is a screen shot of an authoring computer program created in the Delphi programming environment [24-28]. Two nonequivalent Ga atoms [Ga1 and Ga2] and three nonequivalent O atoms [O1, O2 and O3] are showed on Fig. 2.

№	x	y	z	sort
1	0,00980027299030384	3,49024519729932E-16	4,47755899835075	1 Ga1
2	1,50905469516035	1,52	1,76949795703763	2 Ga2
3	1,86100699505957	4,82291621776322E-17	0,618721341579301	3 O1
4	1,34581298558789	2,47383097800023E-16	3,17362349341951	4 O2
5	-1,02117977115405	1,52	4,18904777167625	5 O3

Fig. 1. Laboratory Cartesian coordinates of five atoms in nonequivalent atomic positions

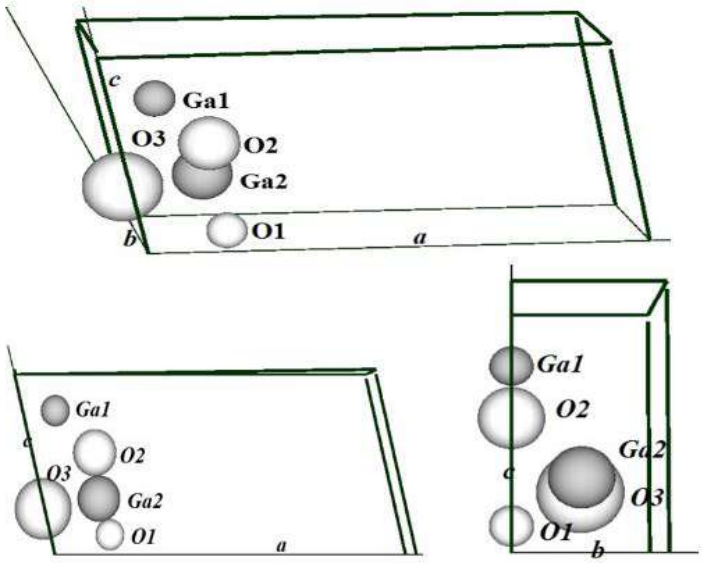

Fig. 2. Unit cell of β-Ga_2O_3, which possesses two nonequivalent Ga sites: Ga1, Ga2 (gray spheres) and three nonequivalent O-sites: O1, O2 and O3 (white spheres) in different angles of observation. The image is built in a laboratory Cartesian coordinate system using an author's computer program

To construct the images of basis (nonequivalent) atoms, symmetry operations are applied for *C2/m* Fedorov group:

$C2/m$ Symmetry Operators

$1\ x,y,z \qquad 1$

$2\ \bar{x},y,\bar{z} \qquad 2\ (0,y,0)$

$3\ \bar{x},\bar{y},\bar{z} \qquad \bar{1}\ (0,0,0)$

$4\ x,\bar{y},z \qquad m\ (x,0,z)$

$5\ \frac{1}{2}+x,\frac{1}{2}+y,z \quad t_c\left[\frac{1}{2},\frac{1}{2},0\right]$

$6\ \frac{1}{2}-x,\frac{1}{2}+y,\bar{z} \quad 2_1\ \left(\frac{1}{4},y,0\right)\left[0,\frac{1}{2},0\right]$

$$7\ \ \frac{1}{2}-x,\frac{1}{2}-y,\bar{z}\ \ \bar{1}\ \ (\frac{1}{4},\frac{1}{4},0)$$

$$8\ \ \frac{1}{2}+x,\frac{1}{2}-y,z\ \ a\ \ \left(x,\frac{1}{2},z\right)\ \ [\frac{1}{2},0,0]$$

The lattice vectors of the unit cell are given in the (x,y,z)-system as:

$$a_1 = T(1,0,0)$$
$$a_2 = T(0,1,0)$$
$$a_3 = T(0,0,1)$$

with the transformation matrix given by the formula (10):

$$T = \begin{pmatrix} -a & 0 & c\ cos\beta \\ 0 & b & 0 \\ 0 & 0 & c\ sin\beta \end{pmatrix} \quad (10)$$

As a result, the elementary cell is filled with thirty atoms, which are shown in fig.3**.** Their values are shown in Fig. 4, which is a screen shot of an authoring computer program

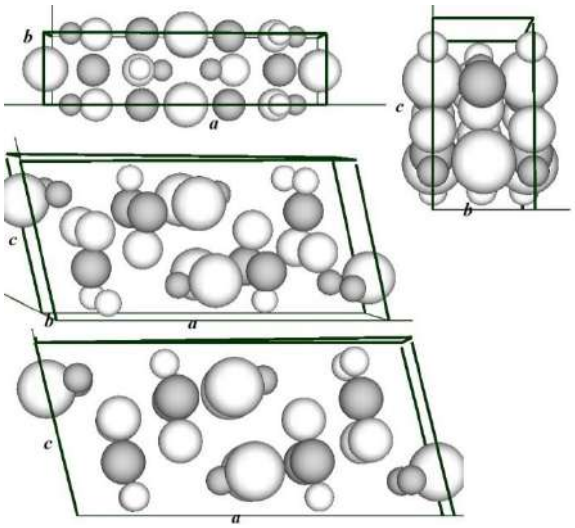

Fig. 3. Unit cell of β-Ga2O3 in different angles of observation.
The image is built in a laboratory Cartesian coordinate system using an author's computer program

Table 3.

Geometric parametres (Å, °) that are calculated using laboratory Cartesian coordinates

Ga1-O1	1.835
Ga1-O2	1.867
Ga1-O3	1.859
O1-Ga1-O2	119.59
O1-Ga1-O3	106.79
O2-Ga1-O3	106.77
O3-Ga1-O3	114.72
O1-Ga2-O1	103.26
O1-Ga2-O2	80.89
Ga2-O1	1.939
Ga2-O2	2.076
Ga2-O2	2.009
Ga2-O3	1.889
O1-Ga2-O2	91.95
O1-Ga2-O3	94.43
O2-Ga2-O2	94.15
O2-Ga2-O2	80.85
O2-Ga2-O3	92.20

We have transformed the coordinate from the crystallographic monoclinic system to Cartesian, and the geometry of the crystal does not distort (Tabl. 3). So, our actions were correct and the obtained set of atomic coordinates can be used to calculate the characteristics of the electronic subsystem of the crystal.

№	x	y	z	sort
1	0,00980027299030384	3,49024519729932E-16	4,47755899835075	1
2	1,50905469516035	1,52	1,76949795703763	2
3	1,86100699505957	4,82291621776322E-17	0,618721341579301	3
4	1,34581298558789	2,47383097800023E-16	3,17362349341951	4
5	-1,02117977115405	1,52	4,18904777167625	5
6	4,73153847982911	1,52	1,1574258976356	1
7	3,23228405765906	3,01313667309765E-16	3,86548693894871	2
8	2,88033175775984	1,52	5,01626355440705	3
9	3,39552576723152	1,52	2,46136140256684	4
10	5,09382022884595	3,26535147202658E-16	4,18904777167625	5
11	11,8775185239735	1,52	1,4459371243101	5
12	0,00980027299030403	3,04	4,47755899835075	1
13	1,86100699505957	3,04	0,618721341579301	3
14	1,34581298558789	3,04	3,17362349341951	4
15	10,8465384798291	3,04	1,1574258976356	1
16	9,34728405765906	1,52	3,86548693894871	2
17	8,99533175775984	3,04	5,01626355440705	3
18	9,51052576723152	3,04	2,46136140256684	4
19	6,1248002729903	1,52	4,47755899835075	1
20	7,62405469516035	3,04	1,76949795703763	2
21	7,97600699505957	1,52	0,618721341579301	3
22	7,46081298558789	1,52	3,17362349341951	4
23	5,76251852397346	3,04	1,4459371243101	5
24	10,8465384798291	9,02210374434031E-17	1,1574258976356	1
25	8,99533175775984	3,91016394995703E-16	5,01626355440705	3
26	9,51052576723152	1,91862459373313E-16	2,46136140256684	4
27	5,09382022884595	3,04	4,18904777167625	5
28	5,76251852397346	1,12710409970678E-16	1,4459371243101	5
29	3,23228405765906	3,04	3,86548693894871	2
30	7,62405469516035	1,37931889863571E-16	1,76949795703763	2

Fig. 4. Laboratory Cartesian coordinates of thirty atoms in unit cell

Conclusions

The technique of converting of the coordinates of the basis atoms in a unit cell of crystal, specified in a crystallographic system, in the Cartesian coordinates is described. This technique is applied to crystalline β-Ga_2O_3 for construction in the laboratory Cartesian coordinate system associated with a computer-generated author program of an atomic environment within a unit cell β-Ga_2O_3. Conversion of the coordinates from the crystallographic monoclinic system to Cartesian did not distort the geometry of the crystal.

References

1. Stepanov, S.I., Nikolaev, V.I., Bourgov, V.E., Romanov, A.E. Gallium Oxide: properties and applications – a review. *Rev. Adv. Mater. Sci.* **2016**, *44*, 63-86.
2. Pearton S.J., Ren Fan, Tadjer Marko, Kim Jihyun Perspective: Ga_2O_3 for ultra-high power rectifiers and MOSFETS. *J. Appl. Phys.* **2018,** *124*(22), 220901.
3. Galazka Z. β-Ga2O3 for wide-bandgap electronics and optoelectronics. *Semicond. Sci. Technol.* **2018**, *33*(11), 113001.
4. Park J., McClintock R., Razeghi M. Ga_2O_3 metal-oxide-semiconductor field effect transistors on sapphire substrate

by MOCVD. *Semicond. Sci. Technol.* **2019**, *34*(8), 08LT01.
5. K.D. Chabak et.al. Lateral β-Ga_2O_3 field effect transistors. *Semicond. Sci.* Technol. **2020,** *35*, 013002.
6. He H., Orlando R., Blanco M.A., Pandey R., Amzallag E., Baraille I., Rerat M. First-principles study of the structural, electronic, and optical properties of Ga_2O_3 in its monoclinic and hexagonal phases. *Phys. Rev.* **2006,** *B74*, 195123.
7. He H., Blanco M.A., Pandey R. Electronic and thermodynamic properties of β-Ga_2O_3. Appl. Phys. Lett. **2006,** *88*(26), 261904.
8. Higashiwaki M., Sasaki K., Murakami H., Kumagai Y., Koukitu A., Kuramata A., Masui T., Yamakosh S. Recent progress in Ga_2O_3 power devices. *Semicond. Sci. Technol.* **2016,** *31*, 034001.
9. Mastro M.A., Kuramata A., Calkins J., Kim J., Ren F., Pearton S.J. Opportunities and future directions for Ga_2O_3. *ECS J. Solid State Sci. Technol.* **2017,** 6, P356-P359.
10. Higashiwaki M., Murakami H., Kumagai Y., Kuramata A. Current status of Ga_2O_3 power devices. *Jpn. J. Appl. Phys.* **2016,** *55*, 1202A1.
11. Higashiwaki H., Kuramata A., Murakami H., Kumagai Y. State-of-the-art technologies of gallium oxide power devices. *J. Phys. D Appl. Phys.* **2017,** *50*, 333002.
12. Peelaers H., Van de Walle C.G. Brillouin zone and band structure of β-Ga_2O_3. *Phys. Stat. Solidi* **2015,** *B252*, 828–832.
13. Varley J. B., Janotti A., Franchini C., Van de Walle C.G. Role of self-trapping in luminescence and p-type conductivity of wide-band-gap oxides. *Phys. Rev.* **2012,** *B85*, 081109(R).
14. Furthmuller J., Bechstedt F. Quasiparticle bands and spectra of Ga_2O_3 polymorphs. *Phys. Rev.* **2016,** *B93*, 115204.
15. Mohamed M., Janowitz C., Unger I., Manzke R., Galazka Z., Uecker R., Fornari R., Weber J.R., Varley J.B., Van de Walle C. G. The electronic structure of β-Ga_2O_3. *Appl. Phys. Lett.*, **2010,** *97*, 211903.
16. Dong L., Jia R., Xin B., Peng B., Zhang Y. et al. Effects of oxygen vacancies on the structural and optical properties of β-Ga_2O_3. *Sci. Rep.* **2017,** *7*, 40160.
17. Shaskolskaya M.P. Crystallography / M.P. Shaskolskaya. - M .: Higher. school, **1996**. - 459 p.
18. Henry N., Lonsdale K. *International tables for X-ray crystallography* / N. Henry, K. Lonsdale Symmetry Groups The Kynoch Press, Birmingham, **1999;** Vol. 1, p. 372.

PACS 538.9

R.M. Balabai, M.V. Naumenko

METHODOLOGY OF CONVERTING OF THE COORDINATES OF THE BASIS ATOMS IN A UNIT CELL OF CRYSTALLINE β -Ga_2O_3, SPECIFIED IN A MONOCLINIC CRYSTALLOGRAPHIC SYSTEM, IN THE LABORATORY CARTESIAN COORDINATES FOR COMPUTER APPLICATIONS

Summary. One of the most important areas of modern technology is the creation of new structural materials with predetermined properties. Along with industrial methods for their preparation and technologies associated with the artificial growth of crystalline structures, various methods of computer modeling of new materials have recently become increasingly important. Such approaches can significantly reduce the number of full-scale experiments. Many applications of the computational materials science are related to the need to establish a relationship between structure and electronic characteristics, and other physical properties of crystals. This article on the example of crystalline β-Ga_2O_3 presents the algorithms used in the converting of the coordinates of the basis atoms in a unit cell of crystal, specified in a crystallographic system, in the Cartesian coordinates for the computational experiment.

Key words: crystalline β-Ga_2O_3, unit cell, basis atoms, monoclinic crystallographic system, Cartesian coordinates

УДК 538.9

Р.М. Балабай, М.В. Науменко

МЕТОДОЛОГІЯ ПЕРЕРАХУНКУ КООРДИНАТ АТОМІВ БАЗИСУ В ЕЛЕМЕНТАРНІЙ КОМІРЦІ КРИСТАЛІЧНОГО β-Ga_2O_3, ЩО ЗАДАНІ В МОНОКЛІННІЙ КРИСТАЛОГРАФІЧНІЙ СИСТЕМІ, В ЛАБОРАТОРНІ ДЕКАРТОВІ КООРДИНАТИ ДЛЯ КОМП'ЮТЕРНОГО ЗАСТОСУВАННЯ

Резюме. Одним із найважливіших напрямків сучасних технологій є створення нових конструкційних матеріалів з наперед заданими властивостями. Поряд з промисловими способами їх отримання і технологіями, пов'язаними з штучним вирощуванням кристалічних структур, останнім часом все більшого значення набувають різні методи комп'ютерного моделювання нових матеріалів. Такі підходи дозволяють істотно скоротити число натурних експериментів. Багато задач прикладного обчислювального матеріалознавства пов'язані з необхідністю встановлення взаємозв'язку між структурою та електронними характеристиками, іншими фізичними властивостями кристалів. У статті на прикладі кристалічного β-Ga_2O_3 представлені алгоритми, використовувані при проектуванні кристалічних структур, що дозволяють досліджувати їх властивості в обчислювальному експерименті.

Ключові слова: кристалічний β-Ga_2O_3, елементарна комірка, атомні базиси, моноклінна кристалографічна система, декартові координати

УДК 538.9

Р.М. Балабай, М.В. Науменко

МЕТОДОЛОГИЯ ПЕРЕРАСЧЕТА КООРДИНАТ АТОМОВ БАЗИСА В ЭЛЕМЕНТАРНОЙ ЯЧЕЙКЕ КРИСТАЛЛИЧЕСКОЙ β-Ga_2O_3, ЗАДАННЫЕ В МОНОКЛИННОЙ КРИСТАЛЛОГРАФИЧЕСКОЙ СИСТЕМЕ, В ЛАБОРАТОРНЫЕ ДЕКАРТОВЫЕ КООРДИНАТЫ ДЛЯ КОМПЬЮТЕРНОГО ПРИМЕНЕНИЯ.

Резюме. Одним из важнейших направлений современных технологий является создание новых конструкционных материалов с заранее заданными свойствами. Наряду с промышленными способами их получения и технологиями, связанными с искусственным выращиванием кристаллических структур, в последнее время все большее значение приобретают различные методы компьютерного моделирования новых материалов. Такие подходы позволяют существенно сократить число натурных экспериментов. Многие задачи прикладного вычислительного материаловедения связанные с необходимостью установления взаимосвязи между структурой и электронными характеристиками, другими физическими свойствами кристаллов. В статье на примере кристаллического β-Ga_2O_3 представлены алгоритмы, используемые при проектировании кристаллических структур, позволяющие исследовать их свойства в вычислительном эксперименте.

Ключевые слова: кристаллический β-Ga_2O_3, элементарная ячейка, атомные базисы, моноклинная кристаллографическая система, декартовые координаты

UDC 621.315.592

Kulikov S.S., Brytavskyi Ye.V., Borshchak V.A., Zatovskaya N.P., Kutalova M.I., Karakis Y.N.

Odesa I. I. Mechnikov National University, 42, Pastera str.; phone: 723-34-61

THE STUDY OF HOMOGENEOUS AND HETEROGENEOUS SENSITIZED CRYSTALS OF CADMIUM SULFIDE. PART IV. FEATURES OF THE REVERSE PHOTOEXCITATION METHOD

For the first time, a reverse method of studying the spectral distribution curves of the photocurrent was applied, which allows to separate the contribution of equilibrium and non-equilibrium carriers.

This publication is a continuation of the reviews [1-3]. In order to preserve the generality of the work, the numbering of sections is selected to be general. Numbers of formulas and figures are presented in sections. References to literature in each review are given individually.

Cadmium sulfide crystals are used in our research as a convenient model material. The results obtained on them and the constructed models are also applied to other semiconductor substances.

6.1. The features of spectral distribution of the photocurrent in terms of the reverse excitation

In the vast majority of cases, various spectral characteristics of semiconductor samples are measured from small to large wavelengths of light. This is not of fundamental importance in the study of its intrinsic conductivity. However, this is not the case for studying the processes associated with entrapment.

With this method of measurement production, the process of filling-emptying the traps goes with an additional stage. First, when excited by wavelengths from the self-absorption band, a large concentration of non-equilibrium carriers is created. Some of them settle on the traps. At sufficiently high light intensities and the rate of change in the wavelength of light, it is possible to create conditions under which the trap at the time of its excitation is completely filled with a non-equilibrium charge, regardless of the background of the processes.

This is convenient. In this case, due to a significant release media photo response is greater, which facilitates the definition of the main parameter – the activation energy, i.e. trap depth, the same, of course, as for equilibrium and nonequilibrium charge.

However, it is absolutely impossible to study the processes associated with the concentrations of charge carriers on the traps that existed there initially, before light exposure. Due to the receipt of a large number of non-equilibrium charges, such processes are completely camouflaged.

Or it is necessary to wait for the relaxation times when each wavelength is illuminated from different points in the spectrum, when the concept of the direction of its change in the direction of increase or decrease becomes meaningless. Each wavelength of light used causes an independent action that is not related to the previous exposure.

In addition, traps that have a small capture cross-section and /or whose concentration in the crystal is insignificant are not able to change the stationary current level and appear only in the first moments of its establishment.

When studying equilibrium processes in a crystal involving traps, it is necessary to apply a reverse change in the wavelength of radiation from large values (usually infrared) to small (visible region) [4,5]. In this case, the light acts only as a tool. By exciting carriers from traps, the light only reads the concentration of the captured charge that already existed there.

Note that this creates a rather peculiar situation. Perhaps because of this, this method of changing the spectral composition of excitation is not widely used.

Although carriers transferred by light from the bound state to the free state are by definition non-equilibrium, their concentration, at usually used sufficiently high

levels of excitation, is uniquely determined by the equilibrium charge that was on the traps before illumination.

Even more complicated is the situation with a system of interacting traps, as in our case, between the main and excited States of R-centers. Consideration of the processes that take place in this case is highlighted in a separate Section 6.2.

With all the nuances of current generation in a semiconductor crystal, the versatility of the reverse method allows measurements to be performed both traditionally in stationary mode and in dynamic mode with different rates of change in the wavelength of exciting light. Classical measurements with a fixed wavelength at each point act as a special case of the dynamic reverse method.

The selection of phenomena that occur in different order of excitation opens up a previously unused opportunity to clarify the nuances of ongoing processes.

Figure 6.1 shows graphs of the photocurrent at various modes and rates of change in the wavelength of exciting light in the visible region. At the edges of the spectrum – at 400 and 900 nm, the crystal was kept for 20 minutes until stationary conditions were reached. Technologically, in all cases, the curve was measured first when the wavelength increased, then when it decreased.

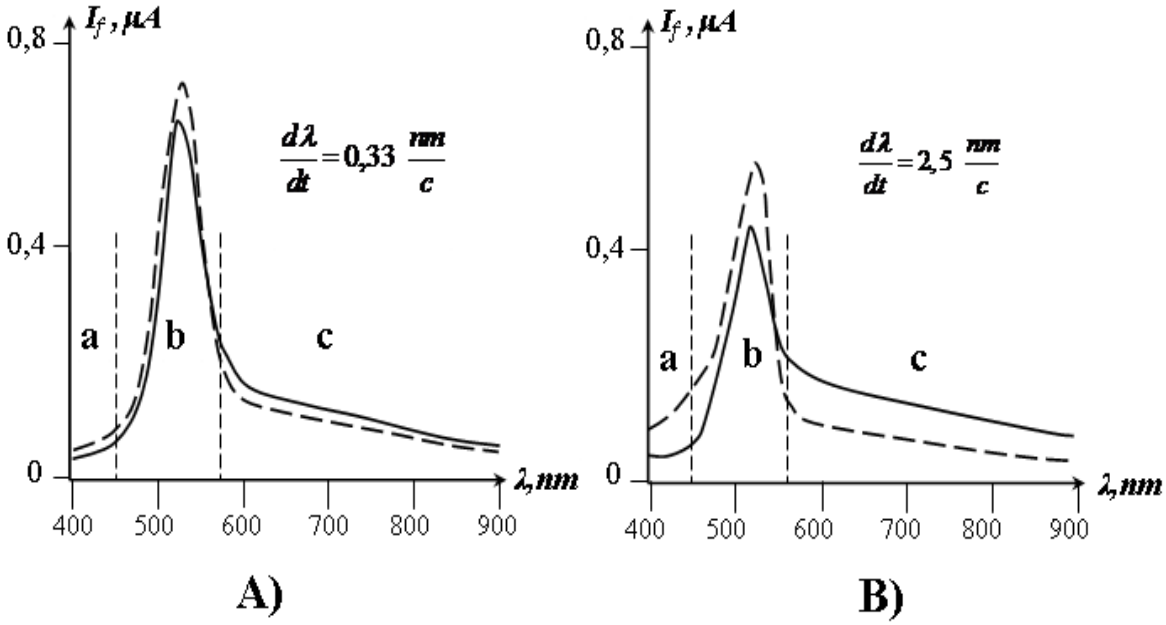

Fig. 6.1. Typical curves of the spectral distribution of the photocurrent of the studied samples when the wavelength changes from small to large values (solid line) and from large to small (dotted line). The speed of change in the wavelength of light: **A)** – 0.33 nm/s and **B)** - 2.5 nm/s. в рисунке исправить с на s.

According to the nature of the processes occurring the graphs of the spectral distribution of the photocurrent are divided into three regions:

a) ***The region of fundamental absorption, 400 – 450 nm.***

At wavelengths of 400 – 450 nm, due to the strong absorption of light, the photocurrent is formed mainly in the near-surface layers, despite the fact that under the conditions of our experiment, mainly transverse conductivity was studied. In these conditions, due to the small size of the sample (the interelectrode distance was less than 1 mm), the contact areas begin to play a significant role.

This is where the highest concentration of R-centers is located. The barrier field accumulates them both from the depth of the crystal volume relative to the light flux, and from the near-surface layers of the frontal surface. According to [6,7], R-centers due to their intrinsic charge and field drift inside the lattice tend to accumulate precisely in the SCR of the shut – off contacts at the surface.

The current flow is controlled by barriers at both edges of the sample. This is supported by further research carried out current-voltage characteristics.

R-centers play a compensating role in forming the barrier. If the barrier is repulsive for electrons (and in CdS these are the main carriers), then the accumulation of a positive charge on the R-centers leads to a decrease in the barrier and an increase in the transverse photocurrent. A similar role can be played, depending on the charge state of the R-centers [6,7,8], by reducing the negative charge when holes are captured on them.

In this case, the spectrum $I_f(\lambda)$ must be separated. Previous illumination with the energy of photons of the order E_g (λ~450 nm) in the conditions of the retracting field, it contributes to filling holes in the R-levels, lowering the barrier and increasing the photocurrent (see Sections 3.1–3.2).

If the excitation first occurs from the side of short wavelengths (λ~400 nm, $E_{photon} > E_g$), then a competing mechanism is activated – due to the above-barrier emission of hot electrons and their tunneling in the narrow upper part of the barrier, the negative charge at the geometric border of the crystal increases, which contributes to the formation of a higher barrier and a smaller photocurrent.

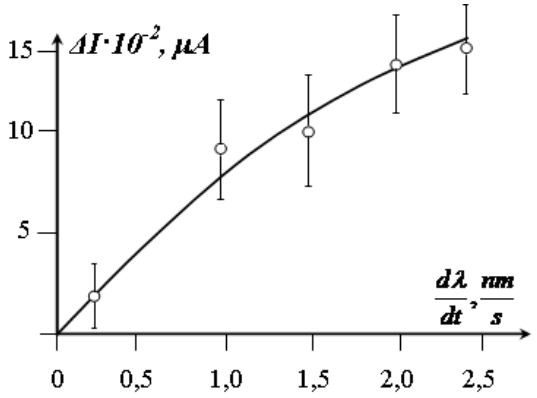

Fig. 6.2. Discrepancy of the short-wave value of the photocurrent for forward and reverse changes in the wavelength of light.

All these processes – both those that lower the barrier and those that increase it - take some time to implement. As a result, both the value of the short-wave photocurrent itself and the value of the divergence of graphs in reverse excitation turn out to be dependent on the rate of change in the wavelength.

We observed an almost double increase in the maximum photocurrent at λ~400 nm, if increased from 0,33 to 2,5 nm/s (Fig. 6.1).

At the same time, the spread of the initial and final values of the photocurrent also increased. Figure 6.2 shows the divergence of the photocurrent graphs for forward and reverse changes in the light wavelength of figure 6.1 in a 400 nm section. The number of measurements for each applied speed was 5, and the confidence probability was assumed to be 0.95. It can be seen that the value ΔI almost linearly increases by more than a dozen times when moving from a rate of 0.33 to 2.5 nm/s.

Both of these changes are easy to understand, given that if the changes occur quickly, then the process of localization of holes is advantageous, since the barrier field itself contributes to the accumulation of positive charge and the extraction of negative.

On the contrary, with a long – term control experiment (up to 3 hours) with constant illumination λ=400 nm, it was possible to increase the photocurrent from 0.030 to 0.050 μA.

Note that the revealed regularities are the prerogative of the proposed reverse method and do not appear in stationary measurements.

b) *The area of intrinsic absorption, 450 – 570 nm.*

In the area of intrinsic absorption, the number of current carriers that have passed into the free state depends only on the ratio between the energy of the incident photons and the width of the band gap. However, this is not enough to form a photocurrent. As shown in [9], the maximum dependence is $I_f(\lambda)$ the current value is defined by the expression $I_0 = e\,L\,\tau_n\,\mu_n\,\frac{b}{c}$, when, – mobility μ, the current-voltage U and geometric dimensions of the sample, - includes the

lifetime τ. Earlier [8], it was found that the lifetime of the main carriers in the sensed samples can significantly increase (up to five orders of magnitude) if the concentration of charged R-centers is comparable to the existing number of S-centers. This makes the graph view dependent $I_f(\lambda)$ from the prehistory of semiconductor excitation. As noted above, the proper absorption remains almost adequate for both directions of change in λ. However, when the wavelength of light increases to the left of the maximum, the excitation of the semiconductor occurs after activation of the near-surface layers and extraction of holes mainly in the contact areas. The filling of R-centers in the volume of the crystal is relatively small. On the contrary, if the maximum is approached from the right, the preliminary emptying of traps is added to the interzone excitation (see point "**c**"). This leads to a greater concentration of free holes, an increase in the population of R-centers, and with it, the lifetime of the main carriers.

Indeed, in the vast majority of cases, we observed an increase in the photocurrent in the long-wave part of the graphs in the "**b** " region of Fig. 6.1.The value of the photocurrent at the maximum was also higher, so there was a slight shift of the graph to the right.

The filling-emptying processes of traps cannot be balanced instantly. In addition, the crystal's sensitivity is based on the interaction between spatially distant R and S centers. And that takes time. As a result, the type of dependency changes $I_f(\lambda)$ it turned out to be related to the rate of change in the wavelength.

The graph was modified slightly for too high or too low speed. Accordingly, either the process of insensitivity did not have time to be established, or the mechanisms of thermal distribution had time to turn on, etc. The greatest changes in the photocurrent of the studied samples at the applied intensities of light flows occurred at *~1-2 nm/s*. This is what determined the choice of the interval of the used rates of change in the wavelength of light in Fig. 6.1.

It should be emphasized that the recorded changes, as for point "**a**", are due to the applied reverse excitation method and are not available for observation or analysis in traditional stationary measurements.

c) ***The region of impurity absorption, 570 – 900 nm.***

The curves of the spectral distribution of the photocurrent after a relatively rapid decrease (by 7 to 10 times) had a well – distinguishable fracture at a wavelength of 550-580 nm. Then, in the long-wave region of the spectrum, they were characterized by a slow decrease in the photocurrent in a wide range that exceeds the total width of the first two described regions (Fig. 6.1). As expected, the photocurrent measured with a set wavelength always turned out to be greater than when the excitation wavelength was reduced. Moreover, this discrepancy turned out to be different for different values (Fig. 6.1).

The presence of a contribution to the photocurrent when excited by light with wavelengths of 600 – 900 nm indicates the presence of deep traps in the samples in the middle and below the middle of the band gap.

Since the most common crystals were used for measurements and no special culling was carried out, they did not have mainly one class of adhesion levels. Numerous contributions of traps with different activation energies provided the wide area of impurity conductivity noted above. We deliberately went to this expense in order to demonstrate the advantages of the proposed method on conventional, non-selective samples.

As shown in point "**b**", in the field of intrinsic sensitivity, the current at the reverse change of the wavelength – from large values to small – on the contrary, was always greater than at the direct change – from small to large. For this reason there are graphs on the borders of these areas $I(\lambda\downarrow)$ and $I(\lambda\uparrow)$ always intersected (Fig. 6.1). This effect, which is very convenient for unambiguously separating the region of interband transitions from the impurity excitation, is by definition a feature of the exclusively reversible method and does not

appear in any way in traditional measurements.

It is recorded that as the growth the intersection point shifts slightly towards shorter wavelengths. This correlates with the fact that $I(\lambda\uparrow)$ for such speeds, it turns out to be higher (see below), which, for a sharp front of the photocurrent decline in the "**b**" region, should lead to exactly this result for geometric reasons.

Since the detected traps were deep enough, the process of thermal emptying did not play a significant role for them. Thus, subtracting for each wavelength from the forward current $I(\lambda\uparrow)$ return $I(\lambda\downarrow)$, it is easy to get the contribution to the photocurrent of only non-equilibrium carriers (Fig. 6.3).

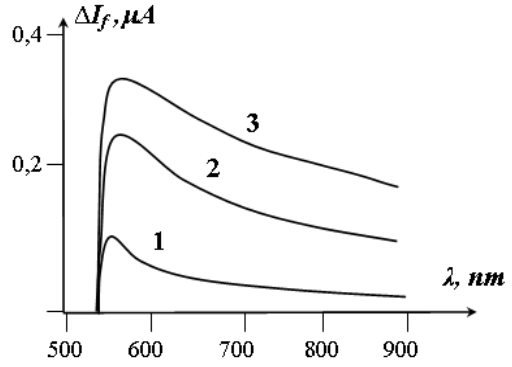

Fig. 6.3. Spectral distribution of the photocurrent signal difference for the speed of light wavelength change: 1 – 0,33; 2 – 1,5; 3 – 2,5 nm/s.

As expected, the higher the rate of change in the wavelength, the less time to affect competing processes – additional spontaneous loss of electrons to the capture centers and their relaxation return to equilibrium. As can be seen from Fig. 6.3, the non-equilibrium contribution to the current as it increases at first, it increased rapidly, and then it almost stabilized at 2,5 nm/s. This also served as an additional determinant for selecting the range of values . We can say that in our case, the curve 3 in figure 6.3 already reflects the net value of the non-equilibrium trap contribution. It was possible to observe this value only due to the reverse method.

As can be seen from Fig. 6.3, the curves $\Delta I(\lambda)$ they were characterized by a fast increase at the beginning of the impurity region (550-570 nm), then a maximum at 570-580 nm and a prolonged decrees to 900 nm. The first circumstance is provided by the competition noted above on the border with the area of its intrinsic absorption. The second indicates, of course, better retention of the pre-captured charge by deeper traps. The third, as already noted, is the presence of a whole family of other capture traps.

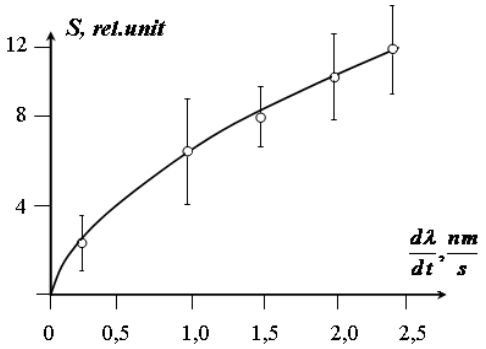

Fig. 6.4. Dependence of the area of divergence of reverse photocurrent graphs in the area of impurity absorption (600-900 nm) on the rate of change of the excitation wavelength.

In addition, the curves of the spectral distribution of the contribution to the photocurrent of each of the traps must have an asymmetric maximum. Due to the circumstances already considered, when excited from a large wave length to a small one, the equilibrium charge is mainly ejected from the traps. This is usually characterized by a bell-shaped maximum trap contribution. The samples had a high dark resistance, so the contribution of such a charge could not be significant. On the contrary, when excited from small to large wavelengths (i.e. first, the traps are significantly more pre-filled with a non-equilibrium charge, and second, they are intensively emptied in the short-wave part of the spectrum. When excited by long-wave quanta, due to the already reduced

population, the number of emissions is less. As a result, the difference curve is not symmetrical. The sum of the tighter short-wave tails of the trap maxima may provide the overall maximum of the graphs in figure 6.3 at wavelengths of 550-600 nm.

Total value of the impurity conductivity contribution can be estimated from the area bounded by the curves in figure 6.1 $I(\lambda\uparrow)$ and $I(\lambda\downarrow)$ for wavelengths from 600 to 900 nm. At Fig. 6.4 shows how this value changes for different values . To calculate the average value and confidence interval, the measurements were repeated five times. The curve in the figure is obtained using two different methods. First, using the image program *Photoshop*. Second, the graphs of Fig. 6.1 in the range of wavelengths 550-900 nm were constructed at the same scale, then a segment of paper was mechanically cut out, bounded along the axis of the abscissus by straight lines λ =550 and λ =900, and on the axis of the ordinate curves $I(\lambda\uparrow)$ and $I(\lambda\downarrow)$ and its weight was determined. The results obtained by both methods gave an identical picture, as shown in figure 6.4.

It is characteristic that with the growth of the speed of change in the wavelength of light, the lower limit of the segment $I(\lambda\downarrow)$ changed slightly. The increase in the area of divergence in the area of trap deposits was mainly due to an increase in the values $I(\lambda\uparrow)$.

We interpret this as additional confirmation that in reverse measurement, the contribution to the current is carried out by an equilibrium trap charge. Its value is small for the entire area of applied speeds there is a complete emptying of the traps. The non-equilibrium charge accumulated on the traps after passing the wavelengths of their intrinsic excitation is, of course, much larger, which ensures the predominance of the curve I(λ↑).

This also explains the sublinear nature of the graph Fig. 6.4. at high speeds, the traps do not have time to completely empty.

Note that thanks to the applied method, it is possible for the first time to clearly separate the contribution of an equilibrium and non-equilibrium trap charge.

As follows from the above, it is the reverse method, and with the maximum speed , allows you to best identify both existing electronic traps and some of their features.

6.2. Reverse spectral characteristics in the region of IR - quenching. The case of interacting traps

Section 6.1 describes the nuances of filling-emptying traps and the advantages of the reverse excitation method. The situation with a system of interacting traps, as in our case, between the main and excited States of R-centers is even more complicated.

In this case, the long-wave light effect is symmetrical. For any sequence of excitation, the levels are activated in turn. The direction of change in the wavelength: from large to small, or from small to large, determines only the order of activation of the holes – either first they are activated from the shallower excited state, and then from the deep ground state, or Vice versa.

In the latter case, we should also consider the possibility that a part of the IR radiation quanta with an energy of 1.1 eV (for cadmium sulfide) can also excite R-centers at a depth of 0.9 with the formation of hot free holes.

Comparing traditional stationary measurements for complex traps and the proposed method of operation at different speeds , the following should be noted:

1. First, both of these methods are not antagonistic. On the contrary, the stationary method should be understood as a special case of zero-speed measurements $\frac{d\lambda}{dt} = 0$. Features that can be analyzed for other values , they are omitted.

2. A stationary measurement method with an already established photocurrent works well for significantly filled traps with a high concentration. More typical is a small charge accumulated on the traps

and/or their low concentration. The processes associated with the influence of this component on the formation of photocurrent affect only in the first seconds at the beginning of exposure. No analysis can detect them from the stationary value of the photocurrent, since they are no longer there.

In dynamic measurements, the role of relaxation changes. From a hindering factor, it becomes an ally. For measurements, especially fast ones, with large values $\frac{d\lambda}{dt}$, relaxation phenomena, of course, will affect the behavior of the photocurrent. It is it is possible to identify these mechanisms and, ultimately, the parameters of the traps that form these mechanisms from comparing the results at different values $\frac{d\lambda}{dt}$ (this means with different degrees of relaxation influence).

3. Non-equilibrium carriers, exchanging with the lattice, in a very small order time 10^{-3} – 10^{-1} s [10] they balance their energy with it. As a result, it is completely impossible to separate the contributions to the current of equilibrium and non-equilibrium carriers for stationary measurements. If the dark current is formed solely by the equilibrium component of the charge, then for the light current it is assumed that its value is associated only and exclusively with non-equilibrium charges. This can be justified for high levels of illumination, and serve as a source of inaccuracy at low light levels. As will be shown below, the proposed method of measurement, especially with the maximum possible speeds $\frac{d\lambda}{dt}$, removes this contradiction.

4. In the case of interacting capture traps, as in our case, between the ground and excited state of the R-centers, the processes of charge redistribution must occur fairly quickly, since geometrically this is the same center. Carriers don't need to spend time drifting from one center to another. Note that the nuances of these processes remain unexplored to date. As an effective tool for such research, the method of high-speed measurements can be used $\frac{d\lambda}{dt}$ in the infrared region.

The range of excitation energies used is called the region of interacting traps in the sense that the effect on the R and R' levels is the excitation of a physically unified center, in contrast to the usual situation with different groups of centers, considered in [4,5].

In General, the spectral distribution of the quenching coefficient [5.11] as the excitation wavelength increases $Q(\lambda\uparrow)$ and when it decreases $Q(\lambda\downarrow)$ for different speeds $\frac{d\lambda}{dt}$ it was characterized by a certain decrease in the Q value and a sliding of the short-wave maximum towards smaller wavelengths, and for the long – wave-large ones. For a stationary graph, measurements with a relaxation of up to 20 min at each point were used to avoid transients [6,7]. The sample was also kept for a long time in each cycle at the edges of the spectrum at 1000 and 1600 nm to prevent interference of graphs.

The reverse graphs for the value were chosen as the reference ones $\frac{d\lambda}{dt}$ ~1 nm/s, causing the most discernible modifications. The characteristic changes observed on the photocurrent quenching curve over the entire range of used speeds (from 0.33 to 2.5 nm/s) are summarized in table 6.1.

Feature A:

The value of Q in each of the peaks is proportional to the number embossed light holes, respectively, for short-wave maximum – from the ground state of R-centers, and for wavelengths from excited. As the wavelength increases in the quenching region, starting from 900 nm, the exciting light first acts on a deeper basic level. The initial filling of this center is the same as for stationary measurements, but the number of activated holes is less, because, depending on the speed $\frac{d\lambda}{dt}$, the total time of exposure to it is less.

Therefore, the value of $Q_{max1}(\lambda\uparrow)$ it turns out to be less than the stationary value. If the excitation is carried out from

long to short waves, the excited state R' is pre-emptied (see Fig. 7.2). Due to an increase in the number of vacancies on it, the flow of thermally excited holes from the ground state increases. As a result, when the wavelength of light decreases to values of the order of 1100 nm, the population of the R-centers is less and the value of $Q_{max1}(\lambda\downarrow)$ it goes down even more. There is an optimal speed when the discrepancy $\Delta Q = Q_{max1}(\lambda\uparrow) - Q_{max1}(\lambda\downarrow)$ the largest according to the model developed in [4,5]. In our case it turned out to be about 1 nm/s. With a further increase in the speed, the discrepancy decreases, since the forward change of λ does not have time to excite the state R, and with the reverse – R'.

Feature B:

Now the excitation from the side of long waves meets first the undisturbed filling of the States R' and the value of the maximum $Q_{max2}(\lambda\downarrow)$ it is determined only by the time of action on the excited States R', which means the speed . In direct measurements, however, with increasing wavelength, another reason is imposed on this [5]. Before this occurred, the excitation of R-States. If **Feature A** is characterized by an increase in the thermal flow of holes, now this causes it to decrease. The population of R ' centers is less, $Q_{max2}(\lambda\downarrow) > Q_{max2}(\lambda\uparrow)$.

Table 6.1. Analysis of characteristic changes on the graphs of Q(λ) for different speeds of changing the wavelength of the quenching light.

Axis graphics / Position maximum	The Ordinate Y (the amount of damping Q, %)	Abscissa X (radiation wavelength λ)
Short-wave maximum quenching (1000 – 1100 nm)	**A.** As the speed increases , discrepancy $\Delta Q = Q_{max1}(\lambda\uparrow) - Q_{max1}(\lambda\downarrow)$ increases, reaching the highest values at about 1 nm/s, and then decreases again.	**C.** Both values $Q_{max1}(\lambda\downarrow)$ and $Q_{max1}(\lambda\uparrow)$ are shifted towards short wavelengths relative to the stationary maximum, but $Q_{max1}(\lambda\downarrow)$ stronger. As the speed increases these deviations first increase, reaching their greatest values at about 1 nm/s, and then decrease again.
Long-wave maximum quenching (1300 - 1400 nm)	**B.** As the speed increases , discrepancy $\Delta Q = Q_{max2}(\lambda\downarrow) - Q_{max2}(\lambda\uparrow)$ increases, reaching the highest values at about 1 nm/s, and then decreases again.	**D.** Both values $Q_{max2}(\lambda\downarrow)$ and $Q_{max2}(\lambda\uparrow)$ are biased towards longer wavelengths relative to stationary maximum, but $Q_{max2}(\lambda\uparrow)$ stronger. As the speed increases these deviations first increase, reaching their greatest values at about 1 nm/s, and then decrease again.

Let's note a characteristic feature. Since it is true for the left maximum $Q_{max1}(\lambda\uparrow) > Q_{max1}(\lambda\downarrow)$, then, according to the Bolzano – Cauchy theorem, the curves $Q(\lambda\uparrow)$ and $Q(\lambda\downarrow)$ they must intersect. Indeed, at any speed of change in the wavelength of light, at all lighting intensities, we observed this effect. At the speed ~1 nm/s value Q~31% it occurred at a wavelength of 1238 nm, regardless of which way the wavelength changed. Such a nuance is the prerogative of the applied technique and, of course, it is impossible to observe it in principle with traditional measurements.

Feature C:

Values $Q_{max1}(\lambda\uparrow)$ and $Q_{max1}(\lambda\downarrow)$ they sink down in different ways. Plot $Q(\lambda\uparrow)$ it is associated with undisturbed settlement of main state and reflects a simple scaling of a stationary short wave maximum $Q(\lambda)$. Both of its ramps undergo almost the same reduction. The right one is slightly larger, because for measurements with a wavelength greater than the maximum, there is a slight shift in the balance of captures-devastations that the exciting light itself caused during measurements at wavelengths less than 1100 nm. As a result, the maximum $Q_{max1}(\lambda\uparrow)$ moves slightly to the left. The pattern changes with measurements as the wavelength of light decreases. As already noted, the excited level was previously emptied. Thermal excitation from the R-centers increased. Their population has decreased. On the long-wave slope of the maximum, this is reflected to a greater extent than on the short-wave, measured later. As a result, the maximum loses its symmetry and depending on the speed it is mostly shifted to the left. It is obvious that as the speed of change in the wavelength of light increases, this effect will be weakened, because as the time of exposure to the center decreases, the light manages to knock out fewer holes.

Feature D:

Similar changes with a shift to the right are formed for the long-wave maximum. Now it's a graph $Q_{max2}(\lambda\uparrow)$ subsides asymmetrically due to the fact that the main level was previously emptied, the thermal transfer of holes from R to R' decreased on the left slope. $Q(\lambda\uparrow)$ this reflected more.

Note that all the variety of graph changes was explained using only one mechanism [4,5] – increasing or decreasing, depending on the direction of the change in the wavelength of light, the thermal excitation of holes from the main to the excited states. It is the presence of several simultaneous effects that allows us to consider the existence of such a channel for intra-center redistribution of charge concentrations as proven. The detection was made possible thanks to the use of reversible method of excitation.

7.1. Features of thermo-optical transitions with excited states of the sensing centers

Two-level model of A.Rose – R.Bube [12,13] qualitatively explains quite well the phenomenon of insensitivity of semiconductors in the presence of slow recombination centers. However, the created model is semifenomenological. Its disadvantages include the following:

I. If localized holes of R' levels were thermally transferred to a free state (Fig. 7.1 B) with an activation energy of 0.2 eV, then light quanta with an energy from 0.2 to 0.9 eV could also release them. In this case, hot holes would simply appear in the valence band. But in this case, the long-wave sensitivity in the range of 1400-1600 nm would not decrease (Fig. 7. 1, feature “a”).

II. For the same reason, there would be no cleavage between the maxima of figure 7.1 a, feature “b”. Light quanta in the range from λ_1=1100 to λ_2=1400 nm (from 1,1 to 0,9 eV) could release media with R' states

III. In the maximum at 1400 nm (Fig.7.1 A, feature “c”), the value of Q would be less than in the short-wave (1100 nm). This should be done because the centers R and R' have equal capture sections for

holes, but the level R' is affected by the thermal outflow of carriers. As a result, the stationary population of R' levels would have to be less than for the ground state of R. At the moment of illumination by radiation with an energy of 0.9 eV, the picture is blurred by an additional non-equilibrium charge as a result of the transition of holes from R to R' centers. However, both to the right and left of point "c" Fig. 7.1 A ($\lambda_{max} + d\lambda$ and $\lambda_{max} - d\lambda$) resonant light excitation of holes does not occur. If the curve $Q(\lambda)$ smooth (and only such are observed experimentally), then $Q(\lambda_2)$ and in this case, it would be less than $Q(\lambda_1)$.

But even if the Bube model remained true, and the singularity at the maximum λ_2 it simply remained unnoticed by numerous researchers, but its interpretation would still require additional considerations. As shown in [14,15], the intensity of IR light cannot be too significant. For sure observation of the quenching effect, the number of IR photons absorbed should approximately correspond to the concentration of R-centers. Since the capture cross sections $S_{pR} = S_{pR'}$, that and IR photons are divided roughly in half between the R and R' centers. Two photons are required to transit holes first from the R to the R'-level, and then to the V-zone. Therefore, even in this case, the long-wave maximum would generally be provided with fewer released holes than the short-wave maximum.

In addition, such processes would require a large amount of time.

IV. If the Fig model were implemented. 7.1B, then there should be an additional maximum quenching with an energy of 0.2 eV ($\lambda \sim 7500$ nm) in the far-IR region when thermal transitions are replaced by optical ones. Moreover, if it is masked by phonon activity, its intensity should increase as the illumination of the crystal increases with its intrinsic light, when the population of R' levels increases. Until now (see, for example, the review [16]), such a maximum of quenching has not been detected.

The height of the quenching maxima in the near-IR region (1100 and 1400 nm) decreases as the intrinsic excitation increases according to our data (Fig. 1.1 of Section 1).

V. The symmetry of the quenching maxima at λ_1 and λ_2 indicates against the Bub model (see Fig. 7.1 A). Experimentally, two fairly wide bands are observed, both slightly blurred to the left of the maxima, in the direction of high energies. This is easy to understand if the release of holes from levels R and R' is carried out directly into the zone. At photon energies exceeding the activation energy of the trap, the holes are able to move to deeper levels in the valence band. Meanwhile, if the Bube model were implemented, the long-wave maximum at 0.9 eV (λ=1400 nm) would have to be an order of magnitude lower than the short-wave one and strictly symmetrical, since the transitions R → R' are essentially resonant.

VI. The same considerations require an almost vertical wall after the second maximum. Photons with an energy less than 0.9 eV cannot transfer holes from the ground state to the excited state.

VII. If the Bube model works, the distance between the main and excited states of the centers of sensitivity (see Fig. 7.1B), $E_R - E_{R'} = h\nu(\lambda_2) = 0{,}9$ eV. For the room temperature at which the spectrum $Q(\lambda)$ is taken (Fig.7.1 a), this is 36 times more than the phonon energy kT = 0.026 eV. If we consider that it is the temperature that causes the separation of the excited state of the R' centers from the main one, then this discrepancy seems too fantastic.

VIII. If, according to the Bube model, when illuminated by a light with a wavelength of λ_2, intra-center transitions occur R → R′ (рис. 7.1B), then the population of levels R' should increase, and the main states R - decrease. Experimentally, we observe smooth dependences on the intensity of long-wave light. This indicates that the process follows a single pattern without changing the mechanism over the entire interval. In this case and in high light conditions $p_{R'} >> p_R$. Due to the large concentration of holes on the centers R', they must be **under** the quasi-Fermi level. F_p^* lies in the interval between $E_{R'}$ and E_v. On the other hand, since the population of pR at high light intensities is low, these levels are **above** the

quasi-Fermi level F_p^* **under** E_R. This cannot be done simultaneously, because $E_R > E_{R'}$ (see Fig. 7.1B).

IX. The excited state of the trap interacts with the ground state at any temperature [10]. However, in the Bube model, even at 300 K, the R' states exchange holes exclusively with the valence band. And the main level, because of its depth, can at best only capture carriers from there. There is no interaction between levels.

7.2. An alternative model of phonon-photon energy absorption in case of holes activated from the centers of slow recombination

The basis for creating a zone model (Fig. 7.1B) served the type of spectral characteristic Q (λ) shown on Fig. 7.1 A. However, the presence of two quenching maxima with the same activation energies can be interpreted in a different way [17], as shown in Fig. 7.2.

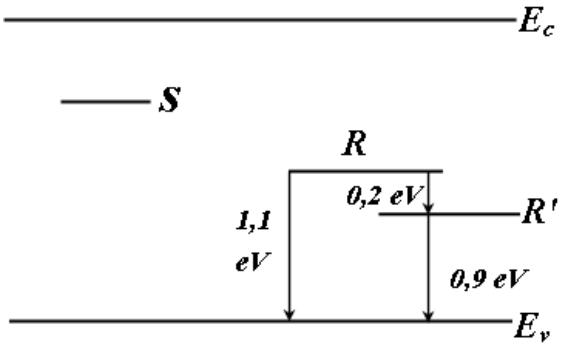

Fig. 7.2. Alternative zone diagram.

This is supported by the following experimental facts:

1. Relaxation curves.

A) The Steady-state value of the photocurrent I_0 (Section 3.4. Fig. 3.7 [2]) is determined by the stationary population of the levels. In full accordance with Fig.1.1 of Section 1.1 [1] for the short-wave maximum Q at 1100 nm, a smaller photocurrent drop was also observed on the curve 1 of Fig. 3.7.

B) For the same reason, the slope of the graph at t=0 for this curve is less, since it is determined by the number of carriers knocked out, and it is proportional to the concentration of holes located at the R-levels.

C) In figure 3.7, the time to establish a stationary photocurrent differs by about three times in graph 1 and 2. This is due to the fact that for both wavelengths the damping levels interact with each other. Light with a wavelength of 1100 nm (Fig. 7.1 a marked λ_1) knocks holes out of the main state of R. In this case, the excited state R' performs the function of a damper – part of the holes from it falls on the centers of R and delays relaxation. When activating the R ' levels with a light with a wavelength λ_2, (1400 nm, 1,1 eV) the role of the damper goes to the centers of R. Since there are fewer holes, relaxation ends much faster.

Thus, all three features of the relaxation curves indicate that the ground state of the R-centers is less populated (see section 7.1, paragraph III). This corresponds to the level model in figure 7.2.

2. Migration and relaxation changes. Large interelectrode distance.

According to the current model in Section 3.1, 3.2 [2], when illuminated by its intrinsic light, under conditions of applied external voltage, charged R-centers migrate from the OPZ contacts to the Central part of the crystal due to diffusion and drift, insensiting it (Fig. 3.4).

Elevated temperatures increase their mobility without changing the charge state. This corresponds to figure 7.2, since the thermal transitions are intra-center.

An increase in temperature in the Bube model should lead to the emptying of the excited states. Therefore, in the same field, they, on the contrary, would have to move slower.

It is experimentally recorded that IR light (λ_2), according to the model of Fig. 7.2, it knocks holes from the most filled R'-levels. This inhibits both diffusion and drift.

On the contrary, if the Bube model were operating (figure 7.1 B), IR light would cause intra-center transitions. The charge state of the R-centers should not change, since the carrier continues to remain within the center. Accordingly, the diffusion and drift would remain the same.

In addition, the depth of R'-levels 0.2 eV in the model Fig. 7.1 B is not able to provide long term retention of charge in the dark and accumulation of traps in the SCR.

3. Migration and relaxation changes. Small interelectrode distance.

The graph in Fig. 3.3 of Section 3.2. [2] was explained by the migration of charged R-centers. To test this model, the concentration of the charged impurity was artificially reduced by IR radiation with an energy of 0.9 eV (Section 3.3). At the same time, all the features of relaxation disappeared. The photocurrent curve without the formation of a depression reached saturation for long times, several times exceeding the time of reaching the maximum I_f. Absolute value of the photocurrent I_f at the same time, it turned out to be an order of magnitude smaller.

This confirms the viability of the zone diagram 7.2 and is completely inconsistent with the Fig model. 7.1 B for the same reason as stated in paragraph 2 above. in the Bube model, infrared light causes only intra-center transitions.

4. Lux-ampere dependencies.

A) Dependence of the quenching coefficient Q on the intensity of the exciting and quenching light based on the model of Fig. 7.2 is obtained in Section 1.1 [1]. The formula is fully confirmed experimentally. As the number of self-absorbed photons increases, Q decreases, while as the intensity of long-wave light increases, the quenching increases (see figure 1.1 of Section 1.1).

Meanwhile, according to Bube, IR light should only cause transitions from the main to the excited state, and only indirectly, due to temperature, the release of holes into the valence band. A two-step transition would hide the effect of this light on the quenching coefficient.

B) Analysis of the rate of increase of the walls of the quenching maxima also leads to a contradiction with the Bube model. As the number of infrared photons increases, the experimental value of the cleavage between the maxima grows. This is not difficult to understand from Fig. 7.2-photons with energy in the region between maxima from 0.9 to 1.1 eV can be effectively absorbed by both levels.

In the Bube model, this would require creating hot holes in the valence band with an energy from 0.7 to 0.9 eV.

In addition, in the Bube model, the long-wave wall with $\lambda > \lambda_2$ it should not react at all to changes in the intensity of the quenching light, since (see Fig. 7.1 B) photons with an energy less than 0.9 eV are not absorbed at all (see section 7.1, paragraph **VI**.).

C) In the narrow region of the ratio between the applied field, temperature and intensity of long-wave light with $\lambda_1 \sim 1100$ nm we were able to create conditions when the first maximum of figure 1.1 a was practically absent ([1] Section 1.2). We explained this by re-grabbing holes. Immediately after activation, the hole is located in the vicinity of the mother center and it is energetically advantageous for it to return back. This is also confirmed by the value of the quantum output for IR light, defined in Section 5.2, at the level of 0.03-0.07. That is, abnormally low.

This fits well with the alternative model and contradicts the Bube model, which assumes a large population of ground states. Accordingly, the probability of capturing holes at these levels, proportional to the number of available places, is much lower. The quantum output can't be small.

D) Dependencies Fig. 5.2 of Section 5.2 [3] for the zone diagram Fig. 7.1 B is not possible. When activated by light with a wavelength of 1100 nm, the hole in this model does not leave the center and therefore no changes from the outside should appear.

The presence of experimental graphs in Fig. 5.2 at different IR radiation intensities confirms the alternative model.

E) In Section 2.2 [1] it is shown that when the crystal is exposed only to its intrinsic excitation, the Lux-ampere characteristics $I_f(L)$ they are linear. With the use of additional infrared illumination, they become superlinear, although at lower absolute values of the current (Fig. 2.2). And this was observed as for the wavelength λ_1, and λ_2 Fig. 7.1 A.

This fully corresponds to the zone diagram in Fig. 7.2. Transitions from both R - and R'-levels are equivalent here. In contrast to the Bube model, where a transition with an energy of 0.9 eV does not lead directly to the release of the hole, and, accordingly, should not give the observed result on the LAC graphs.

5. Reverse graphs.

In Section 6.2.the behavior of q(λ) graphs under the reverse excitation method is investigated. We compared graphs measured at different rates of change in the wavelength, first in the direction of increasing, and then in the direction of decreasing. The difference is in the order in which the centers are excited.

The Bub model does not involve interaction between levels (see section 7.1, paragraph **IX**). Therefore, for any method of measurement, regardless of the rate of increase or decrease in the wavelength, the type of maxima Q(λ) should not change. Infrared light simply reveals the extent to which holes fill the R and R' levels.

If the levels thermally interact with each other, as in the alternative model, the picture changes. In this case, the impact on one level changes the situation on the other. If the measurements are from a large wavelength of light to a small one, the R' centers are first excited. The transitions of holes from the main states are amplified to the vacant places. Therefore, when the wavelength is reduced to λ_1, due to the smaller filling of the R-centers, the maximum Q(λ1) will be smaller. Thermal transitions $R \rightarrow R'$ take time. Therefore the amount of subsidence will depend on the rate of change in the wavelength $\frac{d\lambda}{dt}$. The higher it is, the smaller the change. Thus, in this case, the maximum $Q(\lambda_2)$ turns out to be unchanged, and the maximum $Q(\lambda_1)$ decreases depending on the applied speed $\frac{d\lambda}{dt}$.

If the spectrum is measured traditionally in the direction of increasing the wavelength, the maximum is stable $Q(\lambda_1)$. But it is the effect of light on it during measurements that simultaneously reduces the thermal flow of holes to the R' centers. When the light energy drops to $E_{R'}$, there will also be fewer transitions of holes to the free state from it. In this case the maximum is reduced $Q(\lambda_2)$. Moreover, the more time it took to organize thermal transitions from R-levels. That is, the slower the wave length changed, the speed $\frac{d\lambda}{dt}$ was smaller. The alternate subsidence of the maxima Q (λ) in the far spectral region, depending on the direction of the wavelength change, is an additional argument in favor of the model Fig. 7.2.

6. Processes at the short-wave boundary of quenching.

Section 4 shows [3] that at the short-wave boundary of the quenching region, the I_f it does not change, because the intensity of the photoexcitation and quenching processes are equal. Since each of them depends on external influences in different ways – the magnitude of light flows, temperature, applied voltage-then changing these parameters should lead to the creep of the wavelength of the beginning of quenching.

A) We were not able to find any useful changes in the scope of the implemented model λ_0 (Fig. 7.1 A), related to the variation of the voltage applied to the sample or the intensity of its intrinsic light. Increasing your own arousal works equally in both models. This leads to an increase in level filling. When exposed to them, the recoil is higher, the rate of recombination increases, and faster than the rate of photoexcitation at the edge of absorption. Border λ_0 it should be shifted towards shorter wavelengths for both models.

Indistinguishable results were obtained for different intensities of the infrared light when measuring the spectral dependencies from small to large wavelengths. This is a predictable situation. The greatest impact on the situation λ_0 the spectral region that follows it has an effect $Q(\lambda_1)$. And it is associated with transitions from ground states that work equally in both models.

B) Another thing when measuring $Q(\lambda)$ from large wavelengths to small ones with different speeds (see previous paragraph 5 "Reverse graphs"). In this case, transitions with an energy of 0.9 eV are organized first, and then 1.1 eV. Moreover, the higher the light intensity, the brighter the features appear.

If the Bube model works, the R levels are emptied when pre-lit with a light with an energy of 0.9 eV, and when the subsequent excitation of 1.1 eV, the photo response from them will be less. Accordingly, the rate of quenching in the area λ_0 decreases. Value λ_0 should move to the right. The higher the speed $\frac{d\lambda}{dt}$, the better it should be shown. First, the population of R-centers does not have time to recover, and secondly, transitions from R-levels due to temperature do not have time to interfere.

The opposite situation was observed experimentally. The higher the speed change the wavelength, the lower limit of the damping λ_0 it shifted towards higher values.

This fully corresponds to the alternative model of Fig. 7.2. Light of 0.9 eV energy empties the R'-centers. The thermal emission of holes $R \rightarrow R'$ increases because there are more empty spaces on the R'-centers. At the moment of lighting with an energy of 1.1 eV, the emission of holes from the R-centers will be less due to less population. Reducing the rate of recombination also leads to bias λ_0 in the direction of long wavelengths, however, this is already an inertial process, since it includes an additional stage of thermal transitions limited by probabilistic phenomena.

C) The distinction between temperature changes at a fixed voltage and light intensity works Even better. This was shown better when measuring in the direction of increasing the wavelength of the quenching light.

In the Bube model, holes from R'-States are knocked out using thermal energy. The population of the main levels does not change. The influence of high $Q(\lambda_1)$ remain stable. A fixed value should be expected λ_0.

In fact, as the temperature increased, it crept away from 920 to 940 nm (see Fig. 4.2, Section 4 [3]). This happens because the holes are thermally transferred from R to R'-levels. Then the lighting with the wavelength λ_1 knocks out fewer carriers. Quenching processes are suppressed, and restoration of equality with the rate of excitation is possible only at large wavelengths.

7. Oscillation of holes.

There can be no oscillation of holes at a wavelength of 1100 (0.9 eV) in the Bube model, since the hole does not transit to the free state at all.

Meanwhile, as can be seen from Fig. 5.1 of Section 5.1 [3], it is for the short-wave maximum that the greatest changes are observed with increasing external voltage. It is in full accordance with the alternative model of Fig. 7.2.

7.3. Experiment Éntre - Éntre (either-or).

A selective property of the crystal that allows determining an adequate model between the zone diagrams in the “either-or” mode Fig. 7.1B and 7.2, is the population of the excited states R' when the temperature changes.

In the Bub model [13], the R' levels interact with the V-zone. Heating activates the media from these traps. These are the **giving** centers. When the temperature increases, the population **decreases**.

On the contrary, in the alternative model of figure 7.2, the R'-centers interact with the ground States. Phonons activate media from R-levels to R'-levels. Now the traps R' are the **receiving** centers. As the temperature increases, their population **increases**.

To clarify these circumstances, we used a change in the type of spectral distri-

bution of the quenching coefficient Q (λ) with temperature. The temperature range is selected from room temperature to 50 ^{0}C in order to avoid the phenomena associated with temperature damping of the photocurrent described in [13].

1. The short-wave maximum of this distribution at 1100 nm (1.1 eV) is determined by transitions from the ground States. In the Bube model, this part of the graph should not change. The R-levels are too deep and cannot be noticeably activated by thermal energy. In the first approximation, their population remains the same.

In practice, the Q values are lower here (Fig. 7.3), which fully corresponds to the expected value for the alternative model.

2. The long-wavelength maximum at 1400 nm (at 0.9 eV) increased by about the same amount as the first maximum decreased. Given that the dispersion of the monochromator was equalized not by energy, but by the number of quanta, this indicates in favor of an alternative model Fig. 7.2.

Note that the observed differences were observed only for high IR radiation intensities. We attribute this to the fact that for small light streams, the number of displaced carriers is limited only by the number of photons absorbed. If the number of quanta is comparable and more than the number of traps, the activation processes are determined by the already populated levels and the mechanisms described above take effect.

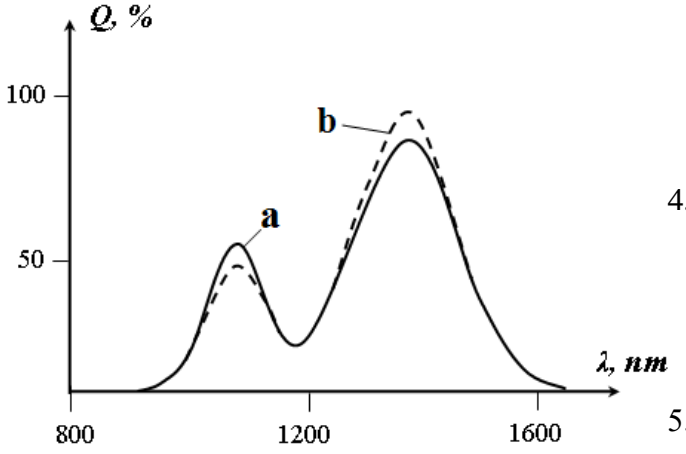

Fig. 7.3. Influence of temperature on the spectral distribution of the quenching coefficient. **a)** - measurements were made at 24 ^{0}C; **b)** - the temperature was 50 ^{0}C..

Thus, the created model of thermooptic transitions lacks the disadvantages of the **I–IX** model R.Bube and confirmed by experimental data **1-7**. The scenario of releasing holes from the ground state - through the excited state – to the valence band first involves a transition with **phonon** absorption $E_R \rightarrow E_{R'}$ with energy 0,2 eV, and only then arousal in a free state $E_{R'} \rightarrow E_v$ due to the energy of a **photon** hν=0,9 eV. The zone diagram is implemented in Fig. 7.2.

References

1. Simanovych N.S., Brytavskyi Ye.V., Kutalova M.I., Borshchak V.A., Karakis Y.N. The study of heterogeneous sensitized crystals of cadmium sulfide. Part I. About charge state of the centers recombination // “Photoelectronics”, n. 26. Odessa, “Одеський національний університет” 2017. s. 124 – 138 .
2. Kulikov S.S., Brytavskyi Ye.V., Kutalova M.I., Zatovskaya N.P., Borshchak V.A., Konopel’skaya N.V., Karakis Y.N. The study of cadmium sulfide heterogeneously sensitized crystals. Part II. Relaxation characteristics // “Photoelectronics”, n. 27. Odessa, “Одеський національний університет” 2018. s. 79 – 93 .
3. Kulikov S.S., Brytavskyi Ye.V., , Kutalova M.I., Zatovskaya N.P., Borshchak V.A., Karakis Y.N. The study of cadmium sulfide heterogeneously sensitized crystals. Part III. Oscillations of excited carriers // “Photoelectronics”, n. 28. Odessa, “Одеський національний університет” 2019. s. 133 – 144.
4. Британвський Є., Каракіс Ю. Особливості спектрального розподілу фотоструму в умовах реверсного збудження // Вісник Львівського університету. Серія Фізична. –Львів – 2010. – Випуск 45. – с. 199 – 205.
5. Британвський Є.В., Каракіс Ю.М. Спектральні характеристики напівпровідників із центрами чутливості при реверсному способі збудження // International Conference of Students and Young Scientists in Theoretical and Ex-

perimental Physics HEUREKA – Lviv 2009. May 20 – 22 – Book of abstracts., Ukraine. s. A6.
6. Каракис Ю.Н., Затовская Н.П., Зотов В.В., Куталова М.И. Особенности релаксации фототока в кристаллах сульфида кадмия с запорными контактами // 1-а Українська наукова конференція з фізики напівпровідників – Одеса, 10-14 вересня 2002. Тези доповідей. Т.2. – с.138
7. Каракис Ю.Н., Борщак В.А., Зотов В.В., Куталова М.И. Релаксационные характеристики кристаллов сульфида кадмия с ИК-гашением // Фотоэлектроника 2002. – вып.11. – с.51 – 55.
8. Britavsky E.V., Karakis Y.N., Kutalova M.I., Chemeresyuk G.G. On the charge state of rapid and slow recombination centers in semiconductors // Photoelectronics. 2008. – n.17. – 2009. – n. 18 – s. 65 – 69.
9. Чемересюк Г.Г., Каракис Ю.Н. Методические указания к лабораторным работам по спецпрактикуму "Фотоэлектрические процессы в полупроводниках. Часть I" // Одесса. Издательство Одесского национального университета. – 2011. – с. 1 – 59.
10. Бонч-Бруевич В.Л., Калашников С.Г. Физика полупроводников // М.: Наука, 2007. – с. 220-222.
11. Brytavskyi Ye.V., Karakis Yu.N., Kutalova M.I., Chemeresyuk G.G. Reversive spectral characteristics in IR-quenching range of photocurrent. The case of interacting holes // Photoelectronics. – 2010. – n. 19. – s. 56 – 60.
12. Роуз А.. Основы теории фотопроводимости // М.:Мир, 1966. – 192 с.
13. Бьюб Р. Фотопроводимость твёрдых тел // М.:Из-во ин.лит, 1992. – с.558 .
14. Драгоев А.А. Визначення квантового виходу інфрачервоного гасіння фототоку // Робота – лауреат Областної сесії Малої Академії наук України. Одеське територіальне відділення. Секція "Фізика". – Одеса 2006. с 32
15. Novikova M.A., Karakis Yu.N., Kutalova M.I. Particularities of current transfer in the crystals with two types of Recombination centers // Photoelectronics – 2005. n.14. s. 58-61.
16. Лашкарёв В.Е., Любченко А.В., Шейкман М.К. Неравновесные процессы в фотопроводниках // К.: Наукова думка, 1981. – с. 264.
17. Mel A.S., Karakis Y.N.. Kutalova M.I., Chemeresjuk G.G. Features of thermo-optical transitions from the recombination centers excited states // Photoelectronics. –2011. – n. 20. – s. 2 –27.

UDC 621.315.592

Kulikov S.S., Brytavskyi Ye.V., Borshchak V.A., Zatovskaya N.P., Kutalova M.I., Karakis Y.N.

THE STUDY OF HOMOGENEOUS AND HETEROGENEOUS SENSITIZED CRYSTALS OF CADMIUM SULFIDE.
PART IV. FEATURES OF THE REVERSE PHOTOEXCITATION METHOD

For the first time, a reverse method of studying the spectral distribution curves of the photocurrent was applied, which allows to separate the contribution of equilibrium and non-equilibrium carriers.

This publication is a continuation of the reviews [1-3]. In order to preserve the generality of the work, the numbering of sections is selected to be general. Numbers of formulas and figures are presented in sections. References to literature in each review are given individually.

Cadmium sulfide crystals are used in our research as a convenient model material. The results obtained on them and the constructed models are also applied to other semiconductor substances.

Keywords: cadmium sulfide, photoexcitation, photocurrent quenching

УДК 621.315.592

Куликов С. С., Бритавский Е. В, Борщак В. А., Затовская Н. П.
Куталова М. И., Каракис Ю. Н.

ИССЛЕДОВАНИЕ ОДНОРОДНЫХ И ГЕТЕРОГЕННЫХ СЕНСИБИЛИЗИРОВАННЫХ КРИСТАЛЛОВ СУЛЬФИДА КАДМИЯ. ЧАСТЬ IV. ОСОБЕННОСТИ МЕТОДА ОБРАТНОГО ФОТОВОЗБУЖДЕНИЯ

Впервые применен обратный метод исследования кривых спектрального распределения фототока, позволяющий разделить вклад равновесных и неравновесных носителей. Данная публикация является продолжением обзоров [1-3]. В целях сохранения общности работы нумерация разделов выбрана общей. Номера формул и рисунков представлены в разделах. Ссылки на литературу в каждом обзоре даются индивидуально. Кристаллы сульфида кадмия используются в наших исследованиях как удобный модельный материал. Полученные на них результаты и построенные модели применимы и к другим полупроводниковым веществам.

Ключевые слова: сульфид кадмия, фотовозбуждение, гашение фототока

УДК 621.315.592

Куликов С.С., Бритавський Є.В, Борщак В.А., Затовська Н.П. Куталова М.І., Каракіс Ю.М.

ДОСЛІДЖЕННЯ ОДНОРІДНИХ І ГЕТЕРОГЕННИХ СЕНСЕБЕЛІЗОВАНИХ КРИСТАЛІВ СУЛЬФІДУ КАДМІЮ. ЧАСТИНА IV. ОСОБЛИВОСТІ МЕТОДУ ЗВОРОТНОГО ФОТОЗБУДЖЕННЯ

Вперше застосований зворотний метод дослідження кривих спектрального розподілу фотоструму, що дозволяє розділити вклад рівноважних і нерівноважних носіїв. Дана публікація є продовженням оглядів [1-3]. З метою збереження спільності роботи нумерація розділів обрана загальною. Номери формул і малюнків представлені в розділах. Посилання на літературу в кожному огляді даються індивідуально. Кристали сульфіду кадмію використовуються в наших дослідженнях як зручний модельний матеріал. Отримані на них результати і побудовані моделі застосовні і до інших напівпровідникових речовин.

Ключові слова: сульфід кадмію, фотозбудження, гасіння фотоструму

This article has been received in September 2020/

PACS 33.20.-t

Glushkov A.V., Kovalchuk V.V., Sofronkov A.N., Svinarenko A.A.

Odesa State Environmental University, 15, Lvovskaya str., Odesa, 65016
E-mail: odeku.intsci@gmail.com

OPTIMIZED QUASIPARTICLE DENSITY FUNCTIONAL APPROACH FOR MULTIELECTRON ATOMIC SYSTEMS

We present the optimized version of the quasiparticle density functional theory (DFT), constructed on the principles of the Landau-Migdal Fermi-liquids theory and principles of the optimized one-quasiparticle representation in theory of multielectron systems. The master equations can be naturally obtained on the basis of variational principle, starting from a Lagrangian of an atomic system as a functional of three quasiparticle densities. These densities are similar to the Hartree-Fock (HF) electron density and kinetical energy density correspondingly, however the third density has no an analog in the Hartree-Fock or the standard DFT theory and appears as result of account for the energy dependence of the mass operator Σ. The elaborated approach to construction of the eigen-functions basis can be characterized as an improved one in comparison with similar basises of other one-particle representations, namely, in the HF, the standard Kohn-Sham approximations etc**.**

1. At present time a density functional theory (DFT) became by a powerful tool in studying the electron structure of different materials, including atomic and molecular systems, solids, semiconductors etc. [1-42]. A construction of the correct energy functionals of a density for multi-body systems represents very actual and important problem of the modern theory of semiconductors and solids, thermodynamics, statistical physics (including a theory of non-equilibrium thermodynamical processes), quantum mechanics and others.

In last time a development of formalism of the energy density functional has been considered in many papers (see [1–7]). Its application is indeed based on the two known theorems by Hohenbreg-Kohn ($\tau = 0$, where τ is a temperature) and Mermin ($\tau \neq 0$) [1,2]. According to these theorems, an energy and thermodynamical potential of the multi-body system are universal density functionals. Though these theorems predict an existence of such a density functional, however its practical realization is connected with a number of the significant difficulties (see [1-3,8-17]). The problem is complicated under consideration of the non-stationary tasks (the known theorem by Runge-Gross about 1-1 mapping between time-dependent densities and the external potentials [2]).

Let us remind some important results of the density functional theory. It should be mentioned a constructive approach to delivering optimal representations for an exact density functional [1,2,8-16], which has been used for generalization of the Hohenberg-Kohn theorem in order to get an effective density functional for large molecules. As alternative version one could consider a quasiparticle conception of Kohn-Sham and the Levi-Valone method [2,3]. In fact it has been done an attempt practically to realize an idea of the Hohenberg-Kohn theorem.

More advanced analogous approach with account of the multi-particle correlations is developed in ref. [8,17,18].

The quasiparticle Fermi-liquid version of the DFT has been earlier developed in Refs. [1-3,8,17] and based on the principles of the Landau-Migdal Fermi liquids theory. In refs. [4,5] it has been firstly developed a consistent relativistic quasiparticle theory of a density functional formalism and constructed an optimized one-quasiparticle representation in a theory of multi-electron systems. The lowest order multi-body effects, in particular, the gauge dependent radiative contribution for the certain class of the photon propagators calibration are treated in QED formulation and new density functional integral-differential equations are derived. The

minimal value of the gauge dependent radiative contribution is considered to be the typical representative of the multi-electron correlation effects, whose minimization is a reasonable criteria in the searching for the optimal QED perturbation theory one-electron basis. In this paper we present the optimized version of the quasiparticle DFT (a Fermi-liquid version of the DFT), based on the principles of the Landau-Migdal Fermi-liquids theory and performance of the gauge invariant principle.

The elaborated approach to construction of the eigen-functions basis can be characterized as an improved one in comparison with similar basises of other one-particle representations, namely, in the HF, the standard Kohn-Sham approximations [12-17] etc.

Below we present only the key points of the theory for multielectron atomic systems.

2. According to Refs. [1-5], the master equations can be obtained on the basis of variational principle, if we start from a Lagrangian of an atomic system L_q. It should be defined as a functional of quasiparticle densities:

$$\nu_0(r) = \sum_\lambda n_\lambda |\Phi_\lambda(r)|^2,$$
$$\nu_1(r) = \sum_\lambda n_\lambda |\nabla\Phi_\lambda(r)|^2, \qquad (1)$$
$$\nu_2(r) = \sum_\lambda n_\lambda [\Phi_\lambda^* \Phi_\lambda - \Phi_\lambda^* \Phi_\lambda].$$

The densities ν_0 and ν_1 are similar to the HF electron density and kinetical energy density correspondingly; the density ν_2 has no an analog in the Hartree-Fock (HF) or the standard DFT theory and appears as result of account for the energy dependence of the mass operator Σ. The functions Φ_λ are the solutions of the master equations for multielectron atomic systems with a nuclear charge Z (in atomic units) as follows:

$$[p^2/2 - \sum_\alpha Z_\alpha / r_\alpha + \sum\nolimits_0(x) +$$
$$p(\partial\sum/\partial p^2)p]\Phi_\lambda(x) =$$
$$(1 - \partial\sum/\partial\varepsilon)\varepsilon_\lambda \Phi_\lambda(x) \qquad (2)$$

The functions Φ_λ in (5) are orthogonal with a weight

$$\rho_k^{-1} = a^{-1} = [1 - \partial\sum/\partial\varepsilon]. \quad (3)$$

Now one can introduce the wave functions of the quasiparticles

$$\varphi_\lambda = a^{-1/2}\Phi_\lambda, \qquad (4)$$

which are, as usually, orthogonal with weight 1. For complete definition of $\{\varphi_\lambda\}$ it should be determined the values $\sum_0, \partial\sum/\partial p^2, \partial\sum/\partial\varepsilon$.

A Lagrangian L_q can be written as a sum of a free Lagrangian and Lagrangian of interaction:

$$L_q = L_q^{\,0} + L_q^{\,int}, \qquad (5)$$

where a free Lagrangian L_q^0 has a standard form:

$$L_q^0 = \int dr \sum_\lambda n_\lambda \Phi_\lambda^* (i\partial/\partial t - \varepsilon_p)\Phi_\lambda, \qquad (6)$$

The interaction Lagrangian is defined in the form, which is characteristic for a standard (Kohn-Sham) density functional theory (as a sum of the Coulomb and exchange-correlation terms), however, it takes into account for the energy dependence of a mass operator $\sum$:

$$L_q^{\text{int}} = L_K - \frac{1}{2}\sum_{i,k=0}^{2}\int \beta_{ik} F(r_1, r_2)\nu_i(r_1)\nu_k(r_2)dr_1 dr_2 \qquad (7)$$

where β_{ik} are some constants (look below), F is an effective potential of the exchange-correlation interaction

In the local density approximation in the density functional the potential F can be expressed through the exchange-correlation pseudo-potential V_{XC} as follows [1-5]:

$$F(r_1, r_2) = \delta V_{XC}/\delta\nu_0 \cdot \delta(r_1 - r_2). \qquad (8)$$

According to ref. [1-4], one can get the following expressions for $\sum_i = -\delta L_q^{\text{int}}/\delta\nu_1$:

$$\sum\nolimits_0 = (1-\sum\nolimits_e)V_K + \sum\nolimits_0^{ex} +$$

$$\frac{1}{2}\beta_{00}\delta^2 V_{XC}/\delta\nu^2 \cdot \nu_0^2 + \beta_{00}\delta V_{XC}/\delta\nu_0 \cdot \nu_0 +$$

$$+ \beta_{01}\delta V_{XC}/\delta\nu_0 \cdot \nu_1 + \beta_{01}\delta^2 V_{XC}/\delta\nu_0^2 \cdot \nu_0\nu_1 +$$

$$\beta_{02}\delta^2 V_{XC}/\delta\nu_0^2 \cdot \nu_0\nu_2 + \beta_{02}\delta V_{XC}/\delta\nu_0 \cdot \nu_2$$

$$\sum\nolimits_1 = \beta_{01}\delta V_{XC}/\delta\nu_0 \cdot \nu_0 +$$

$$+ \beta_{12}\delta V_{XC}/\delta\nu_0 \cdot \nu_2 + \beta_{11}\delta V_{XC}/\delta\nu_0 \cdot \nu_1;$$

$$\sum\nolimits_2 = \beta_{02}\delta V_{XC}/\delta\nu_0 \cdot \nu_0 +$$

$$+ \beta_{12}\delta V_{XC}/\delta\nu_0 \cdot \nu_1 + \beta_{22}\delta V_{XC}/\delta\nu_0 \cdot \nu_2; \quad (9)$$

Here V_K is the Coulomb term (look above), $\sum_0^{ex}$ is the exchange term. Using the known canonical relationship:

$$H_q = \Phi_\lambda^* \delta L_q/\delta\Phi_\lambda^* + \Phi_\lambda \delta L_q/\delta\Phi_\lambda - L_q \quad (10)$$

after some transformations one can receive the expression for the quasiparticle Hamiltonian, which is corresponding to a Lagrangian L_q:

$$\begin{aligned} H_q &= H_q^0 + H_q^{\text{int}} = H_q^0 - L_K + \\ &+ \frac{1}{2}\beta_{00}\delta V_{XC}/\delta\nu_0 \cdot \nu_0^2 + \\ &+ \beta_{01}\delta V_{XC}/\delta\nu_0 \cdot \nu_0 \cdot \nu_1 + \\ &\frac{1}{2}\beta_{11}\delta V_{XC}/\delta\nu_0 \cdot \nu_1^2 - \\ &- \frac{1}{2}\beta_{22}\delta V_{XC}/\delta\nu_0 \cdot \nu_2^2 \end{aligned} \quad (11)$$

It is obvious that omitting the energy dependence of the mass operator (i.e. supposing $\beta_{02} = 0$) the quasiparticle density functional theory can be resulted in the standard Kohn-Sham theory.

Further let us give the corresponding comments regarding the constants β_{ik}. Without a detailed explanation, we note here that the corresponding constants in our theory approximately possess the same universality as ones in the Landau Fermi-liquid theory and Migdal finite Fermi-systems theory. Though it is well known that the entire universality is absent. First of all, it is obvious that the terms with constants $\beta_{01}, \beta_{11}, \beta_{12}, \beta_{22}$ give omitted contribution to the energy functional (at least in the zeroth approximation in comparison with others), so they can be equal to zero in the simple approximation. The value for a constant β_{00} in some degree is dependent upon the definition of the potential V_{XC}. If as V_{XC} it is use one of the correct exchange-correlation potentials from the standard density functional theory, then without losing a community of statement, the constant β_{00} can be equal to 1. The constant β_{02} can be in principle calculated by analytical way, but it is very useful to remember its connection with a spectroscopic factor F_{sp} of atomic or molecular system (it is usually defined from the ionization cross-sections) [5]:

$$F_{sp} = \left\{1 - \frac{\partial}{\partial \in}\sum\nolimits_{kk}\left[-(I.P.)_k\right]\right\} \quad (12)$$

where I.P. is a ionization potential. It is easily to understand the this definition is in fact corresponding to the pole strength of the corresponding Green's function [62]. The simple approximation for the I.P. is as follows [2-4]:

$$(I.P.)_k = -(\in_k + F_k), \quad (13)$$

$$F_k = \Sigma_{kk}\left(-(.I.P.)_k\right) \approx \frac{1}{1 - \partial\Sigma_{kk}(\in_k)/\partial_\in}\Sigma_{kk}(\in_k) \quad (14)$$

.

It is well known that can be determined by the following standard expression (in the second order of the perturbation theory):

$$\sum\nolimits_{kk}^{(2)}(\in)=\sum_{\substack{i,j\\ s\notin F}}\frac{(V_{ksij}-V_{ksji})V_{ksij}}{\in+\in_s-\in_i-\in_j}+\sum_{\substack{i,j\\ s\notin F}}\frac{(V_{ksij}-V_{ksji})V_{ksij}}{\in+\in_s-\in_i-\in_j} \quad (15)$$

Other details can be found in Refs. [1-10]).

3. As application of the quasiparticle theory we present the estimates for the atomic spectroscopic factors. Using the above written formula, one can simply define the values (3)-(12) one could the quantity (12). In the concrete calculation as potential V_{XC} we use the exchange-correlation pseudo-potential which contains the correlation (Gunnarsson-Lundqvist) potential and relativistic exchanger Kohn-Sham one [4,5].

As example in table 1 we present our calculational data for spectroscopic factors of some atoms.

Table 1.Spectroscopic factors of the external ns^2 shells of some atoms and ions

Atom, ion	N	F_{sp}	Atom, ion	n	F_{sp}
Ar	3	0.58	As	6	0.30
Exp.	3	0.56	As^-	6	0.31
RPA	3	0.70	Rn	6	0.29
TI (IV)	3	0.60	Fr^+	6	0.28
Xe	6	0.36	Fr	6	0.28
TI	6	0.36	Ra	7	0.43
Pb	6	0.34	Ac	7	0.42
Bi	6	0.33	Th	7	0.42
Po+	6	0.31	Pa	7	0.42
Po	6	0.31	U	7	0.42

There are also listed for the argon atom the experimental value of the spectroscopic factor and the value, obtained in the random phase approximation (RPA) with exchange. It should be noted that the Hartree-Fock theory gives the value of 1. In conclusion let us remind that the presented approach to definition of the functions basis $\{\Phi_\lambda\}$ of a Hamiltonian H_q can be treated as an improved in comparison with similar basises of other one-particle representations (for example, the HF, the Hatree-Fock-Slater, the standard Kohn-Sham approximations etc.). Naturally, this advancement can be manifested during studying those properties of the multi-electron systems, when an accurate account for the complex exchange-correlation effects, including the continuum pressure, energy dependence of a mass operator etc, is critically important [28-40].

References

1. Glushkov A.V., New approach to theoretical definition of ionization potentials for molecules on the basis of Green's function method. *Journ.of Phys.Chem*.-**1992,** 66, 2671-2677.
2. Glushkov A.V., An universal quasiparticle energy functional in a density functional theory for relativistic atom. *Optics and Spectr*. **1989,** 66, 31-36.
3. Glushkov A.V., Quasiparticle approach in the density functional theory under finte temperatures and dynamics of effective Bose –condensate. *Ukr. Phys. Journ*., **1993**, 38(8), 152-157.
4. Glushkov, A.V. *Relativistic Quantum theory. Quantum mechanics of atomic systems*. Astroprint: Odessa, **2008**
5. Glushkov, A.V. *Relativistic and correlation effects in spectra of atomic systems*. Astroprint: Odessa, **2006**.
6. Glushkov A.V., The Green's functions and density functional approach to vibrational structure in the photoelectron spectra of molecules: Review of method// *Photoelectronics*.-**2014,** *23,* 54-72.
7. Glushkov A.., Koltzova N., Effective account of polarization effects in calculation of oscillator strengths and energies for atoms and molecules by method of equations of motion. *Opt. Spectr.* **1994**, *76*(6), 885-890.
8. Khetselius, O.Yu. *Quantum structure of electroweak interaction in heavy finite Fermi-systems.* Astroprint: Odessa, **2011**.
9. Khetselius, O.. Relativistic perturbation theory calculation of the hyperfine structure parameters for some heavy-element isotopes. *Int. Journ. Quant.Chem.* **2009,** *109*, 3330-3335.
10. Khetselius, O. Relativistic calculation of the hyperfine structure parameters for

heavy elements and laser detection of the heavy isotopes. *Phys.Scr.* **2009,** *T135*, 014023.
11. Khetselius, O.Yu. *Hyperfine structure of atomic spectra*. Astroprint: Odessa, **2008**.
12. Kohn, J.W.; Sham, L.J. Self-Consistent Equations Including Exchange and Correlation Effects. *Phys. Rev. A* **1964,** *140*, 1133.
13. Hohenberg, P.; Kohn, W. Inhomogeneous Electron Gas. *Phys. Rev. B* **1964,** *136*, 864.
14. Feller, D.; Davidson, E.R. An approximation to frozen natural orbitals through the use of the Hartree–Fock exchange potential. *J. Chem. Phys.* **1981,** *74*, 3977-3989.
15. Davidson E.R., Natural Orbitals. *Adv. Quant. Chem*. **1972,** *6*, 235-266
16. Suaud N.; Malrieu, J.-P. Natural molecular orbitals: limits of a Lowdin's conjecture, *Mol. Phys.* **2017**, 115(21-22), 2684-2695.
17. Gross E.; Dreizler R. *Density Functional Theory*; Springer: New York, 1995.
18. Glushkov, A.V. Correction for exchange and correlation effects in multielectron system theory. *Journ. of Struct. Chem*. **1990**, *31*(4), 529-532.
19. Köppel H., Domcke W., Cederbaum L.S., Green's function method in quantum chemistry. *Adv. Chem. Phys*. **1984,** 57, 59.
20. Glushkov A.V., Atom in electromagnetic field.-Kiev: KNT, 2005.-450P.
21. Glushkov A.V., Kondratenko P.A., Buyadzhi V., Kvasikova A.S., Shakhman A., Sakun T., Spectroscopy of cooperative laser electron-γ-nuclear processes in polyatomic molecules. *J. of Phys.: Conf. Ser*. **2014**, *548*, 012025.
22. Khetselius, O.Yu. Relativistic Energy Approach to Cooperative Electron-γ-Nuclear Processes: NEET Effect *In Quantum Systems in Chemistry and Physics, Series: Progress in Theoretical Chemistry and Physics;* Nishikawa, K., Maruani, J., Brändas, E., Delgado-Barrio, G., Piecuch, P., Eds.; Springer: Dordrecht, **2012;** Vol. 26, pp 217-229.
23. Khetselius, O.Yu. Relativistic perturbation theory calculation of the hyperfine structure parameters for some heavy-element isotopes. *Int. Journ.Quant.Chem.* **2009,** *109*, 3330-3335.
24. Khetselius, O.Yu. Relativistic calculation of the hyperfine structure parameters for heavy elements and laser detection of the heavy isotopes. *Phys.Scripta.* **2009,** *135*, 014023.
25. Khetselius, O.Yu. Optimized Perturbation Theory for Calculating the Hyperfine Line Shift and Broadening of Heavy Atoms in a Buffer Gas. *In Frontiers in Quantum Methods and Applications in Chemistry and Physics*, *Series: Progress in Theoretical Chemistry and Physics;* Nascimento, M., Maruani, J., Brändas, E., Delgado-Barrio, G., Eds.; Springer: Cham, **2015;** Vol. 29, pp. 55-76.
26. Khetselius, O.Yu. Relativistic calculating the spectral lines hyperfine structure parameters for heavy ions.*AIP Conf. Proc.* **2008,** *1058*, 363-365.
27. Khetselius, O.Yu. Hyperfine structure of energy levels for isotopes ^{73}Ge, ^{75}As, ^{201}Hg. *Photoelectr*. **2007,** *16*, 129-132
28. Ivanov, L.N.; Ivanova, E.P. Method of Sturm orbitals in calculation of physical characteristics of radiation from atoms and ions. *JETP*. **1996,** *83*, 258-266.
29. Glushkov, A.V., Ivanov, L.N. Radiation decay of atomic states: atomic residue polarization and gauge noninvariant contributions. *Phys. Lett. A* **1992,** *170*, 33.
30. Glushkov, A.V.; Ivanov, L.N. DC strong-field Stark effect: consistent quantum-mechanical approach. *J. Phys. B: At. Mol. Opt. Phys.* **1993,** *26*, L379-386.
31. Ivanova, E.P., Ivanov, L.N., Glushkov, A., Kramida, A. High order corrections in the relativistic perturbation theory with the model zeroth approximation, Mg-Like and Ne-Like Ions. *Phys. Scripta* **1985**, *32*, 513-522.
32. Glushkov, A.V. Multiphoton spectroscopy of atoms and nuclei in a laser field: Relativistic energy approach and radiation atomic lines moments method. *Adv. in Quantum Chem.* **2019**, *78*, 253-285.
33. Khetselius, O.Yu. Optimized relativistic

many-body perturbation theory calculation of wavelengths and oscillator strengths for Li-like multicharged ions. Adv. Quant. Chem. **2019**, *78*, 223-251.
34. Svinarenko, A., Glushkov, A, Khetselius, O., Ternovsky, V., Dubrovskaya Y., Kuznetsova A., Buyadzhi V. Theoretical spectroscopy of rare-earth elements: spectra and autoionization resonances. *Rare Earth Element*, Ed. J. Orjuela (InTech). **2017**, pp 83-104.
35. Glushkov, A., Khetselius, O., Svinarenko A., Buyadzhi, V., Ternovsky, V. Kuznetsova, A., Bashkarev, P. Relativistic perturbation theory formalism to computing spectra and radiation characteristics: application to heavy element. *Recent Studies in Perturbation Theory*, ed. D. Uzunov (InTech). **2017**, 131-150.
36. Glushkov, A. Spectroscopy of cooperative muon-gamma-nuclear processes: Energy and spectral parameters *J. Phys.: Conf. Ser.* **2012,** *397*, 012011.
37. Glushkov, A.V. Spectroscopy of atom and nucleus in a strong laser field: Stark effect and multiphoton resonances. *J. Phys.: Conf. Ser*. **2014**, *548*, 012020.
38. Glushkov, A.V., Khetselius, O.Yu., Svinarenko A.A. Theoretical spectroscopy of autoionization resonances in spectra of lanthanides atoms. *Phys. Scripta*. **2013**, *T153*, 014029.
39. Glushkov, A.V., Svinarenko, A.A., Ternovsky, V.B., Smirnov, A.V., Zaichko, P.A. Spectroscopy of the complex autoionization resonances in spectrum of helium: Test and new spectral data. *Photoelectronics*. **2015**, *24*, 94-102.
40. Glushkov, A.V., Ternovsky, V.B., Buyadzhi, V., Zaichko, P., Nikola, L. Advanced relativistic energy approach to radiation decay processes in atomic systems. *Photoelectr*. **2015**, *24*, 11-22.
41. Glushkov A., Khetselius O., Kruglyak Yu., Ternovsky V. *Calculational Methods in Quantum Geometry and Chaos theory*. P.3. Odessa , **2014.**
42. Glushkov A., Khetselius O., Svinarenko A, Buyadzhi V. *Methods of computational mathematics and mathematical phys*. P.1.TES, Odessa, **2015.**

PACS 33.20.-t

Glushkov A.V., Kovalchuk V.V., Sofronkov A.N., Svinarenko A.A.

OPTIMIZED QUASIPARTICLE DENSITY FUNCTIONAL APPROACH FOR MULTIELECTRON ATOMIC SYSTEMS

Summary. We present the optimized version of the quasiparticle density functional theory (DFT), constructed on the principles of the Landau-Migdal Fermi-liquids theory and principles of the optimized one-quasiparticle representation in theory of multielectron systems. The master equations can be naturally obtained on the basis of variational principle, starting from a Lagrangian of an atomic system as a functional of three quasiparticle densities. These densities are similar to the Hartree-Fock (HF) electron density and kinetical energy density correspondingly, however the third density has no an analog in the Hartree-Fock or the standard DFT theory and appears as result of account for the energy dependence of the mass operator Σ. The elaborated approach to construction of the eigen-functions basis can be characterized as an improved one in comparison with similar basises of other one-particle representations, namely, in the HF, the standard Kohn-Sham approximations etc**.**

Key words: quasiparticle density functional theory, exchange-correlation corrections

PACS 33.20.-t

Глушков А.В., Ковальчук В.В., Софронков А.Н., Свинаренко А.А.

ОПТИМИЗИРОВАННАЯ КВАЗИЧАСТИЧНАЯ ТЕОРИЯ ФУНКЦИОНАЛА ПЛОТНОСТИ ДЛЯ МНОГОЭЛЕКТРОННЫХ АТОМНЫХ СИСТЕМ

Резюме. Представлена оптимизированная версия квазичастичной теории функционала плотности (ТФП), построенная на принципах теории ферми-жидкости Ландау-Мигдала и введении оптимального одноквазичастичного представления в теории многоэлектронных систем. Основные уравнения могут быть естественно получены на основе вариационного принципа, исходя из лагранжиана атомной системы, представленного в виде функционала трех квазичастичных плотностей. Последние аналогичны стандартным электронной плотности Хартри-Фока (ХФ) и плотности кинетической энергии; однако третья плотность не имеет аналога в теории ХФ или стандартной ТФП и появляется как результат учета энергетической зависимости массового оператора квазичастиц. Разработанный подход к построению базиса собственных функций представляется более эффективным в сравнении с аналогичными базисами других одночастичных представлений, в частности, в приближениях ХФ или стандартном приближении Кона-Шэма и др.

Ключевые слова: квазичастичная теория функционала плотности, обменно-корреляционные поправки

PACS 33.20.-t

Глушков О.В., Ковальчук В.В., Софронков О.Н., Свинаренко А.А.

ОПТИМІЗОВАНА КВАЗІЧАСТИНКОВА ТЕОРІЯ ФУНКЦІОНАЛА ГУСТИНИ ДЛЯ БАГАТОЕЛЕКТРОННИХ АТОМНИХ СИСТЕМ

Резюме. Представлена оптимізована версія квазічастинкової теорії функціонала густини (ТФГ), побудованої на принципах теорії фермі-рідини Ландау-Мігдала і введенні оптимального одноквазічастинкового уявлення в теорії багатоелектронних систем. Основні рівняння теорії можуть бути природно отримані на основі варіаційного принципу, виходячи з лагранжіану атомної системи, представленого у вигляді функціоналу трьох квазічастинкових густин. Останні аналогічні стандартним електронній густині Хартрі-Фока (ХФ) і густині кінетичної енергії; однак, третя густина не має аналога в теорії ХФ або стандартній ТФГ і з'являється як результат урахування енергетичної залежності масового оператора квазічастинок. Розроблений підхід до побудови базису власних функцій видається більш ефективним у порівнянні з аналогічними базисами інших одночасткових уявлень, зокрема, в наближеннях ХФ або стандартному наближенні Кона-Шема і ін.

Ключові слова: квазічастинкова теорія функціоналу густини, обмінно-кореляційні поправки

PACS 33.20.-t

Bakunina E. V., Dykyi O. V.

National University "Odesa Law Academy", 28, Rishel'evskaya str., Odesa, 65012
E-mail: bakuninaev09@gmail.com

SIGNAL PROCESSING AND CYBERSECURITY IN SOME CHAOTIC OPTICAL COMMUNICTAION SYSTEMS

A chaos –geometric approach to investigation of complex chaotic dynamical systems is applied to an analysis, modeling and processing the time series of emission intensities of chaotic transmitter/receiver systems (two unidirectionally coupled semiconductor laser systems in the all-optical scheme) suited for encoding at rates of GBit/s. the problem of a signal processing is directly connected with the corresponding cybersecurity in some optical chaos communictaion systems. The estimated values for the dynamic and topologic invariants such as the correlation and Kaplan-York dimensions, Lyapunov indicators, Kolmogorov entropy etc for investigated chaotic signal time series of two unidirectionally coupled semiconductor laser systems in the all-optical scheme.

1. At present time there are carried out the intensive investigations in the field of signal processing and cybersecurity in different optical chaos communictaion systems that is provided by a great importance and interst due to its technical applicatioons [1-6].

The use of methods of a chaos theory has been considered as an effective alternative technique to encrypt information that provides a high level of cyber security for complex information. There have been published sufficiently large number of papers, but, hitherto it is absent an full understanding all mathematical computational, informational and technological aspects of this problem (c.g., [1,2] and Refs therein).

According to ref. [1,2], there are papers, where it has been shown that a message could be encoded and decoded within a high dimensional chaotic carrier in devices with using coupled single-mode semiconductor lasers subjected to coherent optical feedback or injection, or erbium doped fiber ring lasers.

The important feature of such schemes is connected with successful possibilities to synchronize two spatially separated chaotic semiconductor lasers to each other. The authors [2] have reviewed review the main characteristics of the emitter/receiver devices concentrating on two kind of chaotic systems: a semiconductor laser subject to a delayed all-optical feedback and a semiconductor lasers subject to a delayed non-linear electro-optical feedback. The important result of Ref. [2] are as follows: firstly, there is generated a direct-chaotic carrier in dynamics of both systems; secondly, availability of chaotic regime in systems sufficient to provides a privacy in the communication as the higher the complexity of the chaotic carrier the more difficult is to decode the message without the appropriate receiver [2].

From the technical viewpoint, message can be hidden in the broad spectrum in the 10-100 GHz range due to the use of semiconductor diode lasers. In Refs. [10-10] the authors presented a general, uniform chaos-geometric formalism to analysis, modelling and prediction of the non-linear dynamics of quantum and laser systems and devices (such as atomic and diatomic systems in an electromagnetic infrared field, laser and quantum generators systems etc) with elements of the deterministic chaos. In particular, the detailed analysis and modelling has been realized and the results of studying the low- and high dimensional dynamics of a chaos generation in the semiconductor GaAs/GaAlAs laser with the retarded feedback as well as the results of non-linear analysis of the chaotic oscillations in a grid o two autogenerators have been listed. It should be noted that the dynamics of this systems has been also studied from the viewpoint of the corresponding differential equations solutions (e.g. [12,24,44]). At the same time, in a case of different quite complex systems a

similar analysis and differential equations solving is not possible at least in the simplified form, so here one may make processing the experimental time series of the fundamental dynamical variables.

Through there are many papers, where the different methods and algorithms of processing temporal and spatial dynamics of the complex systems are developed and intensively used (see references [1-24].

However, below we will follow a chaos – geometric approach, developed in refs. [20-20]. It includes the advanced generalized techniques such as the wavelet analysis, multi-fractal formalism, mutual information approach, correlation integral analysis, false nearest neighbour algorithm, the Lyapunov exponent's analysis, and surrogate data method, and principally new methods and algorithms of prediction etc.

In this paper we apply a chaos –geometric approach to analysis, modeling and processing the time series of emission intensities of chaotic transmitter/receiver systems (two unidirectionally coupled semiconductor laser systems in the all-optical scheme) suited for encoding at rates of GBit/s [2].

We will list the estimated values for the dynamic and topologic invariants such as the correlation and Kaplan-York dimensions, Lyapunov indicators, Kolmogorov entropy etc for investigated chaotic signal time series.

According to Refs. [20-20], the general chaos–geometric scheme of analysis, modeling and processing the time series of the cited intensities time series includes the following points. The first point is processing the input data, which contain a time series with N discrete values of the scalar variable, namely, intensity measurements:

$$I(t) = I(t_0 + j\Delta t)=I(j) \qquad (1)$$

So the first step is connected with preparing the corresponding numerical data about the intensity measurements. In the general case, s (n) can be any time series (populations or polarization of atoms or molecules, radiation intensities of systems, etc.).

In our case below speech is about the time series of emission intensities of chaotic transmitter/receiver systems (two unidirectionally coupled semiconductor laser systems in the all-optical scheme). This scheme is in details described in Ref. [2]. It is a characteristic feature of this system is availability of a hyper-chaotic carrier, i.e. a high dimensional chaotic attractor. This circumstance has a direct relation to ensuring privacy in the communication as the higher complexity of a chaotic carrier the more difficult is to decode the message without the appropriate receiver (see details in Ref. [2]). Usually these characteristic can be provided by using the semiconductor diode lasers, which, according to different estimates, are able to exhibit a broad spectrum in the range about 10-100 GHz.

The characteristics of chaotic systems signals (time series) and respectively a mechanism of encoding the messages are realized by such a way with a guarantee of impossibility to extract the message by means of any linear filtering process etc. The technical parameters of the chaotic optical communication system are described in ref. [2].

Here we only note that the setup is used to study experimentally all-optical chaos phenomenon. It consists of an external cavity semiconductor laser and several detection devices, namely, a cavity semiconductor laser consists of an edge emitting laser which is driven by a low noise direct current source, a collimation lens, a variable neutral density filter and a high reflecting mirror with a reflectivity of approximately 99 % terminating the external cavity [2]. The semiconductor laser with the facet reflectivities is electronically pumped by a low noise current source with the injection current I_{DC}. The internal round trip time of the light is τ. The emitted light is reflected from a distant mirror with the reflectivity and reinjected into the laser system with some time delay.

A system is constructed so in order to use chaotic fluctuations of intensity (-or amplitude) of a semiconductor laser. As a rule, one keep in mind that some message is masked as a small amplitude modulation with a masking

efficiency (order about -15 dB). In Ref. [2] there are presented the data on the temporal intensity dynamics obtained for an injection current of $I_{DC} = 1.2\ I_{th}$ and a length of the external cavity 3.9 cm. The temporal dynamics comprises fast chaotic pulsations in the GHz range representing as chaotic carrier signal for communication experiments.

From the theoretical viewpoint, analysis of the corresponding time series in further includes reconstruction of the phase space of a system.

More exactly, according to Refs. [20-20], speech is about calculation the respective embedding dimension and reconstruction of an Euclidean space large enough so that the set of points d_A can be unfolded without ambiguity. The well-known approach to perform this reconstruction is in utilizing the correlation dimension method, which allows to calculate so called correlation integral and its dependence upon a radius of the correlation sphere. There are a few versions of numerical realization of the correlation dimension algorithm.

Usually, simultaneously one should check the correctness of the processed data by means of utilizing a surrogate data algorithm (see al details in Refs. [20-20]), which allows to create the substitute data sequences generated in accordance to the probabilistic structure underlying the original data.

It is important to underline that simulteniously an autociolrelation function alsofythm as well as method of average mutual information are utilized to calculate very important numerical parameter of the all algorithm such as a delay time ν (or lag). The matter is in the fact that the series (1) is exchanged by the series with delayed variables I (j+ν) and further one should construct the corresponding vector in the D-dimensional space:

$$[I(j), I(j+\nu), I(j+2\nu), \ldots, I(j+(D-1)\nu)]. \quad (2)$$

It should be noted As it has been noted in [20], if a number ν is too big, then I(j + nν) and I(J +(n+1)ν) will be completely independent of each other in the statistical sense and the projections of the orbits on the attractor will be directed at two completely unrelated directions.

In order to check any complex system on an availability of the elements of a chaos any researcher usually utilizes a procedure of calculation of the such important dynamical invariants as the Lyapunov indicators δ_i (look details in Refs. [17-20]). These indicators determine an invariant measure of chaotic attractor. The latter are very useful when considering the physics of the process and, moreover, determine the limited predictability of the chaotic motion of the physical system. Using only topological or only dynamic invariants to characterize the attractor is unlikely to give a "complete" set of invariants, so it is necessary to use them together. It is worth to remind that there is another very important characteristics such as Kolmogorov entropy E_K which is defined as a sum of the positive Lyapunov indicators.

In order to calculate a dimension of the chaotic attractor one could use the Kaplan-York formula :

$$D_L = i + \sum_{m=1}^{i} \delta_m / |\delta_{i+1}|, \quad (3)$$

where the Lyapunov's exponents δ are taken in descending order, and the number is such that the quantities $\sum_{m=1}^{i} \delta_m > 0$ and $\sum_{m=1}^{i+1} \delta_m < 0$. To calculate the Lyapunov indicators δ_i , one could use one of the existing numerical algorithms and the corresponding PC codes. In this paper we have used the algorithm, which is based on the Jacobi matrix of system and the numerical codes Tisean, Quantum Chaos and Geomath [20]). The details of the utilized methods and algorithms can be found in Refs. [20-20].

3. Below we present the concrete data of analysis and modeling time series of emission intensities of chaotic transmitter/receiver systems (two coupled semiconductor laser systems in the all-optical scheme) suited presented in Ref. [2] for encoding at rates of GBit/s; the typical time series of emission

intensities of chaotic transmitter/receiver systems with two coupled semiconductor laser systems is presented in figure 1.

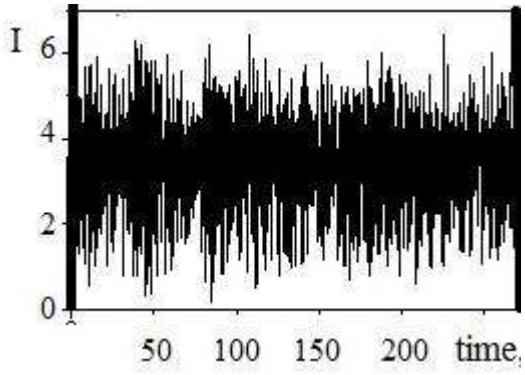

Figure 1. A typical time (ns) series of emission intensity I of the chaotic transmitter/receiver system with two coupled semiconductor laser systems ($8x10^3$ points and Δt=0.0125 ns).

The concrete step is an analysis of the corresponding time series with $8x10^3$ points and Δt=0.0125 ns. The corrective algorithms have been used in order to reconstruct the missing time series terms. The calculation allows to get the following values of the main topologic and dynamic invariants, namely, the time lag ν=8, the embedding dimension D_E=5, the correlation dimension D_C=3.2, the Kaplan-York dimension: D_L=2.3, the positive and negative Lyapunov indicators δ_1=0.233, δ_2=0.003, δ_3=-0.004,…, the Kolmogorov entropy: E_K=0.236. Surely, there is an important chaos availability parameter such as the Gottwald-Melbourne E_{gm} , however here we did not calculate E_{gm}. The performed calculation allows to pay attention at a few important dynamic features in the system. Firstly, availability of two positive Lyapunov indicators is an evidence of a chaos availability in the temporal dynamics and existence of the respective strange attractor in a phase space.

It is important to underline that the Kaplan-York dimension is very close to the correlation dimension, but indeed is smaller than the embedding dimension. The latter confirms the correctness of the choice of the latter. In order to conclude, let us underline that in this work a chaos –geometric approach (in versions [20-20]) has been applied to investigation of complex chaotic optical communication dynamical systems with the aim of modeling and processing data of the time series for emission intensities of chaotic transmitter/receiver systems.

The latter is provided by using two unidirectionally coupled semiconductor laser systems of Ref. [2]. The numerical data on the some dynamic and topologic invariants (the correlation and embedding dimensions, the Kaplan-York parameter, the Lyapunov indicators, Kolmogorov entropy) for investigated chaotic signal time series are obtained and analyzed in order to estimate quantitatively the chaos phenomenon in characteristic chaotic optical communication system. It is important to underline that a changing the governed parameters in a system will result in changing the main dynamic and topologic parameters and can be performed in regime of the numerical experiment.

As the problem of a signal processing in investigated chaotic optical communictaion system is directly connected with the corresponding cybernetic security, it is obvious that the obteined data on the chaotic dynamic parameters and carrier can be utilized for indirect estimate of a privacy in the communication as the higher the complexity of the carrier the more difficult is to decode a e message without the appropriate receiver [2].

References

1. Feature Section on Optical Chaos and Applications to Cryptography, IEEE vol. 38, Ed. by S. Donati and C. R.Mirasso, IEEE J. Quantum Electron., **2002**.
2. Mirasso, C.R., Fischer I., Peil M., Larger L. Optoelectronic Devices For Optical Chaos Communications. *Proc. Spie* 5248, Semiconductor Optoelectronic Devices For Lightwave Communication (8 Dec. 2003).
3. Bakunina E.V., Dikyi O.V., Signal processing and cybersecurity in some information technology systems: Chaos-geometric approach. These add. All-Ukrainian scientific-practical. Conf.

"Cybersecurity in the modern world: current challenges" ("Odessa Law Academy"). **2020**.
4. Schreiber, T. Interdisciplinary application of nonlinear time series methods. *Phys.Rep*. **1999,** ***308***, 1-64.
5. Glushkov, A.V. *Methods of a Chaos Theory*. Astroprint: Odessa, **2012**
6. Abarbanel, H.; Brown, R.; Sidorowich, J; Tsimring, L. The analysis of observed chaotic data in physical systems. *Rev. Mod. Phys*. **1993**, *65*, 1331- 1392.
7. Kennel, M.; Brown, R.; Abarbanel, H. Determining embedding dimension for phase-space reconstruction using geometrical construction. *Phys. Rev. A*. **1992**, *45*, 3403-3412.
8. Glushkov A.V., Khetselius O.Y., Brusentseva S.V., Zaichko P.A., Ternovsky V.B., Studying interaction dynamics of chaotic systems within a nonlinear prediction method: application to neurophysiology. In Advances in Neural Networks, Fuzzy Systems and Artificial Intelligence, Series: Recent Advances in Computer Engineering, Ed. J.Balicki.(Gdansk, WSEAS Pub.) **2014**, *21*, 69-75.
9. Glushkov, A.V. *Atom in an electromagnetic field*. KNT: Kiev, **2005**.
10. Khetselius, O. Forecasting evolutionary dynamics of chaotic systems using advanced non-linear prediction method *In Dynamical Systems Applications;* Łódz, **2013**; Vol T2, pp 145-152.
11. Glushkov, A.V.; Khetselius, O.Yu.; Brusentseva, S.; Duborez, A. Modeling chaotic dynamics of complex systems with using chaos theory, geometric attractors, and quantum neural networks. *Proc. Intern. Geometry Center*. **2014**, *7(3)*, 87-94.
12. Glushkov, A.V.; Malinovskaya, S.V.; Shpinareva, I.M.; Kozlovskaya, V.P.; Gura, V.I. Quantum stochastic modelling energy transfer and effect of rotational and v-t relaxation on multi-photon excitation and dissociation for CF_3Br molecules. *Int. Journ. Quant. Chem.* **2005**, *104(4)*, 512-516.
13. Glushkov, A.V.; Buyadzhi, V.V.; Ponomarenko, E.L. Geometry of Chaos: Advanced approach to treating chaotic dynamics in some nature systems. *Proc. Int. Geom. Center***. 2014** *7(1)*,24-30.
14. Glushkov A., Ternovsky V., Buyadzhi V, Prepelitsa G. Geometry of a relativistic quantum chaos: New approach to dynamics of quantum systems in electromagnetic field and uniformity and charm of a chaos. *Proc. Int. Geom. Center*. **2014,** *7*(4), 60-71.
15. Glushkov A.V.; Ivanov, L.N. DC strong-field Stark effect: consistent quantum-mechanical approach. *J. Phys. B: At. Mol. Opt. Phys.* **1993,** *26*, L379-386
16. Glushkov, A.V. *Relativistic Quantum theory. Quantum mechanics of atomic systems*. Astroprint: Odessa, **2008.**
17. Khetselius, O.Yu. Quantum structure of electroweak interaction in heavy finite Fermi-systems. Astroprint: Odessa, **2011.**
18. Glushkov, A.; Ambrosov, S.; Ignatenko, A. Non-hydrogenic atoms and Wannier-Mott excitons in a DC electric field: Photoionization, Stark effect, Resonances in ionization continuum and stochasticity. *Photoelectronics*, **2001,** *10*, 103-106.
19. Khetselius, O.. Relativistic perturbation theory calculation of the hyperfine structure parameters for some heavy-element isotopes. *Int. Journ.Quant.Chem.* **2009,** *109*, 3330-3335.
20. Glushkov, A.V.; Ternovsky, V.B.; Buyadzhi, V.; Prepelitsa, G.P. Geometry of a Relativistic Quantum Chaos: New approach to dynamics of quantum systems in electromagnetic field and uniformity and charm of a chaos. *Proc. Intern. Geom. Center*. **2014**, *7(4)*, 60-71.
21. Kuznetsova, A.A.; Glushkov, A.V.; Ignatenko, A.V.; Svinarenko, A.A.; Ternovsky V.B. Spectroscopy of multielectron atomic systems in a DC electric field. *Adv. Quant. Chem*. (Elsevier) **2018**, *78*, 287-306.
22. Glushkov, A., Buyadzhi, V., Kvasikova, A., Ignatenko, A., Kuznetsova, A., Pre-

pelitsa, G., Ternovsky, V. Non-Linear chaotic dynamics of quantum systems: Molecules in an electromagnetic field and laser systems. In: *Quantum Systems in Physics, Chemistry, and Biology*. Springer, Cham. **2017**, *30*, 169-180
23. Glushkov A., Khetselius O., Bunyakova Yu., Prepelitsa G., Solyanikova E., Serga E. Non-linear prediction method in short-range forecast of atmospheric pollutants: low-dimensional chaos. In: *Dynamical Systems - Theory and Applications*. Lodz Univ. **2011**, LIF111
24. Glushkov A., Khetselius O., Kuzakon V., Prepelitsa G., Solyanikova E., Svinarenko A. Modeling of interaction of the non-linear vibrational systems on the basis of temporal series analyses (application to semiconductor quantum generators*). Dynamical Systems - Theory and Applications*. Lodz. **2011**, BIF110.
25. Glushkov, A.V., Khetselius, O.Yu., Svinarenko, A., Buyadzhi, V. *Methods of computational mathematics and mathematical physics. P.1*. Odessa: **2015**.
26. Ignatenko A., Buyadzhi A., Buyadzhi V., Kuznetsova, A.A., Mashkantsev, A.A., Ternovsky E. Nonlinear chaotic dynamics of quantum systems: molecules in an electromagnetic field. *Adv. Quant Chem.* **2019**, *78*, 149-170.
27. Mashkantsev, A. A. ; Ignatenko, A.V. ; Kirianov, S.V. ; Pavlov, E.V. Chaotic dynamics of diatomic molecules in an electromagneic field**.** *Photoelectronics.* **2018,** *27*, 103-112**.**

PACS 33.20.-t

Bakunina E.V., Dykyi O.V.

SIGNAL PROCESSING AND CYBERSECURITY IN SOME CHAOTIC OPTICAL COMMUNICTAION SYSTEMS

Summary. A chaos –geometric approach to investigation of complex chaotic dynamical systems is applied to an analysis, modeling and processing the time series of emission intensities of chaotic transmitter/receiver systems (two unidirectionally coupled semiconductor laser systems in the all-optical scheme) suited for encoding at rates of GBit/s. The problem of a signal processing is directly connected with the corresponding cybersecurity in some optical chaos communictaion systems. The estimated values for the dynamic and topologic invariants such as the correlation and Kaplan-York dimensions, Lyapunov indicators, Kolmogorov entropy etc for investigated chaotic signal time series of two unidirectionally coupled semiconductor laser systems in the all-optical scheme.

Key words: complex chaotic dynamical systems, signal processing and cybersecurity

PACS 33.20.-t

Бакунина Е.В., О.В. Дикий

ОБРАБОТКА СИГНАЛОВ И КИБЕРБЕЗОПАСНОСТЬ В НЕКОТОРЫХ ХАОТИЧЕСКИХ ОПТИЧЕСКИХ СИСТЕМАХ КОММУНИКАЦИИ

Резюме. Хаос-геометрический подход к исследованию сложных хаотических динамических систем применяется для анализа, моделирования и обработки временных рядов интенсивности излучения хаотических систем передатчика/приемника (две связанные полупроводниковые лазерные системы в полностью оптической схеме), пригодные для кодирования со скоростью порядка Гбит /с. Вопрос обработки и кодирования сигналов непосредственно связано с соответствующим вопросом кибербезопасности в соответствующих хаотических оптических системах связи. Выполнен расчет значений динамических и топологических инвариантов, таких как корреляционная размерность, размерность Каплана-Йорка, показатели Ляпунова, энтропия Колмогорова и др., для изучаемых временных рядов хаотического сигнала двух связанных полупроводниковых лазерных систем в общей оптической схеме.

Ключевые слова: сложные хаотические динамические системы, связанные полупроводниковые лазерные системы, обработка сигналов и кибербезопасность

PACS 33.20.-t

Бакуніна Є.В., О.В. Дікий

ОБРОБКА СИГНАЛІВ І КІБЕРБЕЗПЕКИ В ДЕЯКИХ ХАОТИЧНИХ ОПТИЧНИХ СИСТЕМАХ КОМУНІКАЦІЇ

Резюме. Хаос-геометричний підхід до дослідження складних хаотичних динамічних систем застосовується для аналізу, моделювання та обробки часових рядів інтенсивності випромінювання хаотичних систем передавача / приймача (дві пов'язані напівпровідникові лазерні системи в повністю оптичній схемі), придатні для кодування зі швидкістю Гбіт / с. Питання обробки та кодування сигналів безпосередньо пов'язане із відповідним питанням кібербезпеки у відповідних хаотичних оптичних системах зв'язку. Виконаний розрахунок значень динамічних та топологічних інваріантів, таких як кореляційна розмірність, розмірність Каплана-Йорка, показники Ляпунова, ентропія Колмогорова та ін., для вивчаємих часових рядів хаотичного сигналу двох пов'язаних напівпровідникових лазерних систем у загальнооптичній схемі.

Ключові слова: складні хаотичні динамічні системи, пов'язані напівпровідникові лазерні системи, обробка сигналів та кібербезпека.

PACS 31.30.Gs

Makushkina M. P., Antoshkina O. A., Khetselius O. Yu.

Odesa State Environmental University, L'vovskaya str.15, Odesa-9, 65016, Ukraine
E-mail: nuclei08@gmail.com

HYPERFINE STRUCTURE PARAMETERS FOR COMPLEX ATOMS WITHIN RELATIVISTIC MANY-BODY PERTURBATION THEORY

Abstract. The calculational results for the hyperfine structure (HFS) parameters for the Mn atom (levels of the configuration $3d^6 4s$) and the results of advanced calculating the HFS constants and nuclear quadrupole moment for the radium isotope $^{223}_{88}Ra$ are obtained on the basis of computing within the relativistic many-body perturbation theory formalism with a correct and effective taking into account the exchange-correlation, relativistic, nuclear and radiative corrections. Analysis of the data shows that an account of the interelectron correlation effects is crucial in the calculation of the hyperfine structure parameters. The fundamental reason of physically reasonable agreement between theory and experiment is connected with the correct taking into account the inter-electron correlation effects, nuclear (due to the finite size of a nucleus), relativistic and radiative corrections. The key difference between the results of the relativistic Hartree-Fock Dirac-Fock and many-body perturbation theory methods calculations is explained by using the different schemes of taking into account the inter-electron correlations as well as nuclear and radiative ones.

1. Introduction

The study of the parameters of the hyperfine structure (HFS) and the characteristics associated with it is of great importance for modeling the properties of nuclei, the search for superdense nuclei, and a number of other problems in nuclear physics. Nuclear size effects in the energy structure of the states of the electron shell of a heavy atom are essentially used in physical research and for technological purposes. The scheme for measuring isotopic shifts of atomic levels based on the method of laser photoionization has become classical, in particular, for Hg isotopes (A = 193-201), this method has been used to measure the root-mean-square radii of the charge distribution in the nucleus and the total moments. Such information can, in principle, be used to simulate intranuclear forces.

In connection with the foregoing, interest has sharply increased in the corresponding theoretical calculations of the HFS characteristics of the spectra of heavy atoms and ions with allowance for relativistic, correlation, and nuclear effects and, of course, in testing new effects predicted on the basis of quantum electrodynamics (QED). It is known that QED corrections (vacuum polarization, self-energy contribution) to the energies of transitions with the participation of K and L-electrons, as well as the effects of the finiteness of the nucleus at large nuclear charges Z> 60, are on the order of the binding energy of valence electrons. Taking them into account is fundamental for determining the energetically allowed channels of decay of states with vacancies and predicting the complete kinetics of decay.

The multi-configuration relativistic Hartree-Fock (RHF), Dirac-Fock (DF), multi-configuration DF (MCDF) approaches (see, for example, refs. [1-33]) are the most reliable versions of calculation for multi-electron systems with a large nuclear charge.

In this paper we present the calculational results for the HFS structure parameters for the Mn atom (levels of the configuration $3d^6 4s$) and the results of advanced calculating the HFS constants and nuclear quadrupole moment for the radium isotope $^{223}_{88}Ra$, using the optimized method of the relativistic many-body perturbation theory with the Dirac-Kohn-Sham zeroth approximation and a correct and effective taking into account the exchange-correlation, relativistic, nuclear and radiative corrections [9-30]. Analysis of the data shows that an account of the cited cor-

rections is crucial in the calculation of the hyperfine structure parameters.

2. Relativistic method to computing hyperfine structure parameters of atoms and ions

Let us describe the key moments of the approach **(**more details can be found in refs. [19-30]). The electron wave functions (the PT zeroth basis) are found from solution of the relativistic Dirac equation with potential, which includes ab initio mean-field potential, electric, polarization potentials of a nucleus. The charge distribution in the Li-like ion is modelled within the Gauss model. The nuclear model used for the Cs isotope is the independent particle model with the Woods-Saxon and spin-orbit potentials (see refa. [20]). Let us consider in details more simple case of the Li-like ion. We set the charge distribution in the Li-like ion nucleus $\rho(r)$ by the Gaussian function:

$$\rho(r|R) = \left(4\gamma^{3/2}/\sqrt{\pi}\right)\exp\left(-\gamma r^2\right) \qquad (1)$$

where $\gamma=4/\pi R^2$ and R is the effective nucleus radius. The Coulomb potential for the spherically symmetric density $\rho(r)$ is:

$$V_{nucl}(r|R) = -\left((1/r)\int_0^r dr' r'^2 \rho\left(r'\middle|R\right) + \int_r^\infty dr' r' \rho\left(r'\middle|R\right)\right) \qquad (2)$$

Consider the DF type equations. Formally they fall into one-electron Dirac equations for the orbitals with the potential $V(r|R)$ which includes the electrical and the polarization potentials of the nucleus; the components of the Hartree potential (in the Coulomb units):

$$V(r|i) = \frac{1}{Z}\int d\vec{r}'\rho(r|i)/|\vec{r}-\vec{r}'| \qquad (4)$$

Here $\rho(r|i)$ is the distribution of the electron density in the state $|i>$, V_{ex} is the exchange inter-electron interaction. The main exchange and correlation effects will be taken into account in the first two orders of the PT by the total inter-electron interaction [21,22].

A procedure of taking into account the radiative QED corrections is in details given in the refs. [19,20].

Regarding the vacuum polarization effect let us note that this effect is usually taken into consideration in the first PT theory order by means of the Uehling-Serber potential. This potential is usually written as follows:

$$U(r) = -\frac{2\alpha}{3\pi r}\int_1^\infty dt \exp(-2rt/\alpha Z)\left(1+1/2t^2\right)\frac{\sqrt{t^2-1}}{t^2} \equiv$$

$$= -\frac{2\alpha}{3\pi r}C(g), \qquad (5)$$

where $g=r/(\alpha Z)$. In our calculation we use more exact approach [20]. The Uehling potential, determined as a quadrature (5), may be approximated with high precision by a simple analytical function. The use of new approximation of the Uehling potential permits one to decrease the calculation errors for this term down to 0.5 – 1%.

A method for calculation of the self-energy part of the Lamb shift is based on the methods [19-24]. The radiative shift and the relativistic part of energy in an atomic system are, in principle, defined by one and the same physical field. One could suppose that there exists some universal function that connects the self-energy correction and the relativistic energy.

Its form and properties are in details analyzed in Refs.[19-24,30-35]. Unlike usual purely electronic atoms, the Lamb shift self-energy part in the case of a pionic atom is not significant and much inferior to the main vacuum-polarization effect.

The energies of electric quadruple and magnetic dipole interactions are defined by a standard way with the hyperfine structure constants, usually expressed through the standard radial integrals:

$$A=\{[(4,32587)10^{-4}Z^2\chi g_I]/(4\chi^2-1)\}(RA)_{-2},$$

$$B=\{7.2878\ 10^{-7}\ Z^3Q/[(4\chi^2-1)I(I-1)\}\ (RA)_{-3}, \qquad (7)$$

Here g_I is the Lande factor, Q is a quadruple momentum of nucleus (in Barn); $(RA)_{-2}$, $(RA)_{-3}$ are the radial integrals usually defined as follows:

$$(RA)_{-2} = \int_0^\infty dr r^2 F(r)G(r)U(1/r^2, R),$$

$$(RA)_{-3} = \int_0^\infty dr r^2 [F^2(r) + G^2(r)U(1/r^2, R) \cdot \quad (8)$$

The radial parts F and G of the Dirac function two components for electron, which moves in the potential $V(r,R)+U(r,R)$, are determined by solution of the Dirac equations. The key elements of the numerical approach to computing the corresponding matrix elements are presented in [31-44]. All calculations are performed on the basis of the numeral code Superatom-ISAN (version 93).

3. Results and Conclusions

In this subsection we go on the presentation of the experimental data and the results of the calculation of the HFS parameters for the Mn element. Let us remind that Mn has one stable isotope with a mass number of 55, a nuclear spin of 5/2, a magnetic dipole moment of 3.46871668 $\mu_я$ and an electric quadrupole moment of Q = 0.33 (1) barn. Basic electronic configuration: $3d^5 4s^2$ ($^6S_{5/2}$). Given the complexity of the spectrum, theoretical study of the HFS should be based on a full multi-electron calculation. An useful review and detailed analysis of the studies of the HFS of the Mn atom was given, for example, in [6].

In table 1 we present the available experimental (A_{exp}, B_{exp}) and theoretical (our calculation) values of the energy levels and the HFS parameters for the Mn levels of the configuration $3d^6 4s$. Earlier [37] we have presented the analogous data for the levels of configuration $3d^5 4s^2$,3d64s. The reasonable agreement between theoretical and measured data can be reached by way of using the optimized wave functions basises and complete, correct accounting for the exchange-correlation corrections.

Table 1. Experimental (A_{exp}, E_{exp}) and theoretical values of the energies of the levels (cm^{-1}) and HFS constants (MHz) (see text) for the levels of the configuration $3d^6 4s$.

Level	Term	E_{exp}	E_{th}
$3d^6 4s$	$a^4F_{9/2}$	34938.7	34882
$3d^6 4s$	$a^4F_{7/2}$	35041.4	34977
$3d^6 4s$	$a^4F_{5/2}$	35115.0	35042
$3d^6 4s$	$a^4D_{7/2}$	-	23208
$3d^6 4s$	$a^4D_{5/2}$	-	23473
Level	Term	A_{exp}	A_{th}
$3d^6 4s$	$a^4F_{9/2}$	649(7)	646
		643(4)	646
$3d^6 4s$	$a^4F_{7/2}$	588(5)	580
		576(12)	580
$3d^6 4s$	$a^4F_{5/2}$	437(3)	436
		440(5)	436
$3d^6 4s$	$a^4D_{7/2}$	171(15)	170
$3d^6 4s$	$a^4D_{5/2}$	-	136
Level	Term	B_{exp}	B_{th}
$3d^6 4s$	$a^4F_{9/2}$	200	198
$3d^6 4s$	$a^4F_{7/2}$	150	149
$3d^6 4s$	$a^4F_{5/2}$	-	21

Further we present experimental data and the results of advanced calculating the HFS constants and nuclear quadrupole moment for the radium isotope $^{223}_{88}Ra$. The mercury atom has an external valet configuration $7s^2$ and is considered by us as a two-quasiparticle system.

Table 2 shows the experimental and calculated data on the HTS magnetic dipole constant A (MHz) for the7s7p $^1P_1$, $^3P_1$, $^3P_2$ states of the atom $^{223}_{88}Ra$. The data of calculations within the framework of the standard uncorrelated DF method, MCDF taking into account the Breit and standard QED corrections, the relativistic method of configuration interaction taking into account the correlation corrections in the framework of the random phase approximation (RCI-RPA) [6], as well as our QED approach (Gaussian model for charge distribution in the nucleus) [8,33,35].

Table 2. The experimental and calculated data on the HTS magnetic dipole constant A (MHz) for the7s7p $^1P_1$, $^3P_1$, $^3P_2$ states of the atom $^{223}_{88}Ra$ (see text).

Method/ State	$^1P_1$	$^3P_1$	$^3P_2$
DF	-226.59	803.97	567.22
MCDF (Breit+QED)	-330.3	1251.9	737.1
RCI-RPA	-242.4	-	-
RMBPT	-339.1	1209	704.5
This work	-340.4	1207.4	703.9
Experiment	-344.5 (0.9)	1201.1 (0.6)	699.6 (3.3)

In Table 3 we present the measured values of the nuclear quadrupole moment Q (in barns) for the isotope obtained experimentally by the ISOLDE Collaboration (CERN) group based on various techniques (see [6]). In addition, this table presents the calculated values, obtained on the basis of calculations within the framework of the MCDF method (taking into account the Breit and QED corrections), relativistic many-particle PT (RMBPT) and our approach (Refs. [1-6]).

Table 3. The values of electric quadrupole moment Q (mb) for isotope of $^{223}_{88}Ra$

Method	*Q* (mb)
MCDF (Breit+QED)	1.21 (0.03)
ISOLDE Collaboration fs RaII	1.254 (0.003) [0.066]
Wendt et al, fs RaI	1.19 (0.12)
RMBPT	1.28
ISOLDE Collaboration fs RaI	1.190 (0.007) [0.126]
ISOLDE Collaboration B(E2)	1.20
This work	1.225 (0.005)

It is important to note that the key quantitative factor of the agreement between theory and experiment is associated with correct accounting for electron-electron correlations, correction for the finite size of the nucleus, taking into account Breit and QED radiation effects. Analysis shows that the contribution due to electron-electron correlations to the HFS constants is ~ 100-500 MHz for various states. This circumstance explains the low degree of consistency in the accuracy of the data presented, obtained within the framework of various versions of the DF method. The contributions of higher-order corrections to the QED TV and corrections for the finite size of the nucleus can reach 1–2 tens of MHz, and it seems important to take them into account more correctly. In addition, it is necessary to take into account the nuclear polarization contributions directly, which can be done within the framework of solving the corresponding nuclear problem, for example, using the shell model with Woods-Saxon and spin-orbit potentials. Such an approach is outlined in [34, 35]. The key difference between the results of calculations within the different theoretical schemes is associated with different methods of accounting for electron-electron correlations.

References

1. Grant I. *Relativistic Quantum Theory of Atoms and Molecules*. Oxford, **2007**.
2. Glushkov, A; Khetselius, O; Svinarenko, A; Buyadzhi, V. *Spectroscopy of autoionization states of heavy atoms and multiply charged ions*. Odessa: **2015**.
3. Khetselius, O.Yu. *Hyperfine structure of atomic spectra*. Astroprint: **2008**.
4. Pyykko, P. Year2008 nuclear quadrupole moments. *Mol. Phys.* **2008,** *106*, 16.
5. Bieron J., Pyykkő P., Jonsson P. Nuclear quadrupole moment of ^{201}Hg. Phys.Rev. A. **2005**, *71*, 012502.
6. Basar Gu., Basar Go., Acar G., Ozturk I.K., Kroger S. Hyperfine structure investigations of MnI: Experimental and theoretical studies of the hyperfine structure in the even configurations. Phys.Scr. **2003**, *67*, 476-484.
7. Gubanova E., Glushkov A., Khetselius O., Bunyakova Yu., Buyadzhi V.,

Pavlenko E. New methods in analysis and project management of environmental activity: Electronic and radioactive waste. FOP: Kharkiv, **2017.**
8. Florko, T.A.; Tkach, T.B.; Ambrosov, S.V.; Svinarenko, A.A. Collisional shift of the heavy atoms hyperfine lines in an atmosphere of the inert gas. *J. Phys.: Conf. Ser*. **2012**, *397*, 012037.
9. Khetselius, O.Yu., Lopatkin Yu.M., Dubrovskaya, Yu.V, Svinarenko A.A. Sensing hyperfine-structure, electroweak interaction and parity non-conservation effect in heavy atoms and nuclei: New nuclear-QED approach. *Sensor Electr. and Microsyst. Techn*. 2010, 7(2), 11-19
10. Glushkov, A.V. *Relativistic Quantum theory. Quantum mechanics of atomic systems*. Astroprint: Odessa, **2008**.
11. Khetselius, O.Yu. Atomic parity non-conservation effect in heavy atoms and observing P and PT violation using NMR shift in a laser beam: To precise theory. *J. Phys.: Conf. Ser.* **2009,** *194*, 022009
12. Khetselius, O.Yu. Hyperfine structure of radium. *Photoelectronics*. **2005,** *14*, 83.
13. Khetselius, O.. Relativistic perturbation theory calculation of the hyperfine structure parameters for some heavy-element isotopes. *Int. Journ. Quant. Chem.* **2009,** *109*, 3330-3335.
14. Khetselius, O.Yu. Relativistic calculation of the hyperfine structure parameters for heavy elements and laser detection of the heavy isotopes. *Phys.Scripta.* **2009,** *135*, 014023.
15. Khetselius, O.Yu. Relativistic Hyperfine Structure Spectral Lines and Atomic Parity Non-conservation Effect in Heavy Atomic Systems within QED Theory. *AIP Conf. Proc.* **2010,** *1290(1)*, 29-33.
16. Khetselius O.Yu.; Gurnitskaya, E.P. Sensing the hyperfine structure and nuclear quadrupole moment for radium. *Sensor Electr. and Microsyst. Techn.* **2006,** *2*, 25-29.
17. Khetselius, O.Yu.; Gurnitskaya, E.P. Sensing the electric and magnetic moments of a nucleus in the N-like ion of Bi. *Sensor Electr. and Microsyst. Techn.* **2006,** *3*, 35-39.
18. Khetselius, O.Yu. Relativistic calculating the spectral lines hyperfine structure parameters for heavy ions. *AIP Conf. Proc.* **2008,** *1058*, 363-365.
19. Khetselius, O.Yu. *Quantum structure of electroweak interaction in heavy finite Fermi-systems.* Astroprint: Odessa, **2011**.
20. Glushkov, A., Gurskaya, M., Ignatenko, A., Smirnov, A., Serga, I., Svinarenko, A., Ternovsky, E. Computational code in atomic and nuclear quantum optics: Advanced computing multiphoton resonance parameters for atoms in a strong laser field. *J. Phys.: Conf. Ser*. **2017**, *905*(1), 012004.
21. Ambrosov S., Ignatenko V., Korchevsky D., Kozlovskaya V. Sensing stochasticity of atomic systems in crossed electric and magnetic fields by analysis of level statistics for continuous energy spectra. *Sensor Electr. and Microsyst. Techn*. **2005**, Issue 2, 19-23.
22. Glushkov, A.V., Ivanov, L.N. Radiation decay of atomic states: atomic residue polarization and gauge noninvariant contributions. *Phys. Lett. A* **1992,** *170*, 33.
23. Glushkov, A.V.; Ivanov, L.N. DC strong-field Stark effect: consistent quantum-mechanical approach. *J. Phys. B: At. Mol. Opt. Phys.* **1993,** *26*, L379-386.
24. Ivanova, E., Glushkov, A. Theoretical investigation of spectra of multicharged ions of F-like and Ne-like isoelectronic sequences. J. Quant. Spectr. and Rad. Tr. **1986**, *36*(2), 127-145.
25. Ivanova, E.P., Ivanov, L.N., Glushkov, A., Kramida, A. High order corrections in the relativistic perturbation theory with the model zeroth approximation, Mg-Like and Ne-Like Ions. *Phys. Scripta* **1985**, *32*, 513-522.
26. Glushkov, A.V. *Relativistic and correlation effects in spectra of atomic systems*. Astroprint, Odessa, **2006.**.
27. Glushkov, A.V. Multiphoton spectroscopy of atoms and nuclei in a laser field: Relativistic energy approach and radiation atomic lines moments method. *Adv. in Quantum Chem.* **2019**, *78*, 253-285.
28. Chernyakova, Y.G., Ignatenko A.V., Vitavetskaya L.A., Sensing the tokamak plasma parameters by means high resolution x-ray theoretical spectroscopy meth-

od: new scheme. *Sensor Electr. and Microsyst. Techn*. **2004**, *1*, 20-24.
29. Svinarenko, A.A. Study of spectra for lanthanides atoms with relativistic many-body perturbation theory: Rydberg resonances. *J. Phys.: Conf. Ser.* **2014,** *548*, 012039.
30. Svinarenko, A. A., Glushkov, A. V., Khetselius, O.Yu., Ternovsky,V.B., Dubrovskaya, Yu., Kuznetsova, A., Buyadzhi, V. Theoretical spectroscopy of rare-earth elements: spectra and autoionization resonances. *Rare Earth Element*, Ed. J. Orjuela (InTech) **2017**, pp 83-104.
31. Khetselius, O.Yu. Optimized relativistic many-body perturbation theory calculation of wavelengths and oscillator strengths for Li-like multicharged ions. Adv. Quant. Chem. **2019**, *78*, 223-251.
32. Khetselius, O. Optimized perturbation theory for calculating the hyperfine line shift and broadening of heavy atoms in a buffer gas. *In Frontiers in Quantum Methods and Applications in Chemistry and Physics*, Springer: Cham, **2015;** Vol. 29, pp. 55-76
33. Glushkov, A.V., Khetselius, O.Yu., Svinarenko A.A., Buyadzhi, V.V., Ternovsky, V.B, Kuznetsova, A., Bashkarev, P Relativistic perturbation theory formalism to computing spectra and radiation characteristics: application to heavy element. *Recent Studies in Perturbation Theory*, ed. D. Uzunov (InTech) **2017**, 131-150.
34. Glushkov A., Lovett L., Khetselius O., Gurnitskaya E., Dubrovskaya Y., Loboda A. Generalized multiconfiguration model of decay of multipole giant resonances applied to analysis of reaction (μ-n) on the nucleus ^{40}Ca. *Int. J. Mod. Phys. A*. **2009**, *24*(2-3), 611-615
35. Dubrovskaya, Yu., Khetselius, O.Yu., Vitavetskaya, L., Ternovsky, V., Serga, I. Quantum chemistry and spectroscopy of pionic atomic systems with accounting for relativistic, radiative, and strong interaction effects. *Adv. in Quantum Chem*. **2019,** Vol.78, pp 193-222.
36. Bystryantseva A., Khetselius O.Yu., Dubrovskaya Yu., Vitavetskaya L.A., Berestenko A.G. Relativistic theory of spectra of heavy pionic atomic systems with account of strong pion-nuclear interaction effects: ^{93}Nb, ^{173}Yb, ^{181}Ta , ^{197}Au. *Photoelectronics*. **2016**, *25*, 56-61.
37. Khetselius, O., Glushkov, A., Gurskaya M., Kuznetsova, A., Dubrovskaya, Yu., Serga I., Vitavetskaya, L. Computational modelling parity nonconservation and electroweak interaction effects in heavy atomic systems within the nuclear-relativistic many-body perturbation theory. *J. Phys.: Conf. Ser*. ***2017,*** *905*(1), 012029.
38. Khetselius, O.Yu., Glushkov, A.V., Dubrovskaya, Yu.V., Chernyakova, Yu., Ignatenko, A.V., Serga, I., Vitavetskaya, L. Relativistic quantum chemistry and spectroscopy of exotic atomic systems with accounting for strong interaction effects. In: Concepts, *Methods and Applications of Quantum Systems in Chemistry and Physics*. Springer, Cham, **2018,** *31*, 71-91.
39. Svinarenko A., Khetselius O., Buyadzhi V., Florko T., Zaichko P., Ponomarenko E. Spectroscopy of Rydberg atoms in a Black-body radiation field: Relativistic theory of excitation and ionization. *J. Phys.: Conf. Ser*. **2014**, *548*, 012048.
40. Svinarenko, A.; Ignatenko, A.; Ternovsky, V.B.; Nikola, L.; Seredenko, S.S.; Tkach, T.B. Advanced relativistic model potential approach to calculation of radiation transition parameters in spectra of multicharged ions. *J. Phys.: Conf. Ser*. **2014,** *548*, 012047.
41. Glushkov A Spectroscopy of cooperative muon-gamma-nuclear processes: Energy and spectral parameters *J. Phys.: Conf. Ser*. **2012,** *397*, 012011.
42. Glushkov, A.V. Spectroscopy of atom and nucleus in a strong laser field: Stark effect and multiphoton resonances. *J. Phys.: Conf. Ser*. **2014**, *548*, 012020
43. Glushkov A.V.; Ivanov, L.N. DC strong-field Stark effect: consistent quantum-mechanical approach. *J. Phys. B: At. Mol. Opt. Phys.* **1993,** *26*, L379-386.
44. Glushkov A.V., Khetselius O.Yu., Svinarenko A.A., Buyadzhi V.V., *Methods of computational mathematics and mathematical physics*. *P.1*. TES: Odessa, **2015**.

PACS 31.30.Gs

Makushkina M.P., Antoshkina O.A., Khetselius O.Yu.

HYPERFINE STRUCTURE PARAMETERS FOR COMPLEX ATOMS WITHIN RELATIVISTIC MANY-BODY PERTURBATION THEORY

Summary. The calculational results for the hyperfine structure (HFS) parameters for the Mn atom (levels of the configuration $3d^6 4s$) and the results of advanced calculating the HFS constants and nuclear quadrupole moment for the radium isotope ${}^{223}_{88}Ra$ are obtained on the basis of computing within the relativistic many-body perturbation theory formalism with a correct and effective taking into account the exchange-correlation, relativistic, nuclear and radiative corrections. Analysis of the data shows that an account of the interelectron correlation effects is crucial in the calculation of the hyperfine structure parameters. The fundamental reason of physically reasonable agreement between theory and experiment is connected with the correct taking into account the inter-electron correlation effects, nuclear (due to the finite size of a nucleus), relativistic and radiative corrections. The key difference between the results of the relativistic Hartree-Fock Dirac-Fock and many-body perturbation theory methods calculations is explained by using the different schemes of taking into account the interelectron correlations as well as nuclear and radiative ones.

Keywords: Hyperfine structure, Heavy atoms, Relativistic perturbation theory, correlation, nuclear, radiative corrections

PACS 31.30.Gs

Макушкина М.П., Антошкина О.А., Хецелиус О.Ю.

ПАРАМЕТРЫ СВЕРХТОНКОЙ СТРУКТУРЫ СЛОЖНЫХ АТОМОВ В РАМКАХ РЕЛЯТИВИСТСКОЙ МНОГОЧАСТИЧНОЙ ТЕОРИИ ВОЗМУЩЕНИЙ

Резюме. Представлены результаты расчетов параметров сверхтонкой структуры (СТС) атома Mn (уровни конфигурации $3d^6 4s$) и результаты уточненного вычисления а констант СТС и квадрупольного момента ядра для изотопа радия ${}^{223}_{88}Ra$ на основе релятивистской многочастичной теории возмущений с эффективным аккуратным учетом обменно-корреляционных, релятивистских, ядерных и радиационных поправок. Анализ данных показывает, что учет эффектов межэлектронной корреляции имеет критическое значение при вычислении параметров сверхтонкой структуры. Физически разумное согласие теории и прецизионного эксперимента может быть обеспечено благодаря полному последовательному учету межэлектронных корреляционных эффектов, ядерных, релятивистских и радиационных поправок. Ключевое различие между результатами расчетов в приближениях Дирака-Фока, различных версиях формализма теории возмущений в основном связано с использованием различных схем учета межэлектронных корреляций, а также учета ядерных и радиационных поправок.

Ключевые слова: Сверхтонкая структура, тяжелый атом, релятивистская теория возмущений, корреляционные, ядерные, радиационные поправки

Макушкіна М.П., Антошкіна О.О., Хецеліус О.Ю.

ПАРАМЕТРИ НАДТОНКОЇ СТРУКТУРИ СКЛАДНИХ АТОМІВ В РАМКАХ РЕЛЯТИВІСТСЬКОЇ БАГАТОЧАСТИНКОВОЇ ТЕОРІЇ ЗБУРЕНЬ

Резюме. Представлені результати розрахунків параметрів надтонкої структури (НТС) атома Mn (рівні конфігурації $3d^6 4s$) і результати уточненого обчислення a констант НТС і квадрупольного моменту ядра для ізотопу радію $^{223}_{88}Ra$ на основі релятивістської багаточастинкової теорії збурень з ефективним акуратним урахуванням обмінно-кореляційних, релятивістських, ядерних і радіаційних поправок. Аналіз даних показує, що урахування ефектів міжелектронної кореляції має критичне значення при обчисленні параметрів надтонкої структури. Фізично розумне узгодження теорії і прецизійного експерименту може бути забезпечено завдяки повному послідовному обліку міжелектронних кореляційних ефектів, ядерних, релятивістських та радіаційних поправок. Ключова відмінність між результатами розрахунків в наближеннях Дірака-Фока, різних версіях формалізму теорії збурень в основному пов'язано з використанням різних схем обліку міжелектронних кореляцій, а також врахування ядерних і радіаційних поправок.

Ключові слова: Надтонка структура, важкий атом, релятивістська теорія збурень, кореляційні, ядерні, радіаційні поправки

PACS 31.15.-p

Ternovsky E. V., Mykhailov A. L.

Odesa State Environmental University, 15, Lvovskaya str., Odesa-16, 65016, Ukraine
E-mail: ternovskyev@gmail.com

NEW RELATIVISTIC APPROACH TO COMPUTING SPECTRAL PARAMETERS OF MULTICHARGED IONS IN PLASMAS

It is presented a new relativistic approach to computing the spectral parameters of multicharged ions in plasmas for different values of the plasmas screening (Debye) parameter (respectively, electron density, temperature). The approach used is based on the generalized relativistic energy approach combined with the optimized relativistic many-body perturbation theory (RMBPT) with the Dirac-Debye shielding model as zeroth approximation, adapted for application to study the spectral parameters of ions in plasmas. An electronic Hamiltonian for N-electron ion in plasmas is added by the Yukawa-type electron-electron and nuclear interaction potential. The special exchange potential as well as the electron density with dependence upon the temperature are used.

1. Introduction

An accurate data about spectra, radiative decay widths and probabilities, oscillator strengths, electron-collision strengths, collisional excitation and de-excitation rates for atoms and especially ions are of a great interest for different applications, namely, astrophysical analysis, laboratory, thermonuclear plasma diagnostics, fusion research, laser physics etc [1–44]. It is also very important for studying energy, spectral and radiative characteristics of a laser-produced hot and dense plasmas [1,2,9, 10].

Above other stimulating factors to studying electron-collisional spectroscopy of ions one should mention the X-ray laser problem, which has stimulated a great number of papers, devoted to modelling the elementary processes in laser, collisionally pumped plasma (see [1,2] and Refs. therein) and construction of the first VUV and X-ray lasers with using plasma of Li-, Ne-like ions as an active medium. Very useful data on the X-lasers problem are firstly received and collected in the papers by Ivanova et al (see [2] and Refs. therein]. From the other side, studying spectra of ions in plasmas remains very actual in order to understand the plasma processes themselves. In most plasma environments the properties are determined by the electrons and the ions, and the interactions between them. The electron-ion collisions play a major role in the energy balance of plasmas. For this reason, modelers and diagnosticians require absolute cross sections for these processes. Cross sections for electron-impact excitation of ions are needed to interpret spectroscopic measurements and for simulations of plasmas using collisional-radiative models. At present time a considerable interest has been encapsulated to studying elementary atomic processes in plasma environments (for example, see [1,9-18] and Refs. therein) because of the plasma screening effect on the plasma-embedded atomic systems. In many papers the calculations of various atomic and ionic systems embedded in Debye plasmas have been performed [1,9-15]). Different theoretical methods have been employed along with the Debye screening to study plasma environments. Calculation of emission spectra of the plasma ions based in the precise theoretical techniques is practical tool, which may be used instead of very expensive sophisticated experiments. Nevertheless, there are known principal theoretical problems to be solved in order to receive the correct description of the elementary atomic processes in laser, collisionally pumped plasma. First of all, speech is about development of the advanced quantum-mechanical models for the further accurate computing oscillator strengths, electron-collisional strengths and rate coefficients for atomic ions in plasmas, including the Debye plasmas. As usually, a correct accounting for the relativ-

istic, exchange-correlation, plasma environment effects is of a great importance. To say strictly, solving of the whole problem requires a development of the quantum-electrodynamical approach as the most consistent one to problem of the Coulomb many-body system.

In this paper, which goes on our work [15-20], we present a new relativistic approach to computing the spectral parameters of multicharged ions in plasmas for different values of the plasmas screening (Debye) parameter (respectively, electron density, temperature). The approach used is based on the generalized relativistic energy approach combined with the optimized RMBPT with the Dirac-Debye shielding model as zeroth approximation, adapted for application to study the spectral parameters of ions in plasmas. An electronic Hamiltonian for N-electron ion in plasmas is added by the Yukawa-type electron-electron and nuclear interaction potential. The special exchange potential as well as the electron density with dependence upon the temperature is used.

2. Optimized relativistic perturbation theory formalism for ions in plasmas

Some fundamental aspects of the approach developed were earlier presented (see, for example, Refs. [15-20]). Therefore, below we are limited only by the key and as a rule new points of a theory.

The generalized relativistic energy approach combined with the RMBPT has been in detail described in Refs. [6,24-29]. It generalizes earlier developed energy approach. The key idea is in calculating the energy shifts ΔE of degenerate states that is connected with the secular matrix M diagonalization [6,24,25]. To construct M, one should use the Gell-Mann and Low adiabatic formula for ΔE. The secular matrix elements are already complex in the PT second order. The whole calculation is reduced to calculation and diagonalization of the complex matrix M and definition of matrix of the coefficients with eigen state vectors $B^{IK}_{ie,iv}$ [6,25]. To calculate all necessary matrix elements one must use the bases of the 1QP relativistic functions. Within an energy approach the total energy shift of the state is usually presented as [24]:

$$\Delta E = \mathrm{Re}\Delta E + i\,\Gamma/2 \qquad (1)$$

where Γ is interpreted as the level width and decay (transition) possibility $P = \Gamma$. Let us start our consideration from formulation relativistic many-body PT with the Debye shielding model Dirac Hamiltonian for electron-nuclear and electron-electron systems. Formally, a multielectron atomic systems (multielectron atom or multicharged ion) is described by the relativistic Dirac Hamiltonian (the atomic units are used) as follows:

$$H = \sum_i h(r_i) + \sum_{i>j} V(r_i r_j). \qquad (1)$$

Here, $h(r)$ is one-particle Dirac Hamiltonian for electron in a field of a nucleus and V is potential of the inter-electron interaction. According to Refs. [6] it is useful to determine the interelectron potential with accounting for the retarding effect and magnetic interaction in the lowest order on parameter α^2 (α is the fine structure constant) as follows:

$$V(r_i r_j) = exp(i\omega_{ij} r_{ij}) \cdot \frac{(1 - \alpha_i \alpha_j)}{r_{ij}}, \qquad (2)$$

where ω_{ij} is the transition frequency; α_i ,α_j are the Dirac matrices.

In order to take into account the plasmas environment effects already in the PT zeroth approximation we use the known Yukawa-type potential of the following form:

$$V(r_i, r_j) = (Z_a Z_b/|r_a - r_b|) exp\,(-\mu \cdot |r_a - r_b|) \qquad (3)$$

where r_a, r_b represent respectively the spatial coordinates of particles, say, A and B and Z_a, Z_b denote their charges.

The potential (3) is well known (look , for example, [1,12,15] and Refs there) well known, for example, in the classical Debye-Hückel, theory of plasmas. The plasmas environment effect is modelled by the shielding parameter μ , which describes a shape of the

long-rang potential. The parameter μ is connected with the plasma parameters such as the temperature θ and the charge density n as follows:

$$\mu \sim \sqrt{e^2 n / k_B T} \qquad (4)$$

Here e is the electron charge and k_B is the Boltzman constant. The density n is given as a sum of the electron density N_e and the ion density N_k of the k-th ion species with the nuclear charge q_k : $n = N_e + \sum_k q_k^2 N_k$ .It is very useful to remind the simple estimates for the shielding parameter.

For example, under typical laser plasma conditions of T ~ 1keV and n~ 10^{23} cm^{-3} the parameter μ is of the order of 0,1 in atomic units. By introducing the Yukawa-type electron-nuclear attraction and electron-electron repulsion potentials, the Debye shielding model Dirac Hamiltonian for electron-nuclear and electron-electron subsystems is given in atomic units as follows [15]:

$$H = \sum_i [\alpha cp - \beta mc^2 - Z\exp(-\mu r_i)/r_i] + \\ + \sum_{i>j} \frac{\left(1 - \alpha_i \alpha_j\right)}{r_{ij}} \exp(-\mu r_{ij}) \qquad (5)$$

where c is the velocity of light and Z is a charge of the atomic ion nucleus.

The formalism of the relativistic many-body PT is further constructed in the same way as the PT formalism in Refs. [16-26]. In the PT zeroth approximation one should use a mean-field potential, which includes the Yukawa-type potential (insist of the pure Coulomb one) plus exchange potential and additionally the correlation potential (for example, the Lundqvist-Gunnarson potential with the optimization parameter b can be used) as in Refs. [16-18,23,24]. As alternative one could use an optimized model potential by Ivanova-Ivanov (for Ne-like ions) [6], which is calibrated within the special ab initio procedure within the relativistic energy approach [8,16].

Let us concretize the corresponding mean-field potential. In particular, one of the possible versions U(r) is as follows (sum of the Coulomb or Yukawa-type potential plus exchange potential:

$$U(r) = U_{Coul\text{-}Yukn}(r) + U_{ex}(r), \qquad (6)$$

With the exchange potential as follows:

$$U_{обм}(r) = \\ \frac{4\pi}{T}\rho(r)\left[1 + 6\frac{\rho(r)}{T^{3/2}} + \frac{\pi^4}{3}\left(\frac{\rho(r)}{T^{3/2}}\right)^2\right]^{-1/3}, \qquad (7)$$

where $\rho(r)$ is an electron density.

The electron density can be presented as a sum of the following terms:

$$\rho(r) = \rho_1(r) + \rho_2(r), \qquad (8)$$

$$\rho_1(\mathrm{r}) \sim \sum_{n,l} |\Psi_{nl}(r)|^2 \qquad (9)$$

$$\rho_1(r) = \frac{\sqrt{2}T^{3/2}}{\pi^2}\int \sqrt{y}\left[1 + \exp\left(y - \frac{U(r)}{T} + \eta\right)\right]^{-1} dy, \qquad (10)$$

$$\mathrm{y} > \frac{1}{T}\left(U(r) + E_0\right), \qquad (11)$$

where $\eta = -\frac{\mu}{T}$, $\mu$is a chemical potential and E_0 is a boundary between state of discrete spectrum and continuum.

The averaged numbers of fulfilling electron states can be determined on the basis of the Fermi-Dirac expression:

$$\mathrm{N_{nl}} = 2(2l+1)\left[1 + \exp\left(\frac{1}{T}\left(E_{nl} + \mu\right)\right)\right]^{-1} \qquad (12)$$

In order to determine a chemical potential μ one should use the condition electroneutrality of the atomic corel

The point of accounting for the many-body exchange-correlation corrections within

a presented theory can be treated as in an usual perturbation theory for free multicharged ions. As usually, in the PT second order, there are two kinds of the exchange and correlation diagrams: polarization and ladder ones. The polarization diagrams take into account the quasiparticle interaction through the polarizable core, and the ladder diagrams account for the immediate quasiparticle interaction. An effective procedure of their accounting are in details described in Refs. [6-9,20-24]. The modified PC numerical code 'Superatom" is used in all calculations. Other details can be found in Refs. [15-20,22,23,38].

3. Results and conclusion

In Tables 1 and 2 we list the numerical variations in the lifetimes of the $2p_{1/2}$, $3s_{1/2}$, $3p_{1/2}$, $3d_{3/2}$, and $4s_{1/2}$ states in Ca XVIII for different μ values.

Table 1.
The dependence of the lifetimes (ps) of the $2p_{1/2}$ state in the Ca XVIII spectrum upon the screening parameter μ: RCC - relativistic coupled-cluster (RCC) method [3]; This - this work

μ	$2p_{1/2}$	$2p_{1/2}$
	RCC	This
0.133	741	740
0.667	494	493
1.000	334	333
1.250	242	242
1.429	192	191
0.60	140	139

Table 2.
The dependence of the lifetimes (ps) of the 3lj,4lj states in the Ca XVIII spectrum upon the parameter μ (this work)

μ	$3s_{1/2}$	$3p_{1/2}$	$3d_{3/2}$	$4s_{1/2}$
0.133	1.09	0.45	0.16	1.64
0.667	1.28	0.54	0.88	2.56
1.000	1.55	0.68	0.22	4.83
1.250	1.87	0.86	0.28	12.6
1.429	2.22	1.08	0.35	82.9

The analysis shows that the presented data are in physically reasonable agreement with the NIST experimental data and theoretical results by relativistic coupled-cluster (RCC) method calculation [3]. However, some difference between the corresponding results can be explained by using different relativistic orbital bases and by difference in the model of accounting for the screening effect as well as some numerical differences..

References

1. Yongqiang, Li Y., Wu, J., Hou, Y., Yuan, J. Influence of hot and dense plasmas on energy levels and oscillator strengths of ions: Be-like ions for Z = 26–36, *J. Phys. B: At. Mol. Opt. Phys.* **2008,** *41*, 145002.
2. Saha B., Fritzsche S. Influence of dense plasma on the low-lying transitions in Be-like ions: relativistic multiconfiguration Dirac–Fock calculation. *J. Phys. B: At. Mol. Opt. Phys.* **2007,** *40*, 259-270.
3. Madhulita Das, Sahoo B. K., Sourav Pal. Relativistic spectroscopy of plasma embedded Li-like systems with screening effects in two-body Debye potentials. *J. Phys. B: At. Mol. Opt. Phys.* **2014,** *47*, 175701.
4. Han, Y.-C., Madsen, L.B. Comparison between length and velocity gauges in quantum simulations of high-order harmonic generation *Phys. Rev. A.* **2010**, *81*, 06343.
5. Glushkov, A.V., Khetselius, O.Yu., Svinarenko, A.A., Buyadzhi, V.V., *Spectroscopy of autoionization states of heavy atoms and multiply charged ion*s. TEC: Odessa, **2015**.
6. Ivanov, L.N., Ivanova, E.P., Aglitsky, E. Modern trends in the spectroscopy of multicharged ions. *Phys. Rep.* **1988,** *166.*
7. Bandrauk, A.D., Fillion-Gourdeau, F., Lorin, E. Atoms and molecules in intense laser fields: gauge invariance of theory and models *J. Phys. B: At. Mol. Opt. Phys*. **2013**, *46*, 153001
8. Glushkov, A.V., Malinovskaya, S.V., Prepelitsa, G.P., Ignatenko, V. Manifestation

of the new laser-electron nuclear spectral effects in the thermalized plasma: QED theory of co-operative laser-electron-nuclear processes. *J. Phys.: Conf. Ser.* **2005,** *11,* 199-206.
9. Gubanova, E., Glushkov, A.V., Khetselius, O.Yu., Bunyakova, Yu.Ya., Buyadzhi, V.V., Pavlenko, E.P. New methods in analysis and project management of environmental activity: Electronic and radioactive waste. FOP: Kharkiv, **2017**.
10. Glushkov, A.V., Malinovskaya, S.V., Chernyakova Y.G., Svinarenko, A.A. Co-operative laser-electron-nuclear processes: QED calculation of electron satellites spectra for multi-charged ion in laser field. *I. J. Quant. Ch.* **2004,** *99,* 889.
11. Glushkov, A., Malinovskaya, S., Loboda, A., Shpinareva, I., Gurnitskaya, E., Korchevsky, D. Diagnostics of the collisionally pumped plasma and search of the optimal plasma parameters of x-ray lasing: calculation of electron-collision strengths and rate coefficients for Ne-like plasma. *J. Phys.: Conf. Ser.* **2005,** *11*, 188-198.
12. Glushkov, A., Ambrosov, S., Loboda, A., Gurnitskaya, E., Prepelitsa, G. Consistent QED approach to calculation of electron-collision excitation cross sections and strengths: Ne-like ions. *Int. J. Quant. Chem.* **2005,** *104*, 562-569.
13. Ignatenko, A.V. Probabilities of the radiative transitions between Stark sublevels in spectrum of atom in an DC electric field: New approach. *Photoelectronics,* **2007,** *16*, 71-74.
14. Glushkov, A.V., Ambrosov, S.V., Ignatenko, A. Non-hydrogenic atoms and Wannier-Mott excitons in a DC electric field: Photoionization, Stark effect, Resonances in ionization continuum and stochasticity. *Photoelect.,* **2001,** *10,* 103.
15. Buyadzhi, V., Kuznetsova, A., Buyadzhi, A., Ternovsky, E.V., Tkach, T.B. Advanced quantum approach in radiative and collisional spectroscopy of multicharged ions in plasmas. Adv. in Quant. Chem. (Elsevier). **2019**, *78*, 171-191,
16. Glushkov, A., Buyadzhi, V., Svinarenko, A., Ternovsky, E. Advanced relativistic energy approach in electron-collisional spectroscopy of multicharged ions in plasma. *Concepts, Methods, Applications of Quantum Systems in Chemistry and Physics* (Springer). **2018**, *31*, 55-69.
17. Buyadzhi, V.V., Chernyakova, Yu.G., Smirnov, A.V., Tkach, T.B. Electron-collisional spectroscopy of atoms and ions in plasma: Be-like ions. *Photoelectronics*. **2016,** *25*, 97-101.
18. Buyadzhi, V.V., Chernyakova, Yu.G., Antoshkina, O.A., Tkach, T.B. Spectroscopy of multicharged ions in plasmas: Oscillator strengths of Be-like ion Fe. *Photoelectronics.* **2017,** *26,* 94..
19. Buyadzhi, V. Laser multiphoton spectroscopy of atom embedded in Debye plasmas: multiphoton resonances and transitions. *Photoelectronics.* **2015,** *24,* 128-133.
20. Buyadzhi, V., Zaichko, P., Antoshkina, O., Kulakli T., Prepelitsa P., Ternovsky V., Mansarliysky, V. Computing of radiation parameters for atoms and multicharged ions within relativistic energy approach: Advanced Code. *J. Phys.: Conf. Ser*. **2017**, *905*(1), 012003.
21. Glushkov, A., Svinarenko, A., Ignatenko, A. Spectroscopy of autoionization resonances in spectra of the lanthanides atoms. *Photoelectronics*. **2011**, *20*, 90-94.
22. Glushkov, A.V. *Relativistic Quantum theory. Quantum mechanics of atomic systems;* Astroprint: Odessa, **2008**.
23. Khetselius, O.Yu. *Hyperfine structure of atomic spectra*. Astroprint: Odessa, **2008**.
24. Glushkov, A., Ivanov, L., Ivanova, E.P. Autoionization Phenomena in Atoms. *Moscow Univ. Press*, Moscow, **1986,** 58.
25. Glushkov, A.V., Ivanov, L.N. Radiation decay of atomic states: atomic residue polarization and gauge noninvariant contributions. *Phys. Lett.A.* **1992,** *170*, 33.
26. Glushkov, A.V. Spectroscopy of atom and nucleus in a strong laser field: Stark effect and multiphoton resonances. *J. Phys.: Conf. Ser*. **2014**, *548*, 012020.
27. Glushkov, A., Svinarenko, A., Ternovsky,

V., Smirnov, A., Zaichko, P. Spectroscopy of the complex autoionization resonances in spectrum of helium: Test and new spectral data. *Photoelectr*. **2015**, *24*, 94.
28. Glushkov, A.V., Ivanov, L.N. Radiation decay of atomic states: atomic residue polarization and gauge noninvariant contributions. *Phys. Lett. A* **1992,** *170*, 33.
29. Glushkov, A.V.; Ivanov, L.N. DC strong-field Stark effect: consistent quantum-mechanical approach. *J. Phys. B: At. Mol. Opt. Phys.* **1993,** *26*, L379-386.
30. Ivanova, E., Glushkov, A. Theoretical investigation of spectra of multicharged ions of F-like and Ne-like isoelectronic sequences. J. Quant. Spectr. and Rad. Tr. **1986**, *36*(2), 127-145.
31. Ivanova, E.P., Ivanov, L.N., Glushkov, A., Kramida, A. High order corrections in the relativistic perturbation theory with the model zeroth approximation, Mg-Like and Ne-Like Ions. *Phys. Scripta* **1985**, *32*, 513-522.
32. Glushkov, A.V. *Relativistic and correlation effects in spectra of atomic systems*. Astroprint, Odessa, **2006.**
33. Khetselius, O.Yu. *Quantum structure of electroweak interaction in heavy finite Fermi-systems*. Astroprint: Odessa, **2011**.
34. Khetselius, O.Yu., Lopatkin, Yu.M., Dubrovskaya, Yu.V, Svinarenko, A.A. Sensing hyperfine-structure, electroweak interaction and parity non-conservation effect in heavy atoms and nuclei: New nuclear-QED approach. *Sensor Electr. and Microsyst. Techn*. **2010,** 7(2), 11-19.
35. Khetselius, O.Yu. Relativistic perturbation theory calculation of the hyperfine structure parameters for some heavy-element isotopes. *Int. J. Quant. Chem.* **2009,** *109*, 3330–3335.
36. Khetselius, O. Relativistic calculation of the hyperfine structure parameters for heavy elements and laser detection of heavy isotope. *Phys. Scr.* **2009,** *135*,01402
37. Svinarenko, A.A., Glushkov, A.V., Khetselius, O.Yu., Ternovsky, V.B., Dubrovskaya, Yu., Kuznetsova, A., Buyadzhi, V. Theoretical spectroscopy of rare-earth elements: spectra and autoionization resonances. *Rare Earth Element*, Ed. J.Orjuela (InTech). **2017**, 83.
38. Glushkov, A.V., Khetselius, O.Yu., Svinarenko, A.A., Buyadzhi, V.V., Ternovsky, V.B, Kuznetsova, A., Bashkarev, P Relativistic perturbation theory formalism to computing spectra and radiation characteristics: application to heavy element. *Recent Studies in Perturbation Theory*, InTech. **2017**, 131.
39. Dubrovskaya, Yu., Khetselius, O.Yu., Vitavetskaya, L., Ternovsky, V., Serga, I. Quantum chemistry and spectroscopy of pionic atomic systems with accounting for relativistic, radiative, and strong interaction effects. *Adv. Quantum Chem.* **2019,** *78*, 193-222.
40. Khetselius, O.Yu., Glushkov, A.V., Dubrovskaya, Yu.V., Chernyakova, Yu.G., Ignatenko, A.V., Serga, I.N., Vitavetskaya, L. Relativistic quantum chemistry and spectroscopy of exotic atomic systems with accounting for strong interaction effects. In *Concepts, Methods and Applications of Quantum Systems in Chem. and Phys.* Springer. **2018,** *31*, 71.
41. Glushkov, A., Buyadzhi, V., Kvasikova, A., Ignatenko, A., Kuznetsova, A., Prepelitsa, G., Ternovsky, V. Non-Linear chaotic dynamics of quantum systems: Molecules in an electromagnetic field and laser systems. In: Tadjer A, Pavlov R, Maruani J, Brändas E, Delgado-Barrio G (eds) Quantum Systems in Physics, Chemistry, and Biology. Springer, Cham. **2017**, *30*, 169-180.
42. Glushkov A.V., Khetselius O.Yu., Loboda A.V., Ignatenko A., Svinarenko A., Korchevsky D., Lovett L., QED Approach to Modeling Spectra of the Multicharged Ions in a Plasma: Oscillator and Electron-ion Collision Strengths.. *AIP Conference Proceedings***. 2008**. 1058. 175-177
43. Glushkov, A.V. *Atom in an electromagnetic field*. KNT: Kiev, **2005**.
44. Glushkov, A.V., Khetselius, O.Yu., Svinarenko, A.A., Buyadzhi, V.V., *Methods of computational mathematics and mathematical physics. P.1*.TES: **2015**.

PACS 31.15.-p

Ternovsky E.V., Mykhailov A.L.

NEW RELATIVISTIC APPROACH TO COMPUTING SPECTRAL PARAMETERS OF MULTICHARGED IONS IN PLASMAS

Summary. It is presented a new relativistic approach to computing the spectral parameters of multicharged ions in plasmas for different values of the plasmas screening (Debye) parameter (respectively, electron density, temperature). The approach used is based on the generalized relativistic energy approach combined with the optimized RMBPT with the Dirac-Debye shielding model as zeroth approximation, adapted for application to study the spectral parameters of ions in plasmas. An electronic Hamiltonian for N-electron ion in plasmas is added by the Yukawa-type electron-electron and nuclear interaction potential. The special exchange potential as well as the electron density with dependence upon the temperature are used.

Key words: spectroscopy of ions in plasmas, relativistic energy approach, new relativistic quantum mechanical model

PACS 31.15.-p

Терновский Е.В., Михайлов А.Л.

НОВЫЙ РЕЛЯТИВИСТСКИЙ ПОДХОД К РАСЧЕТУ СПЕКТРАЛЬНЫХ ПАРАМЕТРОВ МНОГОЗАРЯДНЫХ ИОНОВ В ПЛАЗМЕ

Резюме. Представлен новый релятивистский подход к расчету спектральных параметров многозарядных ионов в плазме для различных значений параметра экранирования плазмы (дебаевского) (соответственно электронной плотности, температуры).Подход основан на обобщенном релятивистском энергетическом подходе, совмещенном с формализмом оптимизированной релятивистской многочастичной теории возмущений с приближением Дирака-Дебая в качестве нулевого приближения, адаптированной для применения при изучении спектральных параметров ионов в плазме. Электронный гамильтониан для иона N-электронов в плазме добавляется потенциалом электрон-электронного и ядерного взаимодействия типа Юкавы. Используются специальный обменный потенциал, а также плотность электронов с фиксацией явной зависимости от температуры.

Ключевые слова: спектроскопия ионов в плазме, энергетический подход, новая релятивистская квантово-механическая модель

PACS 31.15.-p

Терновський Є В., Михайлов О.Л.

НОВИЙ РЕЛЯТИВІСТСЬКИЙ ПІДХІД ДО РОЗРАХУНКУ СПЕКТРАЛЬНИХ ПАРАМЕТРІВ БАГАТОЗАРЯДНИХ ІОНІВ В ПЛАЗМІ

Резюме. Представлений новий релятивістський підхід до розрахунку спектральних параметрів багатозарядних іонів в плазмі для різних значень параметра екранування плазми (дебаєвсьного) (відповідно електронної щільності, температури). Підхід ґрунтується на узагальненому релятивістському енергетичному підході, поєднаному з формалізмом оптимізованої релятивістської багаточастинкової теорії збурень з наближенням Дірака-Дебая в якості нульового наближення, адаптованого для застосування при вивченні спектральних параметрів іонів у плазмі. Електронний гамільтоніан для іона N-електронів в плазмі додається потенціалом електрон-електронного та ядерного взаємодії типу Юкави. Використовуються спеціальний обмінний потенціал, а також щільність електронів з фіксацією явної залежності від температури.

Ключові слова: спектроскопія іонів в плазмі, енергетичний підхід, нова релятивістська квантово-механічна модель.

PACS 31.15.A-

Kuznetsova A. A., Glushkov A. V., Plisetskaya E. K.

National University "Odesa Maritime Academy", Didrikhson str. 8, Odesa, Ukraine
Odesa State Environmental University, 15, Lvovskaya str., Odesa-16, 65016, Ukraine
E-mail: kuznetsovaa232@gmail.com

THEORETICAL COMPLEX ENERGIES OF STARK RESONANCES IN LITHIUM BY OPERATOR PERTURBATION THEORY APPROACH

The theoretical complex energies of the Stark resonances in the lithium atom (non-hydrogenic atomic system) in a DC electric are calculated within the operator form of the modified perturbation theory for the non-H atomic systems. The method includes the physically reasonable distorted-waves approximation in the frame of the formally exact quantum-mechanical procedure. The calculated Stark resonances energies and widths in the lithium atom are calculated and compared with results of calculations on the basis of the method of complex eigenvalue Schrödinger equation by Themelis-Nicolaides, the complex absorbing potential method by Sahoo-Ho and the B-spline-based coordinate rotation method approach by Hui-Yan Meng et al.

1. Introduction

The Stark effect is one of the best known problems in quantum mechanics, however at the same time one of the most difficult in a case of the strong field one [1-8]. In the last years it attracts a great interest especially outside the weak-field region that is stimulated by a whole range of interesting phenomena to be studied such as the effects of potential barriers (shape resonances), new kinds of resonances above threshold etc [11-42], the DC strong field effect in the heavy atomic systems etc. The great relevance of the Stark resonances characteristics of the multielectron atoms is usually provided by standard requirements in spectroscopic information of a number of physical applications, which include atomic and molecular optics and spectroscopy, quantum electronics, laser physics, quantum computing, the construction of kinetic models of new laser schemes for short-range, physics and chemistry laboratory, astrophysical plasmas, astrophysics and astronomy etc. An external electric field shifts and broadens the bound state levels of an atomic system. The standard quantum-mechanical procedure relates the complex eigenenergies (EE) $E = E_r + i\Gamma/2$ and complex eigenfunctions (EF) to the shape resonances. The field effects drastically increase upon going from one excited level to another. The highest levels overlap forming a "new continuum" with lowered boundary. The computational difficulties (for example, such as the well-known Dyson phenomenon) inherent to the standard quantum mechanical methods are well known. The well-known Wentzel-Kramers-Brillouin (WKB) approximation overcomes these difficulties for the states lying far from the " new continuum" boundary. Some modifications of the WKB method (see review in Ref. [58]) are introduced in Stebbings and Dunning, Kondratovich and Ostrovsky, Popov et al; Ivanov-Letokhov (e.g. citations in refs. [1-42]) have fulfilled the first estimations of the effectiviness of the selective ionization of the Rydberg atom using a DC electric and laser fields within the quasiclassical model.

Different computational procedures are used in the Pade and then Borel summation of the divergent Rayleigh-Schrödinger perturbation theory (PT) series (Franceschini et al 1985, Popov et al 1990) and in the sufficiently exact numerical solution of the difference equations following from expansion of the wave function over finite basis (Benassi ans Grecchi 1980, Maquet et al 1983, Kolosov 1987, Telnov 1989, Anokhin-Ivanov 1994), complex-coordinate method, quantum defect approximation etc [20-39]. Hehenberger, McIntosh and E. Brändas have applied the Weyl's theory to the Stark effect

in the hydrogen atom. They have shown that one of the interesting features of Weyl's theory is that it requires a complex parameter and complex solutions to the differential equations making it a powerful tool for the treatment of resonance states. Brändas and Froelich have shown that a complex scale transformation of the time–dependent Schrödinger equation leads to a symmetric EE value problem containing both bound states and resonance (complex) EE values as solutions. It is worth to note that application of the complex coordinate method to a resonance problem has been justified in [20-33].

Themelis and Nicolaides [2-4] adopted an ab initio theory to compute the complex energy of multielectron atomic states and applied it to computing the energies and widths of the lithium Stark resonances for weak and strong fields. Their approach is based on the state-specific construction of a non-Hermitian matrix according to the form of the decaying-state EF which emerges from the complex eigenvalue Schrodinger equation (CESE) theory. Jianguo Rao et al and Hui-Yan Meng et al [1] have elaborated the B-spline-based coordinate rotation method plus the model potential approach and applied it to investigate the complex energies of low-lying resonances of the hydrogen and lithium atoms in an electric field. Sahoo and Ho [5] carried out the calculation the Stark resonances energies and widths in the lithium atom on the base of the complex absorbing potential (CAP) method. It should be noted that the authors use a model potential to represent the interaction between the inner core electrons with the outside valence electron. In fact, these methods are based on the single-active-electron (SAE) approximation. In Refs.[56-58] it had been presented a consistent uniform quantum approach to the solution of the non-stationary state problems including the DC (Direct Current) strong-field Stark effect and also scattering problem. It is based on the operator form of the perturbation theory (OPT) for the Schrödinger equation. A model potential to represent the interaction between the inner core electrons with the outside valence electron is also used in application of the OPT method to alkali atoms Stark resonances.

In this work we present an advanced calculational approach to computing the Stark resonances energies and widths for the non-hydrogenic (non-H) atomic systems in a DC electric field. Our method is based on the modified OPT method and includes the physically reasonable distorted-waves approximation in the frame of the formally exact quantum-mechanical procedure. The Stark resonances energies and widths are calculated for the 4f lithium state and compared with the data of calculations on the basis of the alternative sophisticated approaches such as the method of complex eigenvalue Schrödinger equation by Themelis-Nicolaides, the complex absorbing potential method by Sahoo-Ho and the B-spline-based coordinate rotation method by Hui-Yan Meng et al [1-5].

2. Operator perturbation theory for multielectron atoms in an electric field

As the principal ideas of the approach have been presented in Ref. [17,18], here we are limited to some key elements. As usually, we start from the Dirac Hamiltonian (in relativistic units):

$$H = \alpha p + \beta - \alpha Z / r_i + \sqrt{\alpha} \cdot \varepsilon \cdot z \,, \quad \textbf{(1)}$$

Here a field strength intensity ε is expressed in the relativistic units ($\varepsilon_{rel} = \alpha^{5/2}\varepsilon_{\text{at.un.}}$; α is the fine structure constant). One could see that a relativistic wave function in the Hilbert space is a bi-spinor. In order to further diagonalize the Hamiltonian (1), we need to choose the correct basis of relativistic functions, in particular, by choosing the following functions as in Ref, [17-20]. The corresponding matrix elements of the total Hamiltonian will be no-zeroth only between the states with the same M_J. In fact this moment is a single limitation of the whole approach. Transformation of co-ordinates in the Pauli Hamiltonian (in comparison with the Schrodinger equation Hamiltonian it contents additional potential term of a magnetic dipole

in an external field) can be performed by the standard way. However, procedure in this case is significantly simplified. They can be expressed through the set of one-dimensional integrals, described in details in Refs. [17-24]. To simplify the calculational procedure, the uniform electric field ε should be substitute by the function (c.g. [17,22]:

$$\varepsilon(\mathrm{t}) = \frac{1}{t}\,\varepsilon\left[(t-\tau)\frac{\tau^4}{\tau^4+t^4}+\tau\right] \qquad (2)$$

with sufficiently large τ (τ=1.5t_2). The motivation of a choice of the $\varepsilon(t)$ and some physical features of electron motion are presented in Refs. [17-20]. Here we only underline that the function $\varepsilon(t)$ practically coincides with the constant ε in the inner barrier motion region, i.e. $t<t_2$ and disappears at $t>t_2$. It is important that the final results do not depend on the parameter τ. It is carefully checked in the numerical calculation.

As usually (see [17-24]), the scattering states energy spectrum now spreads over the range $(-\varepsilon\tau/2,+\infty)$, compared with $(-\infty,+\infty)$ in the uniform field. In contrast to the case of a free atom in scattering states in the presence of the uniform electric field remain quantified at any energy *E*, i.e. only definite values of β_1 are possible. The latter are determined by the confinement condition for the motion along the η-axis.

The same is true in our case, but only for the following interval:

$$E \subset \left(-\frac{1}{2}\varepsilon\tau,+\frac{1}{2}\varepsilon\tau\right).$$

Ultimately, such a procedure provides construction of realistic functions of the bound and scattering states. In a certain sense, this completely corresponds to the advantages of the distorted-wave approximation known in scattering theory [18].

The total Hamiltonian does not possess the bound stationary states. According to Ref. [17-22], one has to define the zero order Hamiltonian H_0, so that its spectrum reproduces qualitatively that of the initial one. To calculate the width Γ of the concrete quasistationary state in the lowest PT order one needs only two zeroth–order EF of H_0: bound state function Ψ_{Eb} and scattering state function Ψ_{Es}. There can be solved a more general problem: a construction of the bound state function along with its complete orthogonal complementary of scattering functions Ψ_E with

$$\mathrm{E} \subset \left(-\frac{1}{2}\varepsilon\tau,+\infty\right).$$

The imaginary part of state energy (the resonance width) in the lowest PT order is determined by the standard way:

$$\mathrm{Im}E = \Gamma/2 = \pi|\langle \Psi_{Eb}\,|H|\,\Psi_{Es}\rangle|^2 \qquad (3)$$

with the total Hamiltonian H.

The state functions Ψ_{Eb} and Ψ_{Es} are assumed to be normalized to 1 and by the $\delta(k-k')$ condition, accordingly. The matrix elements $\langle\Psi_{Eb}|H|\Psi_{E's}\rangle$ entering the high- order PT corrections can be determined in the same way. It is important to underline that These corrections can be expressed through the set of one-dimensional integrals, described in details in Refs. [17-20].

Further the ROPT scheme is combined with the RMBPT in spherical coordinates for a free atom. The details of this procedure can be found in the references [22-24]. The RMBPT formalism is constructed by the following way]. An atomic multielectron system is usually described by the relativistic Dirac Hamiltonian (the atomic units are used) as follows:

$$H = \sum_i \{\alpha c p_i - \beta c^2 - Z/r_i\} + \\ + \sum_{i>j} \exp(i\,|\,\omega\,|\,r_{ij})(1-\alpha_i\alpha_j)/r_{ij} \qquad (4)$$

where *Z* is a charge of nucleus, α_i ,α_j are the Dirac matrices, ω_{ij} is the transition frequency, c – the velocity of light. The interelectron interaction potential (second term in (4)) takes into account the retarding effect and magnetic interaction in the lowest order on

parameter of the fine structure constant. In the PT zeroth approximation it is used ab initio mean-field potential:

$$V^{DKS}(r) = [V^{D}_{Coul}(r) + V_X(r) + V_C(r \mid a)], \quad (5)$$

with the standard Coulomb (or some model potential analog), exchange Kohn-Sham V_X and correlation Vc potentials (look details in Refs. [19,20]). An effective approach to accounting the multi-electron polarization contributions is described earlier and based on using the effective two-QP polarizable operator, which is included into the PT first order matrix elements.

In order to calculate the decay (transition) probabilities and widths an effective relativistic energy approach (version [5,6,40-43]) is used. In particular, a width of the state, connected with an autoionization decay, is determined by a coupling with the continuum states and calculated as square of the matrix element [19]:

$$V_{\beta_1\beta_2;\beta_4\beta_3} = \sqrt{(2j_1+1)(2j_2+1)(2j_3+1)(2j_4+1)}$$
$$(-1)^{j_1+j_2+j_3+j_4+m_1+m_2} \times$$
$$\times \sum_{a\mu} (-1)^{\mu} \begin{pmatrix} j_1 & j_3 & a \\ m_1 & -m_3 & \mu \end{pmatrix} \begin{pmatrix} j_2 & j_4 & a \\ m_2 & -m_4 & \mu \end{pmatrix} \times$$
$$\times Q_a\left(n_1 l_1 j_1 n_2 l_2 j_2; n_4 l_4 j_4 n_3 l_3 j_3\right) \quad (6)$$

Here $Q_a = Q_a^{\mathrm{Qul}} + Q_a^{\mathrm{Br}}$, where Q_a^{Qul}, and Q_a^{Br} correspond to the Coulomb and Breit parts of the interelectron potential and express through Slater-like radial integrals and standard angle coefficients. Other details can be found in Refs. [5,6,40-43].

The most complicated problem of the relativistic PT computing the complex multielectron elements spectra is in an accurate, precise accounting for the multi-electron exchange-correlation effects (including polarization and screening effects, a continuum pressure etc), which can be treated as the effects of the PT second and higher orders. The detailed description of the polarization diagrams and the corresponding analytical expressions for matrix elements of the polarization QPs interaction (through the polarizable core) potential is presented in Refs. [5,6,40-52].

3. Results and Conclusions

Here we present the results of computing the complex energy eigenvalues representing the shifted and broadened 4s state of lithium atom as a function of electric field strength. Meng et al [1] have presented the similar results using an advanced B-spline based coordinate rotation (B-CR) approach plus the model potential method. Themelis and Nicolaides [4] adopted *ab initio* theory to compute the complex energy of multielectron states for atom in an electric field. Their approach is based on the state-specific construction of a non-Hermitian matrix according to the form of the decaying-state eigenfunction which emerges from the CESE theory. Sahoo and Ho [5] performed the calculation of the Stark resonances energies and widths on the basis of a complex absorbing potential (CAP) method.

In Table 1 we present our data on the EE representing the shifted and broadened 4s state of lithium atom as a function of electric field strength (in a.u.). For comparison the analogous results, obtained on the basis of the CAP, CESE, B-CR methods [1-5] as well as semiclassical (SC) estimates , are listed too. Analysis of the results shows that our data on the Stark resonances parameters are in a physically reasonable agreement with theoretical data obtained by other, in particular, CESE and B-CR methods.

However, the results for the 4f lithium state width differ more significantly from each other. For example, the CAP calculation for the width of the 4f state gives systematically less values than obtained by the CESE, B-CR and our methods.

Our resonance width values are higher As it was indicated in Ref. [4], one of the advantages of the B-CR method is possibility to apply in the case of increasing field strengths without a significant computational effort

growth, however, the convergence of the width Γ to obtain reliable complex eigenvalues should be carefully carried out.

Table 1. Complex eigenvalues (in atomic units: a.u.) representing the shifted and broadened 4f state of lithium atom as a function of the field strength ε^* (in 10^{-4} a.u.), calculated by different methods (see text)

Li 4f	B-CR [1]	B-CR [1]	CAP [5]	CAP [5]
ε^*	$-E_r$	$\Gamma/2$	$-E_r$	$\Gamma/2$
2.0	2.8962[−2]	2.36[−8]	2.896[−2]	1.62[−7]
2.5	2.9303[−2]	3.170[−4]	2.834[−2]	1.01[−4]
3.0	3.1036[−2]	9.363[−4]	2.796[−2]	1.76[−4]
4.0	3.4574[−2]	2.385[−3]	2.657[−2]	7.05[−4]
4.5	3.6162[−2]	3.038[−3]	-	-
5.0	3.8008[−2]	3.767[−3]	2.576[−2]	1.51[−3]
6.0	4.1282[−2]	5.929[−3]	-	-
7.0	4.4043[−2]	8.095[−3]	-	-
8.0	4.6559[−2]	1.020[−2]	-	-
10	5.1122[−2]	1.424[−2]	-	-
12	5.5320[−2]	1.805[−2]	-	-
Li	This	This	CESE [4]	SC [4]
ε^*	$-E_r$	$\Gamma/2$	$-E_r$	$\Gamma/2$
2.0	2.8962[−2]	3.401[−8]	3.445[−8]	1.67[−10]
2.5	2.9295[−2]	3.172[−4]	3.172[−4]	1.17[−6]
3.0	3.1028[−2]	9.423[−4]	9.482[−4]	3.38[−4]
4.0	3.4565[−2]	2.386[−3]	2.386[−3]	0.2654
4.5	3.6153[−2]	3.042[−3]	3.049[−3]	-
5.0	3.7998[−2]	3.806[−3]	3.839[−3]	-
6.0	4.1273[−2]	5.974[−3]	6.011[−3]	-
7.0	4.4035[−2]	8.133[−3]	8.169[−3]	-
8.0	4.6550[−2]	1.024[−2]	1.027[−2]	-
10	5.1113[−2]	1.426[−2]	1.427[−2]	-
12	5.5312[−2]	1.807[−2]	1.809[−2]	-

One of the advantages of the modified OPT method is that an increasing a field strength does not lead to an increase of computational effort and there is no a convergence problem. To ensure rapid PT convergence, a physically reasonable spectrum (EE and EF) was chosen as the zero order, similar to the 'distorted waves' method. Indeed, the convergence tests confirmed this fact. The OPT approach provides not only resonance state function definition but also the construction of the complex EE state function along with its complete orthogonal complementary of the scattering functions.

In Refs. [51-61] the operator PT method ideology has been used to consider a problem of resonances in the heavy ions collisions and AC Stark effect as well as the actual problems of a cooperative combined electron-gamma-nuclear spectroscopy. In any case development of advanced computational methods to Stark resonances in atoms is of a great importance for multiple physical applications [51-61].

References

1. Meng, H.-Y.; Zhang, Y.-X.; Kang, S.; Shi, T.-Y.; Zhan, M.-S. Theoretical complex Stark energies of lithium by a complex scaling plus the B-spline approach. *J. Phys. B: At. Mol. Opt. Phys*. **2008**, *41*, 155003.
2. Themelis S I and Nicolaides C. A. , Complex energies and the polyelectronic Stark problem. *J. Phys. B: At. Mol. Opt. Phys.* **2000**, *33*, 5561
3. Themelis S I and Nicolaides C A Complex energies and the polyelectronic Stark problem: II. The Li n = 4 levels for weak and strong fields. *J. Phys. B: At. Mol. Opt. Phys.* **2001**, *34*, 2905
4. Mercouris T and Nikolaides C A Solution of the many-electron many-photon problem for strong fields: Application to Li− in one- and two-color laser fields 2003 *Phys. Rev. A.* **2003**, *67*, 063403
5. Glushkov, A.V. *Relativistic Quantum theory. Quantum mechanics of atomic systems*. Astroprint: Odessa, **2008**.
6. Khetselius, O.Yu. *Quantum structure of electroweak interaction in heavy finite Fermi-systems*. Astroprint: Odessa, **2011**.
7. Sahoo S and Ho Y K Stark effect on the low-lying excited states of the hydrogen and the lithium atoms. *J. Phys. B: At. Mol. Opt. Phys.* **2000,** *33***,** 5151
8. Glushkov, A., Buyadzhi, V., Kvasikova, A., Ignatenko, A., Kuznetsova, A., Prepelitsa, G., Ternovsky, V. Non-Linear chaotic dynamics of quantum systems:

Molecules in an electromagnetic field and laser systems. In*: Quantum Systems in Physics, Chemistry, and Biology*. Springer, Cham. **2017**, *30*, 169-180.
9. Harmin, D.A. Theory of the Stark effect. *Phys. Rev. A* **1982**, *26*, 2656.
10. Popov, V.; Mur, V.; Sergeev A.; Weinberg, V. Strong-field Stark effect: perturbation theory and 1/n expansion. *Phys. Lett. A* **1990**, *149(9)*, 418-424.
11. Glushkov, A.V.; Ambrosov, S.V.; Ignatenko, A.V. Non-hydrogenic atoms and Wannier-Mott excitons in a DC electric field: Photoionization, Stark effect, Resonances in ionization continuum and stochasticity. *Photoelectr.* **2001,** *10*, 103-106.
12. Glushkov, A.V. Spectroscopy of atom and nucleus in a strong laser field: Stark effect and multiphoton resonances. *J. Phys.: Conf. Ser*. **2014**, *548*, 012020
13. Glushkov A. Spectroscopy of cooperative muon- gamma- nuclear processes: Energy and spectral parameters. *J. Phys.: Conf. Ser.* **2012,** *397*, 012011
14. Ignatenko, A.V. Probabilities of the radiative transitions between Stark sublevels in spectrum of atom in an DC electric field: New approach. *Photoelectronics,* **2007,** *16*, 71-74.
15. Glushkov, A.; Ambrosov, S.; Ignatenko, A. Non-hydrogenic atoms and Wannier-Mott excitons in a DC electric field: Photoionization, Stark effect, Resonances in ionization continuum and stochasticity. *Photoelectronics,* **2001,** *10*, 103-106.
16. Glushkov, A.V.; Ternovsky, V.B.; Buyadzhi, V.; Prepelitsa, G.P. Geometry of a Relativistic Quantum Chaos: New approach to dynamics of quantum systems in electromagnetic field and uniformity and charm of a chaos. *Proc. Intern. Geom. Center*. **2014**, *7(4)*, 60-71.
17. Glushkov A.V.; Ivanov, L.N. DC strong-field Stark effect: consistent quantum-mechanical approach. *J. Phys. B: At. Mol. Opt. Phys.* **1993,** *26*, L379-386
18. Glushkov, A.V. Operator Perturbation Theory for Atomic Systems in a Strong DC Electric Field. In: Hotokka M., Brändas E., Maruani J., Delgado-Barrio G. (eds) Advances in Quantum Methods and Applications in Chemistry, Physics, and Biology.Eds.; Springer: Cham. **2013**, *27*, 161–177.
19. Glushkov, A. *Atom in an electromagnetic field*. KNT: Kiev, **2005**.
20. Glushkov, A.V. *Relativistic and correlation effects in spectra of atomic systems;* Astroprint: Odessa, **2006.**
21. Khetselius, O.Yu. *Hyperfine structure of atomic spectra*. Astroprint: Odessa, **2008**
22. Kuznetsova, A.A.; Glushkov, A.V.; Ignatenko, A.V.; Svinarenko, A.A.; Ternovsky V.B. Spectroscopy of multielectron atomic systems in a DC electric field. *Adv. Quant. Chem*. (Elsevier) **2018**, *78*, 287-306.
23. Kuznetsova, A.; Buyadzhi, A.; Gurskaya, M.; Makarova, A. Spectroscopy of multi electron atom in a DC electric field: Modified operator perturbation theory approach to Stark resonances. *Photoelectronics***. 2018**, *27*, 94-102
24. Kuznetsova, A.A.; Glushkov, A.V.; Romanenko, E.S.; Plisetskaya, E.K., Spectroscopy of multielectron atom in dc electric field: relativistic operator perturbation theory. *Photoelectronics*. **2019**, 28, 32-38
25. Froelich, P.; Davidson, E.R.; Brändas, E. Error estimates for complex eigenvalues of dilated Schr6dinger operators. *Phys. Rev. A* **1983**, *28, No. 5*, 2641.
26. Lipkin, N.; Moiseyev, N.; Brändas, E. Resonances by the exterior-scaling method within the framework of the finite-basis-set approximation. *Phys. Rev. A* **1989**, *40, No. 2*, 549.
27. Brändas, E.; Froelich, P.; Obcemea, C.H., Elander, N.; Rittby, M. Note on the complex stabilization method. *Phys. Rev. A* **1982**, *26, No. 6*, 3656.
28. *Resonances. The Unifying Route Towards the Formulation of Dynamical Processes - Foundations and Applications in Nuclear, Atomic and Molecular Physics, Series: Lecture Notes in Physics*; Brändas, E.; Elander, N. Eds.; Springer: Berlin, **1989**, *325*, 1-564.

29. Ostrovsky, V.N.; Elander, N. Scattering resonances and background associated with an asymmetric potential barrier via Siegert pseudostates. *Phys. Rev. A* **2005**, *71,* 052707.
30. Sigal, I. Geometric theory of Stark resonances in multielectron systems. *Comm. Math. Phys*. **1988**, *119*, 287-314.
31. Silverstone, H.J.; Adams, B.G.; Cizek, J.; Otto, P. Stark Effect in Hydrogen: Dispersion Relation, Asymptotic Formulas, and Calculation of the Ioni-zation Rate via High-Order Perturbation Theory. *Phys. Rev. Lett*. **1979**, *43*, *No. 20,* 1498-1501.
32. Cerjan, C.; Hedges, R.; Holt, C.; Reinhardt, W.P.; Scheibner, K.; Wendoloski, J.J. Complex coordinates and the Stark effect. *Int. J. Quant. Chem*. **1978**, *14 (4)*, 393-418.
33. Luc-Koenig, E.; Bachelier, A. Systematic theoretical study of the Stark spectrum of atomic hydrogen. I. Density of continuum states. *J. Phys. B: At. Mol. Phys*. **1980,** *13*, 1743-1756
34. Damburg, R.J.; Kolosov, V.V. A hydrogen atom in a uniform electric field. *J. Phys. B: At. Mol. Phys*. **1976**, *9, No. 18,* 3149.
35. Maquet, A.; Chu, S.I.; Reinhardt, W.P. Stark ionization in dc and ac fields: An L2 complex-coordinate approach. *Phys. Rev. A* **1983**, *27, No. 6,* 2946-2970.
36. Reinhardt, W.P. Padé summations for the real and imaginary parts of atomic stark eigenvalues. *Int. J. Quant. Chem*. **1982**, *21(1),* 133-146.
37. Franceschini, V.; Grecchi, V.; Silverstone, H. Complex energies from real perturbation series for the LoSurdo-Stark effect in hydrogen by Borel-Padé approximants. *J. Phys. Rev. A* **1985**, *32 (3),* 1338.
38. Telnov, D.A. DC Stark effect in a hydrogen atom via Sturmian expansions. *J. Phys. B.: At. Mol. Opt. Phys*. **1989**, *22*, *No. 14*, L399-403.
39. Ivanov, I.; Ho, Y.-K. Complex rotation method for the Dirac Hamiltonian. *Phys. Rev. A* **2004**, *69,* 023407.
40. Ivanov, L.N.; Ivanova, E.P. Method of Sturm orbitals in calculation of physical characteristics of radiation from atoms and ions. *JETP*. **1996,** *83,* 258-266.
41. Ivanova, E.P.; Ivanov, L.N.; Glushkov, A.V.; Kramida, A.E. High order corrections in the relativistic perturbation theory with the model zeroth approximation, Mg-Like and Ne-Like Ions. *Phys. Scripta* **1985**, *32,* 513-522.
42. Ivanova, E.P.; Glushkov, A.V. Theoretical investigation of spectra of multicharged ions of F-like and Ne-like isoelectronic sequences. *J. Quant. Spectr. Rad. Transfer.* 1986, *36,* 127-145.
43. Glushkov, A.V. Advanced relativistic energy approach to radiative decay processes in multielectron atoms and multicharged ions. *In Quantum Systems in Chemistry and Physics: Progress in Methods and Applications.* Springer: Dordrecht, **2012**; Vol. 26, pp 231–252.
44. Svinarenko A., Glushkov, A., Khetselius, O., Ternovsky,V., Dubrovskaya, Yu., Kuznetsova, A., Buyadzhi, V. Theoretical spectroscopy of rare-earth elements: spectra and autoionization resonances. *Rare Earth Element.* InTech, **2017**, pp 83-104.
45. Glushkov, A.V., Khetselius, O.Yu., Svinarenko, A.A., Buyadzhi, V.V., *Spectroscopy of autoionization states of heavy atoms and multiply charged ion*s. TEC: Odessa, **2015.**
46. Glushkov, A.V., Khetselius, O.Yu., Svinarenko, A., Buyadzhi, V. *Methods of computational mathematics and mathematical physics. P.1*. Odessa: **2015**.
47. Khetselius, O., Glushkov, A., Dubrovskaya, Yu., Chernyakova, Yu., Ignatenko, A.V., Serga, I., Vitavetskaya, L. Relativistic quantum chemistry and spectroscopy of exotic atomic systems with accounting for strong interaction effects. In: *Concepts, Methods and Applications of Quantum Systems in Chem. and Phys*. Springer, Cham, **2018,** 31, 71-91.
48. Glushkov, A.V., Khetselius, O.Yu., Svinarenko A.A., Buyadzhi, V.V., Ternovsky, V.B, Kuznetsova, A., Bashkarev,

P Relativistic perturbation theory formalism to computing spectra and radiation characteristics: application to heavy element. *Recent Studies in Perturbation Theory*, ed. D. Uzunov (InTech) **2017**, 131-150.
49. Khetselius, O. Relativistic perturbation theory calculation of the hyperfine structure parameters for some heavy-element isotopes. *Int. Journ. Quant. Chem.* **2009,** *109*, 3330-3335.
50. Khetselius, O. Relativistic calculation of the hyperfine structure parameters for heavy elements and laser detection of the heavy isotopes. *Phys. Scr.* **2009,** *135*, 014023
51. Khetselius, O.Yu., Spectroscopy of cooperative electron-gamma-nuclear processes in heavy atoms: NEET effect. *J. Phys.: Conf. Ser*. **2012**, 3*97*, 012012.
52. Svinarenko, A. Study of spectra for lanthanides atoms with relativistic many-body perturbation theory: Rydberg resonances. *J. Phys.: Conf. Ser.* **2014,** *548*, 012039.
53. Buyadzhi, V., Zaichko, P., Antoshkina, O., Kulakli, T., Prepelitsa, G., Ternovsky, V., Mansarliysky, V. Computing of radiation parameters for atoms and multicharged ions within relativistic energy approach: Advanced Code. *J. Phys.: Conf. Ser*. **2017**, *905*(1), 012003.
54. Buyadzhi, V.V., Glushkov, A.V., Mansarliysky, V.F., Ignatenko, A.V., Svinarenko, A.A. Spectroscopy of atoms in a strong laser field: new method to sensing ac stark effect, multiphoton resonances parameters and ionization cross-sections. *Sensor Electr. and Microsyst. Techn*. **2015**, *12*(4), 27-36.
55. Ambrosov, S., Khetselius, O., Ignatenko, A. Wannier-Mott exciton and H, Rb atom in a DC electric field: Stark effect. *Photoelectronics*. **2008**, *17*, 84-87.
56. Ambrosov S., Ignatenko V., Korchevsky D., Kozlovskaya V. Sensing stochasticity of atomic systems in crossed electric and magnetic fields by analysis of level statistics for continuous energy spectra. *Sensor Electr. and Microsyst. Techn*. **2005**, Issue 2, 19-23.
57. Buyadzhi, V.V. Laser multiphoton spectroscopy of atom embedded in Debye plasmas: multiphoton resonances and transitions. *Photoelectrs.* **2015,** *24*, 128.
58. Buyadzhi, V.V.; Chernyakova, Yu.G.; Smirnov, A.V.; Tkach, T.B. Electron-collisional spectroscopy of atoms and ions in plasma: Be-like ions. *Photoelectronics*. **2016,** *25*, 97-101.
59. Buyadzhi, V.; Chernyakova, Yu.; Antoshkina, O.; Tkach, T. Spectroscopy of multicharged ions in plasmas: Oscillator strengths of Be-like ion Fe. *Photoelectronics*. **2017,** *26*, 94-102.
60. Chernyakova, Y.G., Ignatenko A.V., Vitavetskaya L.A. Sensing the tokamak plasma parameters by means high resolution x-ray theoretical spectroscopy method: new scheme. *Sensor Electr. and Microsyst. Techn*. **2004**, *1*, 20-24
61. Khetselius, O.Yu., Gurnitskaya, E.P., Loboda, A.V., Vitavetskaya, L.A. Consistent quantum approach to quarkony energy spectrum and semiconductor superatom and in external electric field. *Photoelectronics*. **2008**, *17*, 127-130.

PACS 31.15.A-

Kuznetsova A.A., Glushkov A.V., Plisetskaya E.K.

THEORETICAL COMPLEX ENERGIES OF STARK RESONANCES IN LITHIUM BY OPERATOR PERTURBATION THEORY APPROACH

Summary. The theoretical complex energies of the Stark resonances in the lithium atom (non-hydrogenic atomic system) in a DC electric are calculated within the operator form of the modified perturbation theory of the Schrödinger equation for the non-H atomic systems. The method includes the physically reasonable distorted-waves approximation in the frame of the formally exact quantum-mechanical procedure. The Stark resonances energies and widths in the lithium atom spectrum are calculated and compared with results of calculations on the basis of the complex absorbing potential method, the B-spline-based coordinate rotation method approach and direct computing complex Schrödinger equation eigenvalues.

Keywords: multielectron atom, electric field, relativistic operator perturbation theory, excited states.

PACS 31.15.A-

Кузнецова А.А., Глушков А.В., Плисецкая Е.К.

ТЕОРЕТИЧЕСКИЕ ЗНАЧЕНИЯ КОМПЛЕКСНЫХ ЭНЕРГИЙ ШТАРКОВСКИХ РЕЗОНАНСОВ В АТОМЕ ЛИТИЯ В РАМКАХ ОПЕРАТОРНОЙ ТЕОРИИ ВОЗМУЩЕНИЙ

Резюме. Вычислены значения комплексных энергий штарковских резонансов в атоме лития (многоэлектронная атомная система) в постоянном электрическом поле на основе модифицированной операторной теории возмущений для многоэлектронных атомных систем. Теоретический подход включает физически обоснованное приближение искаженных волн в рамках формально точной квантово-механической процедуры. Энергии и ширины штарковских резонансов в спектре атома лития вычисляются и сравниваются с результатами расчетов в рамках метода комплексного оптического потенциала, обобщенного метода вращения координат с использованием B сплайнового алгоритма и данными прямого вычисления собственных значений комплексного уравнения Шредингера.

Ключевые слова: Многоэлектронные атом, электрическое поле, релятивистская операторная теория возмущений оператора, возбужденные состояния

PACS 31.15.A-

Кузнецова Г.О., Глушков О.В., Плісецька Є.К.

ТЕОРЕТИЧНІ ЗНАЧЕННЯ КОМПЛЕКСНИХ ЕНЕРГІЙ ШТАРКІВСЬКИХ РЕЗОНАНСІВ В АТОМІ ЛІТІЮ В РАМКАХ ОПЕРАТОРНОЇ ТЕОРІЇ ЗБУРЕНЬ

Резюме. Обчислені значення комплексних енергій штарківських резонансів в атомі літію (багатоелектронних атомна система) в постійному електричному полі на основі модифікованої операторної теорії збурень для багатоелектронних атомних систем. Теоретичний підхід включає фізично обґрунтоване наближення перекручених хвиль в рамках формально точної квантово-механічної процедури. Енергії і ширини штарківських резонансів в спектрі атома літію обчислюються і порівнюються з результатами розрахунків в рамках методу комплексного оптичного потенціалу, узагальненого методу обертання координат з використанням B-сплайнового алгоритму і даними прямого обчислення власних значень комплексного рівняння Шредінгера.

Ключові слова: багатоелектронний атом, електричне поле, релятивістська операторна теорія збурень оператора, збуджені стани.

PACS 36.10.-k

Dubrovskaya Yu. V., Khetselius O. Yu., Serga I. N., Chernyakova Yu. G.

Odesa State Environmental University, L'vovskaya str., 15, Odesa, 65016, Ukraine
E-mail: dubrovskayayv@gmail.com

RELATIVISTIC THEORY OF SPECTRAL CHARACTERISTICS OF PIONIC ATOMIC SYSTEMS: APPLICATION TO HEAVY SYSTEMS

A new theoretical approach to energy and spectral parameters of the hadronic (pionic and kaonic) atoms in the excited states with precise accounting for the relativistic, radiation and nuclear effects is presented. There are presented data of calculation of the energy and spectral parameters for pionic atoms of the ^{93}Nb, ^{173}Yb, ^{181}Ta , ^{197}
Au, with accounting for the radiation (vacuum polarization), nuclear (finite size of a nucleus) and the strong pion-nuclear interaction corrections. The measured values of the Berkley, CERN and Virginia laboratories and alternative data based on other versions of the Klein-Gordon-Fock theories with taking into account for a finite size of the nucleus in the model uniformly charged sphere and the standard Uhling-Serber potential approach for account for the radiation corrections are listed too.

1. Introduction

Our work is devoted to the further application of earlier developed new theoretical approach [1-8] to the description of spectra and different spectral parameters, in particular, radiative transitions probabilities for hadronic (pionic and kaonic) atoms in the excited states with precise accounting for the relativistic, nuclear and radiative effects. It is well known that studying the energy, spectral, radiation parameters, including the spectral lines hyperfine structure, for heavy exotic (hadronic, kaonic, pionic) atomic systems is of a great interest for the further development as atomic and nuclear theories and quantum chemistry of strongly interacted fermionic systems (see, for example, refs. [1-45]). Really, the exotic atoms enable to probe aspects of atomic and nuclear structure that are quantitatively different from what can be studied in the electronic ("usual") atoms. Besides, the corresponding data on the energy and spectral properties of the hadronic atomic systems can be used as a powerful tool for the study of particles and fundamental properties.

While determining the properties of pion atoms in theory is very simple as a series of H such models and more sophisticated methods such combination chiral perturbation theory (TC), adequate quantitative description of the spectral properties of atoms in the electromagnetic pion sector (not to mention even the strong interaction sector) requires the development of High-precision approaches, which allow you to accurately describe the role of relativistic, nuclear, radiation QED (primarily polarization electron-positron vacuum, etc.). pion effects in the spectroscopy of atoms.

The most popular theoretical models for pionic and kaonic atoms are naturally based on the using the Klein-Gordon-Fock equation, but there are many important problems connected with accurate accounting for as pion-kaon-nuclear strong interaction effects as QED radiative corrections (firstly, the vacuum polarization effect etc.). This topic has been a subject of intensive theoretical and experimental interest (see [1-16]). The perturbation theory expansion on the physical; parameter αZ is usually used to take into account the radiative QED corrections, first of all, effect of the polarization of electron-positron vacuum etc. This approximation is sufficiently correct and comprehensive in a case of the light pionic atoms, however it becomes incorrect in a case of the heavy atoms with large charge of a nucleus Z.

The more correct accounting of the QED, finite nuclear size and electron-screening effects for pionic atoms is also very serious and actual problem to be solved more consistent-

ly in comparison with available theoretical models and schemes.

In this paper we present an effective theoretical approach to computing energy and spectral parameters of the hadronic (pionicc) atoms in the excited states with precise accounting for the relativistic, radiation and nuclear effects. There are presented data of calculation of the energy and spectral parameters for pionic atoms of the ^{93}Nb, ^{173}Yb, ^{181}Ta , ^{197}Au, with accounting for the radiation (vacuum polarization), nuclear (finite size of a nucleus) and the strong pion-nuclear interaction corrections. The measured values of the Berkley, CERN and Virginia laboratories and alternative data based on other versions of the Klein-Gordon-Fock theories with taking into account for a finite size of the nucleus in the model uniformly charged sphere and the standard Uhling-Serber potential approach for account for the radiation corrections are listed too.

2. Theory

The basic topics of our theoretical approach have been earlier presented [3-8,27,28], so here we are limited only by the key elements. The relativistic dynamic of a spinless boson (pion) particle is described by the Klein-Gordon-Fock (KGF) equation. As usually, an electromagnetic interaction between a negatively charged pion and the atomic nucleus can be taken into account introducing the nuclear potential A_ν in the KG equation via the minimal coupling $p_\nu \rightarrow p_\nu - qA_\nu$. Generally speaking, the Klein-Gordon-Fock equation can be rewritten as the corresponding two-component equation :

$$[-(\sigma_3+i\sigma_2)\frac{\nabla^2}{2\mu}+\sigma_3\mu+(\sigma_3+i\sigma_2)V_{opt}^{(0)}+V_C^{(0)}]\Psi_i=E_i\Psi_i, \quad (1)$$

where σ_i are the Pauli spin matrices and

$$\Psi_i=\frac{1}{2}\begin{pmatrix}(1+(E-V_C^{(0)})/\mu)\phi_i\\(1-(E-V_C^{(0)})/\mu)\phi_i\end{pmatrix}. \quad (2)$$

This equation is equivalent to the stationary Klein-Gordon-Fock equation. The corresponding non-stationary Klein-Gordon-Fock equation can be written as follows:

$$\mu^2c^2\Psi(x)=\{\frac{1}{c^2}[i\hbar\partial_t+eV_0(r)]^2+\hbar^2\nabla^2\}\Psi(x) \quad (3)$$

where c is the speed of light, *h* is the Planck constant, μ is the reduced mass of the pion-nuclear system, and $\Psi_0(x)$ is the scalar wave function of the space-temporal coordinates. Usually one considers the central potential $[V_0(r), 0]$ approximation with the stationary solution:

$$\Psi\ (x)\ =\ \exp(-iEt/\hbar)\phi(x), \quad (4)$$

where $\phi(x)$ is the solution of the equation:

$$\{\frac{1}{c^2}[E+eV_0(r)]^2+\hbar^2\nabla^2-\mu^2c^2\}\phi(x)=0 \quad (5)$$

Here *E* is the total energy of the system (sum of the mass energy mc^2 and binding energy ε_0). In principle, the central potential V_0 is the sum of the following potentials: the electric potential of a nucleus, vacuum-polarization potential.

The strong interaction potential can be added below. Generally speaking, an energy of the pionic atomic system can be represented as the following sum:

$$E\approx E_{KG}+E_{FS}+E_{QED}+E_N, \quad (6)$$

where E_{KG} is the energy of a pion in a nucleus (Z,A) with the point-like charge, E_{FS} is the contribution due to the nucleus finite size effect, E_{VP} is the radiation QED correction, E_N is the energy shift due to the strong (pion- or kaon- nuclear) interaction V_N.

In principle, the central potential V_0 should include the central Coulomb potential, the radiative (in particular, vacuum-polarization) potential as well as the electron-screening potential in the atomic-optical (electromagnetic) sector. Surely, the full solution of the pionic atom energy especially

for the low-excited state requires an inclusion the hadron-nuclear strong potential.

The next step is accounting the nuclear finite size effect or the Breit-Rosenthal-Crawford-Schawlow one. In order to do it we use the widespread Gaussian model for nuclear charge distribution. The advantages of this model in comparison with usually used models such as for example an uniformly charged sphere model and others had been analysed in Ref. [3]. Usually the Gauss model is determined as follows:

$$\rho(r|R) = \left(4\gamma^{3/2}/\sqrt{\pi}\right)\exp\left(-\gamma r^2\right), \qquad (7)$$

where $\gamma = 4\pi/R^2$, R is an effective radius of a nucleus.

In order to take into account very important radiation QED effects we use the radiative potential from the Flambaum-Ginges theory [15]. In includes the standard Ueling-Serber potential and electric and magnetic form-factors plus potentials for accounting of the high order QED corrections such as:

$$\Phi_{rad}(r) = \Phi_U(r) + \Phi_g(r) + \Phi_f(r) + .$$

$$+ \Phi_l(r) + \frac{2}{3}\Phi_U^{high-order}(r) \qquad (8)$$

where

$$\Phi_U^{high-order}(r) = -\frac{2\alpha}{3\pi}\Phi(r)\frac{0.092Z^2\alpha^2}{1+(1.62r/r_C)^4}.$$

$$\Phi_l(r) = -\frac{B(Z)}{e}Z^4\alpha^5 mc^2 e^{-Zr/a_B} \qquad (9)$$

Here e – a proton charge and universal function $B(Z)$ is defined by expression: $B(Z)=0.074+0.35Z\alpha$.

At last to take into account the electron screening effect we use the standard procedure, based on addition of the total interaction potential SCF potential of the electrons, which can be determined within the Dirac-Fock method by solution of the standard relativistic Dirac equations. It should be noted however, that contribution of theses corrections is practically zeroth for the pionic nitrogen, however it can be very important in transition to many-electron as a rule heavy hadronic atoms.

Further in order to calculate probabilities of the radiative transitions between energy level of the pionic atoms we have used the well-known relativistic energy approach (c. g.[16-28]). Other details are in Refs. [4,7,8].

3. Results and conclusions

In Table 1 the numerical data on the *4f-3d, 5g-4f* transition energies for pionic atoms of the ^{93}Nb, ^{173}Yb, ^{181}Ta , ^{197}Au are presented. There are also listed the measured values of the Berkley, CERN and Virginia laboratories and alternative data obtained on the basis of computing within alternative versions of the Klein-Gordon-Fock (KGF) theory with taking into account for a finite size of the nucleus in the model uniformly charged sphere and the standard Uehling-Serber radiation correction (see Refs. [5, 6,7,13]).

The analysis of the presented data indicate on the importance of the correct accounting for the radiation (vacuum polarization) and the strong pion-nuclear interaction corrections. The contributions due to the nuclear finite size effect should be accounted in a precise theory too.

More exact knowledge of the electromagnetic interaction parameters for a pionic atom will make more clear the true values for parameters of the pion-nuclear potentials. Further it allows to correct a disadvantage of widely used parameterization of the optical potential. It is especially important if one takes into account an increasing accuracy of the X-ray pionic atom spectroscopy experiments.

Table 1.

Transition energies (keV) in the spectra of some heavy pionic atoms (see text)

π-A	Trans.	Berkley E_{EXP}	CERN E_{EXP}	E_{KGF+EM} [6, 7]
^{93}Nb	5g-4f	-	307.79±0.02	-
^{173}Yb	5g-4f	-	-	-
^{181}Ta	5g-4f	453.1±0.4	453.90±0.20	453.06
^{197}Au	5g-4f	532.5±0.5	533.16±0.20	528.95
^{93}Nb	4f-3d	-	140.3±0.1	-
^{173}Yb	4f-3d	-	-	-
^{181}Ta	4f-3d	-	1008.4±1.3	-
π-A	Trans.	E_{KGF-EM} [13]	E_N [13]	Our data
93Nb	5g-4f	-	-	307.85
173Yb	5g-4f	-	-	412.26
181Ta	5g-4f	453.78	453.52 453.62	453.71
197Au	5g-4f	-	531.88	533.08
93Nb	4f-3d	-	-	140.81
173Yb	4f-3d	-	-	838.67
181Ta	4f-3d	-	992.75	1008.80

It is interesting to note that the contributions into transition energies are about ~5 keV due to the QED effects, ~0,2 keV due to the nuclear finite size effect, and ~0.07keV due to the electron screening effect, provided by the 2[He], 4[Be], 10[Ne] electron shells [5].

References

1. Khetselius, O.Yu. Relativistic perturbation theory calculation of the hyperfine structure parameters for some heavy-element isotopes. *Int. J. Quant. Chem.* **2009,** *109*, 3330–3335.
2. Khetselius, O. Relativistic calculation of the hyperfine structure parameters for heavy elements and laser detection of the heavy isotopes. *Phys. Scripta* **2009,** *135*, 014023.
3. Khetselius, O. *Hyperfine structure of atomic spectra*; Astroprint: Odessa, **2008**.
4. Dubrovskaya, Yu., Khetselius, O.Yu., Vitavetskaya, L., Ternovsky, V., Serga, I. Quantum chemistry and spectroscopy of pionic atomic systems with accounting for relativistic, radiative, and strong interaction effects. *Adv. in Quantum Chem.* **2019,** *78*, 193-222.
5. Khetselius, O.Yu., Glushkov, A.V., Dubrovskaya, Yu.V., Chernyakova, Yu.G., Ignatenko, A.V., Serga, I.N., Vitavetskaya, L. Relativistic quantum chemistry and spectroscopy of exotic atomic systems with accounting for strong interaction effects. In: Wang YA, Thachuk M, Krems R, Maruani J (eds) Concepts, Methods and Applications of Quantum Systems in Chemistry and Physics. Springer, Cham, **2018**; Vol. 31, pp. 71-91.
6. Serga, I.N.; Dubrovskaya, Yu.V.; Kvasikova, A.S.; Shakhman, A.N; Sukharev, D.E. Spectroscopy of hadronic atoms: Energy shifts. *J. Phys.: Conf. Ser*. **2012,** *397***,** 012013.
7. Serga, I.N.; Khetselius, O.Yu.; Vitavetskaya, L.A.; Bystryantseva A.N. Relativistic theory of spectra of pionic atomic systems ^{208}Pb with account of strong pion-nuclear interaction effects. *Photoelectronics*. **2017**, *26*, 68-77.
8. Sukharev, D.E.; Khetselius, O.Yu.; Dubrovskaya, Yu.V. Sensing strong interaction effects in spectroscopy of hadronic atoms. *Sensor Electr. and Microsyst. Techn*. **2009**, *N3*, 16-21.
9. Khetselius, O.Yu. *Quantum structure of electroweak interaction in heavy finite Fermi-systems*. Astroprint: Odessa, **2011**.
10. Khetselius, O.Y.., Glushkov, A.V., Gurskaya, M.Y., Kuznetsova, A.A., Dubrovskaya, Yu.V., Serga, I.N., Vitavetskaya, L.A. Computational modelling parity nonconservation and electroweak interaction effects in heavy atomic systems within the nuclear-relativistic many-body perturbation theory. *J. Phys.: Conf. Ser.* **2017,** *905*(1), 012029.
11. Batty, C.; Eckhause, M.; Gall, K. et al. Strong interaction effects in high-Z K^- atoms. *Phys. Rev. C.* **1989,** *40***,** 2154.
12. Erikcson, M.; Ericson, T. Optical Properties of Low Energy Pions in Nuclei. *Ann. Phys.* **1966,** *36*, 323.
13. Batty, C J.; Friedman, E.; Gal, A. Saturation effects in pionic atoms and the π−-

nucleus optical potential. *Nucl. Phys. A.* **1983,** *402*, 411-428.
14. Indelicato, P. Relativistic effects in few-electron heavy ions. Ab initio evaluation of levels energy and transitions probabilities. *Phys. Scripta* **1996,** *65*, 57.
15. Flambaum, V.; Ginges J. Radiative potential and calculation of QED radiative corrections to energy levels and electromagnetic amplitudes in many-electron atoms. *Phys.Rev.A.* **2005**, *72*, 052115.
16. Glushkov A.V., Malinovskaya S.V., Svinarenko A.A., Vitavetskaya L.A., Sensing spectral hierarchy, quantum chaos, chaotic diffusion and dynamical stabilisation effects in a multi- photon atomic dynamics with intense laser field. *Sensor Electr. and Microsyst. Techn*. **2005**, *2*(2), 29-35.
17. Mohr, P.J. Quantum Electrodynamics Calculations in few-Electron Systems. *Phys. Scripta*. **1993,** *46*, 44.
18. Rusov V., Glushkov A., Vaschenko V., Korchevsky D., Ignatenko A. Stochastic dynamics of the atomic systems in the crossed electric and magnetic field: the rubidium atom recurrence spectra. *Bull.of Kiev Nat. Univ.:Ser.Phys.-Math*. **2004**, N4, 433.
19. Glushkov, A.V. Spectroscopy of cooperative muon-gamma-nuclear processes: Energy and spectral parameters. *J. Phys.: Conf. Ser*. **2012,** *397*, 012011.
20. Gubanova, E.R., Glushkov, A.V., Khetselius, O.Yu., Bunyakova, Yu., Buyadzhi, V., Pavlenko, E. *New methods in analysis and project management of environmental activity: Electronic and radioactive waste*. Kharkiv, FOP**, 2017.**.
21. Khetselius, O.Yu., Lopatkin Yu.M., Dubrovskaya, Yu.V, Svinarenko A.A. Sensing hyperfine-structure, electroweak interaction and parity non-conservation effect in heavy atoms and nuclei: New nuclear-QED approach. *Sensor Electr. and Microsyst. Techn*. **2010,** *7*(2), 11-19.
22. Bystryantseva A., Khetselius O.Yu., Dubrovskaya Yu., Vitavetskaya L.A., Berestenko A.G. Relativistic theory of spectra of heavy pionic atomic systems with account of strong pion-nuclear interaction effects: ^{93}Nb, ^{173}Yb, ^{181}Ta , ^{197}Au. *Photoelectronics*. **2016**,*25*, 56-61.
23. Glushkov, A.V. *Relativistic Quantum theory. Quantum mechanics of atomic systems*; Astroprint: Odessa, **2008**.
24. Kuznetsova A.A., Vitavetskaya L.A., Chernyakova Yu.G., Korchevsky D., Calculating the radiative vacuum polarization contribution to the energy shift of 2p-3s transition in pionic deuterium. *Photoelectronics.* **2013**, *22*, 108-111.
25. Glushkov, A.V.; Khetselius, O.Yu.; Svinarenko, A.A.; Buyadzhi, V.V. *Spectroscopy of autoionization states of heavy atoms and multiply charged ions*. Odessa: TEC**, 2015**.
26. Glushkov, A.V. Spectroscopy of atom and nucleus in a strong laser field: Stark effect and multiphoton Resonances. *J. Phys.: Conf. Ser*. **2014**, 548, 012020.
27. Khetselius, O.Yu. Atomic parity nonconservation effect in heavy atoms and observing P and PT violation using NMR shift in a laser beam: To precise theory. *J. Phys.: Conf. Ser*. **2009,** *194*, 022009.
28. Khetselius, O. Relativistic hyperfine structure spectral lines and atomic parity nonconservation effect in heavy atomic systems within QED theory. *AIP Conf. Proc.* **2010,** *1290*, 29–33.
29. Chernyakova, Y.G., Vitavetskaya L., Bashkaryov, P., Serga I., Berestenko, A. The radiative vacuum polarization contribution to the energy shift of some levels of the pionic hydrogen. *Photoelectronic*s **2015**, *24*, 122-127.
30. Glushkov, A., Gurskaya, M., Ignatenko, A., Smirnov, A., Serga, I., Svinarenko, A., Ternovsky, E. Computational code in atomic and nuclear quantum optics: Advanced computing multiphoton resonance parameters for atoms in a strong laser field. *J. Phys.: Conf. Ser*. **2017**, *905*(1), 012004.
31. Ambrosov S., Ignatenko V., Korchevsky D., Kozlovskaya V. Sensing stochasticity of atomic systems in crossed electric and magnetic fields by analysis of level

statistics for continuous energy spectra. *Sensor Electr. and Microsyst. Techn*. **2005**, Issue 2, 19-23.
32. Glushkov, A.V., Ivanov, L.N. Radiation decay of atomic states: atomic residue polarization and gauge noninvariant contributions. *Phys. Lett. A* **1992,** *170*, 33.
33. Glushkov, A.V.; Ivanov, L.N. DC strong-field Stark effect: consistent quantum-mechanical approach. *J. Phys. B: At. Mol. Opt. Phys.* **1993,** *26*, L379-386.
34. Ivanova, E., Glushkov, A. Theoretical investigation of spectra of multicharged ions of F-like and Ne-like isoelectronic sequences. J. Quant. Spectr. and Rad. Tr. **1986**, *36*(2), 127-145.
35. Ivanova, E.P., Ivanov, L.N., Glushkov, A., Kramida, A. High order corrections in the relativistic perturbation theory with the model zeroth approximation, Mg-Like and Ne-Like Ions. *Phys. Scripta* **1985**, *32*, 513-522.
36. Glushkov, A.V. *Relativistic and correlation effects in spectra of atomic systems*. Astroprint, Odessa, **2006.**.
37. Glushkov, A.V. Multiphoton spectroscopy of atoms and nuclei in a laser field: Relativistic energy approach and radiation atomic lines moments method. *Adv. in Quantum Chem.* **2019**, *78*, 253-285.
38. Chernyakova, Y.G., Ignatenko A.V., Vitavetskaya L.A., Sensing the tokamak plasma parameters by means high resolution x-ray theoretical spectroscopy method: new scheme. *Sensor Electr. and Microsyst. Techn*. **2004**, *1*, 20-24.
39. Glushkov, A.V., Malinovskaya, S.V., Dubrovskaya, Yu.V., Sensing the atomic chemical composition effect on the beta decay probabilities. *Sensor Electr. and Microsyst. Techn*. **2005**, *2*(1), 16-20.
40. Glushkov, A.V., Khetselius, O.Yu., Svinarenko, A.A., Buyadzhi, V.V. *Methods of computational mathematics and mathematical physics. P.1*. Odessa: TES, **2015**.
41. Svinarenko, A. A., Glushkov, A. V., Khetselius, O.Yu., Ternovsky,V.B., Dubrovskaya, Yu., Kuznetsova, A., Buyadzhi, V. Theoretical spectroscopy of rare-earth elements: spectra and autoionization resonances. *Rare Earth Element*, Ed. J. Orjuela (InTech) **2017**, pp 83-104
42. Glushkov, A.V., Khetselius, O.Yu., Svinarenko A.A., Buyadzhi, V.V., Ternovsky, V.B, Kuznetsova, A., Bashkarev, P Relativistic perturbation theory formalism to computing spectra and radiation characteristics: application to heavy element. *Recent Studies in Perturbation Theory*, ed. D. Uzunov (InTech) **2017**, 131-150.
43. Danilov, V., Kruglyak, Y., Pechenaya, V. Electron density-bond order matrix and the spin density in the restricted CI method. *Theor. Chim Acta*. **1969**, *13*(4), 288-296.
44. Glushkov A.V., Khetselius O.Yu., Loboda A.V., Ignatenko A., Svinarenko A., Korchevsky D., Lovett L., QED Approach to Modeling Spectra of the Multicharged Ions in a Plasma: Oscillator and Electron-ion Collision Strengths.. *AIP Conference Proceedings***.** **2008**. 1058. 175-177
45. Glushkov, A.V., Safranov, T.A., Khetselius, O.Yu., Ignatenko, A.V., Buyadzhi, V.V., Svinarenko, A.A. Analysis and forecast of the environmental radioactivity dynamics based on methods of chaos theory: General conceptions. *Environm. Problems*. **2016**, *1*(2), 115-120.

PACS 36.10.-k

Dubrovskaya Yu.V., Khetselius O. Yu., Serga I.N., Chernyakova Yu. G.

RELATIVISTIC THEORY OF SPECTRAL CHARACTERISTICS OF PIONIC ATOMIC SYSTEMS: APPLICATION TO HEAVY SYSTEMS

Summary. A new theoretical approach to energy and spectral parameters of the hadronic (pionic and kaonic) atoms in the excited states with precise accounting for the relativistic, radiation and nuclear effects is presented. There are presented data of calculation of the energy and spectral parameters for pionic atoms of the ^{93}Nb, ^{173}Yb, ^{181}Ta , ^{197}Au, with accounting for the radiation (vacuum polarization), nuclear (finite size of a nucleus) and the strong pion-nuclear interaction corrections. The measured values of the Berkley, CERN and Virginia laboratories and alternative data based on other versions of the Klein-Gordon-Fock theories with taking into account for a finite size of the nucleus in the model uniformly charged sphere and the standard Uhling-Serber potential to account for radiation corrections are listed too.

Keywords: relativistic perturbation theory, energy parameters, pionic atomic systems

PACS 36.10.-k

Дубровская Ю.В., Хецелиус О.Ю., Серга И Н., Чернякова Ю.Г.

РЕЛЯТИВИСТСКАЯ ТЕОРИЯ СПЕКТРАЛЬНЫХ ХАРАКТЕРИСТИК ПИОННЫХ АТОМНЫХ СИСТЕМ: ПРИМЕНЕНИЕ К ТЯЖЕЛЫМ СИСТЕМАМ

Резюме. Разработан новый теоретический подход к описанию энергетических и спектральных параметров адронных (пионных) атомов с аккуратным учетом релятивистских, радиационных и ядерных эффектов. Приведены данные расчета энергетических и спектральных параметров пионных атомов ^{93}Nb, ^{173}Yb, ^{181}Ta , ^{197}Au с учетом радиационных (поляризация вакуума), ядерных (конечный размер ядра) поправок и эффекта и сильного пион-ядерного взаимодействия. Для сравнения также приведены экспериментальные значения (измерения в лабораториях в Беркли, ЦЕРН и Вирджинии) и альтернативные теоретические данные, полученных в рамках других версий теории Клейна-Гордона-Фока с учетом конечного размера ядра в рамках модели однородно заряженной сферы и стандартного потенциалом Улинга-Сербера для учета радиационных поправок. .

Ключевые слова: релятивистская теория возмущений, энергетические параметры, пионные атомные системы.

PACS 36.10.-k

Дубровська Ю.В., Хецеліус О.Ю., Сєрга І.М., Чернякова Ю.Г.

РЕЛАТИВІСТИЧНА ТЕОРІЯ СПЕКТРАЛЬНИХ ХАРАКТЕРИСТИК ПІОННИХ АТОМНИХ СИСТЕМ: ЗАСТОСУВАННЯ ДО ВАЖКИХ СИСТЕМ

Резюме. Розроблено новий теоретичний підхід до опису енергетичних і спектральних параметрів адронних (піонних) атомів з акуратним урахуванням релятивістських, радіаційних і ядерних ефектів.. Наведены дані розрахунку енергетичних і спектральних параметрів піонних атомів ^{93}Nb, ^{173}Yb, ^{181}Ta , ^{197}Au з урахуванням радіаційних (поляризація вакууму), ядерних (кінцевий розмір ядра) поправок і ефекту сильного піон-ядерної взаємодії. Для порівняння також наведені експериментальні значення (вимірювання в лабораторіях в Берклі, ЦЕРН і Вірджинії) і альтернативні теоретичні дані, отримані в рамках інших версій теорії Клейна-Гордона-Фока з урахуванням кінцевого розміру ядра в рамках моделі однорідно зарядженої сфери і стандартним потенціалом Улінга-Сербера для урахування радіаційних поправок.

Ключові слова: релятивістська теорія збурень, енергетичні параметри, піонні атомні системи.

PACS 33.20.-t

Ignatenko A. V., Svinarenko A. A., Mansarliysky V. F., Sakun T. N.

Odesa State Environmental University, 15, Lvovskaya str., Odesa, 65016
National Aviation University, 1, Liubomyra Huzara ave., Kiev, 03058
E-mail: ignatenkoav13@gmail.com

OPTIMIZED QUASIPARTICLE DENSITY FUNCTIONAL AND GREEN'S FUNCTIONS METHOD TO COMPUTING BOND ENERGIES OF DIATOMIC MOLECULES

It is presented an advanced approach to computing the energy and spectral parameters of the diatomic molecules, which is based on the hybrid combined density functional theory (DFT) and the Green's-functions (GF) approach. The Fermi-liquid quasiparticle version of the density functional theory is modified and used. The density of states, which describe the vibrational structure in photoelectron spectra, is defined with the use of combined DFT-GF approach and is well approximated by using only the first order coupling constants in the optimized one-quasiparticle approximation. Using the combined DFT-GF approach to computing the spectroscopic factors of diatomic molecules leads to significant simplification of the calculation procedure and increasing an accuracy of theoretical prediction. As illustration, the results of computing the bond energies in a number of known diatomic molecules are presented and compared with alternative theoretical results, obtained within discrete-variational X_α, muffin-tin orbitals and other methods.

1. Introduction

In this paper we study the problem of calculating the important spectroscopic characteristics of multielectron systems (atoms and molecules), namely, the spectroscopic factor. The spectroscopic factor is one of the most important characteristics of atomic and molecular systems and the precise information about it is very important for many applications [1-47].

In calculations based on the density functional theory (DFT) methods in the local density (LP) approximation, invariants have become widespread: discrete-variational X_α (DV-X_α), muffin-tin orbitals (MTO) method in a version of the linear MTO method and localized orbitals, modified DV-X_α method with using a scheme of the transition state (TS) (see [1]). Although, in computational terms, these methods are highly economical, the error in calculating complex molecules based on them can reach several eV

In this paper we present an advanced approach to computing the spectroscopic factors of the diatomic molecules within the hybrid combined density functional theory (DFT) in the Fermi-liquid formulation and the Green's-functions (GF) approach to quantitative determination of the spectroscopic factors for some molecular systems. The approach is based on the Green's function method (Cederbaum-Domske version) [1,2] and Fermi-liquid DFT formalism [3-7] and using the novel effective density functionalы (see also [11-22]). It is important that the calculational procedure is significantly simplified with using the quasiparticle DFT formalism.

2. Many-body theory

As usually, introducing a field operator $\Psi(R,\theta,x)=\sum_i \phi_i(x,R,\theta)a_i(R,\theta)$ with the Hartree-Fock (HF) one–particle functions ϕ_i ($\in_i(R)$ are the one-particle HF energies and f denotes the set of orbitals occupied in the HF ground state; R_0 is the equilibrium geometry on the HF level) and dimensionless normal coordinates Q_s one can write the standard Hamiltonian as follows [2,7]:

$$H = H_E + H_N + H_{EN}^{(1)} + H_{EN}^{(2)}, \qquad (1)$$

$$H_E = \sum_i \epsilon_i(R_0) a_i^t a_i + \frac{1}{2}\sum V_{ijkl}(R_0) a_i^t a_j^t a_l a_k - \\ - \sum_{i,j} \sum_{k\in f} [V_{ikjk}(R_0) - V_{ikkj}(R_0)] a_i^t a_j \quad , \tag{2}$$

$$H_N = \hbar \sum_{s=1}^{M} \omega_s (b_s^t b_s + \frac{1}{2}),$$

$$H_{EN}^{(1)} = 2^{-1/2} \sum_{s=1}^{M} \left(\frac{\partial \epsilon_i}{\partial Q_s}\right)_0 (b_s + b_s^t)[a_i^t a_i - n_i] + \\ + \frac{1}{4}\sum_i \sum_{s,\, s'=1}^{M} \left(\frac{\partial^2 \epsilon_i}{\partial Q_s \partial Q_{s'}}\right)_0 (b_s + b_s^t)(b_{s'} + b_{s'}^t)[a_i^t a_i - n_i], \tag{3a}$$

$$H_{EN}^{(2)} = 2^{-3/2} \sum \sum_{s=1}^{M} \left(\frac{\partial V_{ijkl}}{\partial Q_s}\right)_0 (b_s + b_s^t)[\delta v_1 a_i^t a_j^t a_k + \\ + \delta v_2 a_l a_k a_i^t a_j^t + 2\delta v_3 a_j^t a_k a_l a_i^t] + \\ + \frac{1}{8}\sum \sum_{s,s'=1}^{M} \left(\frac{\partial^2 V_{ijkl}}{\partial Q_s \partial Q_{s''}}\right)_0 (b_s + b_s^t)(b_{s'} + b_{s'}^t \cdot \\ [\delta v_1 a_i^t a_j^t a_k + \delta v_2 a_l a_k a_i^t a_j^t + 2\delta v_3 a_j^t a_k a_l a_i^t] \quad , \tag{3b}$$

with n_i=1 (0), $i \in f$ ($i \notin f$), $\delta\sigma_f$=1 (0) , $(ijkl) \in \sigma_f$, where the index set v_1 means that at least ϕ_k and ϕ_l or ϕ_i and ϕ_j are unoccupied, v_2 that at most one of the orbitals is unoccupied, and v_3 that ϕ_k and ϕ_j or ϕ_l and ϕ_j are unoccupied. The ω_s are the HF frequencies; b_s, b_s^t are destruction and creation operators for vibrational quanta as

$$Q_s = (1/\sqrt{2})(b_s + b_s^t), \\ \partial/\partial Q_s = (1/\sqrt{2})(b_s - b_s^t). \tag{4}$$

The interpretation of the above Hamiltonian and an exact solution of the one-body HF problem is given in refs. [1,-7]. The usual way is to define the HF-single-particle component H_0 of the Hamiltonian (4) is as in Refs. [1,4]. Correspondingly in the one-particle picture the density of occupied states is given by

$$N_k^0(\epsilon) = \frac{1}{2\pi\hbar}\int_{-\infty}^{\infty} dt e^{i\hbar^{-1}(\epsilon - \epsilon_k)t} \langle 0| \; e^{\pm i\hbar^{-1}\tilde{H}_{0^t}} |0\rangle, \tag{5}$$

$$\tilde{H}_0 = \sum_{s=1}^{M} \hbar\omega_s b_s^t b_s + \sum_{s=1}^{M} g_s^k (b_s + b_s^t) + \\ + \sum_{s,s'=1}^{M} \gamma_{ss'}^k (b_s + b_s^t)(b_{s'} + b_{s'}^t) \tag{6}$$

$$g_s^i = \pm\frac{1}{\sqrt{2}}\left(\frac{\partial \epsilon_i}{\partial Q_s}\right)_0, \quad \gamma_{ss'}^i = \pm\frac{1}{4}\left(\frac{\partial^2 \epsilon_i}{\partial Q_s \partial Q_{s'}}\right)_0. \tag{7}$$

To get function $N_k(\epsilon)$ one calculates the GF $G_{kk'}(\epsilon)$ (see details in Refs. [1-7,31-35]:

$$G_{kk'}(\epsilon) = -i\hbar^{-1}\int_{-\infty}^{\infty} dt e^{i\hbar^{-1}\epsilon t} \langle \psi_0| \; T\{ \; a_k(t) a_k^t(0) \; \} |\psi_0\rangle \tag{8}$$

Choosing the unperturbed H_0 to be $H_0 = \sum \epsilon_i a_i^t a_i + H_N$ one could define GF as

$$G_{kk'}^{OB}(t) = \pm\delta_{kk'} i \exp\left[-in^{-1}(\varepsilon_k \mp \Delta\varepsilon)t\right] \cdot \\ \cdot \sum_n \left|\langle \hat{n}_k | U_k | 0\rangle\right|^2 \exp(\pm i n_k \cdot \hat{\omega}_k t) \quad , \tag{9}$$

The direct method for calculation of $N_k(\in)$ as the imaginary part of the GF includes a definition of the vertical I.P. (V.I.P.s) of the reference molecule and then of $N_k(\in)$.

The zeros of the functions:

$$D_k(\in) = \in - \left[\in^{op} + \Sigma(\in)\right]_k, \tag{10}$$

where $\left(\in^{op} + \Sigma\right)_k$ denotes the k-th eigenvalue of the diagonal matrix of the one-particle energies added to matrix of the self-energy part, are the negative V. I. P. 's for a given geometry. One can write [2,4]:

$$(V.I.P.)_k = -(\in_k + F_k), \\ F_k = \Sigma_{kk}\left(-(V.I.P.)_k\right) \approx \frac{1}{1 - \partial\Sigma_{kk}(\in_k)/\partial_\in}\Sigma_{kk}(\in_k) \\ . \tag{11}$$

Expanding the ionic energy E_k^{N-1} about the equilibrium geometry of the reference molecule in a power series of the normal coordinates leads to a set of linear equations for the unknown normal coordinate shifts δQ_S, and new coupling constants:

$$g_1 = \pm\left(1/\sqrt{2}\right)\left[\partial\left(\in_k + F_k\right)/\partial Q_l\right]_0 \qquad (12)$$

$$\gamma_{ll'} = \pm\left(\frac{1}{4}\right)\left[\partial^2\left(\in_k + F_k\right)/\partial Q_l/\partial Q_{l'}\right]_0$$

The coupling constants $g_l, y_{ll'}$ are calculated by the well-known perturbation expansion of the self-energy part. One could write:

$$\sum\nolimits_{kk}^{(2)}(\in) = \sum_{\substack{i,j \\ s\notin F}} \frac{\left(V_{ksij} - V_{ksji}\right)V_{ksij}}{\in + \in_s - \in_i - \in_j} + \sum_{\substack{i,j \\ s\notin F}} \frac{\left(V_{ksij} - V_{ksji}\right)V_{ksij}}{\in + \in_s - \in_i - \in_j} \qquad (13)$$

and the coupling constant g_l, are as [17]:

$$g_l \approx \pm\frac{1}{\sqrt{2}}\frac{\partial \in_k}{\partial Q_l}\frac{1 + q_k\left(\partial/\partial\in\right)\sum_{kk}\left[-\left(V.I.P.\right)_k\right]}{1 - \left(\partial/\partial\in\right)\sum_{kk}\left[-\left(V.I.P.\right)_k\right]} \qquad (14)$$

The pole strength of the corresponding GF:

$$\rho_k = \left\{1 - \frac{\partial}{\partial\in}\sum\nolimits_{kk}\left[-\left(V.I.P.\right)_k\right]\right\}^{-1}; 1 \geq \rho_k \geq 0,$$

$$g_l \approx g_l^0\left[\rho_k + q_k\left(\rho_k - 1\right)\right],$$

$$g_l^0 = \pm 2^{-1/2}\partial \in_k / \partial Q_l \qquad (15)$$

3. Fermi-liquid quasiparticle density functional theory

The quasiparticle Fermi-liquid version of the DFT [3-8,31,36] is used to determine the coupling constants etc. The master equations can be obtained on the basis of variational principle, if we start from a Lagrangian of a molecule L_q. It should be defined as a functional of quasiparticle densities:

$$\nu_0(r) = \sum_\lambda n_\lambda \left|\Phi_\lambda(r)\right|^2,$$

$$\nu_1(r) = \sum_\lambda n_\lambda \left|\nabla\Phi_\lambda(r)\right|^2, \qquad (16)$$

$$\nu_2(r) = \sum_\lambda n_\lambda\left[\Phi_\lambda^*\Phi_\lambda - \Phi_\lambda^*\Phi_\lambda\right].$$

The densities ν_0 and ν_1 are similar to the HF electron density and kinetical energy density correspondingly; the density ν_2 has no an analog in the HF or DFT theory and appears as result of account for the energy dependence of the mass operator Σ. A Lagrangian L_q can be written as a sum of a free Lagrangian and Lagrangian of interaction: $L_q = L_q^0 + L_q^{int}$, where the interaction Lagrangian is defined in the form, which is characteristic for a standard DFT (as a sum of the Coulomb and exchange-correlation terms), but, it takes into account for a mass operator energy dependence of Σ :

$$L_q^{\text{int}} = L_K - \frac{1}{2}\sum_{i,k=0}^{2}\int \beta_{ik}F(r_1,r_2)\nu_i(r_1)\nu_k(r_2)dr_1dr_2 \qquad (17)$$

where F is an effective exchange-correlation interaction potential. The constants β_{ik} are defined in Refs. [3-5]. The constant β_{02} can be calculated by analytical way, but it is very useful to keep in mind its connection with a spectroscopic factor F_{sp} [4,5]:

$$F_{sp} = \left\{1 - \frac{\partial}{\partial\in}\sum\nolimits_{kk}\left[-\left(V.I.P.\right)_k\right]\right\} \qquad (18)$$

The new element is linked with using the DFT correlation Gunnarsson-Lundqvist, Lee-Yang-Parrr functionals (c.g.[12-16]).

The multiplier $[1 - \sum_2]$ is easily calculated if the Gunnarsson-Lundqvist-like correlation potential is used as V_{XC} and $\sum_2$ is determined as follows:

$$\sum(r) = 0{,}254\rho(r)[0{,}328\rho^{-2/3}(r) +$$

$$+ 0{,}204\rho^{-2/3}(r)/\{1 + 18{,}376\rho^{1/3}(r)\}]$$

4. Results and conclusions

Let us present the results of calculating the binding energies and equilibrium distances in molecules N_2, O_2, F_2 belonging to the class of complex from the point of view of taking into account the correlation effects. Effective approach to this topic can be performed within different versions of the standard DV approach such as: DV-X_α, DV-X_α(TS), MTO (see Table 1, where experimental data are also presented for comparison).

Table 1

Bond energies (eV) and equilibrium distances (a.u.): 1 – experiment; 2- DV-X_α, 3- DV-X_α-TS, 4- MTO, 5 – Green function approach, 6 - present work

	E_B	R_e	E_B	R_e	E_B	R_e
	N_2		O_2		F_2	
1	9,91	2,07	5,22	2,28	1,67	2,68
2	9,39	2,11	8,15	2,35	8,97	2,35
3	10,86	2,11	4,14	2,33	3,54	2,61
4	7,8	2,16	4,10	2,30	0,6	2,91
5	9,99	2,11	3,78	2,33	3,21	2,6
6	9,95	2,09	5,12	2,31	1,58	2,70

As follows from the comparison of the energy values presented in Table 1 and the values of the molecular constants are sensitive to the calculation scheme. A more careful consideration of multiparticle correlation effects within the framework of this procedure leads to an improvement in the agreement between the calculation and experiment (in particular, this is observed for molecules; for there is some deterioration). The results obtained in this calculation are in slightly better agreement with experiment than the results of calculations in other versions of the DV method.

It can be concluded that the development of a more perfect than the existing methods to computing molecular constants may be associated with careful consideration of complex correlation effects, including many-body corrections. The one-quasiparticle representation used here can be taken as the zeroth one in one of the sophisticated versions of the many-body PT such as , for example, the Möller-Plesset PT (see e.g. [6]).

References

1. Köppel, H., Domcke, W., Cederbaum, L.S., Green's function method in quantum chemistry. *Adv. Chem. Phys*. **1984**, *57*, 59-132
2. Cederbaum, L., Domcke, W., On vibrational structure of photoelectron spectra by the Green's functions method. *J.Chem. Phys*. **1984**, *60*, 2878-2896.
3. Glushkov, A. An universal quasiparticle energy functional in a density functional theory for relativistic atom. *Opt. and Spectr*. **1989**, *66*(1), 31-36.
4. Glushkov, A.V. New approach to theoretical definition of ionization potentials for molecules on the basis of Green's function method. *J. Phys. Chem*. **1992**, 66, 2671-2677.
5. Glushkov, A.V. *Relativistic and correlation effects in spectra of atomic systems*. Astroprint: Odessa, **2006**.
6. Glushkov, A.V. *Relativistic Quantum theory. Quantum mechanics of atomic systems.* Astroprint: Odessa, **2008**.
7. Ignatenko, A.V. and Lavrenko, A.P., Spectroscopic factors of diatomic molecules: optimized green's functions and density functional method. Photoelectronics. **2019**. Vol.28. P.83-89.
8. Ignatenko, A.V., Glushkov, A.V., Lepikh, Ya.I., Kvasikova, A.S. Photoelectron spectroscopy of diatomic molecules:optimized Green's functions and density functional approach**.** *Photoelectronics*. **2018**, *27*, 44-51.
9. Glushkov A., Khetselius O., Svinarenko A., Buyadzhi V. *Spectroscopy of autoionization states of heavy atoms and multiply charged ion*s. TEC, **2015**.

10. Ponomarenko, E.L., Kuznetsova, A.A., Dubrovskaya, Yu.V., Bakunina, E.V. Energy and spectroscopic parameters of diatomics within generalized equation of motion method. *Photoelectronics*. **2016**, *25*, 114-118.
11. Svinarenko, A.A., Glushkov, A. V., Khetselius, O.Yu., Ternovsky,V.B., Dubrovskaya, Yu., Kuznetsova, A., Buyadzhi, V. Theoretical spectroscopy of rare-earth elements: spectra and autoionization resonances. *Rare Earth Element*, Ed. J. Orjuela (InTech) **2017**, pp 83-104
12. Glushkov, A.V., Khetselius, O.Yu., Svinarenko A.A., Buyadzhi, V.V., Ternovsky, V.B, Kuznetsova, A., Bashkarev, P Relativistic perturbation theory formalism to computing spectra and radiation characteristics: application to heavy element. *Recent Studies in Perturbation Theory*, ed. D. Uzunov (InTech) **2017**, 131-150.
13. Kobayashi, K., Kurita, N., Kumahora, H., Kuzatami, T. Bond-energy calculations of Cu, Ag, CuAg with the generalized gradient approximation. *Phys.Rev.A.* **1991**, *43*, 5810
14. Lagowscki, J., Vosko, S. Analysis of local and gradient-correction correlation energy functionals using electron removal energies. *J. Phys.B: At. Mol. Opt. Phys*. **1988**, *21*(1), 203-208.
15. Guo, Y., Whitehead, M. Effect of the correlation correction on the ionization potential and electron affinity in atoms. *Phys.Rev.A.* **1989**, *39*(1), 28-34.
16. Khetselius, O.Yu., Lopatkin Yu.M., Dubrovskaya, Yu.V, Svinarenko A.A. Sensing hyperfine-structure, electroweak interaction and parity non-conservation effect in heavy atoms and nuclei: New nuclear-QED approach. *Sensor Electr. And Microsyst. Techn*. **2010,** 7(2), 11-19.
17. Florko, T., Ambrosov, S., Svinarenko A., Tkach, T. Collisional shift of the heavy atoms hyperfine lines in an atmosphere of the inert gas. *J. Phys: Conf. Ser*. **2012**, *397*(1), 012037.
18. Khetselius, O. Relativistic perturbation theory calculation of the hyperfine structure parameters for some heavy-element isotopes. *Int. J. Quant. Chem.* **2009,** *109,* 3330–3335.
19. Khetselius, O. Relativistic calculation of the hyperfine structure parameters for heavy elements and laser detection of the heavy isotopes. *Phys. Scr.* **2009,** *135,* 014023.
20. Glushkov A.V., *Atom in electromagnetic field*. KNT: Kiev, **2005**.
21. Khetselius, O. Yu. *Hyperfine structure of atomic spectra*; Astroprint: Odessa, **2008**.
22. Khetselius, O.Yu. *Quantum structure of electroweak interaction in heavy finite Fermi-systems*. Astroprint: Odessa, **2011**.
23. Khetselius, O.Y.., Glushkov, A.V., Gurskaya, M.Y., Kuznetsova, A.A., Dubrovskaya, Yu.V., Serga, I.N., Vitavetskaya, L.A. Computational modelling parity nonconservation and electroweak interaction effects in heavy atomic systems within the nuclear-relativistic many-body perturbation theory. *J. Phys.: Conf. Ser.* **2017,** *905*(1), 012029.
24. Glushkov, A., Gurskaya, M., Ignatenko, A., Smirnov, A., Serga, I., Svinarenko, A., Ternovsky, E. Computational code in atomic and nuclear quantum optics: Advanced computing multiphoton resonance parameters for atoms in a strong laser field. *J. Phys.: Conf. Ser*. **2017**, *905*(1), 012004.
25. Ambrosov S., Ignatenko V., Korchevsky D., Kozlovskaya V. Sensing stochasticity of atomic systems in crossed electric and magnetic fields by analysis of level statistics for continuous energy spectra. *Sensor Electr. and Microsyst. Techn*. **2005**, Issue 2, 19-23.
26. Buyadzhi, V.V., Glushkov, A.V., Mansarliysky, V.F., Ignatenko, A.V., Svinarenko, A. Spectroscopy of atoms in a strong laser field: new method to sensing ac stark effect, multiphoton resonances parameters and ionization cross-sections. *Sensor Electr. and Microsyst. Techn*. **2015**, *12*(4), 27-36.
27. Svinarenko A.A., Mischenko E., Loboda A., Dubrovskaya Yu. Quantum measure of frequency and sensing the collisional

shift of the ytterbium hyperfine lines in medium of helium gas. *Sensor Electr. and Microsyst. Techn*. **2009**, 1, 25-29.
28. Malinovskaya S.V., Dubrovskaya Yu.V., Zelentzova T.N. The atomic chemical environment effect on the b decay probabilities: Relativistic calculation. *Herald of Kiev Nat. Univ. Ser.: Phys.-Math*. **2004**, N4, 427-432.
29. Glushkov A., Khetselius O., Svinarenko A., Prepelitsa G., Mischenko E., The Green's functions and density functional approach to vibrational structure in the photoelectron spectra for molecules. *AIP Conf. Proc*. **2010**, *1290*, 263-268.
30. Khetselius O., Florko T., Svinarenko A., Tkach T. Radiative and collisional spectroscopy of hyperfine lines of the Li-like heavy ions and Tl atom in an atmosphere of inert gas. *Phys.Scripta*. **2013**, *T153*, 014037.
31. Glushkov, A.V., Kivganov, A.F., Khokhlov, V.N., Buyadzhi, T.V., Vitavetskaya, L.A., Borovskaya, G.A., Polishchuk, V.N. Calculation of the spectroscopic characteristics of diatomic van der Waals molecules and ions: Inert gas atom—halogen-type inert gas ion in the ground state. *Russian Phys. Journ*. **1998**, *41*(3), 223-226
32. Glushkov, A., Malinovskii, A., Efimov, V., Kivganov, A., Khokhlov, V., Vitavetskaya, L., Borovskaya, G., Calculation of alkaline metal dimers in terms of model perturbation theory. *J. Struct. Chem*. **1998**, *39*(2), 179-185.
33. Khetselius, O.Yu. Hyperfine structure of radium. *Photoelectron*. **2005**, *14*, 83-85
34. Khetselius O.Yu., Quantum Geometry: New approach to quantization of the quasistationary states of Dirac equation for super heavy ion and calculating hyper fine structure parameters. *Proc. Int. Geometry Center*. **2012**, *5*(3-4), 39-45.
35. Dubrovskaya, Yu., Khetselius, O.Yu., Vitavetskaya, L., Ternovsky, V., Serga, I. Quantum chemistry and spectroscopy of pionic atomic systems with accounting for relativistic, radiative, and strong interaction effects. *Adv. in Quantum Chem.* **2019,** Vol.78, pp 193-222.
36. Khetselius, O.Yu., Glushkov, A.V., Dubrovskaya, Yu.V., Chernyakova, Yu.G., Ignatenko, A.V., Serga, I.N., Vitavetskaya, L. Relativistic quantum chemistry and spectroscopy of exotic atomic systems with accounting for strong interaction effects. In: Wang YA, Thachuk M, Krems R, Maruani J (eds) *Concepts, Methods and Applications of Quantum Systems in Chemistry and Physics*. Springer, Cham, **2018**; Vol. 31, pp. 71-91.
37. Glushkov, A.V., Ivanov, L.N. Radiation decay of atomic states: atomic residue polarization and gauge noninvariant contributions. *Phys. Lett. A* **1992,** *170*, 33.
38. Glushkov, A.V.; Ivanov, L.N. DC strong-field Stark effect: consistent quantum-mechanical approach. *J. Phys. B: At. Mol. Opt. Phys.* **1993,** *26*, L379-386.
39. Ivanova, E., Glushkov, A. Theoretical investigation of spectra of multicharged ions of F-like and Ne-like isoelectronic sequences. J. Quant. Spectr. and Rad. Tr. **1986**, *36*(2), 127-145.
40. Ivanova, E.P., Ivanov, L.N., Glushkov, A., Kramida, A. High order corrections in the relativistic perturbation theory with the model zeroth approximation, Mg-Like and Ne-Like Ions. *Phys. Scripta* **1985**, *32*, 513-522.
41. Glushkov, A.V. Multiphoton spectroscopy of atoms and nuclei in a laser field: Relativistic energy approach and radiation atomic lines moments method. *Adv. in Quantum Chem.* **2019**, *78*, 253-285.
42. Glushkov, A.V., Khetselius, O.Yu., Svinarenko, A.A., Buyadzhi, V. *Methods of computational mathematics and mathematical physics*. *P.1*. TES: Odessa, **2015.**
43. Glushkov, A.V., Safranov, T.A., Khetselius, O.Yu., Ignatenko, A.V., Buyadzhi, V.V., Svinarenko, A.A. Analysis and forecast of the environmental radioactivity dynamics based on methods of chaos theory: General conceptions. *Environm. Problems*. **2016**, *1*(2), 115-120.
44. Glushkov, A., Buyadzhi, V., Kvasikova,

A., Ignatenko, A., Kuznetsova, A., Prepelitsa, G., Ternovsky, V. Non-Linear chaotic dynamics of quantum systems: Molecules in an electromagnetic field and laser systems. In: Tadjer A, Pavlov R, Maruani J etal, (eds) *Quantum Systems in Physics, Chemistry, and Biology*. Springer, Cham. **2017**, *30*, 169

45. Robert, C., Morrison, R., Liu, G., Extended Koopmans theorem: approximate ionization energies from MCSCF Wave Functions. *J. Comp. Chem*. **1992**, *13*, 1004-1010.
46. Glushkov A.V., Khetselius O.Yu., Loboda A.V., Ignatenko A., Svinarenko A., Korchevsky D., Lovett L., QED Approach to Modeling Spectra of the Multicharged Ions in a Plasma: Oscillator and Electron-ion Collision Strengths.. *AIP Conference Proceedings***. 2008**. 1058. 175-177
47. Svinarenko, A. Spectroscopy of autoionization resonancesin spectra of barium. *Photoelectronics*. *2014*, *23*, 86-90.

PACS 33.20.-t

Ignatenko A.V., Svinarenko A.A., Mansarliysky V.F., Sakun T.N.

SPECTROSCOPIC FACTORS OF DIATOMIC MOLECULES: OPTIMIZED GREEN'S FUNCTIONS AND DENSITY FUNCTIONAL METHOD

Summary. It is presented an advanced approach to computing the energy and spectral parameters of the diatomic molecules, which is based on the hybrid combined density functional theory (DFT) and the Green's-functions (GF) approach. The Fermi-liquid quasiparticle version of the density functional theory is modified and used. The density of states, which describe the vibrational structure in photoelectron spectra, is defined with the use of combined DFT-GF approach and is well approximated by using only the first order coupling constants in the optimized one-quasiparticle approximation. Using the combined DFT-GF approach to computing the spectroscopic factors of diatomic molecules leads to significant simplification of the calculation procedure and increasing an accuracy of theoretical prediction. As illustration, the results of computing the bond energies in a number of known diatomic molecules are presented and compared with alternative theoretical results, obtained within discrete-variational X_α, muffin-tin orbitals and other methods.

Key words: diatomic molecules, Green's functions, density functional

PACS 33.20.-t

Игнатенко А.В., Свинаренко А.А., Мансарлийский В.Ф., Сакун Т.Н.

ОПТИМИЗИРОВАННЫЙ МЕТОД ФУНКЦИОНАЛА ПЛОТНОСТИ И ФУНКЦИЙ ГРИНА В РАСЧЕТАХ ЭНЕРГИИ СВЯЗИ ДВУХАТОМНЫХ МОЛЕКУЛ

Резюме. Представлен усовершенствованный подход к вычислению энергетических и спектральных параметров двухатомных молекул, базирующийся на гибридной комбинированной теории функционала плотности (ТФП) и методе функций Грина (ФГ). Используется модель ферми-жидкостная квазичастичная версия ТФП. Плотность состояний, которая описывает колебательную структуру в фотоэлектронных спектрах, определяется с использованием комбинированного подхода ТФП - ФГ. Использование комбинированного ТФП-ФГ подхода приводит к значительному упрощению процедуры расчета и повышению точности теоретического прогнозирования. В качестве иллюстрации представлены результаты расчета энергий связи в ряде известных двухатомных молекул, которые сравниваются с альтернативными теоретическими результатами, полученными с помощью дискретно-вариационного X_α и других подходов.

Ключевые слова: двухатомные молекулы, функция Грина, функционал плотности

PACS 33.20.-t

Ігнатенко Г.В., Свинаренко А.А., Мансарлійський В.Ф. , Сакун Т.М.

ОПТИМІЗОВАНИЙ МЕТОД ФУНКЦІОНАЛУ ГУСТИНИ І ФУНКЦІЙ ГРІНА В РОЗРАХУНКАХ ЕНЕРГІЇ ЗВ'ЯЗКУ ДВОАТОМНИХ МОЛЕКУЛ

Резюме. Представлений вдосконалений метод обчислення енергетичних та спектральних параметрів 2-атомних молекул, що базується на гібридній теорії функціонала щільності (ТФП) і методі функцій Гріна (ФГ). Використано фермі-рідинну квазічастинкову версію ТФП. Густина станів, які описує коливальну структуру фотоелектронного спектру, визначається в межах ТФП-ФГ методу. Використання комбінованого ТФП-ФГ методу призводить до спрощення процедури обчислень, підвищення точності прогнозу. В якості ілюстрації представлені результати розрахунку енергій зв'язку в ряді відомих двоатомних молекул, які порівнюються з альтернативними теоретичними результатами, отриманими за допомогою дискретно-варіаційного і інших підходів.

Ключові слова: двоатомні молекули, функція Гріна, функціонал густини.

PACS 31.15.A-; 32.30.-r

Chernyshev A. S., Efimova E. A., Buyadzhi V. V., Nikola L. V.

I.I. Mechnikov Odesa National University, Dvoryanskaya str. , 2, Odesa, 65000
Odesa State Environmental University, 15, Lvovskaya str., Odesa-16, 65016
E-mail: buyadzhivv@gmail.com

CASCADE OF AUGER TRANSITIONS IN SPECTRUM OF XENON: THEORETICAL DATA

The energy parameters of the Auger transitions for the xenon atomic system are calculated within the combined relativistic energy approach and relativistic many-body perturbation theory with the zeroth order density functional approximation. The results are compared with reported experimental data as well as with those obtained by semiempirical method. The important point is linked with an accurate accounting for the complex exchange-correlation (polarization) effect contributions and using the optimized one-quasiparticle representation in the relativistic many-body perturbation theory zeroth order that significantly provides a physically reasonable agreement between theory and experiment.

1. Introduction

Development of the novel experimental methods in a modern Auger- spectroscopy allows to open new interesting features especially for the heavy complex atomic systems. It is easily to understand that a synchrotron radiation sources provide an effective way to ionize deep core hole States in heavy multielectron systems (e.g. [1]). As result, new advanced data on the energy and spectral parameters of the complex atomic systems can be obtained.

Let us remind following to ref . [2] that studies in modern atomic physics (spectroscopy, spectral lines theory, theory of atomic collisions etc), astrophysics, plasma physics, laser physics and quantum and photoelectronics requires an availability of sets of correct data on the energetic, spectroscopic and structural properties of atoms, including the data on the Auger transitions [1-8]. The kinetic energy of the ejected Auger electron is measured by Auger-electron spectroscopy (AES). Sensing the Auger spectra in atomic systems and solids gives the important data for the whole number of scientific and technological applications. So called two-step model is used most widely when calculating the Auger decay characteristics [1-5]. Since the vacancy lifetime in an inner atomic shell is rather long (about 10^{-17} to 10^{-14}s), the atom ionization and the Auger emission are considered to be two independent processes. In the more correct dynamic theory of the Auger effect [2,3] the processes are not believed to be independent from one another. The fact is taken into account that the relaxation processes due to Coulomb interaction between electrons and resulting in the electron distribution in the vacancy field have no time to be over prior to the transition.

In fact, a consistent Auger decay theory has to take into account correctly a number of correlation effects, including the energy dependence of the vacancy mass operator, the continuum pressure, spreading of the initial state over a set of configurations etc [1-19]. The most widespread theoretical studying the Auger spectra parameters is based on using the multi-configuration Dirac-Fock (MCDF) calculation [2,3]. The theoretical predictions based on MCDF calculations have been carried out within different approximations and remained hitherto nonsatisfactory in many relations. Earlier [8-13] it has been proposed relativistic perturbation theory (PT) method of the Auger decay characteristics for complex atoms, which is based on the Gell-Mann and Low S-matrix formalism energy approach) and QED PT formalism [4-7]. The novel element consists in using the optimal basis of the electron state functions derived from the minimization condition for the calibration-non-invariant

contribution (the second order PT polarization diagrams contribution) to the imaginary part of the multi-electron system energy already at the first non-disappearing approximation of the PT. Earlier it has been applied in studying the Auger decay characteristics for a set of neutral atoms, quasi-molecules and solids. Besides, the ionization cross-sections of inner shells in various atoms and the Auger electron energies in solids were estimated. Here we apply the combined relativistic energy approach and relativistic many-body perturbation theory with the zeroth order density functional approximation is applied to determination of the energy parameters of the Auger transitions of the xenon atomic system.

2. The theoretical method

In Refs. [2, 8-17] the fundamentals of the relativistic many-body PT formalism have been in detail presented, so further we are limited only by the key elements, following the cited Refs. Let us remind that the majority of complex atomic systems possess a dense energy spectrum of interacting states. In Refs. [2-13, 19-38] there is realized field procedure for calculating the energy shifts ΔE of degenerate states, which is connected with the secular matrix *M* diagonalization. The whole calculation of the energies and decay probabilities of a non-degenerate excited state is reduced to the calculation and diagonalization of the *M*. The complex secular matrix *M* is represented in the form [2,9,10]:

$$M = M^{(0)} + M^{(1)} + M^{(2)} + M^{(3)}. \qquad (1)$$

where $M^{(0)}$ is the contribution of the vacuum diagrams of all order of PT, and $M^{(1)}$, $M^{(2)}, M^{(3)}$ those of the one-, two- and three-QP diagrams respectively. The diagonal matrix $M^{(1)}$ can be presented as a sum of the independent 1QP contributions. The optimized 1-QP representation is the best one to determine the zeroth approximation. In the relativistic energy approach [4-9], which has received a great applications during solving numerous problems of atomic, molecular and nuclear physics (e.g., see Refs. [10-13]), the imaginary part of electron energy shift of an atom is directly connected with the radiation decay possibility (transition probability). An approach, using the Gell-Mann and Low formula with the QED scattering matrix, is used in treating the relativistic atom. The total energy shift of the state is usually presented in the form:

$$\Delta E = \mathrm{Re}\Delta E + i\,\Gamma/2\,, \qquad (2)$$

where Γ is interpreted as the level width, and the decay possibility P = Γ. The imaginary part of electron energy of the system, which is defined in the lowest order of perturbation theory as [4]:

$$\mathrm{Im}\Delta E(B) = -\frac{e^2}{4\pi} \sum_{\substack{\alpha>n>f \\ [\alpha<n\le f]}} V^{|\omega_{\alpha n}|}_{\alpha n \alpha n}\,, \qquad (3)$$

where (α>n>f) for electron and (α<n<f) for vacancy. Under calculating the matrix elements (3) one should use the angle symmetry of the task and write the expansion for potential $\sin|\omega|r_{12}/r_{12}$ on spherical functions as follows [4]:

$$\frac{\sin|\omega|r_{12}}{r_{12}} = \frac{\pi}{2\sqrt{r_1 r_2}} \sum_{\lambda=0}^{\infty} (\lambda) J_{\lambda+1/2}(|\omega|r_1) \cdot J_{\lambda+1/2}(|\omega|r_1) J_{\lambda+1/2}(|\omega|r_2) P_\lambda(\cos \boldsymbol{r}_1 \boldsymbol{r}_2)\,, \qquad (4)$$

where J is the Bessel function of first kind and (λ)= 2λ + 1. This expansion is corresponding to usual multipole one for probability of radiative decay.

Within the frame of QED PT approach the Auger transition probability and the Auger line intensity are defined by the square of an electron interaction matrix element having the form [4]:

$$V^{\omega}_{1234} = [(j_1)(j_2)(j_3)(j_4)]^{1/2} \sum_{\lambda\mu} (-1)^{\mu} \begin{pmatrix} j_1 j_3 & \lambda \\ m_1 - m_3 & \mu \end{pmatrix} \times \mathrm{Re}\, Q_\lambda(1234);$$

$$Q_\lambda = Q_\lambda^{\mathrm{Qul}} + Q_\lambda^{\mathrm{Br}} \cdot \qquad (5)$$

The terms Q_λ^{Qul} and Q_λ^{Br} correspond to subdivision of the potential into Coulomb part $cos|\omega|r_{12}/r_{12}$ and Breat one, $cos|\omega|r_{12}\alpha_1\alpha_2/r_{12}$. The real part of the electron interaction matrix element is determined using expansion in terms of Bessel functions:

$$\frac{\cos|\omega|r_{12}}{r_{12}} = \frac{\pi}{2\sqrt{r_1 r_2}} \sum_{\lambda=0} (\lambda) J_{\lambda+1/2}(|\omega|r_<) J_{-\lambda-1/2}(|\omega|r_>) P_\lambda(\cos \mathbf{r}_1\mathbf{r}_2) \qquad (6)$$

where J is the 1st order Bessel function, $(\lambda)=2\lambda+1$.

The Coulomb part Q_λ^{Qul} is expressed in terms of radial integrals R_λ , angular coefficients S_λ [4]:

$$\mathrm{Re}\,Q_\lambda^{\mathrm{Qul}} = \frac{1}{Z}\mathrm{Re}\{R_l(1243)S_\lambda(1243) + R_\lambda(\tilde{1}24\tilde{3})S_\lambda(\tilde{1}24\tilde{3}) +$$

$$+ R_\lambda(1\tilde{2}\tilde{4}3)S_\lambda(1\tilde{2}\tilde{4}3) + R_\lambda(\tilde{1}\tilde{2}\tilde{4}\tilde{3})S_\lambda(\tilde{1}\tilde{2}\tilde{4}\tilde{3})\}. \qquad (7)$$

As a result, the Auger decay probability is expressed in terms of $\mathrm{Re}Q_\lambda(1243)$ matrix elements:

$$\mathrm{Re}\,R_\lambda(1243) = \iint d\eta r_1^2 r_2^2 f_1(\eta_1) f_3(\eta_1) f_2(r_2) f_4(r_2) Z_\lambda^{(1)}(r_<) Z_\lambda^{(1)}(r_>) \qquad (8)$$

where f is the large component of radial part of single electron state Dirac function; function Z and angular coefficient are defined in Refs. [4-7]. The other items in (7) include small components of the Dirac functions; the sign «~» means that in (7) the large radial component f_i is to be changed by the small g_i one and the moment l_i is to be changed by $\tilde{l}_i = l_i - 1$ for Dirac number æ$_1$> 0 and l_i+1 for æ$_i$<0. The Breat part of Q is defined in [4,11]. The Auger width is obtained from the adiabatic Gell-Mann and Low formula for the energy shift [4].

The direct contribution to the Auger level width with a vacancy $n_\alpha l_\alpha j_\alpha m_\alpha$ is as follows:

$$\sum_\lambda \frac{2}{(\lambda)(j_\alpha)} \sum_{\beta\gamma\le f} \sum_{k>f} Q_\lambda(\alpha k\gamma\beta) Q_\lambda(\beta\gamma k\alpha), \qquad (9)$$

while the exchange diagram contribution is:

$$\frac{2}{(j_\alpha)} \sum_{\lambda_1\lambda_2} \sum_{\beta\gamma\le f} \sum_{k>f} Q_{\lambda_1}(\alpha k\gamma\beta) Q_{\lambda_2}(\beta\gamma k\alpha) \begin{Bmatrix} j_\alpha & j_\gamma & \lambda_2 \\ j_k & j_\beta & \lambda_1 \end{Bmatrix}. \qquad (10)$$

The partial items of the $\sum_{\beta\gamma} \sum_{k}^{\wedge}$ sum answer to contributions of $\alpha^{-1} \to (\beta\gamma)^{-1}K$ channels resulting in formation of two new vacancies $\beta\gamma$ and one free electron k: $\omega_k = \omega_\alpha + \omega_\beta - \omega_\alpha$.

The calculating of all matrix elements, wave functions, Bessel functions etc is reduced to solving the system of differential equations. The formulas for the autoionization (Auger) decay probability include the radial integrals $R_\alpha(\alpha k\gamma\beta)$, where one of the functions describes electron in the continuum state.

When calculating this integral, the correct normalization of the wave functions is very important, namely, they should have the following asymptotic at $r \to 0$:

$$\left.\begin{matrix} f \\ g \end{matrix}\right\} \to (\lambda\omega)^{-1/2} \begin{cases} \left[\omega + (\alpha Z)^{-2}\right]^{-1/2} sin(kr + \delta), \\ \left[\omega - (\alpha Z)^{-2}\right]^{-1/2} cos(kr + \delta). \end{cases} \qquad (12)$$

The important aspect of the whole procedure is an accurate accounting for the exchange-correlation effects. We have used the generalized relativistic Kohn-Sham density functional [8-17] in the zeroth approximation of relativistic PT; naturally, the perturbation operator contents the operator (7) minus the cited Kohn-Sham density functional. Further the wave functions are corrected by accounting of the first order PT contribution. Besides, we realize the procedure of optimization of relativistic orbitals base. The main idea is based on using ab initio optimization procedure, which is reduced to minimization of the gauge dependent multielectron contribution $Im\Delta E_{ninv}$ of the lowest QED PT corrections to the radiation widths of atomic levels.

The formulae for the Auger decay probability include the radial integrals $R_\alpha(\alpha k\gamma\beta)$, where one of the functions describes electron in the continuum state. The energy of an electron formed due to a transition *jkl* is defined by the difference between energies of atom with a hole at *j* level and double-ionized atom at *kl* levels in final state:

$$E_A(jkl, {}^{2S+1}L_J) = E_A^{+}(j) - E_A^{2+}(kl, {}^{2S+1}L_J) \quad (13)$$

To single out the above-mentioned correlation effects, the equation (13) can be presented as [8,9]:

$$E_A(jkl, {}^{2S+1}L_J) = E(j) - E(k) - E(l) - \Delta(k,l; {}^{2S+1}L_J), \quad (14)$$

where the item Δ takes into account the dynamic correlation effects (relaxation due to hole screening with electrons etc.) To take these effects into account, the set of procedures elaborated in the atomic theory [8-13] is used. All calculations are performed on the basis of the modified numeral code Superatom (version 93).

3. Results and conclusion

Below the energy parameters of the Auger transitions for the xenon are presented and compared with the experimental data as well as with those obtained by semiempirical and perturbation theory methods. In table 1 we present data on the initial and final states of the most intense $4d^{-2}\rightarrow 4d^{-1}\rightarrow 5p^{-2}$ and $4d^{-1}5p^{-2}\rightarrow 5p^{-}4$ Auger transitions in the neutral xenon.

Our theoretical data (the relativistic many-body PT) and the theoretical semiempirical data by Jonauskas et al [1], and relativistic perturbation theory data [9] for the energies of the Auger transitions are also given.

The analysis of the presented results in table 1 results in the conclusions that the précised description of the Auger processes requires the detailed accurate accounting for the exchange-correlation effects, including the particle-hole interaction, screening effects and iterations of the mass operator.

Table 1. Calculated and experimental energies of the Auger transitions E_k for Xe (see text)

Initial state	Final state	E_{th} [1]	E_{th}, [9]	E_{th}, our	E_{ex} [1]
$4d^{-2}\ {}^1G_4$	$4d^{-1}\ 5p^{-2}({}^1D)\ {}^2F_{5/2}$	31.5	31.3	31.2	
$4d^{-2}\ {}^1G_4$	$4d^{-1}\ 5p^{-2}\ ({}^3P)\ {}^2F_{7/2}$	31.2	31.0	30.9	30.8
$4d^{-2}\ {}^1G_4$	$4d^{-1}\ 5p^{-2}\ ({}^1D)\ {}^2G_{9/2}$	30.9	30.6	30.5	
$4d^{-2}\ {}^1D^2$	$4d^{-1}\ 5p^{-2}\ ({}^3P)\ {}^2D_{5/2}$	30.5	30.3	30.2	30.3
$4d^{-2}\ {}^1G_4$	$4d^{-1}\ 5p^{-2}\ ({}^3P)\ {}^2D_{3/2}$	30.1	30.0	29.9	29.9
$4d^{-2}\ {}^1G_4$	$4d^{-1}\ 5p^{-2}\ ({}^1D)\ {}^2D_{5/2}$	29.3	29.2	29.1	
$4d^{-2}\ {}^1D_2$	$4d^{-1}\ 5p^{-2}\ ({}^1D)\ {}^2F_{7/2}$	29.1	29.1	29.0	29.1
$4d^{-2}\ {}^1G_4$	$4d^{-1}\ 5p^{-2}\ ({}^1D)\ {}^2F_{7/2}$	29.1	29.1	29.1	
$4d^{-2}\ {}^3F_4$	$4d^{-1}\ 5p^{-2}\ ({}^3P)\ {}^4F_{9/2}$	29.1	29.1	29.1	
$4d^{-2}\ {}^3F_4$	$4d^{-1}\ 5p^{-2}\ ({}^3P)\ {}^4F_{5/2}$	28.4	28.3	28.2	
$4d^{-2}\ {}^3F_4$	$4d^{-1}\ 5p^{-2}\ ({}^3P)\ {}^2F_{5/2}$	28.1	28.0	28.2	28.3
$4d^{-2}\ {}^1G_4$	$4d^{-1}\ 5p^{-2}\ ({}^1S)\ {}^2D_{5/2}$	27.8	27.8	27.8	27.9
$4d^{-2}\ {}^3F_2$	$4d^{-1}\ 5p^{-2}\ ({}^1D)\ {}^2G_{9/2}$	27.4	27.3	27.2	27.1
$4d^{-2}\ {}^3P_1$	$4d^{-1}\ 5p^{-2}\ ({}^1S)\ {}^2D_{5/2}$	27.0	26.9	26.8	
$4d^{-2}\ {}^3F_4$	$4d^{-1}\ 5p^{-2}\ ({}^3P)\ {}^2F_{5/2}$	26.5	26.5	26.4	26.5
$4d^{-2}\ {}^1D_2$	$4d^{-1}\ 5p^{-2}\ ({}^1S)\ {}^2D_{3/2}$	26.1	26.2	26.1	
$4d^{-2}\ {}^`1G_4$	$4d^{-1}\ 5p^{-2}\ ({}^1S)\ {}^2D_{3/2}$	26.1	26.2	26.1	
$4d^{-2}\ {}^3P_2$	$4d^{-1}\ 5p^{-2}\ ({}^1S)\ {}^2D_{5/2}$	25.9	26.0	25.9	
$4d^{-2}\ {}^3F_4$	$4d^{-1}\ 5p^{-2}\ ({}^1D)\ {}^2G_{9/2}$	25.6	25.9	25.8	-
$4d^{-2}\ {}^3F_2$	$4d^{-1}\ 5p^{-2}\ ({}^1S)\ {}^2D_{5/2}$	24.3	24.6	24.6	24.7
$4d^{-2}\ {}^3F_4$	$4d^{-1}\ 5p^{-2}\ ({}^1S)\ {}^2D_{5/2}$	22.5	22.9	22.8	

The relativistic many-body PT approach provides physically reasonable results in comparison with the fine experimental results due to a considerable extent to more correct accounting for complex inter electron exchange-correlation effects. It is important to note that using more correct gauge-invariant procedure of generating the relativistic orbital bases in the zeroth approximation of the consistent relativistic perturbation theory is directly connected with correctness of accounting for the exchange-correlation effects. The further theoretical progress can be reached by the next refinement of theoretical procedure.

References

[1] Jonauskas V., Partanen L., Kucas S., Karazjia R., Huttula M., Aksela S., Aksela H., Auger cascade satellites following 3d ionization in xenon. J. *Phys.B. Atom.Mol.Opt. Phys*. 2003, *36*, 4403-4416.

[2] Efimova E, Chernyshev A, Buyadzhi V., Nikola L,Theoretical Auger spectroscopy of the neon: transition energies and widths.*Photoelectronics.* **2019.** *28*, 24-31

[3] Chernyakova, Y., Ignatenko, A., Vitavetskaya, L.A. Sensing the tokamak plasma parameters by means high resolution x-ray theoretical spectroscopy method: new scheme. *Sensor Electr. and Microsyst. Techn*. **2004**, *1*, 20-24.

[4] Aglitsky, E., Safronova, U. *Spectroscopy of autoionization states of atomic systems*. Energoat: Moscow, 1992**.**

[5] Glushkov, A.V., Khetselius, O.Yu., Svinarenko, A.A., Buyadzhi, V.V., *Spectroscopy of autoionization states of heavy atoms and multiply charged ions*. TEC: Odessa, **2015**.

[6] Buyadzhi, V., Kuznetsova, A., Buyadzhi, A., Ternovsky, E., Tkach, T. Advanced quantum approach in radiative and collisional spectroscopy of multicharged ions in plasmas. *Adv. in Quant. Chem*. **2019**, *78*, 171-191.

[7] Glushkov, A., Buyadzhi, V., Svinarenko, A., Ternovsky, E. Advanced relativistic energy approach in electron-collisional spectroscopy of multicharged ions in plasma. *Concepts, Methods, Applications of Quantum Systems in Chemistry and Physics* (Springer). **2018**, *31*, 55-69.

[8] Glushkov, A., Ambrosov, S., Prepelitsa, G., Kozlovskaya, V. Auger effect in atoms and solids: Calculation of characteristics of Auger decay in atoms, quasimolecules and solids with apllication to surface composition analysis. *Funct. Materials*. **2003**, *10*, 206.

[9] Nikola, L. Resonant Auger spectroscopy of the atoms of inert gases. *Photoelectr*. 2011, *20*, 104.

[10] Khetselius, O.Yu. Quantum Geometry: New approach to quantization of quasistationary states of Dirac equation for superheavy ion and calculating hyperfine structure parameters. *Proc. Int. Geometry Center*. 2012, *5*(3-4), 39-45.

[11] Ivanov, L.N., Ivanova, E.P., Aglitsky, E. Modern trends in the spectroscopy of multicharged ions. *Phys. Rep.* **1988,** *166.*

[12] Svinarenko, A., Khetselius, O., Buyadzhi, V., Florko, T., Zaichko, P., Ponomarenko E. Spectroscopy of Rydberg atoms in a Black-body radiation field: Relativistic theory of excitation and ionization. *J. Phys.: Conf. Ser*. **2014**, *548*, 012048.

[13] Glushkov A.V., Ivanov, L.N. DC strong-field Stark effect: consistent quantum-mechanical approach. *J. Phys. B: At. Mol. Opt. Phys.* **1993,** *26*, L379-386.

[14] Glushkov, A. Spectroscopy of atom and nucleus in a strong laser field: Stark effect and multiphoton resonances. *J. Phys.: Conf. Ser*. **2014**, *548*, 012020.

[15] Osmekhin, S., Fritzsche, S., Grum-Grzhimailo, A.N., Huttula1, M., Aksela, H., Aksela S. Angle-resolved study of the Ar $2p^{-1}_{1/2}3d$ resonant Auger decay. *J. Phys. B: At. Phys*. **2008**, *41*, 145003.

[16] Pahler, M., Caldwell, C., Schaphorst, S., Krause, M. Intrinsic linewidths of

neon $2s2p^5(^{1,3}P)nl^2L$ correlation satellites. *J. Phys. B. At. Phys*. **1993**, *26*, 1617-1622.

[17] Sinanis, C., Aspromallis, G., Nicolaides, C. Electron correlation in Auger spectra of the Ne^+ K $2s2p^5(^{3,1}P^0)3p^2S$ satellites. J. Phys. B. At. Phys. **1995**, *28*, L423-428.

[18] Armen, G.B., Larkins, F.P. Valence Auger and X-ray participator and spectator processes for neon and argon atoms. *J. Phys. B. At. Mol. Opt. Phys*. **1991**, *24*, 741-760.

[19] Glushkov, A.V. Relativistic and correlation effects in spectra of atomic systems. Astroprint: Odessa, **2006**.

[20] Khetselius, O.Yu. *Quantum structure of electroweak interaction in heavy finite Fermi-systems.* Astroprint: Odessa, **2011**.

[21] Glushkov A, Spectroscopy of cooperative muon-gamma-nuclear processes: Energy and spectral parameters *J. Phys.: Conf. Ser.* **2012,** *397*, 012011.

[22] Khetselius, O.Yu. Hyperfine structure of atomic spectra.-Odessa: Astroprint, **2008.**

[23] Glushkov, A.V., Ivanov, L.N. Radiation decay of atomic states: atomic residue polarization and gauge noninvariant contributions. *Phys. Lett. A* **1992,** *170*, 33.

[24] Glushkov, A.V.; Ivanov, L.N. DC strong-field Stark effect: consistent quantum-mechanical approach. *J. Phys. B: At. Mol. Opt. Phys.* **1993,** *26*, L379-386.

[25] Ivanova, E., Glushkov, A. Theoretical investigation of spectra of multicharged ions of F-like and Ne-like isoelectronic sequences. J. Quant. Spectr. and Rad. Tr. **1986**, *36*(2), 127-145.

[26] Ivanova, E.P., Ivanov, L.N., Glushkov, A., Kramida, A. High order corrections in the relativistic perturbation theory with the model zeroth approximation, Mg-Like and Ne-Like Ions. *Phys. Scripta* **1985**, *32*, 513-522.

[27] Dubrovskaya, Yu., Khetselius, O.Yu., Vitavetskaya, L., Ternovsky, V., Serga, I. Quantum chemistry and spectroscopy of pionic atomic systems with accounting for relativistic, radiative, and strong interaction effects. *Adv. Quantum Chem.* **2019,** *78*, 193-222.

[28] Khetselius, O.Yu., Glushkov, A.V., Dubrovskaya, Yu., Chernyakova, Yu., Ignatenko, A., Serga, I., Vitavetskaya, L. Relativistic quantum chemistry and spectroscopy of exotic atomic systems with accounting for strong interaction effects. In: *Concepts, Methods and Applications of Quantum Systems in Chem. and Phys.* Springer. **2018,** *31*, 71.

[29] Khetselius, O. Relativistic perturbation theory calculation of the hyperfine structure parameters for some heavy-element isotopes. *Int. J. Quant. Chem.* **2009,** *109*, 3330–3335.

[30] Buyadzhi, V.V., Chernyakova, Yu.G., Antoshkina, O., Tkach, T. Spectroscopy of multicharged ions in plasmas: Oscillator strengths of Be-like ion Fe. *Photoelectronics*. **2017,** *26*, 94-102.

[31] Malinovskaya, S., Dubrovskaya, Yu., Zelentzova, T. The atomic chemical environment effect on the b decay probabilities: Relativistic calculation. *Herald of Kiev Nat. Univ. Ser.: Phys.-Math*. **2004**, N4, 427-432.

[32] Bystryantseva, A., Khetselius, O.Yu., Dubrovskaya, Yu., Vitavetskaya, L.A., Berestenko, A.G. Relativistic theory of spectra of heavy pionic atomic systems with account of strong pion-nuclear interaction effects: ^{93}Nb, ^{173}Yb, ^{181}Ta, ^{197}Au. *Photoelectronics*. **2016**, *25*, 56-61.

[33] Buyadzhi, V., Zaichko, P., Antoshkina, O., Kulakli, T., Prepelitsa, P., Ternovsky, V., Mansarliysky, V. Computing of radiation parameters for atoms and multicharged ions within relativistic energy approach: Advanced Code. *J. Phys.: Conf. Ser*. **2017**, *905*(1), 012003.

[34] Khetselius, O.Yu., Lopatkin, Yu.M., Dubrovskaya, Yu.V, Svinarenko, A.A. Sensing hyperfine-structure, electro-

weak interaction and parity non-conservation effect in heavy atoms and nuclei: New nuclear-QED approach. *Sensor Electr. and Microsyst. Techn*. **2010,** 7(2), 11-19.
[35] Danilov, V., Kruglyak, Y., Pechenaya, V. The electron density-bond order matrix and the spin density in the restricted CI method. *Theor. Chim. Act*. **1969**, *13*(4), 288-296.
[36] Kruglyak, Yu. Configuration interaction in the second quantization representation: basics with application up to full CI. *Science Rise*. **2014**, *4*(2), 98-115.
[37] Glushkov, A.V., Khetselius, O.Yu., Svinarenko, A., Buyadzhi, V. *Methods of computational mathematics and mathe-matical physics*. TES: Odessa, **2015**.
[38] Ignatenko, A.V., Svinarenko, A.A., Prepelitsa, G.P., Perelygina, T.B. Optical bi-stability effect for multi-photon absorption in atomic ensembles in a strong laser field. *Photoelectronics*. **2009**, *18*, 103-105.
[39] De Fanis, A., Tamenori, Y., Kitajima, M., Tanaka, H., Ueda, K. Doopler-free resonant Auger Raman spectroscopy on atoms and molecules at Spring-8. *J. Phys.: Conf. Ser***. 2004**, 183, 63-72.

PACS 31.15.A-; 32.30.-r

Chernyshev A.S., Efimova E.A., Buyadzhi V.V., Nikola L.V.

CASCADE OF AUGER TRANSITIONS IN SPECTRUM OF XENON: THEORETICAL DATA

Summary. The energy parameters of the Auger transitions for the xenon atomic system are calculated within the combined relativistic energy approach and relativistic many-body perturbation theory with the zeroth order density functional approximation. The results are compared with reported experimental data as well as with those obtained by semiempirical methods. The important point is linked with an accurate accounting for the complex ex-change-correlation (polarization) effect contributions and using the optimized one-quasiparticle representation in the relativistic many-body perturbation theory zeroth order that significantly provides a physically reasonable agreement between theory and experi-ment.

Key words: relativistic theory, Auger spectroscopy, xenon

PACS 31.15.A-; 32.30.-r

Чернышев А.С., Ефимова Е.А., Буяджи В.В.. Никола Л.В.

КАСКАД ОЖЕ-ПЕРЕХОДОВ В СПЕКТРЕ КСЕНОНА: ТЕОРЕТИЧЕСКИЕ ДАННЫЕ

Резюме. Энергетические параметры оже-переходов для атомной системы ксенона рассчитаны в рамках комбинированного релятивистского энергетического подхода и релятивистской многочастичной теории возмущений с приближением функционала плотности нулевого порядка. Результаты сравниваются с экспериментальными результатами, а также с полуэмпирическими теоретическими данными. Важный момент связан с учетом вкладов сложных многочастичных обменных корреляционных ‘ффектов и использованием оптимизированного одноквазичастичного представления в нулевом приближении многочастичной теории возмущений, что определяет физически разумное согласие между теорией и экспериментом.

Ключевые слова: релятивистская теория, Оже-спектроскопия, ксенон

PACS 31.15.A-; 32.30.-r

Чернишев О.С., Ефимова Є.О., Буяджи В.В.. Нікола Л.В.

КАСКАД ОЖЕ-ПЕРЕХОДІВ В СПЕКТРІ КСЕНОНА: ТЕОРЕТИЧНІ ДАНІ

Резюме. Енергетичні параметри оже-переходів для атомної системи ксенону обчислені на основі комбінованого релятивістського енергетичного підходу і релятивістської багаточастинкової теорії збурень з наближенням функціонала щільності нульового порядку. Результати порівнюються з експериментальними результатами, а також з напівемпіричними дтеоретичними даними. Важливий момент пов'язаний з урахуванням вкладів складних багаточасткових обмінних кореляційних ефектів та з використанням оптимізованого одноквазічастічного уявлення в нульовому наближенні релятивістської багаточастинкової теорії збурень, що визначає фізично певну згоду між теорією і експериментом.

Ключові слова: релятивістська теорія, Оже-спектроскопія, ксеон.

PACS 31.15.-p

Buyadzhi V. V.

Odesa State Environmental University, 15, Lvovskaya str., Odesa-16, 65016, Ukraine
E-mail: buyadzhivv@gmail.com

RELATIVISTIC ENERGY APPROACH AND MANY-BODY PERTURBATION THEORY TO COMPUTING ELECTRON-COLLISION CROSS-SECTIONS OF COMPLEX MULTIELECTRON IONS

An advanced relativistic energy approach combined with a relativistic many-body perturbation theory with ab initio zeroth approximation is used to calculate the electron-collision excitation cross-sections for complex multielectron systems. The relativistic many-body perturbation theory is used alongside the gauge-invariant scheme to generate an optimal Dirac-Kohn-Sham- Debye-Hückel one-electron representation. The results of relativistic calculation (taking into account the exchange and correlation corrections) of the electron collision cross-sections of excitation for the neon-like ion of the krypton are presented and compared with alternative results calculation on the basis of the R-matrix method in the Breit-Pauli approximation, in the relativistic distorted wave approximation and R- matrix method in combination with Dirac-Fock approximation.

2. Introduction

Electron-collisional spectroscopy of atoms and multicharged ions is one of the most fast developing branches of modern atomic spectroscopy. The properties of laboratory and astrophysical plasmas have drawn considerable attention over the last decades [1-50]. It is known that multicharged ions play an important role in the diagnostics of a wide variety of plasmas. Similar interest is also stimulated by importance of this information for correct determination of the characteristics for plasma in thermonuclear (tokamak) reactors, searching new mediums for X-ray range lasers.

In the last years an especial interest attracts study of multicharged ions of isoelectronic sequences of the inert atoms (neon, krypton, argon). The sought objects of research, firstly, belong to the class of complex relativistic many-electron atomic systems, in connection with which the approbation of the theory is extremely important and indicative just for such systems. Second, the sought multiply charged ions are of great interest for a number of applications in the field of laser physics and quantum electronics, in particular, the use of the plasma of the corresponding ions as an active medium for short-wavelength lasers, further in the field of diagnostics of astrophysical, laboratory and fusion reactor plasma, tokamak and EBIT devices, as well as, of course, laser plasma

In the case of solving collision problems involving multi-electron atomic systems, as well as low-energy processes, etc., the structure of atomic systems should be described on the basis of rigorous methods of quantum theory. As a rule, the Hartree-Fock (HF) or Hartree-Fock-Slater (HFS) models implemented in the tight-binding approximation were used to describe the wave functions of the bound states of atoms and ions. Another direction is the models of the central potential (model potential, pseudopotential) implemented in the distorted wave approximation (DWA). It should be mentioned the currently widespread and widely used R-matrix method and its various promising modifications, as well as a generalization of the well-known Dirac-Fock method to the case of taking into account multipolarity in the corresponding operators (see, e.g. , [1-7]). It should be noted that, depending on the perturbation theory (PT) basis used, different versions of the R-matrix method received the corresponding names. For example, in specific calculations such versions as R-MATR-CI3-5R and R-MATR-41 R-matrix method were used using respectively wave functions in the multiconfiguration approximation, in particular, 5- and 41- configuration wave

functions. As numerous applications of the R-matrix method have shown, it has certain advantages in terms of accuracy and consistency over such popular approaches as the first-order PT method, as well as the distorted wave approximation taking into account configuration interaction (CI-DWBA); --- approximation of distorted waves using the HF basis (HF-DWBA), finally, the relativistic approximation of distorted waves with a 1-configuration and multi-configuration wave function of the ground state (SCGS-RDWA, MCGS-RDWA, etc.). Improved models have also appeared in theories of the coupled-channel (VC) type VCDWA (Variational Continuum Distorted Wave), for example, a modification of the Vraun-Scroters type and others (see [1-5]). Various cluster methods have also been widely used (see in more details [1-3,14,15]).

In this paper, we present and use an advanced relativistic energy approach to calculate the electron-ion collision strengths, effective collision strengths and the associated cross sections. The relativistic many-body PT is utilised alongside the gauge-invariant scheme to generate an optimal one-electron representation. The calculated effective collision strengths of the Ne-like krypton excitation are listed.

2. Advanced energy approach to electron collision strengths for atomic systems

The detailed description of our approach was earlier presented (see, for example, Refs. [7-9,13]). Therefore, below we are limited only by the key points. The generalized relativistic energy approach combined with the RMBPT has been in details described in Refs. [6,14-18]. It generalizes earlier developed energy approach [6,16].

The key idea is in calculating the energy shifts ΔE of degenerate states that is connected with the secular matrix M diagonalization [6,16]. To construct M, one should use the Gell-Mann and Low adiabatic formula for ΔE. The secular matrix elements are already complex in the PT second order. The whole calculation is reduced to calculation and diagonalization of the complex matrix M .and definition of matrix of the coefficients with eigen state vectors $B^{IK}_{ie,iv}$ [6,8,9].

To calculate all necessary matrix elements one must use the basis's of the 1QP relativistic functions. Within an energy approach the total energy shift of the state is usually presented as [6,16]:

$$\Delta E = \mathrm{Re}\Delta E + i\,\Gamma/2 \qquad (1)$$

where Γ is interpreted as the level width and decay possibility $P = \Gamma$. The imaginary part of electron energy of the system, which is defined in the lowest PT order as [6]:

$$\mathrm{Im}\Delta E(B) = -\frac{e^2}{4\pi} \sum_{\substack{\alpha>n>f \\ [\alpha<n\le f]}} V^{|\omega_{\alpha n}|}_{\alpha n \alpha n}, \qquad (2)$$

where $\sum_{\alpha>n>f}$ for electron and $\sum_{\alpha<n\le f}$ for vacancy. The separated terms of the sum in (3) represent the contributions of different channels. It is known that their adequate description requires using the optimized basis's of wave functions. In [6] it has been proposed "ab initio" optimization principle for construction of cited basis's. It uses a minimization of the gauge dependent multielectron contribution of the lowest QED PT corrections to the radiation widths of atomic levels. This contribution describes collective effects and it is dependent upon the electromagnetic potentials gauge (the gauge non-invariant contribution δE_{ninv}). The minimization of $\mathrm{Im}\delta E_{ninv}$ leads to integral differential equation, that is numerically solved. In result one can get the optimal one-electron basis of the PT [14,16,17]. It is worth to note that this approach was used under solving of multiple problems of modern atomic , nuclear and molecular physics (see [14-25]). The scattered part of $\mathrm{Im}\Delta E$ appears first in the second order of the atomic PT. The collisional de-excitation cross section is defined as follows [6,8,9]:

$$\sigma(IK \to 0) = 2\pi \sum_{j_{in}, j_{sc}} (2 j_{sc} + 1) * \qquad (3)$$

$$*\{\sum_{j_{ie},j_{iv}} < 0 \mid j_{in}, j_{sc} \mid j_{ie}, j_{iv}, J_i > B^{IK}_{ie,iv}\}^2 ,$$

$$< 0 \mid j_{in}, j_{sc} \mid j_{ie}, j_{iv}, J_i >=$$

$$\sqrt{(2j_{ie}+1)(2j_{iv}+1)}(-1)^{j_{ie}+1/2} \times \sum_{\lambda} (-1)^{\lambda+J_i} \times$$

$$\times \{\delta_{\lambda,J_i} /(2J_i+1) Q_\lambda(sc,ie;iv,in) + ,$$

$$\begin{bmatrix} j_{in} \ldots j_{sc} \ldots J_i \\ j_{ie} \ldots j_{iv} \ldots\ldots \lambda \end{bmatrix} Q_\lambda(ie;in;iv,sc)\} \qquad (4)$$

where Q_λ is the sum of the known Coulomb and Breit matrix elements [6,14,16]. The effective collision strength $\Omega(I \to F)$ is associated with a collisional cross section σ as follows (in the Coulomb units):

$$\sigma(I \to F) = \Omega(I \to F) \cdot \pi / \qquad (5)$$

$$/\{(2J_i+1)\varepsilon_{in}[(\alpha Z)^2 \varepsilon_{in} + 2]\}$$

where Z is the nucleus charge and α is the fine structure constant, ε_{in} is the incident energy. Further let us firstly consider the Debye shielding model according to Refs. [7-9]. It is known in the classical theory of plasmas developed by Debye-Hückel, the interaction potential between two charged particles is modelled by the Yukawa-type potential, which contains the shielding parameter μ. The parameter μ is connected with the plasma parameters such as the temperature T and the charge density n as follows: $\mu \sim \sqrt{e^2 n / k_B T}$. Here, as usually, e is the electron charge and $\kappa_Б$ is the Boltzman constant.

It should be noted that indeed the Debye screening for the atomic electrons in the Coulomb field of nuclear charge is well understood due to the presence of the surrounding plasma electrons with high mobility. On the other hand, the contribution due to the Debye screening between electrons would be of smaller magnitude orders.

Majority of the previous works on the spectroscopy study have considered the screening effect only in the electron-nucleus potential where the electron-electron interaction potential is truncated at its first term of the standard exponential expansion for its dominant contribution [3-69]. However, it is also important to take into account the screening in the electron- electron interactions for large plasma strengths to achieve more realistic results in the search for stability of the atomic structure in the plasma environment.

By introducing the Yukawa-type e-N and e-e interaction potentials, an electronic Hamiltonian for N-electron ion in a plasma is in atomic units as follows [7]:

$$H = \sum_i [\alpha cp - \beta mc^2 - Z \exp(-\mu r_i)/r_i] + \sum_{i>j} \frac{(1-\alpha_i \alpha_j)}{r_{ij}} \exp(-\mu r_{ij}) \qquad (6)$$

To generate the wave functions basis we use the optimized Dirac-Kohn-Sham potential with one parameter [14,15], which calibrated within the special ab initio procedure within the relativistic energy approach [16,17]. More details, including the procedures of computing amplitudes, radial intagrals, matrix elements etc, can be found in Refs. [7-23]. All calculations are performed on the basis of the code Superatom-ISAN (version 93).

3. Results and conclusion

Table 1 shows the values of the cross sections for the excitation of some states of the Kr^{26+} multicharged ion from the ground state (the energy of the incident electron are 4.082 keV) obtained within the framework of the relativistic many-body perturbation theory and relativistic energy formalism [7-23].

In Table 1 there are also listed the data (for the first 26 excited states) of the calculation by the R-matrix method in the Breit-Pauli approximation by Gupta et al (BP-RM), in the relativistic distorted wave approximation

(RDWA), R- matrix method in the DF approximation by Griffin et al (MCDF-RM) (e.g. [2] and Refs. therein).

Table 1.
Cross sections for excitation by electron impact of the Kr^{26+} excited states at the incident electron energy of 4.082 keV

Level	BP-R-M	RDWA
$2p^5 3s\ (3/2,1/2)_2$	8.94(-23)	8.80(-23)
$2p^5 3s\ (3/2,l/2)_1$	5.22(-22)	6.63(-22)
$2p^5 3p\ (3/2,l/2)_1$	1.60(-22)	1.73(-22)
$2p^5 3p\ (3/2,1/2)_2$	4.25(-22)	4.72(-22)
$2p^5 3s\ (1/2,l/2)_0$	1.90(-23)	1.76(-23)
$2p^5 3s\ (1/2,l/2)_1$	2.99(-22)	4.16(-22)
$2p^5 3p\ (3/2,3/2)_3$	2.30(-22)	2.20(-22)
$2p^5 3p\ (3/2,3/2)_1$	1.10(-22)	1.06(-22)
$2p^5 3p\ (3/2,3/2)_2$	3.81(-22)	3.90(-22)
$2p^5 3p\ (3/2,3/2)_0$	2.06(-21)	2.05(-21)
$2p^5 3p\ (1/2,l/2)_1$	9.44(-23)	9.09(-23)
$2p^5 3p\ (1/2,3/2)_1$	1.11(-22)	1.11(-22)
$2p^5 3p\ (1/2,3/2)_2$	3.81(-22)	4.31(-22)
$2p^5 3d\ (3/2,3/2)_0$	9.85(-23)	9.97(-23)
$2p^5 3p\ (1/2.1/2)_0$	5.48(-21)	5.40(-21)
$2p^5 3d\ (3/2,3/2)_1$	3.08(-22)	3.11(-22)
$2p^5 3d\ (3/2,3/2)_3$	4.75(-22)	4.66(-22)
$2p^5 3d\ (3/2,5/2)_2$	2.92(-22)	2.90(-22)
$2p^5 3d\ (3/2,5/2)_4$	3.11(-22)	2.99(-22)
$2p^5 3d\ (3/2,3/2)_2$	1.33(-22)	1.26(-22)
$2p^5 3d\ (3/2.5/2)_3$	3.67(-22)	3.61(-22)
$2p^5 3d(3/2,5/2)_l$	1.30(-20)	1.46(-20)
$2p^5 3d\ (1/2,3/2)_2$	1.55(-22)	1.47(-22)
$2p^5 3d\ (1/2,5/2)_2$	2.44(-22)	2.32(-22)
$2p^5 3d\ (1/2,5/2)_3$	4.40(-22)	4.25(-22)
$2p^5 3d\ (1/2,3/2)_2$	1.64(-20)	1.46(-20)
Level	DF-RM	Our data
$2p^5 3s\ (3/2,1/2)_2$	9.98(-23)	9.75(-23)
$2p^5 3s\ (3/2,l/2)_1$	7.29(-22)	7.05(-22)
$2p^5 3p\ (3/2,l/2)_1$	1.85(-22)	1.80(-22)
$2p^5 3p\ (3/2,1/2)_2$	4.88(-22)	4.81(-22)
$2p^5 3s\ (1/2,l/2)_0$	2.01(-23)	1.97(-23)
$2p^5 3s\ (1/2,l/2)_1$	4.52(-22)	4.38(-22)
$2p^5 3p\ (3/2,3/2)_3$	2.34(-22)	2.32(-22)
$2p^5 3p\ (3/2,3/2)_1$	1.20(-22)	1.17(-22)
$2p^5 3p\ (3/2,3/2)_2$	4.17(-22)	4.13(-22)
$2p^5 3p\ (3/2,3/2)_0$	2.02(-21)	1.98(-21)
$2p^5 3p\ (1/2,l/2)_1$	1.01(-22)	9.98(-23)
$2p^5 3p\ (1/2,3/2)_1$	1.21(-22)	1.18(-22)
$2p^5 3p\ (1/2,3/2)_2$	4.41(-22)	4.37(-22)
$2p^5 3d\ (3/2,3/2)_0$	1.04(-22)	1.01(-22)
$2p^5 3p\ (1/2.1/2)_0$	5.08(-21)	5.03(-21)
$2p^5 3d\ (3/2,3/2)_1$	3.34(-22)	3.30(-22)
$2p^5 3d\ (3/2,3/2)_3$	4.78(-22)	4.71(-22)
$2p^5 3d\ (3/2,5/2)_2$	3.00(-22)	2.98(-22)
$2p^5 3d\ (3/2,5/2)_4$	3.17(-22)	3.14(-22)
$2p^5 3d\ (3/2,3/2)_2$	1.42(-22)	1.39(-22)
$2p^5 3d\ (3/2.5/2)_3$	3.62(-22)	3.60(-22)
$2p^5 3d(3/2,5/2)_l$	1.45(-20)	1.42(-20)
$2p^5 3d\ (1/2,3/2)_2$	1.58(-22)	1.57(-22)
$2p^5 3d\ (1/2,5/2)_2$	2.44(-22)	2.42(-22)
$2p^5 3d\ (1/2,5/2)_3$	4.31(-22)	4.29(-22)
$2p^5 3d\ (1/2,3/2)_2$	1.72(-20)	1.69(-20)

Analyzing the presented data, it should be noted that shortened bases are used in the BP-RM methods and the relativistic distorted wave approximation by Reed et al (RDWA), as a result of which, as noted also by Griffin et al [20], the data on the cross sections of state excitation the krypton ion are strongly underestimated.

References

1. Badnell, N.R. Calculations for electron-ion collisions and photoionization processes for plasma modeling. *J. Phys.: Conf. Ser*. **2007**, *88*, 012070.
2. Griffin, D.C., Balance, C., Mitnik, D., Berengut, J.C. Dirac *R*-matrix calculations of electron-impact excitation of neon-like krypton. *J. Phys. B: At. Mol. Opt. Phys*. **2008**, *41*, 215201.
3. Yongqiang, Li; Jianhua, Wu; Yong, Hou, Jianmin Yuan. Influence of hot and dense plasmas on energy levels and oscillator strengths of ions: Be-like ions for *Z* = 26–36, *J. Phys. B: At. Mol. Opt. Phys.* **2008,** *41*, 145002.
4. Bannister, M. E., Djurić, N., Woitke, O., Dunn, G., Chung, Y. -S, Smith, A. C. H., Wallbank, B., Berrington, K. A. Absolute cross-sections for near–threshold electron-impact excitation of

Be-like C^{2+}, N^{3+}, O^{4+}. *Int. J. Mass Spectr*. **1999**, *192*, 39-48.
5. Smith, A. C. H., Bannister, M. E., Chung, Y. -S, Djuri,ć N., Dunn, G. H., Wallbank, B., Woitke, O. Near-threshold Electron-impact Excitation of Multiply-charged Be-like Ions. *Phys.Scr*. 1999, T80, 283-287.
6. Ivanov, L.N.; Ivanova, E.P.; Knight, L. Energy approach to consistent QED theory for calculation of electron-collision strengths: Ne-like ions. *Phys. Rev. A.* **1993,** *48*, 4365-4374.
7. Buyadzhi, V.V. Laser multiphoton spectroscopy of atom embedded in Debye plasmas: multiphoton resonances and transitions. *Photoelectronics.* **2015,** *24*, 128-133.
8. Buyadzhi, V.V.; Chernyakova, Yu.G.; Smirnov, A.V.; Tkach, T.B. Electron-collisional spectroscopy of atoms and ions in plasma: Be-like ions. *Photoelectronics*. **2016,** *25*, 97-101.
9. Buyadzhi, V.; Chernyakova, Yu.; Antoshkina, O.; Tkach, T. Spectroscopy of multicharged ions in plasmas: Oscillator strengths of Be-like ion Fe. *Photoelectronics*. **2017,** *26*, 94-102.
10. Glushkov, A.V.; Malinovskaya, S.V.; Prepelitsa, G.P.; Ignatenko, V. Manifestation of the new laser-electron nuclear spectral effects in the thermalized plasma: QED theory of co-operative laser-electron-nuclear processes. *J. Phys.: Conf. Ser*. **2005,** *11*, 199-206.
11. Glushkov, A.V.; Malinovskaya, S.V.; Chernyakova Y.G.; Svinarenko, A.A. Cooperative laser-electron-nuclear processes: QED calculation of electron satellites spectra for multi-charged ion in laser field. *Int. Journ. Quant. Chem.* **2004,** *99*, 889-893.
12. Glushkov, A.V.; Malinovskaya, S.V.; Loboda, A.V.; Shpinareva, I.M.; Gurnitskaya, E.P.; Korchevsky, D.A. Diagnostics of the collisionally pumped plasma and search of the optimal plasma parameters of x-ray lasing: calculation of electron-collision strengths and rate coefficients for Ne-like plasma. *J. Phys.: Conf. Ser*. **2005,** *11*, 188-198.
13. Glushkov, A.V.; Ambrosov, S.V.; Loboda, A.V.; Gurnitskaya, E.P.; Prepelitsa, G.P. Consistent QED approach to calculation of electron-collision excitation cross sections and strengths: Ne-like ions. *Int. J. Quantum Chem.* **2005,** *104*, 562-569.
14. Glushkov, A.V. *Relativistic Quantum theory. Quantum mechanics of atomic systems;* Astroprint: Odessa, **2008**.
15. Khetselius, O.Yu. *Hyperfine structure of atomic spectra*. Astroprint: Odessa, **2008**.
16. Glushkov, A.V.; Ivanov, L.N.; Ivanova, E.P. Autoionization Phenomena in Atoms. *Moscow Univ. Press*, **1986,** 58-160
17. Glushkov, A.; Ivanov, L. Radiation decay of atomic states: atomic residue polarization and gauge noninvariant contributions. *Phys. Lett. A* **1992,** *170*, 33.
18. Glushkov, A.V. Spectroscopy of atom and nucleus in a strong laser field: Stark effect and multiphoton resonances. *J. Phys.: Conf. Ser*. **2014**, *548*, 012020
19. Ivanov, L.N.; Ivanova, E.P. Method of Sturm orbitals in calculation of physical characteristics of radiation from atoms and ions. *JETP*. **1996,** *83*, 258-266.
20. Glushkov, A.V., Ivanov, L.N., Ivanova, E.P. Autoionization Phenomena in Atoms. *Moscow Univ. Press*, Moscow, **1986,** 58.
21. Glushkov, A.V., Ivanov, L.N. Radiation decay of atomic states: atomic residue polarization and gauge noninvariant contributions. *Phys. Lett. A* **1992,** *170*, 33.
22. Glushkov, A.V.; Ivanov, L.N. DC strong-field Stark effect: consistent quantum-mechanical approach. *J. Phys. B: At. Mol. Opt. Phys.* **1993,** *26*, L379-386.
23. Ivanova, E., Glushkov, A. Theoretical investigation of spectra of multicharged ions of F-like and Ne-like isoelectronic

sequences. J. Quant. Spectr. and Rad. Tr. **1986**, *36*(2), 127-145.
24. Ivanova, E.P., Ivanov, L.N., Glushkov, A., Kramida, A. High order corrections in the relativistic perturbation theory with the model zeroth approximation, Mg-Like and Ne-Like Ions. *Phys. Scripta* **1985**, *32*, 513-522.
25. Glushkov, A.V. *Relativistic and correlation effects in spectra of atomic systems*. Astroprint: Odessa, **2006**.
26. Glushkov, A.V. Multiphoton spectroscopy of atoms and nuclei in a laser field: Relativistic energy approach and radiation atomic lines moments method. *Adv. in Quantum Chem.* **2019**, *78*, 253-285.
27. Glushkov, A., Loboda, A., Gurnitskaya, E., Svinarenko, A. QED theory of radiation emission and absorption lines for atoms in a strong laser field. *Phys. Scripta*. **2009,** *T135*, 014022.
28. Glushkov, A. Spectroscopy of cooperative muon-gamma-nuclear processes: Energy and spectral parameters *J. Phys.: Conf. Ser*. **2012,** *397*, 012011.
29. Glushkov, A.V. Spectroscopy of atom and nucleus in a strong laser field: Stark effect and multiphoton resonances. *J. Phys.: Conf. Ser*. **2014**, *548*, 012020.
30. Glushkov, A.V., Ternovsky, V.B., Buyadzhi, V., Prepelitsa, G.P. Geometry of a Relativistic Quantum Chaos: New approach to dynamics of quantum systems in electromagnetic field and uniformity and charm of a chaos. *Proc. Int. Geom. Center*. **2014,** *7*(4), 60-71.
31. Glushkov, A., Buyadzhi, V., Kvasikova, A., Ignatenko, A., Kuznetsova, A., Prepelitsa, G., Ternovsky, V. Non-Linear chaotic dynamics of quantum systems: Molecules in an electromagnetic field and laser systems. In: *Quantum Systems in Physics, Chemistry, and Biology*. Springer, Cham. **2017**, *30*, 169-180.
32. Glushkov, A.V. Relativistic polarization potential of a many-electron atom. *Sov. Phys. Journal.* **1990**, *33(1)*, 1-4.
33. Glushkov, A., Svinarenko, A., Ignatenko, A. Spectroscopy of autoionization resonances in spectra of the lanthanides atoms. *Photoelectronics*. **2011**, *20*, 90-94.
34. Glushkov, A., Gurskaya, M., Ignatenko, A., Smirnov, A., Serga, I., Svinarenko, A., Ternovsky, E. Computational code in atomic and nuclear quantum optics: Advanced computing multiphoton resonance parameters for atoms in a strong laser field. *J. Phys.: Conf. Ser*. **2017**, *905*, 012004.
35. Glushkov, A; Khetselius, O; Svinarenko, A; Buyadzhi, V. *Spectroscopy of autoionization states of heavy atoms and multiply charged ions*. Odessa: **2015**
36. Glushkov, A.V., Khetselius, O.Yu., Svinarenko, A.A., Buyadzhi, V.V. *Methods of computational mathematics and mathematical physics*. *P.1*. TES: Odessa, **2015**.
37. Khetselius, O.Yu. Spectroscopy of cooperative electron-gamma-nuclear processes in heavy atoms: NEET effect. *J. Phys.: Conf. Ser*. **2012**, 3*97*, 012012.
38. Buyadzhi, V., Zaichko, P., Antoshkina, O., Kulakli, T., Prepelitsa, G., Ternovsky, V.B., Mansarliysky, V. Computing of radiation parameters for atoms and multicharged ions within relativistic energy approach: Advanced Code. *J. Phys.: Conf. Ser*. **2017**, *905*(1), 012003. Ignatenko, A.V. Probabilities of the radiative transitions between Stark sublevels in spectrum of atom in an DC electric field: New approach. *Photoelectronics,* **2007,** *16*, 71-74.
39. Glushkov, A.V.; Ambrosov, S.V.; Ignatenko, A.V. Non-hydrogenic atoms and Wannier-Mott excitons in a DC electric field: Photoionization, Stark effect, Resonances in ionization continuum and stochasticity. *Photoelectronics,* **2001,** *10*, 103-106.
40. Glushkov A., Ternovsky V., Buyadzhi V., Prepelitsa G., Geometry of a rela-

tivistic quantum chaos: New approach to dynamics of quantum systems in electromagnetic field and uniformity and charm of a chaos. *Proc. Intern. Geom. Center*. **2014,** *7*(4), 60-71.
41. Glushkov A V, Ambrosov S V, Loboda A V, Chernyakova Yu G, Svinarenko A A and Khetselius O Yu QED calculation of the superheavy elements ions: energy levels, radiative corrections, and hfs for different nuclear models Nucl Phys A Nucl Hadr Phys **2004,** 734, 21
42. Khetselius, O.Yu. Relativistic perturbation theory calculation of the hyperfine structure parameters for some heavy-element isotopes. *Int. Journ.Quant Chem*. **2009,** *109*, 3330-3335.
43. Khetselius, O. Hyperfine structure of radium. *Photoelectronic*. **2005,** *14*, 83-85.
44. Sukharev, D.E.; Khetselius, O.Yu.; Dubrovskaya, Yu.V. Sensing strong interaction effects in spectroscopy of hadronic atoms. *Sensor Electr. and Microsyst. Techn*. **2009**, *N3*, 16-21.
45. Khetselius, O.Yu. *Quantum structure of electroweak interaction in heavy finite Fermi-systems*. Astroprint: Odessa, **2011**.
46. Khetselius, O.Y.., Glushkov, A.V., Gurskaya, M.Y., Kuznetsova, A.A., Dubrovskaya, Yu.V., Serga, I.N., Vitavetskaya, L.A. Computational modelling parity nonconservation and electroweak interaction effects in heavy atomic systems within the nuclear-relativistic many-body perturbation theory. *J. Phys.: Conf. Ser*. **2017,** *905*(1), 012029.
47. Svinarenko, A. A., Glushkov, A. V., Khetselius, O.Yu., Ternovsky,V.B., Dubrovskaya, Yu., Kuznetsova, A., Buyadzhi, V. Theoretical spectroscopy of rare-earth elements: spectra and autoionization resonances. *Rare Earth Element*, Ed. J. Orjuela (InTech) **2017**, pp 83-104
48. Glushkov, A.V., Khetselius, O.Yu., Svinarenko A.A., Buyadzhi, V.V., Ternovsky, V.B, Kuznetsova, A., Bashkarev, P Relativistic perturbation theory formalism to computing spectra and radiation characteristics: application to heavy element. *Recent Studies in Perturbation Theory*, ed. D. Uzunov (InTech) **2017**, 131-150.
49. Danilov, V., Kruglyak, Y., Pechenaya, V. Electron density-bond order matrix and the spin density in the restricted CI method. *Theor. Chim Acta*. **1969**, *13*(4), 288-296.
50. Glushkov A.V., Khetselius O.Yu., Loboda A.V., Ignatenko A., Svinarenko A., Korchevsky D., Lovett L., QED Approach to Modeling Spectra of the Multicharged Ions in a Plasma: Oscillator and Electron-ion Collision Strengths. *AIP Conference Proceedings***. 2008**. 1058. 175-177

PACS 31.15.-p

Buyadzhi V.V.

ELECTRON-COLLISIONAL SPECTROSCOPY OF ATOMS AND IONS: ADVANCED ENERGY APPROACH

Summary. An advanced relativistic energy approach combined with a relativistic many-body perturbation theory with ab initio zeroth approximation is used to calculate the electron-collision excitation cross-sections for complex multielectron systems. The relativistic many-body perturbation theory is used alongside the gauge-invariant scheme to generate an optimal Dirac-Kohn-Sham- Debye-Hückel one-electron representation. The results of relativistic calculation (taking into account the exchange and correlation corrections) of the electron collision cross-sections of excitation for the neon-like ion of the krypton are presented and compared with alternative results calculation on the basis of the R-matrix method in the Breit-Pauli approximation, in the relativistic distorted wave approximation and R- matrix method in combination with Dirac-Fock approximation

Key words: spectroscopy of ions, relativistic energy approach, collision cross-sections.

PACS 31.15.-p

Буяджи В.В.

РЕЛЯТИВИСТСКИЙ ЭНЕРГЕТИЧЕСКИЙ ПОДХОД И МНОГОЧАСТИЧНАЯ ТЕОРИЯ ВОЗМУЩЕНИЙ ДЛЯ ОПРЕДЕЛЕНИЯ СЕЧЕНИЙ ЭЛЕКТРОННО-СТОЛКНОВЕННОГО ВОЗБУЖДЕНИЯ ДЛЯ СЛОЖНЫХ МНОГОЭЛЕКТРОННЫХ ИОНОВ

Резюме. Эффективный релятивистский энергетический подход в комбинации с многочастичной теорией возмущений с неэмпирическим нулевым приближением используется для расчета сечений электрон-столкновительного возбуждения для ряда сложных релятивистских многоэлектронных систем. Релятивистская многочастичная теория возмущений наряду с эффективной калибровочно-инвариантной схемой используется для генерации оптимального одноэлектронного представления Дирака-Кона-Шама-Дебая-Хюккеля. Приведены результаты релятивистского расчета (с учетом обменных и корреляционных поправок) сечений электрон-столкновительного возбуждения неоноподобного иона криптона и проведено сравнение с альтернативными результатами расчета на основе R-матричного метода в приближении Брейта-Паули, в релятивистском приближении искаженных волн и на основе R-матричного метода в сочетании с приближением Дирака-Фока.

Ключевые слова: спектроскопия ионов, энергетический подход, сечения столкновений

PACS 31.15.-p

Буяджи В.В.

РЕЛЯТИВІСТСЬКИЙ ЕНЕРГЕТИЧНИЙ ПІДХІД І БАГАТОЧАСТИНКОВА ТЕОРІЯ ЗБУРЕНЬ ДЛЯ ВИЗНАЧЕННЯ ПЕРЕТИНІВ ЕЛЕКТРОННОГО ЗБУДЖЕННЯ ЗА РАХУНОК ЗІТКНЕНЬ ДЛЯ СКЛАДНИХ БАГАТОЕЛЕКТРОННІ ИОНОВ

Резюме. Ефективний релятивістський енергетичний підхід в комбінації з багаточастинкової теорією збурень з неемпіричним нульовим наближенням використуються для розрахунку перетинів електронного збудження за рахунок зіткнень для ряду складних релятивістських багатоелектронних систем. Релятивістська багаточастинкова теорія збурень поряд з ефективною калібрувально-інваріантної схемою використуються для генерації оптимального одноелектронного уявлення Дірака-Кона-Шама-Дебая-Хюккеля. Наведены результати релятивістського розрахунку (з урахуванням обмінних і кореляційних поправок) перетинів електрон-зіткнень збудження неоноподібного іона кріптону і проведено порівняння з альтернативними результатами розрахунків на основі R-матричного методу в наближенні Брейта-Паулі, в релятивістському наближенні спотворених хвиль і на основі R-матричного методу в поєднанні з наближенням Дірака-Фока.

Ключові слова: спектроскопія іонів, енергетичний підхід, перерізи зіткнень.
PACS 42.55.-f

Tsudik A. V., Glushkov A. V., Ternovsky V. B., Zaichko P. A.

Odesa National Maritime Academy, Didrikhsona str. 4, Odesa, 65001
Odesa State Environmental University, L'vovskaya str.15, Odesa-16, 65016, Ukraine
E-mail: tsudikav@gmail.com

ADVANCED COMPUTING TOPOLOGICAL AND DYNAMICAL INVARIANTS OF RELATIVISTIC BACKWARD-WAVE TUBE TIME SERIES IN CHAOTIC AND HYPERCHAOTIC REGIMES

The advanced results of computing the dynamical and topological invariants (correlation dimensions values, embedding, Kaplan-York dimensions, Lyapunov's exponents, Kolmogorov entropy etc) of the dynamics time series of the relativistic backward-wave tube with accounting for dissipation and space charge field and other effects are presented for chaotic and hyperchaotic regimes. It is solved a system of equations for unidimensional relativistic electron phase and field unidimensional complex amplitude. The data obtained make more exact earlier presented preliminary data for dynamical and topological invariants of the relativistic backward-wave tube dynamics in chaotic regimes and allow to describe a scenario of transition to chaos in temporal dynamics.

1. Introduction

Powerful generators of chaotic oscillations of microwave range of interest for radar, plasma heating in fusion devices, modern systems of information transmission using dynamic chaos and other applications. Among the most studied of vacuum electronic devices with complex dynamics are backward-wave tubes (BWT) , for which the possibility of generating chaotic oscillations has been theoretically and experimentally found [1-20]. The BWT is an electronic device for generating electromagnetic vibrations of the superhigh frequencies range. Authors [6] formally considered the possible chaos scenario in a single relativistic BWT. Authors [4,5] have numerically studied dynamics of a non-relativistic BWT, in particular, phase portraits, statistical quantifiers for a weak chaos arising via period-doubling cascade of self-modulation and the same characteristics of two non-relativistic backward-wave tubes. The authors of [4-7] have solved the equations of nonstationary nonlinear theory for the O-type BWT without account of the spatial charge, relativistic effects, energy losses etc. It has been shown that the finite-dimension strange attractor is responsible for chaotic regimes in the BWT. The multiple studies [1-13], increasing the beam current in the system implemented complex pattern of alternation of regular and chaotic regimes of generation, completes the transition to a highly irregular wideband chaotic oscillations with sufficiently uniform continuous spectrum.

In this work we have performed an advanced numerical analysis and modelling and presented some results of computing the dynamical and topological invariants (correlation dimensions values, embedding, Kaplan-York dimensions, Lyapunov's exponents, Kolmogorov entropy etc) of the dynamics time series of the relativistic backward-wave tube with accounting for dissipation and space charge field and other effects are presented for chaotic and hyperchaotic regimes. The system of equations for unidimensional relativistic electron phase and field unidimensional complex amplitude is numerically solved using the Runge-Cutta method. The data presented make more exact the preliminary data for dynamical and topological invariants of the relativistic backward-wave tube dynamics in chaotic regimes and allow to describe a scenario of transition to chaos in temporal dynamics.

2. Relativistic model and some results

As the key ideas of our technique for nonlinear analysis of chaotic systems have been in

details presented in refs. [9-28], here we pay attention only on the kew and some new elements. Below we follow to the version of a standard non-stationary theory [9], however, despite the above cited papers we take into account a number of effects, namely, influence of space charge, dissipation, the waves reflections at the ends of the system and others (a modification of model of Refs.[5-13]).

The standard relativistic dynamics is described system of equations for unidimensional relativistic electron phase $\theta(\zeta,\tau,\theta_0)$ (which moves in the interaction space with phase θ_0 ($\theta_0 \in [0; 2\pi]$) and has a coordinate ζ at time moment τ) and field unidimensional complex amplitude $F(\zeta,\tau) = \tilde{E} / (2\beta_0 UC^2)$ as [11]:

$$\partial^2\theta / \partial\zeta^2 = -L^2\gamma_0^3[(1+\frac{1}{2\pi N}\partial\theta / \partial\zeta)^2 - \beta_0^2]^{3/2}$$

$$\mathrm{Re}[F\exp(i\theta) + \frac{4QC}{ik}\sum_{k=1}^{M} I_k \exp(ik\theta)]$$

$$\partial F / \partial\tau - \partial F / \partial\zeta + dF = -L\tilde{I}\ ,$$

$$I_k = -\frac{1}{\pi}\int_0^{2\pi} e^{-ik\theta} d\theta_0 \qquad (1)$$

with the corresponding boundary and initial conditions. The dynamical system studied has several controlling parameters which are characteristic for distributed relativistic electron-waved self-vibrational systems: i) electric length of an interaction space N; ii) bifurcation parameter $L = 2\pi CN / \gamma_0$ (here C- is the known Piers parameter) ; iii) relativistic factor, which is determined as:

$$\gamma_0 = (1 - \beta_0^2)^{-1./2}. \qquad (2)$$

It should be also noted that an influence of reflections leads to the fact that bifurcational parameter L begins to be dependent on the phase φ of the reflection parameter (see discussion regarding it in [7,8]).

3. Chaos-dynamic approach to analysis of time series

The basic idea of the construction of our approach to prediction of chaotic properties of complex systems is in the use of the traditional concept of a compact geometric att (CGA) in which evolves the measurement data, plus the neural networks (NNW) algorithm implementation [14-38].

Really, one should consider some scalar measurements $s(n) = s(t_0 + n\Delta t) = s(n)$, where t_0 is the start time, Δt is the time step, and n is the number of the measurements. The main task is to reconstruct phase space using as well as possible information contained in $s(n)$. To do it, the method of using time-delay coordinates by Packard et al [28] can be used. The direct using lagged variables $s(n+\tau)$ (here τ is some integer to be defined) results in a coordinate system where a structure of orbits in phase space can be captured. A set of time lags is used to create a vector in d dimensions, $\mathbf{y}(n)$= [$s(n)$, $s(n+\tau)$, $s(n+2\tau)$, .., $s(n+(d-1)\tau)$], the required coordinates are provided. Here the dimension d is the embedding dimension, d_E. To determine the proper time lag at the beginning one should use the known method of the linear autocorrelation function (ACF). The alternative additional approach is provided by the average mutual information (AMI) method as an approach with so called nonlinear concept of independence.

The further next step is to determine the embedding dimension, d_E, and correspondingly to reconstruct a Euclidean space R^d large enough so that the set of points d_A can be unfolded without ambiguity. The dimension, d_E, must be greater, or at least equal, than a dimension of attractor, d_A, i.e. $d_E > d_A$. To reconstruct the attractor dimension and to study the signatures of chaos in a time series, one could use such methods as the correlation integral algorithm (CIA) by Grassberger

and Procaccia [32] or the false nearest neighbours (FNN) method by Kennel et al [27. The principal question of studying any complex chaotic system is to build the corresponding prediction model and define how predictable is a chaotic system. The new element of our approach is using the NNW algorithm in forecasting nonlinear dynamics of chaotic systems [7,14,15].

The fundamental parameters to be computed are the Kolmogorov entropy (and correspondingly the predictability measure as it can be estimated by the Kolmogorov entropy), the Lyapunov's exponents (LE), the Kaplan-Yorke dimension (KYD) etc. The LE are usually defined as asymptotic average rates and they are related to the eigenvalues of the linearized dynamics across the attractor. Naturally, the knowledge of the whole LE allows to determine other important invariants such as the Kolmogorov entropy and the attractor's dimension. The Kolmogorov entropy is determined by the sum of the positive LE.

The estimate of the dimension of the attractor is provided by the Kaplan and Yorke conjecture:

$$d_L = j + \sum_{i=1}^{j} \lambda_i / |\lambda_{j+1}|,$$

where j is such that $\sum_{i=1}^{j} \lambda_i > 0$ and $\sum_{i=1}^{j+1} \lambda_i < 0$, and the LE are taken in descending order.

In Fig. 1 we present the flowchart of the combined chaos-geometric and NNW computational approach to nonlinear analysis and prediction of dynamics of any system [1,11,14-48]. All calculations are carried out with using the PC Codes "Geomath", "Superatom", "Quantum Chaos" (e.g. [1,16-26,39-48]).

I. General analysis of the dynamical problem, processing dynamical variable series for studied complex system (preliminary general analysis of dynamics, evolutionary differential equations treating,…)

⇓

II. Chaos-geometric method: assessment of the presence of chaos:
1. The Gottwald-Melbourne test: $K \to 1$ – chaos;
2. Fourier decompositions, irregular nature of change – chaos;
3. Spectral analysis, Energy spectra statistics, the Wigner distribution, the spectrum of power, "Spectral rigidity";

⇓

III. The geometry of phase space. Fractal Geometry:
4. Computation time delay τ using ACF or AMI;
5. Determining embedding dimension d_E by the CIA method or FNN points;
6. Calculation multi-fractal spectra. Wavelet analysis;

⇓

IV. Prediction model:
7. Computing global LE: λ_α; KYD d_L, average predictability measure Pr_{max};
8. Determining the number of FNN points for the best prediction results;
9. Methods of nonlinear prediction: nonlinear parameterized function; NNW; optimized trajectories (propagators) algorithms, ...;

Figure 1. Flowchart of the combined chaos-geometric approach and NNW to nonlinear analysis and prediction of chaotic dynamics of the complex systems (devices)

4. Illustrative results and conclusions

In Figure 2 we present the numerical temporal dependence of the output signal amplitude of the relativistic backward-wave tube for parameter L=6.1 (b) (see other details, e.g. [7]).

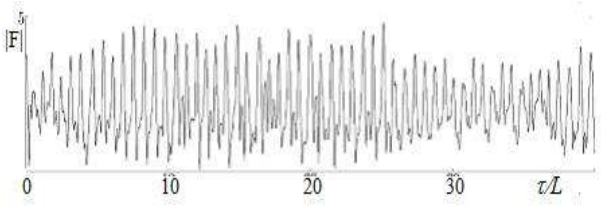

Figure 2. Numerical temporal dependence of the output signal amplitude of the relativistic BWT for L=6.1.

In Table 1 we present our data on the correlation dimension d_2, the embedding dimension determined based on the algorithm of false nearest neighboring points (d_N) with percentage of false neighbors (%) calculated for different values of time lag τ. The values of the time lag are also listed in this table for the both regimes as chaotic as hyperchaotic one.

Table 1.

Correlation dimension d_2, the dimension of the attachment determined based on the algorithm of false nearest neighboring points (d_N) with percentage of false neighbors (%) calculated for different values of time lag τ

Chaos (I)			Hyperchaos (II)		
τ	d_2	(d_N)	τ	d_2	(d_N)
60	3.62	5 (5.6)	67	7.23	10 (13)
6	3.13	4 (1.1)	10	6.44	8 (2.2)
8	3.11	4 (1.2)	12	6.42	8 (2.2)

In Table 2 we list the results of computing the Lyapunov's exponents, the, Kolmogorov entropy K_{entr}. For the studied series there are positive and negative values of the Lyapunov's exponents. Naturally, an availability of the positive values of the Lyapunov's exponents is a characteristic feature of the chaotic dynamics of the studied systems. It shoyld be noted that the latter is an example of distributed multiparametric system that provides the known difficulties under studying of such systems.

Table 2.

The Lyapunov's exponents for the backward-wave tube time series in the chaotic (L=4.2) and hyperchaotic regimes (L=6.1): λ_1–λ_4 in descending order and *K* is the Kolmogorov entropy

Regime	λ_1	λ_2	λ_3	λ_4	*K*
Chaos	0.261	0.0001	-0.0004	–0.528	0.26
Hyper chaos	0.514	0.228	0.0000	–0.0002	0.74

References

1. Glushkov, A.V.; Prepelitsa, G.P.; Svinarenko, A.A. ; Zaichko, P.A. Studying interaction dynamics of the non-linear vibrational systems within non-linear prediction method (application to quantum autogenerators) *In Dynamical Systems Theory;* Awrejcewicz, J., Kazmierczak, M., Olejnik, P., Mrozowski, J., Eds.; Wyd. Politech. Łódz.: Łódz, **2013**; Vol T1, pp 467-477.
2. Ignatenko, A.V.; Buyadzhi, A.; Buyadzhi, V.; Kuznetsova,A.; Mashkantsev, A.; Ternovsky, E. Nonlinear chaotic dynamics of quantum systems: molecules in an electromagnetic field// Adv. Quant. Chem. **2018**,*78* doi.org/10.1016/bs.aiq.2018.06.006.
3. Ginsburg, H. S.; Kuznetsov, S.P.; Fedoseyev, T.N. Theory of transients in relativistic BWO. *Izv. Vuzov. Ser. Radiophys*. **1978,** *21*, 1037-1052.
4. Ginzburg, N.S.; Zaitsev, N.A.; Ilyakov, E.; Kulagin, V.I.; Novozhilov, Yu. Rosenthal P., Sergeev V., Chaotic generation in backward wave tube of the megawatt power level. *Journ. of Techn.Phys*. **2001,** *71*, 73-80.
5. Kuznetsov A.P., Kuznetsov S.P., Ryskin N.M., Isaeva O.B., *Non-linearity: From oscillations to chaos*.-Moscow: NIS RHD.-2006.
6. Kuznetsov A.P., Shirokov A.P., Discretre model of relativistic backward-wave

tube. *Russian J.of Phys. Ser.PND*. **1997**. 5, 76-83.
7. Kuznetsov S.P., Trubetskov D.I., Chaos and hyperchaos in backward-wave tube. *Russian Journ.of Phys. Ser.Radiophys*.- **2004**, XLVII(5), 1-8
8. Ryskin N.M., Titov V.N., The transition to the development of chaos in a chain of two unidirectionally-coupled backward-wave tubes. *Journ.Techn.Phys*. **2003**. 73, 90-94.
9. Glushkov, A.V.; Buyadzhi, V.V.; Ternovsky V.B. Geometry of Chaos: Consistent combined approach to treating of chaotic self-oscillations in backward-wave tube. *Proc. Intern. Geometry Center*. **2013**, *6*(2), 6-12.
10. Ternovsky V.B., Geometry and Dynamics of a Chaos: Modelling non-linear processes in relativistic backward-wave tubes chain. *Proc. of Int. Geom. Center*. **2014**, 7(3), 79-86
11. A.V. Glushkov, A.V. Tsudik, D.A. Novak, O.B. Dubrovsky, Chaotic dynamics of relativistic backward-wave tube with accounting for space charge field and dissipation effects: New effects. *Photoelectronics*. **2018.** 27, 44-51.
12. Levush, B.; Antonsen, T.M.; Bromborsky, A.; Lou, W.R.; Carmel, Y. Theory of relativistic backward wave oscillator with end reflections. *IEEE Trans. on Plasma Sci.* **1992**, *20*, 263-280.
13. Ryskin, N.M.; Titov, V.N. Self-modulation and chaotic regimes of generation in a relativistic backward-wave oscillator with end reflections. *Radiophys. and Quant.Electr*. **2001**, *44*, 793-806.
14. Glushkov, A.V.; Khetselius, O.Yu.; Svinarenko, A.A.; Prepelitsa, G.P. Energy approach to atoms in a laser field and quantum dynamics with laser pulses of different shape. *In Coherence and Ultrashort Pulsed Laser Emission.* Duarte, F.J., Ed.; InTech: Rijeka, **2010**, 159-186.
15. Levush, B.; Antonsen, T.; Bromborsky, A.; Lou, W. Relativistic backward wave oscillator: theory and experiment. *Phys.Fluid*. **1992**, *B4*, 2293-2299.
16. Glushkov, A.V. *Methods of a Chaos Theory*. OSENU: Odessa, **2012**.
17. Glushkov, A.V. *Atom in an electromagnetic field*. KNT: Kiev, **2005**.
18. Glushkov, A.V.; Khetselius, O.Yu.; Brusentseva, S.V.; Zaichko, P.A.; Ternovsky, V.B. Studying interaction dynamics of chaotic systems within a non-linear prediction method: Application to neurophysiology *In Advances in Neural Networks, Fuzzy Systems and Artificial Intelligence, Series: Recent Advances in Computer Engineering;* Balicki, J., Ed.; WSEAS Press: Gdansk, **2014**; Vol 21, pp 69-75.
19. Khetselius, O.Yu. Forecasting evolutionary dynamics of chaotic systems using advanced non-linear prediction method *In Dynamical Systems Applications;* Awrejcewicz, J., Kazmierczak, M., Olejnik, P., Mrozowski, J., Eds.; Wyd. Politech. Łódz.: Łódz, **2013**; Vol T2, pp 145-152..
20. Glushkov, A.V.; Malinovskaya, S.V.; Gurnitskaya, E.P.; Khetselius, O.Yu.; Dubrovskaya, Yu.V. Consistent quantum theory of recoil induced excitation and ionization in atoms during capture of neutron. *J. Phys.: Conf. Ser.* **2006,** *35*, 425-430.
21. Khetselius, O.Yu. *Hyperfine structure of atomic spectra*. Astroprint: Odessa, **2008**.
22. Khetselius, O.Yu. *Quantum structure of electroweak interaction in heavy finite Fermi-systems.* Astroprint: Odessa, **2011**.
23. Glushkov, A.V. *Relativistic Quantum theory. Quantum mechanics of atomic systems*. Astroprint: Odessa, **2008**.
24. Glushkov, A.V., Khetselius, O.Yu., Svinarenko, A.A., Buyadzhi, V.V. *Spectroscopy of autoionization states of heavy atoms and multiply charged ion*s. TEC: Odessa, **2015**
25. Glushkov, A.V. *Relativistic and correlation effects in spectra of atomic systems*. Astroprint: Odessa, **2006**.
26. Glushkov, A.V.; Prepelitsa, G.P.; Svinarenko, A.A. ; Zaichko, P.A. Studying interaction dynamics of the non-linear vi-

brational systems within non-linear prediction method (application to quantum autogenerators) *In Dynamical Systems Theory;* Awrejcewicz, J., Kazmierczak, M., Olejnik, P., Mrozowski, J., Eds.; Wyd. Politech. Łódz.: Łódz, **2013**; Vol T1, pp 467-477.
27. Abarbanel, H.; Brown, R.; Sidorowich, J; Tsimring, L. The analysis of observed chaotic data in physical systems. *Rev. Mod. Phys*. **1993**, *65*, 1331- 1392.
28. Packard, N.; Crutchfield, J; Farmer, J.; Shaw, R. Geometry from a time series *Phys. Rev. Lett*. **1988**, *45*, 712-716.
29. Kennel, M.; Brown, R.; Abarbanel, H. Determining embedding dimension for phase-space reconstruction using a geometrical construction. *Phys. Rev. A*. **1992**, *45*, 3403-3412.
30. Packard N., Crutchfield J., Farmer J., Shaw R., Geometry from a time series//Phys Rev Lett.-1988.-Vol.45.-P.712–716.
31. Gallager, R. *Information theory and reliable communication.* N.-Y., **1986**.
32. Grassberger, P. ; Procaccia, I. Measuring the strangeness of strange attractors. *Physica D*. **1983**, *9*, 189-208.
33. Theiler, J.; Eubank, S.; Longtin, A.; Galdrikian, B.; Farmer, J. Testing for nonlinearity in time series: The method of surrogate data. *Physica D*. **1992**, *58*, 77-94.
34. Glushkov, A.V.; Malinovskaya, S.V.; Loboda, A.V.; Shpinareva, I.M.; Gurnitskaya, E.P.; Korchevsky, D.A. Diagnostics of the collisionally pumped plasma and search of the optimal plasma parameters of x-ray lasing: calculation of electron-collision strengths and rate coefficients for Ne-like plasma. *J. Phys.: Conf. Ser*. **2005,** *11*, 188-198.
35. Taken, F. Detecting strange attractors in turbulence. *Lecture notes in mathematics (Springer)* **1981**, *898*, 366–381.
36. Glushkov, A.V.; Buyadzhi, V.V.; Ponomarenko, E.L. Geometry of Chaos: Advanced approach to treating chaotic dynamics in some nature systems// Proc. Intern. Geom. Center. 2014 *7(1)*,24-30.
37. Sano, M.; Y. Sawada, Y. Measurement of the Lyapunov spectrum from chaotic time series. *Phys Rev.Lett*. **1995**, *55*, 1082-1085
38. Rusov V., Glushkov A., Vaschenko V., Korchevsky D., Ignatenko A. Stochastic dynamics of the atomic systems in the crossed electric and magnetic field: the rubidium atom recurrence spectra. *Bull.of Kiev Nat. Univ.* **2004**, N4, 433.
39. Khetselius, O. Relativistic perturbation theory calculation of the hyperfine structure parameters for some heavy-element isotopes. *Int. J. Quant.Chem.* **2009,** *109*, 3330-3335.
40. Khetselius, O. Relativistic calculation of the hyperfine structure parameters for heavy elements and laser detection of the heavy isotopes. *Phys.Scr.* **2009,** *T135*, 014023.
41. Glushkov, A.; Gurskaya, M.; Ignatenko, A.; Smirnov, A.; Serga, I.; Svinarenko, A.; Ternovsky E. Computational code in atomic and nuclear quantum optics: Advanced computing multiphoton resonance parameters for atoms in a strong laser field. *J. Phys.: Conf. Ser*. **2017**, *905*, 012004.
42. Buyadzhi, V., Zaichko, P., Antoshkina, O., Kulakli, T., Prepelitsa, P., Ternovsky, V., Mansarliysky, V. Computing of radiation parameters for atoms and multicharged ions within relativistic energy approach: Advanced Code. *J. Phys.: Conf. Ser*. **2017**, *905*(1), 012003.
43. Svinarenko, A., Glushkov, A., Khetselius, O., Ternovsky,V., Dubrovskaya, Yu., Kuznetsova, A., Buyadzhi, V. Theoretical spectroscopy of rare-earth elements: spectra and autoionization resonances. *Rare Earth Element*, InTech. **2017**, 83-104.
44. Glushkov A.V., Khetselius O.Yu., Loboda A.V., Ignatenko A., Svinarenko A., Korchevsky D., Lovett L., QED Approach to Modeling Spectra of the Multicharged Ions in a Plasma: Oscillator and Electron-ion Collision Strengths. *AIP Conference Proceedings*.-**2008**. 1058, 175-177

45. Glushkov, A., Khetselius, O., Svinarenko A.A., Buyadzhi, V.V., Ternovsky, V., Kuznetsova, A., Bashkarev, P. Relativistic perturbation theory formalism to computing spectra and radiation characteristics: application to heavy element. *Recent Studies in Perturbation Theory*. InTech. **2017**, 131-150.
46. Glushkov, A.V.; Malinovskaya, S.V.; Prepelitsa, G.P.; Ignatenko, V. Manifestation of the new laser-electron nuclear spectral effects in the thermalized plasma: QED theory of co-operative laser-electron-nuclear proces-ses. *J. Phys.: Conf. Ser.* **2005,** *11*, 199-206.
47. Ivanova, E.P., Ivanov, L.N., Glushkov, A., Kramida, A. High order corrections in the relativistic perturbation theory with the model zeroth approximation, Mg-Like and Ne-Like Ions. *Phys. Scripta* **1985**, *32*, 513-522.
48. Prepelitsa, G.; Glushkov, A.V.; Lepikh, Ya.; Buyadzhi, V.; Ternovsky, V.; Zaichko, P. Chaotic dynamics of non-linear processes in atomic and molecular systems in electromagnetic field and semiconductor and fiber laser devices: new approaches, uniformity and charm of chaos. *Sensor Electr. and Microsyst.Techn*. **2014**, *11*, 43-57.

PACS 42.55.-f

Tsudik A.V., Glushkov A.V., Ternovsky V.B., Zaichko P.A.

ADVANCED COMPUTING TOPOLOGICAL AND DYNAMICAL INVARIANTS OF RELATIVISTIC BACKWARD-WAVE TUBE TIME SERIES IN CHAOTIC AND HYPERCHAOTIC REGIMES

Summary. The advanced results of computing the dynamical and topological invariants (correlation dimensions values, embedding, Kaplan-York dimensions, Lyapunov's exponents, Kolmogorov entropy etc) of the dynamics time series of the relativistic backward-wave tube with accounting for dissipation and space charge field and other effects are presented for chaotic and hyperchaotic regimes. It is solved a system of equations for unidimensional relativistic electron phase and field unidimensional complex amplitude. The data obtained make more exact earlier presented preliminary data for dynamical and topological invariants of the relativistic backward-wave tube dynamics in chaotic regimes and allow to describe a scenario of transition to chaos in temporal dynamics.

Key words: relativistic backward-wave tube, chaotic dynamics, non-linear methods

PACS 42.55.-f

Цудик А.В., Глушков А.В., Терновский В.Б., Заичко П.А.

ХАОТИЧЕСКАЯ ДИНАМИКА РЕЛЯТИВИСТСКОЙ ЛАМПЫ ОБРАТНОЙ ВОЛНЫ С УЧЕТОМ ВЛИЯНИЯ ПОЛЯ ПРОСТРАНСТВЕННОГО ЗАРЯДА И ДИССИПАЦИИ: НОВЫЕ ЭФФЕКТЫ

Резюме. Представлены уточненные данные вычисления динамических и топологических инвариантов (значения корреляционной размерности, размерности вложения, Каплана-Йорка, показатели Ляпунова, энтропия Колмогорова и др) для временных рядов, характеризующих динамику релятивистской лампы обратной волны с учетом эффектов диссипации, пространственного заряда и др. в хаотическом и гиперхаотическом режимов. Получены решения системы уравнений для одномерной релятивистской фазы электрона и одномерной комплексной амплитуды поля. Полученные данные уточняют ранее представленные данные для динамических и топологических инвариантов динамики релятивистской лампы обратной волны в хаотических режимах и позволяют количественно охарактеризовать сценарий перехода к хаосу во временной динамике.

Ключевые слова: релятивистская лампы обратной волны, хаотическая динамика, нелинейные методы

PACS 42.55.-f

Цудік, А.В., Глушков О.В., Терновський В.Б., Заічко П.О.

ХАОТИЧНА ДИНАМІКА РЕЛЯТИВІСТСЬКОЇ ЛАМПИ ЗВЕРНЕНОЇ ХВИЛІ З УРАХУВАННЯМ ВПЛИВУ ПОЛЯ ПРОСТОРОВОГО ЗАРЯДУ ТА ДИСИПАЦІЇ: НОВІ ЕФЕКТИ

Резюме. Представлені уточнені дані обчислення динамічних і топологічних інваріантів (значення кореляційної розмірності, розмірності вкладення, Каплана-Йорка, показники Ляпунова, ентропія Колмогорова та ін) для часових рядів, що характеризують динаміку релятивістської лампи зверненої хвилі з урахуванням ефектів дисипації, просторового заряду і ін. в хаотичному і гіперхаотичному режимах. Отримані рішення системи рівнянь для одновимірної релятивістської фази електрона і одновимірної комплексної амплітуди поля. Отримані дані уточнюють раніше представлені дані для динамічних і топологічних інваріантів динаміки релятивістської лампи зворотної хвилі в хаотичному режимі і дозволяють кількісно охарактеризувати сценарій переходу до хаосу у часовій динаміці.

Ключові слова: релятивістська лампи зворотної хвилі, хаотична динаміка, нелінійні методи

PACS 32.30.-r

Ternovsky V. B., Svinarenko A. A., Dubrovskaya Yu. V.

Odesa National Maritime Academy, Didrikhsona str. 4, Odesa, 65001
Odesa State Environmental University, L'vovskaya str., 15, Odesa, 65016, Ukraine
E-mail: ternovskyvb@gmail.com

THEORETICAL STUDYING EXCITED STATES SPECTRUM OF THE YTTERBIUM WITHIN THE OPTIMIZED RELATIVISTIC MANY-BODY PERTURBATION THEORY

Theoretical studying spectrum of the excited states for the ytterbium atom is carried out within the relativistic many-body perturbation theory with ab initio zeroth approximation and generalized relativistic energy approach. The zeroth approximation of the relativistic perturbation theory is provided by the optimized Dirac-Kohn-Sham ones. Optimization has been fulfilled by means of introduction of the parameter to the Kohn-Sham exchange potentials and further minimization of the gauge-non-invariant contributions into radiation width of atomic levels with using relativistic orbital set, generated by the corresponding zeroth approximation Hamiltonian. The obtained theoretical data on energies E and widths W of the ytterbium excited states are compared with alternative theoretical results (the Dirac-Fock, relativistic Hartree-Fock, perturbation theories) and available experimental data. Analysis shows that the theoretical and experimental values of energies are in good agreement with each other, however, the values of widths differ significantly. In our opinion, this fact is explained by insufficiently accurate estimates of the radial integrals, the use of unoptimized bases, and some other approximations of the calculation.

1. Introduction

A great interest in the study of radiation and autoionization processes involving electrons, photons, atoms and ions is stimulated by new classes of problems, in particular, in modern laser physics and physics of astrophysical, thermonuclear, laser and other plasmas (see [1-52]). In recent years, among atomic systems, special attention has been paid to the experimental and theoretical study of the spectral characteristics of heavy atoms, including atoms of lanthanides and actinides, as well as multiply charged ions. Traditionally, they are used in astrophysical research, in studies of the physics of laboratory plasma generated by various sources: laser pulses, tokamaks, pinches, capillary discharges, etc., in studies of thermonuclear fusion. For several decades, methods for the experimental study of the spectroscopic characteristics of the radiation of multiply charged ions have been developed and improved. A detailed description of experimental techniques can be found in a number of well-known books, reviews, and original experimental works (see, e.g., [1-52]).

A modern quantum mechanics of atoms (as well as molecules) has undergone significant development over the past few decades. It is possible to recall such well-known, along with those mentioned above, methods such as the Rayleigh-Schrödinger, Möller-Plesset perturbation theory (PT) method, PT in 1/Z parameter (Z is the charge of the atomic nucleus) and electron-electron interaction, PT with a model potential approximation, with Hartree-Fock (HF) or Dirac-Fock (DF) zeroth approximations andd many others. The multi-configuration DF method is the most reliable version of calculation for multielectron systems with a large nuclear charge. One should remember about very complicated structure of spectra of the heavy atoms, including actinides, uranium, trans-uranium elements and others and necessity of correct accounting for the different correlation effects such as polarization interaction of the valent quasiparticles and their mutual screening, iterations of a mass operator etc.).

The aim of our present work is to use an effective method of relativistic many-body PT with an optimized ab initio Dirac-Kohn-

Sham approximation [27-30] to study spectrum of excited states for the ytterbium.

2. The relativistic many-body perturbation theory and energy approach

As the method of computing is earlier presented in detail, here we are limited only by the key topics [27-30]. According to these Refs., the majority of complex atomic systems possess a dense energy spectrum of interacting states with essentially relativistic properties. In the theory of the non-relativistic atom a convenient field procedure is known for calculating the energy shifts ΔE of degenerate states. This procedure is connected with the secular matrix *M* diagonalization [30-32]. In constructing *M*, the Gell-Mann and Low adiabatic formula for ΔE is used.

In contrast to the non-relativistic case, the secular matrix elements are already complex in the second order of the electrodynamical PT (first order of the interelectron interaction). Their imaginary part of ΔE is connected with the radiation decay (radiation) possibility. In this approach, the whole calculation of the energies and decay probabilities of a non-degenerate excited state is reduced to the calculation and diagonalization of the complex matrix *M*. In the papers of different authors, the $\mathrm{Re}\,\Delta E$ calculation procedure has been generalized for the case of nearly degenerate states, whose levels form a more or less compact group. One of these variants has been previously introduced: for a system with a dense energy spectrum, a group of nearly degenerate states is extracted and their matrix *M* is calculated and diagonalized. If the states are well separated in energy, the matrix *M* reduces to one term, equal to ΔE. The non-relativistic secular matrix elements are expanded in a PT series for the interelectron interaction. The complex secular matrix *M* is represented in the form [26,27]:

$$M = M^{(0)} + M^{(1)} + M^{(2)} + M^{(3)}. \quad (1)$$

where $M^{(0)}$ is the contribution of the vacuum diagrams of all order of PT, and $M^{(1)}$, $M^{(2)}, M^{(3)}$ those of the one-, two- and three-quasiparticle diagrams respectively. $M^{(0)}$ is a real matrix, proportional to the unit matrix. It determines only the general level shift. We have assumed $M^{(0)} = 0$. The diagonal matrix $M^{(1)}$ can be presented as a sum of the independent one-quasiparticle contributions. For simple systems (such as alkali atoms and ions) the one-quasiparticle energies can be taken from the experiment. Substituting these quantities into (1) one could have summarized all the contributions of the one - quasiparticle diagrams of all orders of the formally exact QED PT. However, the necessary experimental quantities are not often available.

The first two order corrections to $\mathrm{Re}\,M^{(2)}$ have been analyzed previously using Feynman diagrams (look Ref. in [2,3]). The contributions of the first-order diagrams have been completely calculated. In the second order, there are two kinds of diagrams: polarization and ladder ones. The polarization diagrams take into account the quasiparticle interaction through the polarizable core, and the ladder diagrams account for the immediate quasiparticle interaction [30-36]. Some of the ladder diagram contributions as well as some of the three-quasiparticle diagram contributions in all PT orders have the same angular symmetry as the two-quasiparticle diagram contributions of the first order. These contributions have been summarized by a modification of the central potential, which must now include the screening (anti-screening) of the core potential of each particle by the two others. The additional potential modifies the one-quasiparticle orbitals and energies.

Then the secular matrix is as follows:

$$M \to \tilde{M}^{(1)} + \tilde{M}^{(2)}, \quad (2)$$

where $\tilde{M}^{(1)}$ is the modified one-quasiparticle matrix (diagonal), and $\tilde{M}^{(2)}$ the modified two-quasiparticle one. $\tilde{M}^{(1)}$ is calculated by substituting the modified one-quasiparticle energies), and $\tilde{M}^{(2)}$ by means of the first PT

order formulae for $M^{(2)}$, putting the modified radial functions of the one-quasiparticle states in the radial integrals..

Let us remind that in the QED theory, the photon propagator D(12) plays the role of this interaction. Naturally the analytical form of D(12) depends on the gauge, in which the electrodynamical potentials are written. Interelectron interaction operator with accounting for Breit interaction has been taken as follows:

$$V(r_i r_j) = exp(i\omega r_{ij}) \cdot \frac{(1 - \alpha_i \alpha_j)}{r_{ij}}, \qquad (3)$$

where, as usually, α_i are the Dirac matrices. In general, the results of all approximate calculations depended on the gauge. Naturally the correct result must be gauge-invariant. The gauge dependence of the amplitudes of the photoprocesses in the approximate calculations is a known fact and is investigated by Grant, Armstrong, Aymar and Luc-Koenig, Glushkov-Ivanov-Ivanova et al (see review in [9,32]). Grant has investigated the gauge connection with the limiting non-relativistic form of the transition operator and has formulated the conditions for approximate functions of the states, in which the amplitudes of the photo processes are gauge invariant (see review in [9]). These results remain true in the energy approach because the final formulae for the probabilities coincide in both approaches. Glushkov-Ivanov have developed a new relativistic gauge-conserved version of the energy approach [32]. In ref. [27,30,35-40] it has been developed its further generalization. Here we applied this approach for generating the optimized relativistic orbitals basis in the zeroth approximation of the many-body PT. Optimization has been fulfilled by means of introduction of the parameter to the Fock and Kohn-Sham exchange potentials and further minimization of the gauge-non-invariant contributions into radiation width of atomic levels with using relativistic orbital bases, generated by the corresponding zeroth approximation Hamiltonians [26]. Other details can be found in Refs. [9,27-29,41-47].

3. Some results and conclusion

Table 1 shows the experimental and theoretical data for the energies (measured from the energy of the ground state: 4f146s2 1S0) of some YbI singly excited states [2-7, 28-30]: MCHF-BP - data obtained on the basis of the multi-configuration Hartree-Fock method

Table 1.

Energy of the ground state: $4f^{14}6s^2\ ^1S_0$) of some YbI singly excited states: MCHF-BP - data obtained on the basis of the multi-configuration Hartree-Fock method (MCHF) taking into account Breit-Pauli corrections (BP) (C, D different sets of configurations included in the calculation by the MCHF-BP method [4]); RHF — the data by Cowan, RHF method; RMBPT - data of Ivanov-Letokhov et al., Method of the relativistic PT with model zeroth approximation; DF-data of DF analysis of Wyart-Camus with empirical fit, QED-PT data, obtained within the relativistic (QED) theory [28-30].

Config.	J	MCHF BPC	MCHF+ BPD	HFR	DF
$6s_{1/2}{}^{2}$ *	0	0	0	0	0
$6s_{1/2}6p_{1/2}$	0	17262	18730	17320	17312
$6s_{1/2}6p_{1/2}$	1	17568	18813	17954	17962
$6s_{1/2}6p_{3/2}$	1	26667	25257	25069	25075
$6s_{1/2}6p_{3/2}$	2	18249	18999	19710	19716
$6s_{1/2}5d_{3/2}$	1	28871	23740	24489	24489
$6s_{1/2}5d_{3/2}$	2	28973	24172	24484	24751
$6s_{1/2}5d_{5/2}$	2	29633	26841	27677	27654
$6s_{1/2}5d_{5/2}$	3	29374	25500	25271	25270
Config.	J	QED-PT	RMBPT	Our data	Exp
$6s_{1/2}{}^{2}$ *	0	0	0	0	0
$6s_{1/2}6p_{1/2}$	0	17310	17400	17305	17288
$6s_{1/2}6p_{1/2}$	1	18008	18100	18006	17992
$6s_{1/2}6p_{3/2}$	1	25094	25500	25088	25068
$6s_{1/2}6p_{3/2}$	2	19715	19800	19740	19710
$6s_{1/2}5d_{3/2}$	1	24410	23900	24527	24489
$6s_{1/2}5d_{3/2}$	2	24824	24600	24801	24752
$6s_{1/2}5d_{5/2}$	2	26970	26100	26712	27678
$6s_{1/2}5d_{5/2}$	3	25098	24900	25310	25271

Note: * [34] *E*=-148710cm^{-1}; *E1*=-148700cm^{-1}; *E2*=-148695cm^{-1};

(MCHF) taking into account Breit-Pauli corrections (BP) (C, D different sets of configurations included in the calculation by the MCHF-BP method [4]); RHF — Cowen data, RHF method; RMBPT (E1) - data of Ivanov-Letokhov et al., Method - relativistic TV with zero approximation MF; data of DF analysis of Wyart-Camus with empirical fit, data of QED-PT [28-30].

Analysis of the data in Table 1 shows that the role of exchange-correlation effects for the studied atom is extremely significant; The HF method with a small number of considered configurations has an error of more than 100 cm-1. Table 2 shows the experimental and theoretical data of Letokhov et al. [17, 82] for the energy and width of excited (autoionization) states of the 7s6p configuration in the YbI spectrum (which originate from the ground state: $4f^{14}6s^2\ ^1S_0$ Yb): E1, W1 - RMBPT - data of Ivanov et al. [7]; E2, W2 – QED theory [8] (QED-PT); E3- MCHF-BP data from Karacoban-Özdemir [4] (classification in [4] differs from our classification). E4W4 – our data.

Table 2.

Widts W (cm^{-1}) of autoionization resonances of the YbI 7s6p configuration (see text)

Term	W3	W1	W2	W4	W_{exp}
$^3P_0^0$	-	0.7	1.15	1.12	1.1
$^3P_1^0$	-	3.0	1.10	0.98	0.95
$^3P_2^0$	-	0.7	1.51	1.58	1.6
$^1P_1^0$	-	1.8	2.48	2.55	2.6

Analysis shows that the values of E1-E3, Eexp are in good agreement with each other, however, the values of W1-4, Wexp differ significantly. In our opinion, this fact is explained by insufficiently accurate estimates of the radial integrals, the use of unoptimized bases, and some other approximations of the calculation. This also applies to data obtained from the MCHF and RHF methods.

In our calculation, we used an optimized basis of the orbitals of the basis states and more accurately took into account important many-particle exchange-correlation effects, including the polarization and screening interactions of quasiparticles above the closed shells core, the pressure of the continuum and some other effects.

References

1. Gubanova, E., Glushkov, A., Khetselius, O., Bunyakova, Y., Buyadzhi, V., Pavlenko, E. *New methods in analysis and project management of environmental activity: Electronic and radioactive waste*. FOP: Kharkiv, **2017**.
2. Svinarenko A.A., Mischenko E.V., Loboda A.V., Dubrovskaya Yu.V. Quantum measure of frequency and sensing the collisional shift of the ytterbium hyperfine lines in medium of helium gas. *Sensors Electronics and Microsystems Technologies*. 2009, N1, 25-29.
3. Chernenko A., Beterov I.M., Permyakova O.I. Modeling of amplification without inversion near transitions from Autoionization levels of ytterbium atom. *Laser Phys.* **2000**, 10, 133-138.
4. Karaçoban B., Özdem L. Energies, Landé Factors, and Lifetimes for Some Excited Levels of Neutral Ytterbium (Z = 70)/ *Acta Phys.Polonica.A.* **2011**, 119, 342-353.
5. Jong-hoon Yi, Lee J., Kong H.J. Autoionizing states of the ytterbium atom by three-photon polarization spectroscopy. *Phys. Rev. A.* **1995**. 51. 3053–3057.
6. Jong-hoon Yi, Park H., Lee J. Investigation of even parity autoionizing states of ytterbium atom by two-photon ionization spectroscopy. *J. Korean Phys. Soc.* **2001.** 39, 916-920.
7. Bekov GI, Vidolova-Angelova E., Ivanov LN, Letokhov VS, Mishin VI, Laser spectroscopy of narrow doubly excited autoionization states of the ytterbium atom. *JETP*. 1**981**. 80 (3), 866-878.
8. Khetselius, O.. Relativistic perturbation theory calculation of the hyperfine structure parameters for some heavy-element isotopes. *Int. Journ. Quant.Chem.* **2009,** *109*, 3330-3335.
9. Khetselius, O. Relativistic calculation of the hyperfine structure parameters for heavy elements and laser detection of the

heavy isotopes. *Phys.Scr.* **2009,** *T135*, 014023.
10. Khetselius, O.Yu. *Hyperfine structure of atomic spectra*. Astroprint: Odessa, **2008**.
11. Khetselius, O.Yu. Optimized relativistic many-body perturbation theory calculation of wavelengths and oscillator strengths for Li-like multicharged ions. Adv. Quant. Chem. **2019**, *78*, 223-251.
12. Glushkov, A.V. *Relativistic Quantum theory. Quantum mechanics of atomic systems*. Astroprint: Odessa, **2008**.
13. Glushkov, A.V., Khetselius, O.Yu., Svinarenko, A.A., Buyadzhi, V.V. *Spectroscopy of autoionization states of heavy atoms and multiply charged ion*s. TEC: Odessa, **2015**.
14. Dubrovskaya, Yu., Khetselius, O.Yu., Vitavetskaya, L., Ternovsky, V., Serga, I. Quantum chemistry and spectroscopy of pionic atomic systems with accounting for relativistic, radiative, and strong interaction effects. *Adv. in Quantum Chem.* **2019,** Vol.78, pp 193-222.
15. Bystryantseva, A., Khetselius, O.Yu., Dubrovskaya, Yu., Vitavetskaya, L.A., Berestenko, A.G. Relativistic theory of spectra of heavy pionic atomic systems with account of strong pion-nuclear interaction effects: ^{93}Nb, ^{173}Yb, ^{181}Ta, ^{197}Au. *Photoelectronics*. **2016**, *25*, 56-61.
16. Khetselius, O., Glushkov, A., Gurskaya, M., Kuznetsova, A., Dubrovskaya, Yu., Serga, I., Vitavetskaya, L. Computational modelling parity nonconservation and electroweak interaction effects in heavy atomic systems within the nuclear-relativistic many-body perturbation theory. *J. Phys.: Conf. Ser.* ***2017,*** *905*(1), 012029.
17. Khetselius, O.Yu., Glushkov, A.V., Dubrovskaya, Yu.V., Chernyakova, Yu., Ignatenko, A.V., Serga, I., Vitavetskaya, L. Relativistic quantum chemistry and spectroscopy of exotic atomic systems with accounting for strong interaction effects. In: Concepts, *Methods and Applications of Quantum Systems in Chemistry and Physics*. Springer, Cham. **2018,** *31*, 71-91.
18. Svinarenko, A., Khetselius, O., Buyadzhi, V.V., Florko, T., Zaichko, P., Ponomarenko, E. Spectroscopy of Rydberg atoms in a Black-body radiation field: Relativistic theory of excitation and ionization. *J. Phys.: Conf. Ser*. **2014**, *548*, 012048.
19. Khetselius, O.Yu. *Quantum structure of electroweak interaction in heavy finite Fermi-systems.* Astroprint: Odessa, **2011**.
20. Khetselius, O.Y. Hyperfine structure of energy levels for isotopes ^{73}Ge, ^{75}As, ^{201}Hg. *Photoelectronics*. **2007,** *16*, 129-132.
21. Khetselius, O.Y., Gurnitskaya, E.P., Sensing the electric and magnetic moments of a nucleus in the N-like ion of Bi. *Sensor Electr. and Microsyst. Techn*. **2006**, *N3*, 35-39.
22. Khetselius, O.Yu., Lopatkin, Yu.M., Dubrovskaya, Yu.V, Svinarenko, A.A. Sensing hyperfine-structure, electroweak interaction and parity non-conservation effect in heavy atoms and nuclei: New nuclear-QED approach. *Sensor Electr. and Microsyst. Techn*. **2010,** 7(2), 11-19.
23. Florko, T.A., Tkach, T.B., Ambrosov, S.V., Svinarenko, A.A. Collisional shift of the heavy atoms hyperfine lines in an atmosphere of the inert gas. *J. Phys.: Conf. Ser*. **2012**, *397*, 012037.
24. Glushkov, A., Vitavetskaya, L. Accurate QED perturbation theory calculation of the structure of heavy and superheavy element atoms and multicharged ions with the account of nuclear size effect and QED corrections. *Herald of Uzhgorod Univ. Ser. Phys*. **2000**, *8*(2), 321-324.
25. Buyadzhi, V.V., Chernyakova, Yu.G., Smirnov, A.V., Tkach, T.B. Electron-collisional spectroscopy of atoms and ions in plasma: Be-like ions. *Photoelectronics*. **2016,** *25*, 97-101.
26. Buyadzhi, V.V., Chernyakova, Yu.G., Antoshkina, O., Tkach, T. Spectroscopy of multicharged ions in plasmas: Oscillator strengths of Be-like ion Fe. *Photoelectronics*. **2017,** *26*, 94-102
27. Ternovsky, V., Theoretical studying Rydberg states spectrum of the uranium atom on the basis of relativistic many-body perturbation theory. Photoelectronics. **2019**, 28, 39-45

28. Glushkov, A.V., Khetselius, O.Yu., Svinarenko A.A. Theoretical spectroscopy of autoionization resonances in spectra of lanthanides atoms. *Phys. Scripta*. **2013**, *T153*, 014029.
29. Svinarenko, A., Glushkov, A, Khetselius, O., Ternovsky, V., Dubrovskaya Y., Kuznetsova A., Buyadzhi V. Theoretical spectroscopy of rare-earth elements: spectra and autoionization resonances. *Rare Earth Element*, Ed. J. Orjuela (InTech). **2017**, pp 83-104.
30. Glushkov, A.V., Khetselius, O.Yu., Svinarenko A.A., Buyadzhi, V.V., Ternovsky, V.B, Kuznetsova, A., Bashkarev, P. Relativistic perturbation theory formalism to computing spectra and radiation characteristics: application to heavy element. *Recent Studies in Perturbation Theory*, ed. D. Uzunov (InTech). **2017**, 131-150.
31. Glushkov, A.V., Svinarenko, A.A., Ternovsky, V.B., Smirnov, A.V., Zaichko, P.A. Spectroscopy of the complex autoionization resonances in spectrum of helium: Test and new spectral data. *Photoelectronics*. **2015**, *24*, 94-102.
32. Glushkov, A.V., Ternovsky, V.B., Buyadzhi, V., Zaichko, P., Nikola, L. Advanced relativistic energy approach to radiation decay processes in atomic systems. *Photoelectr*. **2015**, *24*, 11-22.
33. Ivanov, L.N.; Ivanova, E.P. Method of Sturm orbitals in calculation of physical characteristics of radiation from atoms and ions. *JETP*. **1996,** *83*, 258-266.
34. Glushkov, A.V., Ivanov, L.N., Ivanova, E.P. Autoionization Phenomena in Atoms. *Moscow Univ. Press*, Moscow, **1986,** 58.
35. Glushkov, A.V., Ivanov, L.N. Radiation decay of atomic states: atomic residue polarization and gauge noninvariant contributions. *Phys. Lett. A* **1992,** *170*, 33.
36. Glushkov, A.V.; Ivanov, L.N. DC strong-field Stark effect: consistent quantum-mechanical approach. *J. Phys. B: At. Mol. Opt. Phys.* **1993,** *26*, L379-386.
37. Ivanova, E., Glushkov, A. Theoretical investigation of spectra of multicharged ions of F-like and Ne-like isoelectronic sequences. J. Quant. Spectr. and Rad. Tr. **1986**, *36*(2), 127-145.
38. Ivanova, E.P., Ivanov, L.N., Glushkov, A., Kramida, A. High order corrections in the relativistic perturbation theory with the model zeroth approximation, Mg-Like and Ne-Like Ions. *Phys. Scripta* **1985**, *32*, 513-522.
39. Glushkov, A.V. *Relativistic and correlation effects in spectra of atomic systems*. Astroprint: Odessa, **2006**.
40. Glushkov, A.V. Multiphoton spectroscopy of atoms and nuclei in a laser field: Relativistic energy approach and radiation atomic lines moments method. *Adv. in Quantum Chem.* **2019**, *78*, 253-285.
41. Glushkov, A., Loboda, A., Gurnitskaya, E., Svinarenko, A. QED theory of radiation emission and absorption lines for atoms in a strong laser field. *Phys. Scripta.* **2009,** *T135*, 014022.
42. Glushkov, A. Spectroscopy of cooperative muon-gamma-nuclear processes: Energy and spectral parameters *J. Phys.: Conf. Ser.* **2012,** *397*, 012011.
43. Glushkov, A.V. Spectroscopy of atom and nucleus in a strong laser field: Stark effect and multiphoton resonances. *J. Phys.: Conf. Ser*. **2014**, *548*, 012020.
44. Glushkov, A.V., Ternovsky, V.B., Buyadzhi, V., Prepelitsa, G.P. Geometry of a Relativistic Quantum Chaos: New approach to dynamics of quantum systems in electromagnetic field and uniformity and charm of a chaos. *Proc. Int. Geom. Center*. **2014,** *7*(4), 60-71.
45. Glushkov, A., Buyadzhi, V., Kvasikova, A., Ignatenko, A., Kuznetsova, A., Prepelitsa, G., Ternovsky, V. Non-Linear chaotic dynamics of quantum systems: Molecules in an electromagnetic field and laser systems. In: *Quantum Systems in Physics, Chemistry, and Biology*. Springer, Cham. **2017**, *30*, 169-180.
46. Glushkov, A.V. Relativistic polarization potential of a many-electron atom. *Sov. Phys. Journal.* **1990**, *33(1)*, 1-4.
47. Glushkov, A., Svinarenko, A., Ignatenko, A. Spectroscopy of autoionization reso-

nances in spectra of the lanthanides atoms. *Photoelectronics*. **2011**, *20*, 90-94.
48. Glushkov, A., Gurskaya, M., Ignatenko, A., Smirnov, A., Serga, I., Svinarenko, A., Ternovsky, E. Computational code in atomic and nuclear quantum optics: Advanced computing multiphoton resonance parameters for atoms in a strong laser field. *J. Phys.: Conf. Ser*. **2017**, *905*, 012004.
49. Glushkov, A., Khetselius, O., Svinarenko, A., Buyadzhi, V. *Methods of computational mathematics and mathematical physics*. *P.1*. TES: Odessa, **2015**.
50. Khetselius, O.Yu. Spectroscopy of cooperative electron-gamma-nuclear processes in heavy atoms: NEET effect. *J. Phys.: Conf. Ser*. **2012**, 3*97*, 012012.
51. Buyadzhi, V., Zaichko, P., Antoshkina, O., Kulakli, T., Prepelitsa, G., Ternovsky, V.B., Mansarliysky, V. Computing of radiation parameters for atoms and multicharged ions within relativistic energy approach: Advanced Code. *J. Phys.: Conf. Ser*. **2017**, *905*(1), 012003.
52. Glushkov A.V., Khetselius O.Yu., Loboda A.V., Ignatenko A., Svinarenko A., Korchevsky D., Lovett L., QED Approach to Modeling Spectra of the Multicharged Ions in a Plasma: Oscillator and Electron-ion Collision Strengths.. *AIP Conference Proceedings***. 2008**. 1058. 175-177
53. Ternovsky V. Theoretical study of the Yb spectrum. Preprint OSENU, **2019**, AM-2.

PACS 32.30.-r

Ternovsky V.B., Svinarenko A.A., Dubrovskaya Yu.V.

THEORETICAL STUDYING EXCITED STATES SPECTRUM OF THE YTTERBIUM WITHIN THE OPTIMIZED RELATIVISTIC MANY-BODY PERTURBATION THEORY

Summary. Theoretical studying spectrum of the excited states for the ytterbium atom is carried out within the relativistic many-body perturbation theory with ab initio zeroth approximation and generalized relativistic energy approach. The zeroth approximation of the relativistic perturbation theory is provided by the optimized Dirac-Kohn-Sham ones. Optimization has been fulfilled by means of introduction of the parameter to the Kohn-Sham exchange potentials and further minimization of the gauge-non-invariant contributions into radiation width of atomic levels with using relativistic orbital set, generated by the corresponding zeroth approximation Hamiltonian. The obtained theoretical data on energies E and widths W of the ytterbium excited states are compared with alternative theoretical results (the Dirac-Fock, relativistic Hartree-Fock, perturbation theories) and available experimental data. Analysis shows that the theoretical and experimental values of energies are in good agreement with each other, however, the values of widths differ significantly. In our opinion, this fact is explained by insufficiently accurate estimates of the radial integrals, the use of unoptimized bases, and some other approximations of the calculation.

Keywords: Relativistic perturbation theory, optimized zeroth approximation, ytterbium atom, spectrum of excited states

PACS 32.30.-r

Терновский В.Б., Свинаренко А.А., Дубровская Ю.В.

ТЕОРЕТИЧЕСКОЕ ИССЛЕДОВАНИЕ СПЕКТРА ВОЗБУЖДЕННЫВХ СОСТОЯНИЙ ИТТЕРБИЯ НА ОСНОВЕ РЕЛЯТИВИСТСКОЙ МНОГОЧАСТИЧНОЙ ТЕОРИИ ВОЗМУЩЕНИЙ

Резюме. В рамках релятивистской многочастичной теории возмущений и обобщенного релятивистского энергетического подхода проведено теоретическое исследование спектра ридберговских состояний атома урана. В качестве нулевого приближения релятивистской теории возмущений выбрано оптимизированное приближение Дирака-Кона-Шэма. Оптимизация выполнена путем введения параметра в обменные потенциалы Фока и Кона-Шэма и дальнейшей минимизацией калибровочно-неинвариантных вкладов в радиационные ширины атомных уровней с использованием релятивистского базиса орбиталей, сгенерированного соответствующим гамильтонианом нулевого приближения. Полученные теоретические данные об энергиях E и ширинах W возбужденных состояний иттербия сравниваются с альтернативными теоретическими результатами (теории Дирака-Фока, релятивистского Хартри-Фока, теории возмущений) и имеющимися экспериментальными данными. Анализ показывает, что теоретические и экспериментальные значения энергий хорошо согласуются между собой, однако значения ширин существенно различаются. На наш взгляд, это объясняется недостаточно точными оценками радиальных интегралов, использованием неоптимизированных базисов и некоторыми другими приближениями расчетов.

Ключевые слова: Релятивистская теория возмущений, оптимизированное нулевое приближение, атом иттербия, спектр возбужденных состояний

PACS 32.30.-r

Терновський В.Б., Свинаренко А.А., Дубровська Ю.В.

ТЕОРЕТИЧНЕ ВИВЧЕННЯ СПЕКТРУ ЗБУДЖЕНИХ СТАНІВ ІТЕРБІЮ НА ОСНОВІ РЕЛЯТИВІСТСЬКОЇ БАГАТОЧАСТКОВІ ТЕОРІЇ ЗБУРЕНЬ

Резюме. В рамках релятивістської багаточастинкової теорії збурень і узагальненого релятивістського енергетичного підходу проведено теоретичне дослідження спектра збуджених станів атома ітербію. В якості нульового наближення релятивістської теорії збурень обрано оптимізоване наближення Дірака-Кона-Шема. Оптимізація виконана шляхом введення параметра в обмінний потенціал Кона-Шема і подальшої мінімізації калібрувально-неінваріантних вкладів в радіаційні ширини атомних рівнів з використанням релятивістського базису орбіталей, згенерованого відповідним гамільтоніаном нульового наближення. Отримані теоретичні дані про енергії E і завширшки W збуджених станів ітербію порівнюються з альтернативними теоретичними результатами (теорії Дірака-Фока, релятивістського Хартрі-Фока, теорії збурень) і наявними експериментальними даними. Аналіз показує, що теоретичні і експериментальні значення енергій добре узгоджуються між собою, однак значення ширини істотно розрізняються. На наш погляд, це пояснюється недостатньо точними оцінками радіальних інтегралів, використанням неоптимізованих базисів і деякими іншими наближеннями розрахунків.

Ключові слова: Релятивістська теорія збурень, оптимізоване нульове наближення, атом ітербію, спектр збуджених станів.

UDC 539.182

Zaichko P. A., Kuznetsova A. A., Tsudik A. V., Mansarliysky V. F.

Odesa National Maritime Academy, Odesa, 4, Didrikhsona str., Odesa, Ukraine
e-mail: zaichkopa@gmail.com

RELATIVISTIC CALCULATION OF THE RADIATIVE TRANSITION PROBABILITIES AND LIFETIMES OF EXCITED STATES FOR THE RUBIDIUM ATOM IN A BLACK-BODY RADIATION FIELD

We present the results of relativistic calculation of the radiative transition probabilities and excited states lifetimes for a heavy Rydberg atomic systems in a black-body (thermal) radiation field on example of the rubidium. As theoretical approach we apply the combined generalized relativistic energy approach and relativistic many-body perturbation theory with ab initio Dirac zeroth approximation. There are obtained the calculational data for the radiative transition probabilities and excited states lifetimes, in particular, the rubidium atom in the Rydberg states with principal quantum number n=10-100. It is carried out the comparison of obtained theoretical data on the effective lifetime for the group of Rydberg nS states of the rubidium atom at a temperature of T = 300K with experimental data as well as data of alternative theoretical calculation based on the improved quasiclassical model. It is shown that the accuracy of the theoretical data on the radiative transition probabilities and excited states lifetimes is provided by a correctness of the corresponding relativistic wave functions and accounting for the exchange-correlation effects.

1. Introduction

In the last two decades, a new field of research has been very actively developed in modern optics and spectroscopy, namely quantum optics and spectroscopy of Rydberg atoms (RA) and ions. These are atomic systems that are in highly excited states with large values of the principal quantum number n. By the way, it is known that a number of astrophysical processes in interstellar gas, which interacts with fragments of supernova explosions, collisions of interstellar clouds, and supersonic gas flows during star formation lead to PA with very large n (~ 1000). The reasons for the significant interest in RA are well known and are connected, first, with the properties extraordinary for ordinary atoms, namely: for the lifetime: $n^3 a_0 \hbar / e^2 Z$ ($\tau \sim n^3$ for $l \sim 1$, $\tau \sim n^5$ for $n \sim l$; l--orbital quantum number), geometric dimensions $\sim n^2$ ($n^2 a_0 / Z$, $a_0 = \hbar^2/me^2 =$ 0,5291773Å), geometric cross sections $\pi n^4 a^2{}_0 / Z^2$, Rydberg electron binding energies $Z^2 R_\infty / n^2$ (R_∞ =13.6058 eV), polarizabilities ~ n^2, dipole moments of radiation transitions ~ n^2, shifts due to external fields (Stark shift ~ $n^7 l^5$, Zeeman effect ~ n^2). Moreover, the idea of the existence of the fifth state of matter, namely, the Rydberg substance, is well-founded. As a result, in recent years it has stimulated intensive research in the field of standard fundamental spectroscopy of RA, related to the calculation of energy and spectroscopic parameters of these atoms, important for the general development of relativistic (quantum-electrodynamic, QED) theory of atomic spectra, and applied research in fields of quantum optics, computer science, cryptography, quantum computing (e.g. [1-28]).

The vast majority of existing papers on the description of Rydberg atoms in the thermal radiation field (c.g. [1-32]) are based on the Coulomb approximation (CA), model potential (MP) approach, , different versions of the quantum defect method, classical and quasiclassical model approaches. The authors of the papers [3-10] applied the Coulomb approximation, quantum defect formalism, different versions of the model and pseudopotential method etc. It should be noted separately the cycles of theoretical and experimental works by Nashimento et al and especially Ryabtsev-Beterov et al [2,3], as well as theoretical works of Dyachkov-Pankratov and others (c.g.[1-10]), in which the ad-

vanced versions of a quasi-classical approach to the calculation of radiation amplitudes, oscillator strengths, and cross-sections for the Rydberg atoms in the BBR radiation field were actually developed.

In the papers [1-3,7-10] the authors present the calculational data on the ionization rates for Rydberg atoms of alkali elements (lithium, sodium, potassium, caesium) by a BBR radiation field. The calculations were carried out for the nS, nP, and nD states in the wide range of principal quantum numbers and temperatures. The above theoretical works and relevant models were substantially based on non-relativistic approximation. At the same time one should note that for heavy Rydberg atoms (both in the free state and in an external electromagnetic field) it is fundamentally important to accurately account for both relativistic and exchange-correlation effects.

In this paper the results of relativistic calculation of the radiative transition probabilities and excited states lifetimes for a heavy Rydberg atomic systems in a black-body (thermal) radiation field are presented on example of the rubidium atom. As theoretical approach we apply the combined generalized relativistic energy approach and relativistic many-body perturbation theory with ab initio Dirac zeroth approximation. There are obtained the calculational data for the radiative transition probabilities and excited states lifetimes, in particular, the rubidium atom in the Rydberg states with principal quantum number n=10-100. It is carried out the comparison of obtained theoretical data on the effective lifetime for the group of Rydberg nS states of the rubidium atom at a temperature of T = 300K with experimental data as well as data of alternative theoretical calculation based on the improved quasiclassical model. .

2. Relativistic theory of multielectron atom in a Black-body radiation field: Some theoretical aspects

From the physical viewpoint, a qualitative picture of the BBR Rydberg atoms ionization is easily understandable. Even for temperatures of order $T=10^4$ K, the frequency of a greater part of the BBR photons ω does not exceed 0.1 a.u. Usually, it is enough to use a single- electron approximation for calculating the ionization cross section $\sigma_{nl}(\omega)$.

The latter appears in a product with the Planck's distribution for the thermal photon number density:

$$\rho(w,T)=\frac{\omega^2}{\pi^2 c^3[\exp(\omega/kT)-1]}, \quad (1)$$

where k=3.1668×10^{-6} a.u., K^{-1} is the Boltzmann constant, c = 137.036 a.u. is the speed of light. Ionization rate of a bound state nl results in the integral over the Blackbody radiation frequencies:

$$P_{nl}(T)=c\int_{|E_{nl}|}^{\infty}\sigma_{nl}(\omega)\rho(\omega,T)d\omega. \quad (2)$$

The ionization cross-section from a bound state with a principal quantum number n and orbital quantum number l by photons with frequency ω is as follows:

$$\sigma_{nl}(\omega)=\frac{4\pi^2\omega}{3c(2l+1)}[lM^2_{nl\to El-1}+$$

$$+(l+1)M^2_{nl\to El+1}], \quad (3)$$

where the radial matrix element of the ionization transition from the bound state with the radial wave function $R_{nl}(r)$ to continuum state with the wave function $R_{El}(r)$ normalized to the delta function of energy. The corresponding radial matrix elements are written by the standard way. Other details can be found in Refs. [9-16].

We apply a generalized energy approach [9-20] and relativistic perturbation theory with the zeroth approximation [21-32] to computing the Rydberg atoms ionization parameters. According to Ref. [11,22], the RMBPT zeroth order Hamiltonian of the Rydberg atomic system is as follows:

$$H_0 = \sum_i \{\alpha c p_i - \beta mc^2 + [-Z/r_i + U_{MF}(r_i \mid b) + V_{XC}(r_i)] \qquad (4)$$

where c is the velocity of light, α_i, α_j – the Dirac matrices, ω_{ij} –the transition frequency, Z is a charge of atomic nucleus. The general potential in (4) includes self-consistent Coulomb-like mean-field potential $U_{MF}(r_i \mid b)$, ab ibitio one-particle exchange-correlation (relativistic generalized exchange Kohn-Sham potential plus generalized correlation Lundqvist-Gunnarsson potential) $V_{XC}(r_i \mid b)$ with the gauge calibrated parameter b (it is determined within special relativistic procedure on the basis of relativistic energy approach; c.g. [21-32]).

The perturbation operator is as follows:

$$H^{PT} = \sum_{i>j} exp(i\omega_{ij} r_{ij}) \cdot \frac{(1 - \alpha_i \alpha_j)}{r_{ij}} - \sum_i [U_{MF}(r_i) + V_{XC}(r_i \mid b)] \qquad (5)$$

The multielectron interelectron exchange-correlation effects (the core polarization and screening effects, continuum pressure etc) are taken into consideration as the RMBPT second and higher orders contributions. The details of calculation of the corresponding matrix elements of the polarization and screening interelectron interaction potentials are described in Refs. [9,22,33-38].

In relativistic theory radiation decay probability (ionization cross-section etc) is connected with the imaginary part of electron energy shift. The total energy shift of the state is usually presented in the form: $\Delta E = \mathrm{Re}\Delta E + i\,\Gamma/2$, where Γ is interpreted as the level width, and a decay probability $P = \Gamma$. The imaginary part of electron energy shift is defined in the PT lowest order as:

$$\mathrm{Im}\Delta E(B) = -\frac{e^2}{4\pi} \sum_{\substack{\alpha>n>f \\ [\alpha<n\le f]}} V_{\alpha n \alpha n}^{|\omega_{\alpha n}|}, \qquad (6)$$

where (α>n>f) for electron and (α<n<f) for vacancy.

The matrix element is determined as follows:

$$V_{ijkl}^{|\omega|} = \iint dr_1 dr_2 \Psi_i^*(r_1) \Psi_j^*(r_2) \frac{\sin|\omega| r_{12}}{r_{12}} (1 - \alpha_1 \alpha_2) \Psi_k^*(r_2) \Psi_l^*(r_1) \qquad (7)$$

Their detailed description of the matrix elements and procedure for their computing is presented in Refs. [16-20]. The relativistic wave functions are calculated by solution of the Dirac equation with the potential, which includes the Dirac-Fock consistent field potential and additionally polarization potential [22].

The total ionization rate of the Rydberg atomic system in the BBR radiation field is usually determined as the sum of direct BBR ionization rate of the initially excited state, the ionization (field ionization) rate of highly excited states, which are populated from the initial Rydberg state via absorption of the BBR photons, the rate of direct BBR-induced ionization of atoms from the neighbouring Rydberg states and the rate of field ionization of high-lying Rydberg states (with populating through so called two-step process via the BBR photons absorption).

The total width of the Rydberg state (naturally isolated from all external electromagnetic fields except BBR one) consists, apparently, of natural, spontaneous radiation width Γ_{nl}^{sp} and BBR-induced (thermal) width Γ_{nl}^{BBR}:

$$\Gamma_{nl}^{tot} = \Gamma_{nl}^{sp} + \Gamma_{nl}^{BBR}(T). \qquad (8)$$

Accordingly, the effective lifetime of the Rydberg state is inversely proportional to the total decay rate as a result of spontaneous transitions and transitions induced by the BBR radiation:

$$\frac{1}{\tau_{eff}} = \Gamma_0 + \Gamma_{\mathrm{BBR}} = \frac{1}{\tau_0} + \frac{1}{\tau_{BBR}} \qquad (9)$$

The detailed procedures of calculation of the radial and angular integrals (amplitudes) in

the matrix elements are described in the Refs. [16-44]. All calculations are performed on the basis of the code Superatom.

3. Results and conclusions

In Table 1 we present our theoretical data (Our) values of the lifetimes (in ns) of the group of some excited states of the rubidium atom, as well as experimental data and alternative theoretical results obtained on the basis of different approaches: the Coulomb approximation (QA) and model potential (MP), and PTDFSD (many-body perturbation theory with Dirac-Fock SD zero approximation) plus the same data of this method with compilation contribution; method of model potential with the relativistic energy approach (REA) - MP-REA - (data from Refs. [1-5]).

Table 1.
The theoretical and experimental lifetimes (ns) of the group of the Rb some excited states (see text)

level	QA-MP	PTDF^{SD}	PT- DF^{SDc}
$6s_{1/2}$	-	45.4	45.4
$7s_{1/2}$	-	88.3	88.3
$8s_{1/2}$	-	161.8	161.9
$9s_{1/2}$	266.36	-	271.7
$10s_{1/2}$	417.84	-	426
$6p_{1/2}$	-	123	122.5
$6p_{3/2}$	-	113	112.4
$7p_{1/2}$	-	280	277.8
$7p_{3/2}$	-	258	255.2
$8p_{1/2}$	-	508	501.0
$8p_{3/2}$	-	471	464.2
$7d_{3/2}$	331.08	-	339.5
$7d_{5/2}$	319.57	-	327.0
level	MP-EA	Our	Exp.
$6s_{1/2}$	45.5	45.5	45.57(17)
$7s_{1/2}$	88.1	88.2	88.07(40)
$8s_{1/2}$	161.4	161.5	161(3)
$9s_{1/2}$	262.1	262.1	253(14)
$10s_{1/2}$	421.3	426.4	430(20)
$6p_{1/2}$	124.1	124.1	125(4)
$6p_{3/2}$	112.1	112.6	112(3)
$7p_{1/2}$	274.3	274.1	272(15)
$7p_{3/2}$	249.0	248.8	246(10)
$8p_{1/2}$	497.4	496.9	
$8p_{3/2}$	456.2	455.1	400(80)
$9p_{1/2}$	796.4	795.6	
$9p_{3/2}$	743.6	742.7	665(40)
$10p_{1/2}$	964.2	963.8	
$10p_{3/2}$	921,0	920.5	
$7d_{3/2}$	336.2	340.5	345(9)
$7d_{5/2}$	324.8	328.1	325(22)
$8d_{3/2}$	488.3	490.4	515(30)
$8d_{5/2}$	431.1	432.8	421(25)

Analysis of the data in Table 1 shows that the error in calculating the lifetime of different levels in the rubidium atom obviously depends on the accuracy, consistency and correctness of the main relativistic and correlation corrections, and above all, exchange-polarization.

Next, we present the results of calculating the effective lifetime of the Rydberg states of the rubidium atom depending on the principal quantum number at the fixed temperature T. In Figure 1, we present theoretical data (dashed line) on the dependence of the values of the effective lifetime for the group of Rydberg (a) nS states of the rubidium atom at a temperature of T = 300K), in dependence upon the principal quantum number as well as experimental data – black circles [1] and data of alternative theoretical calculation based on the improved quasiclassical model by Beterov et al [2]. - continuous line.

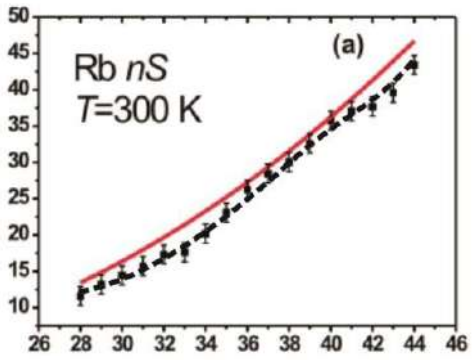

Figure 1. Our theoretical data (dashed line) on the dependence of the values of the effective lifetime for the group of Rydberg (a) nS states of the Rb atom at T = 300K), as well as experimental data – black circles [1] and data of alternative theoretical calculation based on the improved quasiclassical model by Beterov et al [2]. - continuous line

The corresponding values of the lifetimes of the levels are obtained for the values of the principal quantum number n up to 100. In general, the results of our non-empirical relativistic theory are in physically realistic agreement with the experimental data, at least much better than some other alternative theoretical approaches. The same applies to the effect of thermal radiation reduces the value of a lifetime.

References

[1] Nascimento V.A., Caliri L.L., de Oliveira A.L., Bagnato V.S. , Marcassa L.G. Measurement of the lifetimes of S and D states below n=31 using cold Rydberg gas. *Phys.Rev.A.* **2006,** 74, 054501.

[2] Beterov, I.I., Ryabtsev, I., Tretyakov D., Entin, V. Quasiclassical calculations of blackbody-radiation-induce depopulation rates and effective lifetimes of Rydberg *nS*, *nP*, and *nD* alkali-metal atoms with *n*~80. *Phys Rev A.* **2009,** 79, 052504.

[3] Beterov I.I., TretyakovD.V., Ryabtsev I.I., Entin V.M., Ekers A., Bezuglov N.N., Ionization of Rydberg atoms by blackbody radiation. *New J. Phys*. **2009,** *11*, 013052

[4] Safronova U., Safronova M. Third-order relativistic many-body calculations of energies, transition rates, hyperfine constants, blackbody radiation shift in $^{171}Yb^{+}$. *Phys. Rev. A.* **2009**, *79*, 022512.

[5] Angstmann, E., Dzuba, V., Flambaum, V. Frequency shift of hyperfine transitions due to blackbody radiation. *Phys. Rev. A.* **2006**, *74*, 023405.

[6] Gallagher T.F., Cooke W.E. Interactions of Blackbody Radiation with atoms. *Phys. Rev. Lett*. **1979**, *42*, 835–839.

[7] Lehman G. W. Rate of ionization of H and Na Rydberg atoms by black-body radiation. *J. Phys. B: At. Mol. Phys*. **1983**, *16*, 2145-2156.

[8] D'yachkov L., Pankratov P. On the use of the semiclassical approximation for the calculation of oscillator strengths and photoionization cross sections. *J. Phys. B: At. Mol. Opt. Phys*. **1994**, *27*, 461-468.

[9] Svinarenko A.A., Khetselius O.Yu., Buyadzhi V.V., Florko T.A., Zaichko P.A., Ponomarenko E.L., Spectroscopy of Rydberg atoms in a Black-body radiation field: Relativistic theory of excitation and ionization. *J. Phys.: Conf. Ser*. **2014**, *548,* 012048.

[10] Svinarenko A.A., Khetselius O.Yu., Buyadzhi V., Kvasikova A., Zaichko P. Spectroscopy of Rydberg atoms in a Black-body radiation field: Relativistic theory of excitation and ionization. *Photoelectronics*. **2014**, *23*, 147-151.

[11] Glushkov, A.V., Ternovsky, V.B., Buyadzhi, V., Tsudik, A., Zaichko, P. Relativistic approach to calcuation of ionization characteristics for rydberg alkali atom in a black-body radiation field. *Sensor Electr. and Microsyst. Techn*. **2019**, *16*(3), 69-77.

[12] Glushkov, A.V. *Relativistic Quantum theory. Quantum mechanics of atomic systems*. Astroprint: Odessa, **2008**.

[13] Glushkov, A.V., Khetselius, O.Yu., Svinarenko, A.A., Buyadzhi, V.V., *Spectroscopy of autoionization states of heavy atoms and multiply charged ion*s. TEC: Odessa, **2015**.

[14] Glushkov, A., Svinarenko, A., Ternovsky, V., Smirnov, A., Zaichko, P., Spectroscopy of the complex autoionization resonances in spectrum of helium: Test and new spectral data. *Photoelectronics*. **2015**, *24*, 94-102.

[15] Glushkov A.V., Ternovsky V.B., Buyadzhi V., Zaichko P., Nikola L. Advanced relativistic energy approach to radiation decay processes in atomic systems. *Photoelectr*. **2015**, *24*, 11-22.

[16] Ivanov, L.N.; Ivanova, E.P. Method of Sturm orbitals in calculation of physical characteristics of radiation from atoms and ions. *JETP*. **1996,** *83*, 258-266.

[17] Glushkov, A.; Ivanov, L.; Ivanova, E.P. Autoionization Phenomena in Atoms. *Moscow Univ. Press*, Moscow, **1986,** 58.

[18] Glushkov, A.V., Ivanov, L.N. Radiation decay of atomic states: atomic residue polarization and gauge noninvariant con-

tributions. *Phys. Lett. A* **1992,** *170*, 33.
[19] Glushkov, A.V.; Ivanov, L.N. DC strong-field Stark effect: consistent quantum-mechanical approach. *J. Phys. B: At. Mol. Opt. Phys.* **1993,** *26*, L379-386.
[20] Ivanova, E., Glushkov, A. Theoretical investigation of spectra of multicharged ions of F-like and Ne-like isoelectronic sequences. J. Quant. Spectr. and Rad. Tr. **1986**, *36*(2), 127-145.
[21] Ivanova, E.P., Ivanov, L.N., Glushkov, A., Kramida, A. High order corrections in the relativistic perturbation theory with the model zeroth approximation, Mg-Like and Ne-Like Ions. *Phys. Scripta* **1985**, *32*, 513-522.
[22] Glushkov A., Multiphoton spectroscopy of atoms and nuclei in a laser field: Relativistic energy approach and radiation atomic lines moments method. *Adv. in Quantum Chem.* **2019**, *78*, 253-285.
[23] Glushkov, A.V.; Khetselius, O.Yu.; Svinarenko A. Theoretical spectroscopy of autoionization resonances in spectra of lanthanides atoms. *Phys. Scripta*. **2013**, *T153*, 014029.
[24] Glushkov, A.V. *Relativistic and correlation effects in spectra of atomic systems*. Astroprint: Odessa, **2006**.
[25] Khetselius, O.Yu. *Hyperfine structure of atomic spectra*. Astroprint: Odessa, **2008**.
[26] Khetselius, O.Yu. Relativistic perturbation theory calculation of the hyperfine structure parameters for some heavy-element isotopes. *Int. Journ. Quant.Chem.* **2009,** *109*, 3330-3335.
[27] Khetselius, O. Relativistic calculation of the hyperfine structure parameters for heavy elements and laser detection of the heavy isotopes. *Phys.Scr.* **2009,** *T135*, 014023
[28] Khetselius, O.Yu. Optimized relativistic many-body perturbation theory calculation of wavelengths and oscillator strengths for Li-like multicharged ions. Adv. Quant. Chem. **2019**, *78*, 223-251.
[29] Khetselius, O.Yu., Glushkov, A.V., Dubrovskaya, Yu.V., Chernyakova, Yu., Ignatenko, A.V., Serga, I., Vitavetskaya, L. Relativistic quantum chemistry and spectroscopy of exotic atomic systems with accounting for strong interaction effects. In: Concepts, *Methods and Applications of Quantum Systems in Chemistry and Physics*. Springer, Cham, **2018,** *31*, 71-91.
[30] Khetselius, O.Yu. *Quantum structure of electroweak interaction in heavy finite Fermi-systems.* Astroprint: Odessa, **2011**.
[31] Glushkov, A., Vitavetskaya, L. Accurate QED perturbation theory calculation of the structure of heavy and superheavy element atoms and multicharged ions with the account of nuclear size effect and QED corrections. *Herald of Uzhgorod Univ.* **2000**, *8*(2), 321-324.
[32] Svinarenko, A., Glushkov, A, Khetselius, O., Ternovsky, V., Dubrovskaya Y., Kuznetsova A., Buyadzhi V. Theoretical spectroscopy of rare-earth elements: spectra and autoionization resonances. *Rare Earth Element*, Ed. J. Orjuela (InTech) **2017**, pp 83-104.
[33] Glushkov, A.V., Khetselius, O.Yu., Svinarenko A.A., Buyadzhi, V.V., Ternovsky, V.B, Kuznetsova, A., Bashkarev, P Relativistic perturbation theory formalism to computing spectra and radiation characteristics: application to heavy element. *Recent Studies in Perturbation Theory*, ed. D. Uzunov (InTech) **2017**, 131-150.
[34] Glushkov A., Khetselius O., Svinarenko A., Buyadzhi V., *Spectroscopy of autoionization states of heavy atoms and multiply charged ion*s. TEC: Odessa, **2015.**
[35] Glushkov A.V., Khetselius O.Yu., Svinarenko A.A., Buyadzhi V.V., *Methods of computational mathematics and mathematical physics*. *P.1*. TES: Odessa, **2015**.
[36] Dubrovskaya, Yu., Khetselius, O.Yu., Vitavetskaya, L., Ternovsky, V., Serga, I. Quantum chemistry and spectroscopy of pionic atomic systems with accounting for relativistic, radiative, and strong

interaction effects. *Adv. in Quantum Chem.* **2019,** Vol.78, pp 193-222.
[37] Bystryantseva A., Khetselius O.Yu., Dubrovskaya Yu., Vitavetskaya L.A., Berestenko A.G. Relativistic theory of spectra of heavy pionic atomic systems with account of strong pion-nuclear interaction effects: ^{93}Nb, ^{173}Yb, ^{181}Ta , ^{197}Au. *Photoelectronics*. **2016**, *25*, 56-61.
[38] Khetselius, O., Glushkov, A., Gurskaya, M., Kuznetsova, A., Dubrovskaya Yu., Serga I., Vitavetskaya L. Computational modelling parity nonconservation and electroweak interaction effects in heavy atomic systems within the nuclear-relativistic many-body perturbation theory. *J. Phys.: Conf. Ser.* ***2017,*** *905*(1), 012029.
[39] Khetselius O., Gurnitskaya E. Sensing the electric and magnetic moments of a nucleus in the N-like ion of Bi. *Sensor Electr. and Microsyst. Tech.* **2006**, *N3*, 35
[40] Khetselius, O.Yu., Lopatkin Yu.M., Dubrovskaya, Yu.V, Svinarenko A.A. Sensing hyperfine-structure, electroweak interaction and parity non-conservation effect in heavy atoms and nuclei: New nuclear-QED approach. *Sensor Electr. and Microsyst. Techn*. **2010,** 7(2), 11-19.
[41] Glushkov A.V., Malinovskaya S.V., Dubrovskaya Yu.V., Sensing the atomic chemical composition effect on the beta decay probabilities. Sensor Electr. and Microsyst. Techn. **2005**, *2*(1), 16-20.
[42] Florko, T.A.; Tkach, T.B.; Ambrosov, S.V.; Svinarenko, A.A. Collisional shift of the heavy atoms hyperfine lines in an atmosphere of the inert gas. *J. Phys.: Conf. Ser*. **2012**, *397*, 012037.
[43] Buyadzhi V.; Chernyakova Yu.; Smirnov A; Tkach T. Electron-collisional spectroscopy of atoms and ions in plasma: Be-like ions. *Photoelectronics*. **2016,** *25,* 97-101
[44] Buyadzhi, V.V.; Chernyakova, Yu.G.; Antoshkina, O.; Tkach, T. Spectroscopy of multicharged ions in plasmas: Oscillator strengths of Be-like ion Fe. *Photoelectronics*. **2017,** *26,* 94-102

PACS: 31.15.ac, 31.15.ag, 31.15.aj

Zaichko P.A., Kuznetsova A.A., Tsudik A.V., Mansarliysky V.F.

RELATIVISTIC CALCULATION OF THE RADIATIVE TRANSITION PROBABILITIES AND LIFETIMES OF EXCITED STATES FOR THE RUBIDIUM ATOM IN A BLACK-BODY RADIATION FIELD

Summary. We present the results of relativistic calculation of the radiative transition probabilities and excited states lifetimes for a heavy Rydberg atomic systems in a black-body (thermal) radiation field on example of the rubidium. As theoretical approach we apply the combined generalized relativistic energy approach and relativistic many-body perturbation theory with ab initio Dirac zeroth approximation. There are obtained the calculational data for the radiative transition probabilities and excited states lifetimes, in particular, the rubidium atom in the Rydberg states with principal quantum number n=10-100. It is carried out the comparison of obtained theoretical data on the effective lifetime for the group of Rydberg nS states of the rubidium atom at a temperature of T = 300 K with experimental data as well as data of alternative theoretical calculation based on the improved quasiclassical model. It is shown that the accuracy of the theoretical data on the radiative transition probabilities and excited states lifetimes is provided by a correctness of the corresponding relativistic wave functions and accounting for the exchange-correlation effects.

Key words: Rydberg heavy atoms, relativistic theory, black-body radiation field.

PACS: 31.15.ac, 31.15.ag, 31.15.aj

Заичко П.А., Кузнецова А.А., Цудик А.В., Мансарлийский В.Ф.

РЕЛЯТИВИСТСКИЙ РАСЧЕТ ВЕРОЯТНОСТЕЙ РАДИАЦИОННЫХ ПЕРЕХОДОВ И ВРЕМЕНИ ЖИЗНИ ВОЗБУЖДЕННЫХ СОСТОЯНИИ ДЛЯ АТОМА РУБИДИЯ В ПОЛЕ ИЗЛУЧЕНИЯ ЧЕРНОГО ТЕЛА

Резюме. Представлены результаты релятивистского расчета вероятностей радиационных переходов и времен жизни возбужденных состояний для тяжелой ридберговской атомной системы в поле чернотельного (теплового) излучения на примере рубидия. В качестве теоретического подхода мы применяем комбинированный релятивистский энергетический подход и релятивистскую многочастичную теорию возмущений с оптимизированныи дираковским нулевым приближением. Получены расчетные данные для вероятностей радиационных переходов и времен жизни возбужденных состояний, в частности атома рубидия в ридберговских состояниях с главным квантовым числом n = 10-100. Проведено сравнение полученных теоретических данных по эффективным временам жизни для группы ридберговских nS состояний атома рубидия при температуре T = 300 K с экспериментальными данными, а также данными альтернативного теоретического расчета на основе усовершенствованной квазиклассической модели. Показано, что точность теоретических данных обеспечивается корректностью вычисления соответствующих релятивистских волновых функций и полнотой учета обменно-корреляционных эффектов.

Ключевые слова: ридберговские тяжелые атомы, релятивистская теория, тепловое излучение.

PACS: 31.15.ac, 31.15.ag, 31.15.aj

Заічко П.О., Кузнецова А.А., Цудік А.В., Мансарлійський В.Ф.

РЕЛЯТИВІСТСЬКИЙ РОЗРАХУНОК ЙМОВІРНОСТЕЙ РАДІАЦІЙНИХ ПЕРЕХОДІВ І ЧАСУ ЖИТТЯ ЗБУДЖЕНИХ СТАНІВ ДЛЯ АТОМУ РУБІДІЮ В ПОЛІ ВИПРОМІНЮВАННЯ ЧОРНОГО ТІЛА

Резюме. Представлені результати релятивістського розрахунку ймовірностей радіаційних переходів і часів життя збуджених станів для важкої рідбергівської атомної системи в поле чорнотільного (теплового) випромінювання на прикладі рубідію. В якості теоретичного підходу ми застосовуємо комбінований релятивістський енергетичний підхід і релятивістську багаточастинкову теорію збурень з оптимізованим дираківським нульовим наближенням. Отримано розрахункові дані для ймовірностей радіаційних переходів і часів життя збуджених станів, зокрема атома рубідію в рідбергівських станах з головним квантовим числом n = 10-100. Проведено порівняння отриманих теоретичних даних щодо ефективних часів життя для групи рідбергівських nS станів атома рубідію при температурі T = 300 K з експериментальними даними, а також даними альтернативного теоретичного розрахунку на основі удосконаленої квазікласичної моделі. Показано, що точність теоретичних даних забезпечується коректністю обчислення відповідних релятивістських хвильових функцій і повнотою обліку обмінно-кореляційних ефектів.

Ключові слова: рідбергівські важкі атоми, релятивістська теорія, теплове випромінювання.

PACS 31.15.A-; 32.30.-r

Khetselius O. Yu., Mykhailov, A. L.

Odesa State Environmental University, L'vovskaya str.15, Odesa-16, 65016, Ukraine
E-mail: mykhailovol94@gmail.com

RELATIVISTIC CALCULATION OF WAVELENGTHS AND E1 OSCILLATOR STRENGTHS IN LI-LIKE MULTICHARGED IONS AND GAUGE INVARIANCE PRINCIPLE

The spectral wavelengths and oscillator strengths for $1s^22s$ ($^2S_{1/2}$) → $1s^23p$ ($^2P_{1/2}$) transitions in the Li-like multicharged ions with the nuclear charge Z=28,30 are calculated on the basis of the combined relativistic energy approach and relativistic many-body perturbation theory with the zeroth order optimized Dirac-Kohn-Sham one-particle approximation and gauge invariance principle performance. The comparison of the obtained results with available theoretical and experimental (compilated) data is performed. The important point is linked with an accurate accounting for the complex exchange-correlation (polarization) effect contributions and using the optimized one-quasiparticle representation in the relativistic many-body perturbation theory zeroth order that significantly provides a physically reasonable agreement between theory and precise experiment.

1. Introduction

The development of new directions in the The study of spectroscopic and structural properties of the multicharged ions has a subject of significant interest for many physical, astrophysical and chemical applications. The levels energies, transitions probabilities, oscillator strengths and so on are very important in atomic physics (spectroscopy, spectral lines theory), astrophysics, plasma physics, laser physics, quantum electronics. They are very much needed in research of thermonuclear reactions, where the ionic radiation is one of the primary loss mechanisms and so on. The spectral lines belonging to the radiation of many multicharged ions have been identified in both solar flares and nonflaring solar active regions, observed in high-temperature plasmas, such as pinches and laser-produced plasmas, and in beam-foil spectra. The multiple observations of satellite lines of the He-, Li-, Be-like multicharged ions in the solar corona and in laboratory plasmas have emphasized the need for accurate values of the energetic and spectroscopic parameters for multicharged ions. [1-10].

However, a study of the spectral characteristics of heavy atoms and ions in the Rydberg states has to be more complicated as it requires a necessary accounting for the relativistic, exchange-correlations effects and possibly the QED corrections for superheavy atomic systems. The simultaneous correct accounting of relativistic, quantum electrodynamic (QED), and many-particle correlation effects is essential [11–40]. The results of calculating the characteristics of atomic processes based on modern theoretical methods often differ several times.

The difference in the values of the transition amplitudes, the oscillator strengths, and the radiation widths for heavy atoms using various expressions for the photon propagator reaches 5–30% (we are essentially talking about the non-fulfillment of the principle of gauge invariance when calculating physical quantities) [11-18]. From the point of view of applications for the majority of the most important atomic systems, there is very often partially or completely missing information on their energy, radiation or/and autoionization characteristics (heavy atoms, atoms of alkaline-earth elements, lanthanides and actinides).

In this paper The spectral wavelengths and oscillator strengths for $1s^22s$ ($^2S_{1/2}$) → $1s^23p$ ($^2P_{1/2}$) transitions in the Li-like multicharged ions with the nuclear charge Z=28,30 are calculated on the basis of the combined relativistic energy approach and

relativistic many-body perturbation theory with the zeroth order optimized Dirac-Kohn-Sham one-particle approximation and studying an effect of the gauge invariance on the transition amplitude values for some Li-like multicharged ions.

2. Relativistic theory of multicharged ions

In Refs. [2-5,.8,16-25] the fundamentals of the relativistic many-body PT formalism have been in detail presented, so further we are limited only by the novel elements. Let us remind that the majority of complex atomic systems possess a dense energy spectrum of interacting states. In Refs. [16-24] there is realized a field procedure for calculating the energy shifts ΔE of degenerate states, which is connected with the secular matrix *M* diagonalization. The whole calculation of the energies and decay probabilities of a non-degenerate excited state is reduced to the calculation and diagonalization of the *M*. The complex secular matrix *M* is represented in the form:

$$M = M^{(0)} + M^{(1)} + M^{(2)} + M^{(3)}. \qquad (1)$$

where $M^{(0)}$ is the contribution of the vacuum diagrams of all order of PT, and $M^{(1)}$, $M^{(2)}, M^{(3)}$ those of the one-, two- and three-QP diagrams respectively. The diagonal matrix $M^{(1)}$ can be presented as a sum of the independent 1QP contributions. The optimized 1-QP representation is the best one to determine the zeroth approximation. In the relativistic energy approach, which has received a great application during solving numerous problems of atomic, molecular and nuclear physics (e.g., see Refs. [16-54]), the imaginary part of electron energy shift of an atom is directly connected with the radiation decay possibility (transition probability). An approach, using the Gell-Mann and Low formula with the QED scattering matrix, is used in treating the relativistic atom. The total energy shift of the state is usually presented in the form:

$$\Delta E = \mathrm{Re}\Delta E + i\,\Gamma/2 \qquad (2)$$

where Γ is interpreted as the level width, and the decay possibility P = Γ. The imaginary part of electron energy of the system, which is defined in the lowest order of perturbation theory as [16-20]:

$$\mathrm{Im}\Delta E(B) = -\frac{e^2}{4\pi} \sum_{\substack{\alpha>n>f \\ [\alpha<n\le f]}} V^{|\omega_{\alpha n}|}_{\alpha n \alpha n}, \qquad (3)$$

where (α>n>f) for electron and (α<n<f) for vacancy. The matrix element is determined as follows:

$$V^{|\omega|}_{ijkl} = \iint dr_1 dr_2 \Psi^*_i(r_1)\Psi^*_j(r_2)\frac{\sin|\omega| r_{12}}{r_{12}}(1-\alpha_1\alpha_2)\Psi^*_k(r_2)\Psi^*_l(r_1) \qquad (4)$$

where ω_{ij} is the transition frequency; α_i ,α_j are the Dirac matrices. The separated terms of the sum in (1) represent the contributions of different channels and a probability of the dipole transition

Naturally, the physical values should not depend on the calibration of the photonic propagator. In general form, it can be written as

$$D = D_T + C \cdot D_L,$$
$$D_T = \frac{\delta_{\mu\nu}}{k_0^2 - k^2},$$
$$D_L = \frac{k_\mu k_\nu}{k_0^2 - k^2} \qquad (5)$$

where the term D_T is corresponding to exchange by transverse photons, D_L — longitudinal ones, C is the gauge constant. contribution of the main exchange-correlation (the second and higher orders of the atomic perturbation theory or fourth etc of the QED perturbation theory) diagrams to imaginary part of an electron energy shift looks like [17]:

$$\mathrm{Im}\, E_{ninv}(\alpha - s \mid A_d) = -C\frac{e^2}{4\pi}\iiint\int dr_1 dr_2 dr_3 dr_4$$

$$\sum\left(\frac{1}{\omega_{mn}+\omega_{\alpha_s}} + \frac{1}{\omega_{mn}-\omega_{\alpha_s}}\right)\Psi^+_\alpha(r_1)\Psi^+_m(r_2)\Psi^+_s(r_3)\cdot$$

$$\cdot \Psi_n^+(r_4)(1-\alpha_1\alpha_2)/r_{12} \cdot \{[(\alpha_3\alpha_4 - (\alpha_3 n_{34})(\alpha_4 n_{34}))/r_{34} \cdot$$

$$\sin[\omega_{\alpha_n}(r_{12}+r_{34}) + \omega_{\alpha_n} \cdot \cos[\omega_{\alpha_n}(r_{12}+r_{34})](1+(\alpha_3 n_{34})$$

$$(\alpha_4 n_{34}))]\}\Psi_m(r_3)\Psi_\alpha(r_4)\Psi_n(r_2)\Psi_s(r_1) \qquad (6)$$

Expression (6) can be represented as an a sum:

$$\Sigma \langle \alpha m | W_1 | ns \rangle \langle sn | W_2 | m\alpha \rangle / (\omega_{mn} \pm \omega_{\alpha s}) \qquad (7)$$

with (4) different operator combinations W_1, W_2. The sum over n can be calculated by the method of differential equations. The index m numbers a finite number of states occupied in the core and the state of the real continuum. The continuum-related part describes the vacuum polarization of the electron field and leads to divergent integrals in the non-renormalizable theory. Its contribution to the main contribution has an additional order of smallness (αZ^2). The minimization of the density functional $\mathrm{Im}\delta E$ leads to the integral differential equation for the ρ_c, that can be numerically solved. This step allows to determine the optimization parameter b. In Ref. [8] the authors elaborated a simplified computational procedure.

The contribution of the main exchange-correlation (the second and higher orders of the atomic perturbation theory or fourth etc ones of the QED perturbation theory) to imaginary part of an electron energy shift is determined by the polarizability of an atomic core, which is related to the electronic core density ρ_c. The expression (6) can be represented an a functional of the density ρ_c.

Under calculating the matrix elements (2) one should use the expansion for potential $\sin|\omega|r_{12}/r_{12}$ on spherical functions as follows [16-20]:

$$\frac{\sin|\omega|r_{12}}{r_{12}} = \frac{\pi}{2\sqrt{r_1 r_2}} \sum_{\lambda=0}^{\infty} (\lambda) J_{\lambda+1/2}(|\omega|r_1) J_{\lambda+1/2}(|\omega|r_2) P_\lambda(\cos \widehat{r_1 r_2}), \qquad (8)$$

where J is the Bessel function of first kind and $(\lambda) = 2\lambda + 1$. Substitution of the expansion (5) to matrix element of interaction gives as follows [14]:

$$V_{1234}^{\omega} = [(j_1)(j_2)(j_3)(j_4)]^{1/2} \sum_{\lambda\mu} (-1)^{\mu} \begin{pmatrix} j_1 j_3 & \lambda \\ m_1 - m_3 & \mu \end{pmatrix} \times$$

$$\times \mathrm{Im}\{Q_\lambda^{Qul}(1234) + Q_\lambda^{Br}(1234)], \qquad (9)$$

where j_i is the total single electron momentums, m_i – the projections; Q^{Qul} is the Coulomb part of interaction, Q^{Br} - the Breit part. Their detailed definitions are presented in Refs. [10-11,18,19]. The relativistic wave functions are calculated by solution of the Dirac equation with the potential, which includes the "outer electron- ionic core" potential and exchange-polarization potential [20]. In fact, we realize the procedure of optimization of relativistic orbitals base. The main idea is based on using ab initio optimization procedure, which is reduced to minimization of the gauge dependent multielectron contribution $\mathrm{Im}\Delta E_{ninv}$ of the lowest QED PT corrections to the radiation widths of atomic levels. According to [11, 18], "in the fourth order of QED PT (the second order of the atomic PT) there appear the diagrams, whose contribution to the $\mathrm{Im}\Delta E_{ninv}$ accounts for correlation effects and this contribution is determined by the electromagnetic potential gauge (the gauge dependent contribution)". The accurate procedure for minimization of the functional $\mathrm{Im}\delta E_{ninv}$ leads to the Dirac-Kohn-Sham-like equations for the electron density that are numerically solved by the Runge-Cutta standard method It is very important to know that the regular realization of the total scheme allows to get an optimal set of the 1QP functions and more correct results in comparison with so called simplified one, which has been used in Refs. [11-13] and reduced to the functional minimization using the variation of the correlation potential parameter b. Other details can be found in Refs. [8,16,17].

The adequate, precise computation of radiative parameters of the heavy Rydberg alkali-metal atoms within relativistic perturbation theory requires an accurate accounting for the multi-electron exchange-correlation effects (including polarization and screening effects, a continuum pressure etc). These effects within our approach are treated as the effects of the perturbation theory second and

higher orders. Using the standard Feynman diagrammatic technique one should consider two kinds of diagrams (the polarization and ladder ones), which describe the polarization and screening exchange-correlation effects. The detailed description of the polarization diagrams and the corresponding analytical expressions for matrix elements of the polarization interelectron interaction (through the polarizable core of an alkali atom) potential is presented in Refs. [16-40].

An effective approach to accounting for the polarization diagrams contributions is in adding the effective two-quasiparticle polarizable operator into the perturbation theory first order matrix elements. In Ref. [21] the corresponding non-relativistic polarization functional has been derived. More correct relativistic expression has been presented in the Refs. [22,8] and used in our theory.

The corresponding two-quasiparticle polarization potential looks as follows:

$$V_{pol}^{d}(r_1 r_2) = X \left\{ \int \frac{dr' \left(\rho_c^{(0)}(r')\right)^{1/3} \theta(r')}{|r_1 - r'| \cdot |r' - r_2|} - \right.$$

$$\left. - \int \frac{dr' \left(\rho_c^{(0)}(r')\right)^{1/3} \theta(r')}{|r_1 - r'|} \int \frac{dr'' \left(\rho_c^{(0)}(r'')\right)^{1/3} \theta(r'')}{|r'' - r_2|} \Big/ \left\langle \left(\rho_c^{(0)}\right)^{1/3} \right\rangle \right\} \quad (10a)$$

$$\left\langle \left(\rho_c^{(0)}\right)^{1/3} \right\rangle = \int dr \left(\rho_c^{(0)}(r)\right)^{1/3} \theta(r), \quad (10b)$$

$$\theta(r) = \left\{ 1 + \left[3\pi^2 \cdot \rho_c^{(0)}(r) \right]^{2/3} / c^2 \right\}^{1/2}, \quad (10c)$$

where ρ_c^0 is the core electron density (without account for the quasiparticle), X is numerical coefficient, c is the light velocity. The contribution of the ladder diagrams (these diagrams describe the immediate interparticle interaction) is summarized by a modification of the perturbation theory zeroth approximation mean-field central potential (look [2,8]), which includes the screening (anti-screening) of the core potential of each particle by the two others. All computing was performed with using the modified PC code "Superatom-ISAN" (version 93).

3. Results and conclusion

We applied the above described approach to compute the oscillator strengths (reduced dipole matrix elements) for a number of transitions in spectra of the heavy alkali atoms and corresponding ions.

In table 1 we list our computational results on the wavelengths and oscillator strengths gf (upper number in the line "Our work": data, obtained without using the optimized basis set and accounting for the exchange-polarization corrections; lower number in the line "Our work" – with using the optimized basis set and accounting for the exchange-polarization corrections) for $1s^2 2s$ ($^2S_{1/2}$) → $1s^2 3p$ ($^2P_{1/2}$) transitions in the Li-like ions with Z=21,22. In Table 1 the data on the wavelengths, oscillator strengths, calculated by Banglin Deng et al [12] (in the framework of the relativistic configuration-interaction formalism using multiconfiguration DF wave functions and considering the Breit interaction, QED and nuclear mass corrections), Zhang et al (the Dirac-Fock-Slater method and disturbed wave approximation), Martin et al (the relativistic quantum defect method),Nahar (ab initio calculations including relativistic effects employing the Breit-Pauli R-matrix method) and the NIST data [10-15] are listed too. The data by Banglin Deng et al [12] are obtained in the length gauge, and the ratios (V/L; in %) of the velocity and length gauges data to check the accuracy of calculations are listed. We also present our values of the gauge non-invariant contribution (Ninv; in %). Comparison of the presented data shows that the agreement between the theoretical data and experimental results is more or less satisfactory. An estimate of the gauge-non-invariant contributions (the difference between the oscillator strengths values calculated with using the transition operator in the form of "length" G1 and "velocity" G2) is about 0.1%. The theoretical data, obtained with using the different photon propagator gauges

(Coulomb and Babushkin ones) are practically equal.

Table 1.

The calculated wavelengths, oscillator strengths for $1s^2 2s\ (^2S_{1/2}) \rightarrow 1s^2 3p\ (^2P_{1/2})$ transitions in the Li-like ions with Z=28,30; V/L is the ratios of the velocity and length gauges values by Banglin Deng et al [12]; Ninv (in %) is the gauge non-invariant contribution (this work);

Z	Ref.	Wave-length (A)	Oscillator strength (gf, 10^{-1})	V/L; Ninv (%)
28	Banglin Deng et al	9.104	1.2889	V/L~0.2
	NIST	9.105	-	
	Zhang et al	9.099	1.299	
	Nahar	9.1	1.339	
	Martin et al		1.28	
	This work	9.103	1.3285 1.2891	N_{inv}~0.1
30	Banglin Deng et al	7.859	1.2983	V/L~0.2
	Zhang et al	7.854	1.309	
	Martin et al		1.29	
	This work	7.858	1.3387 1.2985	N_{inv}~0.1
	Banglin Deng et al	7.859	1.2983	V/L~0.2

References

[1] Grant, I. *Relativistic Quantum Theory of Atoms and Molecules*. Oxford, **2007.**

[2] Glushkov, A., Khetselius, O., Svinaren-ko, A., Buyadzhi, V. *Spectroscopy of autoionization states of heavy atoms and multiply charged ions*. Odessa: **2015**.

[3] Khetselius, O.Yu. Relativistic Energy Approach to Cooperative Electron-γ-Nuclear Processes: NEET Effect *In Quantum Systems in Chemistry and Physics, Series: Progress in Theoretical Chemistry and Physics;* Nishikawa, K., Maruani, J., Brändas, E., Delgado-Barrio, G., Piecuch, P., Eds.; Springer: Dordrecht, **2012;** Vol. 26, pp 217-229.

[4] Khetselius, O.Yu. Relativistic perturbation theory calculation of the hyperfine structure parameters for some heavy-element isotopes. *Int. Journ. Quant.Chem.* **2009,** *109,* 3330-3335.

[5] Khetselius, O.Yu. Relativistic calculation of the hyperfine structure parameters for heavy elements and laser detection of the heavy isotopes. *Phys.Scripta.* **2009,** *135,* 014023.

[6] Chernyakova, Y., Ignatenko, A., Vitavetskaya, L.A. Sensing the tokamak plasma parameters by means high resolution x-ray theoretical spectroscopy method: new scheme. *Sensor Electr. and Microsyst. Techn*. **2004**, 1, 20-24.

[7] Dzuba, V.A., Flambaum, V.V., Sushkov, O.P. Calculation of energy levels, E1 transition amplitudes, and parity violation in Fr *Phys. Rev. A.* **1995**, 51, 3454.

[8] Khetselius, O.AYu., Mykhailov, A.L., Efimova, E.A., Serga, R.E., Wavelengths and oscillator strengths for Li-like multicharged ions within relativistic many-body perturbation theory. Photoelectronics. **2018**, *27*, 69-78

[9] Safronova, U., Johnson, W., Derevianko, A. Relativistic many-body calculations of energy levels, hyperfine constants, electric-dipole matrix elements, and static polarizabilities for alkali-metal atoms. *Phys. Rev. A.* **1999**, *60*, 4476.

[10] Zhang, H.L.; Sampson, D.H.; Fontes, C.J. Relativistic distorted-wave collision strengths and oscillator strengths for the 85 Li-like ions with 8 <*Z*< 92. Atom. Dat. Nucl. Dat. Tabl. **1990**, *44*, 31-77.

[11] Nahar, S. N. Relativistic fine structure oscillator strengths for Li-like ions: C IV - Si XII,SXIV,ArXVI,CaXVIII,Ti

XX,Cr XXII, Ni XXVI. *Astr. and Astrophys*. **2002**. *389*, 716-728.

[12] Banglin, Deng.; Gang, Jiang; Chuanyu Zhang. Relativistic configuration-interaction calculations of electric dipole n = 2 − n = 3 transitions for medium-charge Li-like ions. *Atom. Dat. and Nucl. Dat. Tabl*. **2014,** *100,* 1337-1355.

[13] Svinarenko, A., Khetselius, O., Buyadzhi, V., Florko, T., Zaichko,P., Ponomarenko, E. Spectroscopy of Rydberg atoms in a Black-body radiation field: Relativistic theory of excitation and ionization. *J. Phys.: Conf. Ser*. **2014**, *548*, 012048.

[14] Ivanov, L.N., Ivanova, E.P., Aglitsky, E. Modern trends in the spectroscopy of multicharged ions. Phys. Rep. **1988**, 166.

[15] Ivanov, L.N.; Ivanova, E.P.; Knight, L. Energy approach to consistent QED theory for calculation of electron-collision strengths: Ne-like ions. *Phys. Rev. A.* **1993,** *48*, 4365-4374.

[16] Glushkov, A.V.; Ivanov, L.N.; Ivanova, E.P. Autoionization Phenomena in Atoms. *Moscow University Press*, Moscow, **1986,** 58-160

[17] Glushkov, A.V.; Ivanov, L.N. Radiation decay of atomic states: atomic residue polarization and gauge noninvariant contributions. *Phys. Lett. A* **1992,** *170,* 33-36.

[18] Glushkov A.V.; Ivanov, L.N. DC strong-field Stark effect: consistent quantum-mechanical approach. *J. Phys. B: At. Mol. Opt. Phys.* **1993,** *26*, L379-386.

[19] Glushkov, A.V. *Relativistic Quantum theory. Quantum mechanics of atomic systems*. Astroprint: Odessa, **2008**.

[20] Ivanova, E., Glushkov, A. Theoretical investigation of spectra of multicharged ions of F-like and Ne-like isoelectronic sequences. J. Quant. Spectr. and Rad. Tr. **1986**, *36*(2), 127-145.

[21] Ivanova, E.P., Ivanov, L.N., Glushkov, A., Kramida, A. High order corrections in the relativistic perturbation theory with the model zeroth approximation, Mg-Like and Ne-Like Ions. *Phys. Scripta* **1985**, *32*, 513-522.

[22] Glushkov, A.V. Relativistic polarization potential of a many-electron atom. *Sov. Phys. Journal*. **1990**, *33(1)*, 1-4.

[23] Glushkov, A.V. Negative ions of inert gases. *JETP Lett.* **1992,** *55*, 97-100.

[24] Glushkov, A.V. Energy approach to resonance states of compound superheavy nucleus and EPPP in heavy nuclei collisions *In Low Energy Antiproton Physics;* Grzonka, D., Czyzykiewicz, R., Oelert,W., Rozek, T., Winter, P., Eds.; AIP: New York, *AIP Conf. Proc*. **2005**, *796*, 206-210.

[25] Glushkov, A.V. Spectroscopy of cooperative muon-gamma-nuclear processes: Energy and spectral parameters *J. Phys.: Conf. Ser*. **2012,** *397*, 012011

[26] Glushkov, A.V. Advanced Relativistic Energy Approach to Radiative Decay Processes in Multielectron Atoms and Multicharged Ions. *In Quantum Systems in Chemistry and Physics: Progress in Methods and Applications, Series: Progress in Theoretical Chemistry and Physics*; Nishikawa, K., Maruani, J., Brandas, E., Delgado-Barrio, G., Piecuch, P., Eds.; Springer: Dordrecht, **2012**; Vol. 26, pp 231–252.

[27] Glushkov, A.V. Multiphoton spectroscopy of atoms and nuclei in a laser field: Relativistic energy approach and radiation atomic lines moments method. *Adv. in Quantum Chem.* **2019**, *78*, 253-285.

[28] Khetselius, O.Yu. *Quantum structure of electroweak interaction in heavy finite Fermi-systems.* Astroprint: Odessa, **2011**

[29] Khetselius, O.Yu. Optimized relativistic many-body perturbation theory calculation of wavelengths and oscillator strengths for Li-like multicharged ions. Adv. Quant. Chem. **2019**, *78*, 223-251.

[30] Khetselius, O.Yu. Relativistic Hyperfine Structure Spectral Lines and Atomic Parity Non-conservation Effect in Heavy Atomic Systems within QED

Theory. *AIP Conf. Proceedings.* **2010,** *1290(1),* 29-33.
[31] Khetselius, O.Yu. Relativistic Calculating the Spectral Lines Hyperfine Structure Parameters for Heavy Ions. *AIP Conf. Proc.* **2008,** *1058,* 363-365.
[32] Khetselius, O.Yu. Hyperfine structure of radium. *Photoelectronics*. **2005,** *14*, 83-85.
[33] Khetselius, O.Yu.; Gurnitskaya, E.P. Sensing the electric and magnetic moments of a nucleus in the N-like ion of Bi. *Sensor Electr. and Microsyst. Techn.* **2006,** *3*, 35-39.
[34] Khetselius O.Yu.; Gurnitskaya, E.P. Sensing the hyperfine structure and nuclear quadrupole moment for radium. *Sensor Electr. and Microsyst. Techn.* **2006,** *2*, 25-29.
[35] Khetselius, O.Yu. Atomic parity nonconservation effect in heavy atoms and observing P and PT violation using NMR shift in a laser beam: To precise theory. *J. Phys.: Conf. Ser*. **2009,** *194,* 022009
[36] Khetselius, O.Yu. Quantum Geometry: New approach to quantization of quasistationary states of Dirac equation for superheavy ion and calculating hyperfine structure parameters. *Proc. Int. Geometry Center*. **2012**, *5(*3-4), 39-45.
[37] Glushkov, A.V. *Relativistic and correlation effects in spectra of atomic systems.* Astroprint: Odessa, **2006**.
[38] Khetselius, O.Yu. Hyperfine structure of atomic spectra.- Odessa: Astroprint, 2008
[39] Glushkov, A., Buyadzhi, V., Svinarenko, A., Ternovsky, E. Advanced relativistic energy approach in electron-collisional spectroscopy of multicharged ions in plasma. Concepts, Methods, Applications of Quantum Systems in Chemistry and Physics (Springer). **2018,** *31*, 55-69.
[40] Dubrovskaya, Yu., Khetselius, O.Yu., Vitavetskaya, L., Ternovsky, V., Serga, I. Quantum chemistry and spectroscopy of pionic atomic systems with accounting for relativistic, radiative, and strong interaction effects. *Adv. Quantum Chem*. **2019**, *78*, 193-222.
[41] Khetselius, O.Yu., Glushkov, A.V., Dubrovskaya, Yu., Chernyakova, Yu., Ignatenko, A., Serga, I., Vitavetskaya, L. Relativistic quantum chemistry and spectroscopy of exotic atomic systems with accounting for strong interaction effects. In Concepts, Methods and Applications of Quantum Systems in Chem. and Phys. Springer. **2018**, *31*, 71.
[42] Buyadzhi, V., Kuznetsova, A., Buyadzhi, A., Ternovsky, E.V., Tkach, T.B. Advanced quantum approach in radiative and collisional spectroscopy of multicharged ions in plasmas. *Adv. in Quant. Chem*. **2019**, *78*, 171-191.
[43] Ignatenko, A.V. Probabilities of the radiative transitions between Stark sublevels in spectrum of atom in an DC electric field: New approach. *Photoelectronics,* **2007,** *16*, 71-74.
[44] Khetselius, O.Yu., Lopatkin, Yu.M., Dubrovskaya, Yu.V, Svinarenko, A.A. Sensing hyperfine-structure, electroweak interaction and parity nonconservation effect in heavy atoms and nuclei: New nuclear-QED approach. *Sensor Electr. and Microsyst. Techn***. 2010**, *7*(2), 11-19.
[45] Glushkov, A.V.; Ambrosov, S.V.; Ignatenko, A.V. Non-hydrogenic atoms and Wannier-Mott excitons in a DC electric field: Photoionization, Stark effect, Resonances in ionization continuum and stochasticity. *Photoelectronics,* **2001,** *10*, 103-106.
[46] Glushkov, A.V.; Gurskaya, M.Yu.; Ignatenko, A.V.; Smirnov, A.V.; Serga, I.N.; Svinarenko, A.A.; Ternovsky, E.V. Computational code in atomic and nuclear quantum optics: Advanced computing multiphoton resonance parameters for atoms in a strong laser field. *J. Phys.: Conf. Ser*. **2017**, *905*, 012004.
[47] Danilov, V., Kruglyak, Y., Pechenaya, V. The electron density-bond order matrix and the spin density in the restrict-

ed CI method. *Theor. Chim. Act*. **1969**, 13(4), 288-296.
[48] Kruglyak, Yu. Configuration interaction in the second quantization representation: basics with application up to full CI. S*cienceRise*. **2014**, *4*(2), 98-115.
[49] Buyadzhi, V.V., Chernyakova, Yu.G., Antoshkina, O., Tkach, T. Spectroscopy of multicharged ions in plasmas: Oscillator strengths of Be-like ion Fe. *Photoelectronics*. **2017**, *26*, 94-102.
[50] Malinovskaya, S.V., Dubrovskaya, Yu.V., Zelentzova, T.N. The atomic chemical environment effect on the b decay probabilities: Relativistic calculation. *Herald of Kiev Nat. Univ. Ser.: Phys.-Math*. **2004**, N4, 427-432.
[51] Bystryantseva, A., Khetselius, O.Yu., Dubrovskaya, Yu., Vitavetskaya, L.A., Berestenk, A.G. Relativistic theory of spectra of heavy pionic atomic systems with account of strong pion-nuclear interaction effects: ^{93}Nb, ^{173}Yb, ^{181}Ta, ^{197}Au. *Photoelectronics*. **2016**, *25*, 56-61.
[52] Buyadzhi, V., Zaichko, P., Antoshkina, O., Kulakli, T., Prepelitsa, P., Ternovsky, V., Mansarliysky, V. Computing of radiation parameters for atoms and multicharged ions within relativistic energy approach: Advanced Code. *J. Phys.: Conf. Ser*. **2017**, *905*(1), 012003.
[53] Glushkov, A.V., Khetselius, O.Yu., Svinarenko, A., Buyadzhi, V. *Methods of computational mathematics and mathematical physics* TES: Odessa, **2015**
[54] Ignatenko, A.V., Svinarenko, A.A., Prepelitsa, G.P., Perelygina, T.B. Optical bi-stability effect for multi-photon absorption in atomic ensembles in a strong laser field. *Photoelectronics*. **2009**, *18*, 103-105.

PACS 31.15.A-; 32.30.-r

Khetselius O.Yu., Mykhailov, A.L.

RELATIVISTIC CALCULATION OF WAVELENGTHS AND E1 OSCILLATOR STRENGTHS IN Li-LIKE MULTICHARGED IONS AND GAUGE INVARIANCE PRINCIPLE

Summary. The spectral wavelengths and oscillator strengths for $1s^22s$ ($^2S_{1/2}$) → $1s^23p$ ($^2P_{1/2}$) transitions in the Li-like multicharged ions with the nuclear charge Z=28,30 are calculated on the basis of the combined relativistic energy approach and relativistic many-body perturbation theory with the zeroth order optimized Dirac-Kohn-Sham one-particle approximation and gauge invariance principle performance. The comparison of the obtained results with available theoretical and experimental (compilated) data is performed. The important point is linked with an accurate accounting for the complex exchange-correlation (polarization) effect contributions and using the optimized one-quasiparticle representation in the relativistic many-body perturbation theory zeroth order that significantly provides a physically reasonable agreement between theory and precise experiment

Key words: relativistic theory, radiative transitions, gauge invariance principle, lithium-like ions

PACS 31.15.A-; 32.30.-r

Хецелиус О.Ю., Михайлов А.Л.

РЕЛЯТИВИСТСКИЙ РАСЧЕТ ДЛИН ВОЛН И E1 СИЛ ОСЦИЛЛЯТОРОВ В LI-ПОДОБНЫХ МНОГОЗАРЯДНЫХ ИОНАХ И ПРИНЦИП КАЛИБРОВОЧНОЙ ИНВАРИАНТНОСТИ

Резюме. Спектральные длины волн и силы осцилляторов для переходов $1s^22s\ (^2S_{1/2}) \rightarrow 1s^23p\ (^2P_{1/2})$ в Li-подобных ионах с зарядом ядра Z = 28,30 вычислены на основе комбинированного релятивистского энергетического подхода и релятивистской многочастичной теории возмущений с дирак-кон-шэмовским одночастичным нулевым приближением и условием соблюдения принципа калибровочноъ инвариантности в радиационных переходах. Проведено сравнение полученных результатов с имеющимися теоретическими и экспериментальными данными. Важный момент связан с аккуратным учетом вкладов сложных многочастичных обменных корреляционных (поляризационных) эффектов и с использованием оптимизированного одноквазичастичного представления в нулевом приближении релятивистской многочастичной теории возмущений, что определяет определенное согласие теории и эксперимента.

Ключевые слова: релятивистская теория, радиационные переходы, принцип калибровочной инвариантности, литий-подобные ионы

PACS 31.15.A-; 32.30.-r

Хецелиус О.Ю., Михайлов О.Л.

РЕЛЯТИВІСТСЬКИЙ РОЗРАХУНОК ДОВЖИН ХВИЛЬ І E1 СИЛ ОСЦИЛЯТОРІВ В Li-ПОДІБНИХ БАГАТОЗАРЯДНИХ ІОНАХ ТА ПРИНЦИП КАЛІБРУВАЛЬНОЇ ІНВАРІАНТНОСТІ

Резюме. Спектральні довжини хвиль і сили осциляторів для переходів $1s^22s\ (^2S_{1/2}) \rightarrow 1s^23p\ (^2P_{1/2})$ в Li-подібних багатозарядних іонах з зарядом ядра Z = 28,30 обчислені на основі комбінованого релятивістського енергетичнго підходу і релятивістської багаточастинкової теорії збурень з дірак-кон-шемівським одночастинковим наближенням нульового порядку і умовою дотримання принципу калібровочно' інваріантності в радіаційних переходах. Проведено порівняння отриманих результатів з наявними теоретичними і експериментальними даними. Важливий момент пов'язаний з акуратним урахуванням внесків складних багаточасткових обмінних кореляційних (поляризаційних) ефектів і з використанням оптимізованого одноквазічастічного уявлення в нульовому наближенні релятивістської багаточастинкової теорії збурень, що визначає певну згоду теорії та експерименту.

Ключові слова: релятивістська теорія, радіаційні переходи, принцип калібрувальної інваріантності, літій-подібні іони

PACS 31.15.Ne, 31.10.1z

Makarova A. O, Buyadzhi A. A. and Dubrovsky O. V.

Odesa State Environmental University, L'vovskaya str.15, Odesa-9, 65016, Ukraine
e-mail: buyadzhiaa@gmail.com

NUMERICAL STUDYING ENERGY PARAMETERS OF MULTIELECTRON ATOM IN A MAGNETIC FIELD: HELIUM

There are presented the results of calculating the energies of the helium atom energy in a homogeneous magnetic field on the basis of the new numerical quantum-mechanical approach. The approach is based on the numerical difference solution of the Schrödinger equation, the model potential method and the operator perturbation theory formalism. The obtained results on energy of the helium atom in dependence upon the magnetic field strength are compared with available theoretical results, obtained on the basis of alternative numerical Hartree-Fock and diagonalization methods.

1. Introduction

The fundamentals of the quantum theory of the Zeeman effect are described in detail in well-known monographs and in courses on quantum mechanics and theoretical spectroscopy. At present time, interest in these effects shifted to the field of applied research (e.g. [1-28]). An important problem is studying the energy characteristics of multielectron atoms in a strong and superstrong magnetic field. At the same time, it was found that many of the results of the theory are either of little use for specific calculations, or even incomplete until recently. Further development of the theory is mainly associated with studies of atomic spectra in a sufficiently strong field B and for highly excited states with n >> 1. As indicated in the introduction, interest in these problems is associated with a wide range of applications, including: absorption spectra excitons in a magnetic field, the structure of atoms in superstrong magnetic fields on the surface of neutron stars, the splitting and broadening of atomic spectral lines in electric and magnetic fields of plasma, the structure of radio lines emitted by excited atoms in the interstellar medium, etc.

Among modern methods for describing atomic spectroscopy in a magnetic field, a series of papers [4-18] should be distinguished, where perturbation theory methods, various schemes, and algorithms have been developed based on the numerical solution of the Schrödinger equation in the Hartree–Fock and other approximations. Based on them, it was possible to obtain a lot of useful numerical data regarding the energies of various states of a number of many-electron atoms at various magnetic field intensities. The imposition of a magnetic field on an atomic system leads to an additional restriction of the electron motion across the field, and with a further increase in the field strength - to a sharp decrease in the transverse motion of the electron and, as a consequence, to the transformation of the three-dimensional potential well of the atom into a one-dimensional one. The consequence of this can be a strong change in the energy spectrum of the atom. For the simplest spinless one-electron (hydrogen) atom, the perturbation Hamiltonian V, caused by the interaction of the orbital momentum *I* of the electron with the field B, has the form $V = -\mu_B IB$.To determine the energy eigenvalues, i.e., diagonalization of the perturbation V, it suffices to choose the wave functions corresponding to a certain projection I onto the direction B. Usually, as such functions, we choose spherical wave functions corresponding to certain values of the total moment $l^2 = l\,(l + 1)$ and its projection $l_z = \hbar m \cdot$ For a hydrogen atom, the Zeeman sublevels corresponding to a certain m remain degenerate in the quantum number l. This specificity of the Coulomb degeneracy is also manifested in the fact that as the diagonalizing *V* wave functions, one can choose parabolic wave functions Ψ_{n_1,n_2}, with the Oz axis along the field B. These states, by virtue of the relation $n_1 + n_2 + |m| = n - 1$ for a given *m*, remain degenerate in the values of n_1,n_2 corresponding

to their equal sum $n_1 + n_2$.. Thus, the Zeeman component of the hydrogen level is characterized not by one, but, generally speaking, by several wave functions.

In this paper we shortly present the results of calculating the energies of the helium atom energy in a homogeneous magnetic field on the basis of the new numerical quantum-mechanical approach [1,12]. The approach is based on the numerical difference solution of the Schrödinger equation, the model potential method and the operator perturbation theory formalism.

2. Theoretical approach

According to the Ref [10], the Hamiltonian of he helium atom in a magnetic field B differs from the operator of the hydrogen atom by the presence of the Coulomb interaction operator, which naturally aggravates the problem of separation of variables in the Schrödinger equation. Introducing a cylindrical coordinate system (ρ, φ,z), with the axis Oz || B and taking into account that the dependence of the wave function on the rotation angle φ around the z axis is trivial:

$$\Psi \sim e^{iM\varphi}\,\psi(\rho,z) \qquad (1)$$

one should write the Schrödinger equation for the one-electron function of an atomic system (atomic units are used here e=h=m=1) as:

$$[\frac{\partial^2}{\partial\rho^2}+\frac{1}{\rho}\frac{\partial}{\partial\rho}+\frac{\partial^2}{\partial z^2}-\frac{M^2}{\rho^2}-4\gamma^2\rho^2+ \\ +\frac{4}{r}+V_c(r)+(\frac{E}{R_y}-\gamma M)]\Psi(\rho,z)=0 \qquad (2)$$

where V_c (r) is the potential that describes the effect of all other electrons on the given one. Naturally, it is absent for the hydrogen atom. As the potential Vc, we use the Green-Miller like potential (c.g.[2]), which approximates the Hartree potential quite accurately.

The required parameters, as a rule, are selected from the condition of the best fitting of the experimental values of the energy levels of free atoms (c.g. [2]).

To take into account the exchange corrections, the exchange potential was taken in the simplest Slater approximation and added to potential (3) [19].

The two-dimensional equation (2) is naturally not solved analytically in a general form. The terms appearing in it: the potential of the Coulomb interaction, which contains $r=(\rho^2+z^2)^{1/2}$,potential V $[(\rho^2+z^2)^{1/2}]$ prevents the separation of variables. One could rewrite the Schrödinger equation as follows:

$$H\,\psi(\rho,z)=E\,\psi(\rho,z) \qquad (3)$$

$$H=-1/2(\partial^2/\partial\rho^2+1/\rho\partial/\partial\rho+ \\ +\partial^2/\partial z^2-m^2/\rho^2),V(\rho,z), \qquad (4)$$

$$V(\rho,z)=-(\rho^2+z^2)^{-1/2}+(N_c-1)\cdot \\ \Omega(\rho^2+z^2)^{-1/2}+1/8\gamma^2\rho^2+\gamma m/2, \qquad (5)$$

The potential $1/8\gamma^2\rho^2$ limits the movement in the direction perpendicular to the field direction. Similarly, in the region $\gamma >> 1$, the motion of an electron across a magnetic field is determined by the size of its cyclotron orbit, $\lambda=(\hbar c/eM)^{1/2}$ and along the field by a modified Coulomb interaction, which takes into account the non-Coulomb character of the potential field in which an electron moves in a many-electron atom [18].

Note that calculations of multielectron atomic systems with introduced potentials are quite well known in the literature (see [2,18-20]); moreover, computational schemes based on them have been tested several times and tested for a number of atoms in the free state. The Green-Miller like potential (c.g.[2]), was successfully used in calculating the energies and forces of atomic oscillators of the 1st period of the periodic table (see review in [21]).

For solution of the Schrödinger equation with hamiltonian equations (7) we constructed the finite differences scheme which is in some aspects simila**r** to method [2]. An infinite region is exchanged by a rectangular region: $0<\rho<L_\rho$, $0<z<L_z$. It has sufficiently large size; inside it a rectangular uniform grid with

steps h_ρ, h_z was constructed. The external boundary condition, as usually, is:

$$(\partial\Psi/\partial n)_r = 0.$$

The knowledge of the asymptotic behaviour of wave function in the infinity allows to get numeral estimates for L_ρ, L_z. A wave function has an asymptotic of the kind as: $exp[-(-2E)^{1/2}r]$, where $(-E)$ is the ionization energy from stationary state to lowest Landau level. Then L is estimated as $L\sim9(-2E)^{-1/2}$. The more exact estimate is found empirically. The three-point symmetric differences scheme is used for second derivative on z. The derivatives on ρ are approximated by (2m+1)-point symmetric differences scheme with the use of the Lagrange interpolation formula differentiation. To calculate the values of the width G for resonances in atomic spectra in a magnetic field one can use the modified operator perturbation theory method (see details in Ref.[12,13]).. Other calculation details can be found in Refs. [2, 19-21].

3. Illustration results and conclusion

As illustration, below we present the data on energies of the electronic excited and ground state of the helium atom in dependence upon the magnetic field strength (parameter γ) and compared with available theoretical results, obtained on the basis of alternative methods.

Parameter γ varies within: $\gamma=B/Bo$=0.00-10, where $B_0 = m^2e^3c/h^3Z^3$.

In Table 1 there are listed the energies of the ground state of the helium atom in dependence upon the parameter γ. For the helium atom there are available the results of calculations for the ground state within other theoretical methods. In particular, the Hartree-Fock (HF) calculation results are in the Refs. [6,7].

As the ground state analysis shows, in whole our data are corresponding to the alternative HF results, however, indeed, they lie a little lower for a weak field regime and more substantially lower in the intermediate regime of the magnetic parameter.

Table 1

The energies (in atomic units) of the ground state of the helium atom as a function of the magnetic field parameter γ

Method	γ=0.5	γ=1	γ=2	γ=5
[15]	-	-2,400	-	-
[12}	-2,700	-3,027	-3,520	-4,624
[13]	-2,616	-2,960	-3,502	-4,617
Our	-2,700	-3,027	-3,520	-4,624
Method	γ=10	γ=20	γ=50	γ=100
[12]	-5,860	-7,450	-10,288	-13,343
[13]	-5,829	-7,428	-10,264	-13,077
Our	-5,860	-7,450	-10,288	-13,343
Method	γ=200	γ=500	γ=1000	γ=10000
[12]	-16,602	-22,471	-28,342	-56,623
[13]	-16,579	-22,467	-28,032	-55,151
Our	-16,602	-22,471	-28,342	-56,623

The difference between the listed data can be explained by the partial account of electron correlation corrections, which is absent in the HF calculation.

References

1. Makarova, A., Buyadzhi, A., Dubrovsky, O. Spectroscopy and dynamics of multielectron atom in a magnetic field: New approach. Photoelectronics. 2019, 28, 19-23.
2. Khetselius, O.Yu. *Hyperfine structure of atomic spectra*. Astroprint: Odessa, **2008**.
3. Khetselius, O.Yu. Optimized relativistic many-body perturbation theory calculation of wavelengths and oscillator strengths for Li-like multicharged ions. Adv. Quant. Chem. **2019**, *78*, 223-251.
4. Glushkov, A.V. *Relativistic Quantum theory. Quantum mechanics of atomic systems*. Astroprint: Odessa, **2008**.
5. Khetselius, O.Yu. *Quantum structure of electroweak interaction in heavy finite Fermi-systems.* Astroprint: Odessa, **2011**.
6. Glushkov, A.V. *Relativistic and correlation effects in spectra of atomic systems*. Astroprint: Odessa, **2006** .
7. Ivanova, E., Glushkov, A. Theoretical investigation of spectra of multicharged ions of F-like and Ne-like isoelectronic sequences. J. Quant. Spectr. and Rad. Tr. **1986**, *36*(2), 127-145.

8. Ivanova, E.P., Ivanov, L.N., Glushkov, A., Kramida, A. High order corrections in the relativistic perturbation theory with the model zeroth approximation, Mg-Like and Ne-Like Ions. *Phys. Scripta* **1985**, *32*, 513-522.
9. Ignatenko, A., Svinarenko A., Prepelitsa, G.P., Perelygina, T.B. Optical bi-stability effect for multi-photon absorption in atomic ensembles in a strong laser field. *Photoelectronics*. **2009**, *18*, 103-105.
10. Rao,J., Liu, W., Li, B. Theoretical complex Stark energies of hydrogen by a complex-scaling plus B-spline approach. *Phys. Rev. A*. **1994**, *50*, 1916-1919.
11. Rao, J.; Li, B. Resonances of hydrogen atom in strong parallel magnetic and electric fields. Phys.Rev.A. **1995,** *51*, 4526
12. Glushkov, A.V. *Atom in an electromagnetic field*. KNT: Kiev, **2005**.
13. Ivanov M.V., Schnelcher P. Ground States of H,…,Ne and their singly positive ions in strong magnetic fields: the high-field regime. Phys.Rev.A.-**2000**., 61, 022505.
14. Jones, M., Ortiz, G., Ceperley, D. Hartree-Fock studies of atoms in strong magnetic fields. *Phys. Rev. A*. **1996,** *54*, 219-231.
15. Gadiyak G., Lozovik Yu.E., Mashchenko A., Obrecht M. Hydrogen-like and helium-like systems in a superstrong magnetic field. Opt. Spectr. **1984**, *56* (1), 26-32
16. Khetselius, O., Lopatkin Y., Dubrovskaya, Y., Svinarenko A. Sensing hyperfine-structure, electroweak interaction and parity non-conservation effect in heavy atoms and nuclei: New nuclear-QED approach. *Sensor Electr. and Microsyst. Techn*. **2010,** 7(2), 11-19.
17. Glushkov, A., Malinovskaya, S, Ambrosov S., Shpinareva I, Troitskaya O. Resonances in quantum systems in strong external fields: consistent quantum approach. *J. Techn.Phys*. **1997**, *38*(2), 215-218.
18. Ambrosov S., Ignatenko V., Korchevsky D., Kozlovskaya V. Sensing stochasticity of atomic systems in crossed electric and magnetic fields by analysis of level statistics for continuous energy spectra. *Sensor Electr. and Microsyst. Techn*. **2005**, Issue 2, 19-23.
19. Glushkov, A.; Ambrosov, S.; Ignatenko, A. Non-hydrogenic atoms and Wannier-Mott excitons in a DC electric field: Photoionization, Stark effect, Resonances in ionization continuum and stochasticity. *Photoelectronics*, **2001,** *10*, 103-106.
20. Glushkov A.V.; Ivanov, L.N. DC strong-field Stark effect: consistent quantum-mechanical approach. *J. Phys. B: At. Mol. Opt. Phys.* **1993,** *26*, L379-386.
21. Rusov V., Glushkov A., Vaschenko V., Korchevsky D., Ignatenko A. Stochastic dynamics of the atomic systems in the crossed electric and magnetic field: the rubidium atom recurrence spectra. *Bull.of Kiev Nat. Univ*. **2004**, N4, 433.
22. Khetselius, O. Relativistic perturbation theory calculation of the hyperfine structure parameters for some heavy-element isotopes. *Int. J. Quant.Chem.* **2009,** *109*, 3330-3335.
23. Khetselius, O. Relativistic calculation of the hyperfine structure parameters for heavy elements and laser detection of the heavy isotopes. *Phys.Scr*. **2009,** *T135*, 014023.
24. Glushkov, A.; Gurskaya, M.; Ignatenko, A.; Smirnov, A.; Serga, I.; Svinarenko, A.; Ternovsky E. Computational code in atomic and nuclear quantum optics: Ad-vanced computing multiphoton resonance parameters for atoms in a strong laser field. *J. Phys.: Conf. Ser*. **2017**, *905*, 012004.
25. Buyadzhi, V., Zaichko, P., Antoshkina, O., Kulakli, T., Prepelitsa, P., Ternovsky, V., Mansarliysky, V. Computing of radiation parameters for atoms and multicharged ions within relativistic energy approach: Advanced Code. *J. Phys.: Conf. Ser*. **2017**, *905*(1), 012003.
26. Svinarenko, A., Glushkov, A., Khetselius, O., Ternovsky,V., Dubrovskaya, Yu., Kuznetsova, A., Buyadzhi, V. Theoretical spectroscopy of rare-earth elements: spectra and autoionization resonances. *Rare Earth Element*, InTech. **2017**, 83-104
27. Glushkov, A., Khetselius, O., Svinarenko A.A., Buyadzhi, V.V., Ternovsky, V., Kuznetsova, A., Bashkarev, P. Relativistic perturbation theory formalism to computing spectra and radiation characteristics: application to heavy element. *Recent Studies in Perturbation Theory*. InTech. **2017**, 131-150.

28. Glushkov A.V., Khetselius O.Yu., Svinarenko A.A., Buyadzhi V.V., *Methods of computational mathematics and mathematical physics*. TES: Odessa, **2015**

29. Khetselius, O., Gurnitskaya, E., Loboda, A., Vitavetskaya, L. Consistent quantum approach to quarkony energy spectrum and semiconductor superatom and in external electric field *Photoelectron*. **2008**, *17*, 127.

PACS 31.15.Ne, 31.10.1z

Makarova A.O, Buyadzhi A.A. and Dubrovsky O.V.

NUMERICAL STUDYING ENERGY PARAMETERS OF MULTIELECTRON ATOM IN A MAGNETIC FIELD: HELIUM

Summary. There are presented the results of calculating the energies of the helium atom energy in a homogeneous magnetic field on the basis of the new numerical quantum-mechanical approach. The approach is based on the numerical difference solution of the Schrödinger equation, the model potential method and the operator perturbation theory formalism. The obtained results on energy of the helium atom in dependence upon the magnetic field strength are compared with available theoretical results, obtained on the basis of alternative numerical Hartree-Fock and diagonalization methods.

Key words: atomic system, magnetic field, quantum mechanical approach

PACS 31.15.Ne, 31.10.1z

Макарова А.О., Буяджи А.А., Дубровский О.В.

ЧИСЛЕННОЕ ИССЛЕДОВАНИЕ ЭНЕРГЕТИЧЕСКИХ ПАРАМЕТРОВ МНОГОЭЛЕКТРОННОГО АТОМА В МАГНИТНОМ ПОЛЕ: ГЕЛИЙ

Резюме. Представлены результаты расчета энергии атома гелия в однородном магнитном поле на основе нового численного квантово-механического подхода. Подход основан на численном конечно--азностном решении уравнения Шредингера, методе модельного потенциала и формализме операторной теории возмущений. Полученные результаты по энергии атома гелия в зависимости от напряженности магнитного поля сравниваются с известными теоретическими результатами, полученными на основе альтернативных численных методов Хартри-Фока и диагонализации.

Ключевые слова: атомная система, магнитное поле, квантово-механический метод

PACS 31.15.Ne, 31.10.1z

Макарова О.О., Буяджи Г.А., Дубровський О.В.

ЧИСЕЛЬНЕ ВИВЧЕННЯ ЕНЕРГЕТИЧНИХ ПАРАМЕТРІВ БАГАТОЕЛЕКТРОННИХ АТОМІВ В МАГНІТНОМУ ПОЛІ: ГЕЛІЙ

Резюме. Представлені результати розрахунку енергії атома гелію в магнітному полі на основі нового чисельного квантово-механічного підходу. Підхід заснований на чисельному скінченно-різницевому розв'язанні рівняння Шредінгера, методі модельного потенціалу та формалізмі операторної теорії збурень. Отримані результати по енергії атома гелію в залежності від напруженості магнітного поля порівнюються з відомими теоретичними результатами, отриманими на основі альтернативних чисельних методів Хартрі-Фока і діагоналізації.

Ключові слова: атомна система, магнітне поле, квантово-механічний метод

PACS 31.15.-p; 33.20.-t

Kirianov S. V., Mashkantsev A. A., Bilan I. I., Ignatenko A. V.

Odesa State Environmental University, 15, L'vovskaya str., Odesa, 65016
E-mail: kirianovserg@gmail.com

DYNAMICAL AND TOPOLOGICAL INVARIANTS OF NONLINEAR DYNAMICS OF THE CHAOTIC LASER DIODES WITH AN ADDITIONAL OPTICAL INJECTION

Nonlinear chaotic dynamics of the of the chaotic laser diodes with an additional optical injection is computed within rate equations model, based on the a set of rate equations for the slave laser electric complex amplitude and carrier density. To calculate the system dynamics in a chaotic regime the known chaos theory and non-linear analysis methods such as a correlation integral algorithm, the Lyapunov's exponents and Kolmogorov entropy analysis are used. There are listed the data of computing dynamical and topological invariants such as the correlation, embedding and Kaplan-Yorke dimensions, Lyapunov's exponents, Kolmogorov entropy etc. New data on topological and dynamical invariants are computed and firstly presented.

1. Introduction

The elements of chaotic dynamics in different laser systems and devices, including semiconductor lasers, laser diodes, resonators etc are of a great importance and interest because of their potential applications in laser physics and quantum electronics, optical secure communications and cryptography, and many others. At the same time, the laser's relaxation oscillation limits the bandwidth of chaotic light emitted from a laser diode and similar devices with single optical injection or feedback. This circumstance as well as a general interest to new theoretical dynamics phenomena make necessary the further studying and improvement the main features of the optical chaos communications.

. From the other side, there is a general interest to studying the chaotic laser systems provided a necessity of the further development of a general theory of dynamic systems and a chaos.

Let us remind that according to Refs. [1-15], under the definite conditions, such systems are described by the corresponding model, when Hamiltonians are possessing only a few degrees of freedom. For the low-dimensional chaotic case the corresponding conditions of transition to deterministic chaos in the system dynamics are quite well understood at the classical level [1-4].

Under quantum treatment of the problem, the similar systems (in particular, the diatomic molecules in a resonant electromagnetic field) are studied with using the known quasiclassical approach [2]. At the theoretical level, the majority of studies, devoted to chaos phenomena in molecular dynamics, is carried out with the using simple tools of dynamical systems theory and qualitative theory of differential equations. New field of investigations of the quantum and other systems has been provided by the known progress in a development of a nonlinear analysis and chaos theory methods [1-12,17-30].

In Refs. [11,27-33] the authors applied different approaches to quantitative studying regular and chaotic dynamics of atomic and molecular systems interacting with a strong electromagnetic field and laser systems.

The most popular approach to studying nonlinear dynamics of chaotic systems includes the combined using the advanced nonlinear analysis and a chaos theory methods such as the autocorrelation function method, multi-fractal formalism, mutual information approach, correlation integral analysis, false nearest neighbour algorithm, Lyapunov exponent's analysis, surrogate data method, stochastic propagators method, memory and Green's functions approaches etc (see details in Refs. [17-24]).

In Ref. [1] the authors experimentally and numerically demonstrate the route to band width enhanced chaos in a chaotic laser diode with an additional optical injection; they used the own unique experimental setup, which includes a distributed feedback (DFB) laser with a 4 m fiber ring feedback cavity (the slave laser) and the other solitary DFB laser as an injection laser (the master laser) to enlarge the bandwidth of the chaotic laser (see detailed description in Ref. [1]). The concrete technological characteristics are as follows: slave laser is biased at 28.0 mA (1.27 times threshold), and its wavelength is stabilized at 1553.8 nm with 0.3 nm linewidth (at −20 dB) and a 35 dB side mode suppression ratio; respectively, the laser's output power is 0.7 mW, and the relaxation frequency and modulation bandwidth were about 2 GHz and 5 GHz. The original set of the chaotic states before optical injection is obtained with −6.1 dB optical feedback (the feedback injection strength with a scale of the solitary slave laser's power).

In this paper we present the corresponding results of computing the characteristic dynamical and topological invariants of the nonlinear dynamics of the chaotic laser diode with an additional optical injection (all characteristics are corresponding to parameters of the Ref. [1]).

2. Chaos-geometric approach to dynamics of the chaotic systems

As the main ideas of the quantum-dynamic approach to diatomic molecule in an electromagnetic field are in details presented in the Refs. [5-7,2], here we will restrict yourself only by some necessary elements.

In order to perform the detailed analysis of the chaotic regime polarization time series, further a total dynamics of the quantum system in an electromagnetic field and to calculate the fundamental topological and dynamical invariants of the system in a chaotic regime we used the universal chaos-geometric approach, presented earlier (see, c.g., [5-7,19-20]).

Generally speaking, the approach includes a set of such non-linear analysis and a chaos theory methods as the correlation integral approach, multi-fractal and wavelet analysis, average mutual information, surrogate data, Lyapunov's exponents and Kolmogorov entropy approach, spectral methods, nonlinear prediction (predicted trajectories, neural network etc) algorithms.

One of the important tasks here is to determine the corresponding embedding dimension and to reconstruct a Euclidean space R^d large enough so that the set of points d_A can be unfolded without ambiguity. In accordance with the embedding theorem, the embedding dimension, d_E, must be greater, or at least equal, than a dimension of attractor, d_A, i.e. $d_E > d_A$.

Usually one should use several standard approaches to reconstruction of the attractor dimension (see, e.g., [17-20]). The correlation integral analysis is one of the widely used techniques to investigate the signatures of chaos in a time series. The analysis uses the correlation integral, $C(r)$, to distinguish between chaotic and stochastic systems.

To compute the correlation integral, the algorithm of Grassberger and Procaccia is the most commonly used approach. According to this algorithm, the correlation integral is

$$C(r) = \lim_{N\to\infty} \frac{2}{N(n-1)} \sum_{\substack{i,j \\ (1\le i<j\le N)}} H\left(r - \| \mathbf{y}_i - \mathbf{y}_j \|\right) \qquad (2)$$

where H is the Heaviside step function with $H(u) = 1$ for $u > 0$ and $H(u) = 0$ for $u \le 0$, r is the radius of sphere centered on $\mathbf{y}_i$ or $\mathbf{y}_j$, and N is the number of data measurements.

In order to perform the verification of the results obtained by means of the correlation integral analysis, one could use so called known surrogate data method. This approach makes use of the substitute data generated in accordance to the probabilistic structure underlying the original data.

The important dynamical invariants of a chaotic system are the Lyapunov's exponents (see, c.g., [17-20]). These characteristics can be defined as asymptotic average rates, they are independent of the initial conditions, and

therefore they do comprise an invariant measure of attractor. Saying simply, the Lyapunov's exponents are the parameters to detect whether the system is chaotic or not.

Another important characteristics, namely, the Kolmogorov entropy K_{ent} measures the average rate at which information about the state is lost with time. According to the definition, the Kolmogorov entropy can be determined as the sum of the positive Lyapunov's exponents.

The estimate of the dimension of the attractor is provided by the Kaplan and York conjecture:

$$d_L = j + \frac{\sum_{\alpha=1}^{j} \lambda_\alpha}{|\lambda_{j+1}|}, \qquad (3)$$

where j is such that $\sum_{\alpha=1}^{j} \lambda_\alpha > 0$ and $\sum_{\alpha=1}^{j+1} \lambda_\alpha < 0$, and the Lyapunov's exponents λ_α are taken in descending order.

There are a few approaches to computing the Lyapunov's exponents. One of them computes the whole spectrum and is based on the Jacobi matrix of system. In this work we use an advanced algorithm with fitted map with higher order polynomials. To calculate the spectrum of the Lyapunov's exponents, one could determine the time delay τ and embed the data in the four-dimensional space. In this point it is very important to determine the Kaplan-York dimension and compare it with the correlation dimension, defined by the Grassberger-Procaccia algorithm].

As a rule, the calculational results of the state-space reconstruction are highly sensitive to the length of data set (i.e. it must be sufficiently large) as well as to the time lag and embedding dimension correctly determined.

Indeed, there are limitations on the applicability of chaos theory for observed (finite) dynamical variable series arising from the basic assumptions that these series must be infinite. A finite and small data set may probably result in an underestimation of the actual dimension of the process. The details of the computational procedures and algorithms can be also found in Refs. [27-46].

3. Nonlinear dynamics of the chaotic laser diode: Some results and conclusions

Below we present the results of of computing the dynamical and topological invariants of the nonlinear dynamics of the chaotic laser diode system with an additional optical injection According to [1], the dynamics of this system can be described by a set of rate equations for the slave laser electric complex amplitude F and carrier density n, correspondingly and is represented as follows:

$$\frac{dF}{dt} = \frac{1+i\beta}{2}\{\frac{g(n-n_0)}{1+\delta|F|^2} - \tau_p^{-1}\}F +$$

$$\frac{k_f}{\tau_i}F(t-\tau)\cdot\exp[-i2\pi\eta\tau] + \frac{k_i}{\tau_i}F_j\exp[i\Delta\eta t],$$

$$\frac{dn}{dt} = \frac{i}{qV} - \frac{n}{\tau_N} - \frac{g(n-n_0)}{1+\delta|F|^2}|F|^2 + G(n)$$

where k_f and k_j denote the feedback and injection strength, the amplitude of injection laser $|F_j|$ is equal to that of the solitary slave laser, and $\Delta\eta = \eta_j - \eta_s$ is the detuning between the injection and the slave lasers. The feedback delay τ=20ns is set in the experimental setup [1]. As the input data for the solving the rate equations system the numerical values of the parameters have been used as follows (see more details in Ref. [1]): transparency carrier density $n_0=0.455\times10^6$ m^{-3}, threshold current $i_{th}r$ =22 mA, differential gain $g=1.414\times10^{-3}$ μm^{3}ns^{-1} , the carrier lifetime τ_N=2.5 ns, photon lifetime τ_p=1.17ps, round-trip time in laser intracavity τ_i=7.38 ps, the linewidth enhancement factor β=5.0, gain saturation parameter $\delta=5\times10^{-3}$ μm^{3}and active layer volume V=324m^3; the simulated slave laser is biased at $1.7i_{thr}$ with 5.2 GHz modulation bandwidth.

According to data [1], under k_j=0, a growth of the parameter k_f results in a period-doubling bifurcation route to chaos, followed

by a reversed route out of chaos. More exatly, a chaos is realized in the region about 0.04–0.16 of k_f and bandwidths are about 4.0–6.2 GHz. The rate equations systems has been numerically solved and the corresponding time series for amplitude and density are obtained. The concrete step is an analysis of the corresponding time series with the $N=\cdot 10^4$ and $\Delta t=2\cdot 10^{-3}$ns. It is very important to declare that the dynamics of the chaotic laser diode system with an additional optical injection has the elements of a deterministic chaos (the strange attractor). In Table 1 we present the computational values of the correlation dimension d_2, the Kaplan-York attractor dimension (d_L), the Lyapunov's exponents (λ_i), Kolmogorov entropy (K_{entr}), the Gottwald-Melbourne parameter.

Table 1

Correlation dimension d_2, Lyapunov's exponents (λ_i, i=1,2), Kaplan-York attractor dimension (d_L), Kolmogorov entropy (K_{entr}), Gottwald-Melbourne parameter K_{GW}

d_2	λ_1	λ_2
2.94	0.358	0.096
d_L	K_{entr}	K_{GW}
2.80	0.454	0.94

To conclude, the values of the dynamical and topological invariants (the correlation, Kaplan-York dimensions, the Lyapunov's exponents etc) for the dynamics of the chaotic laser diode system with an additional optical injection are computed. In particular, the first two Lyapunov's exponents are positive. These data indicate on emerging dynamical chaos elements in the laser diode system dynamics.

References

1. Wang A.-B, , Wang Y.-C., Wang J.-F., Route to broadband chaos in a chaotic laser diode subject to optical injection. Optics Letters. 2009, 34(8), 1144-1146.
2. Pavlov E.V., Ignatenko A.V., Krianov S.V., ,Mashkantsev A.A., Dynamical and topological invariants of PbO dynamics in a resonant electromagnetic field. *Photoelectronics.* **2019**, *28,* 121-126.
3. Zhang C.; Katsouleas T.; Joshi C. Harmonic frequency generation & chaos in laser driven molecular vibrations. *In Proc. of Short-wavelength Physics with Intense Laser Pulses*, San-Diego. **1993**.
4. Berman, G.; Bulgakov, E.; Holm, D. Nonlinear resonance and dynamical chaos in diatomic molecule driven by a resonant IR field. *Phys. Rev. A* **1995,** *52*, 3074
5. Glushkov, A.V. Spectroscopy of atom and nucleus in a strong laser field: Stark effect and multiphoton resonances. *J. Phys.: Conf. Ser*. **2014**, *548*, 012020.
6. Ignatenko A., Buyadzhi A., Buyadzhi V., Kuznetsova, A.A., Mashkantsev, A.A., Ternovsky E. Nonlinear chaotic dynamics of quantum systems: molecules in an electromagnetic field. *Adv. Quant Chem.* **2019**, *78*, 149-170.
7. Glushkov, A., Buyadzhi, V., Kvasikova, A., Ignatenko, A., Kuznetsova, A., Prepelitsa, G., Ternovsky, V. Non-Linear chaotic dynamics of quantum systems: Molecules in an electromagnetic field and laser systems. In: *Quantum Systems in Physics, Chemistry, and Biology*. Springer, Cham. **2017**, *30*, 169-180
8. Mashkantsev, A. A. ; Ignatenko, A.V. ; Kirianov, S.V. ; Pavlov, E.V. Chaotic dynamics of diatomic molecules in an electromagneic field**.** *Photoelectronics.* **2018,** *27*, 103-112**.**
9. Glushkov A., Ternovsky V., Buyadzhi V, Prepelitsa G. Geometry of a relativistic quantum chaos: New approach to dynamics of quantum systems in electromagnetic field and uniformity and charm of a chaos. *Proc. Int. Geom. Center*. **2014,** *7*(4), 60-71.
10. Glushkov A.V.; Ivanov, L.N. DC strong-field Stark effect: consistent quantum-mechanical approach. *J. Phys. B: At. Mol. Opt. Phys.* **1993,** *26*, L379-386.
11. Ignatenko, A.; Buyadzhi ,A.; Buyadzhi, V.; Kuznetsova,A.; Mashkantsev, A.; Ternovsky E. Nonlinear chaotic dynamics of quantum systems: molecules in an

electromagnetic field. Adv. Quant. Chem. **2019**, *78*, 149-170.
12. Glushkov, A.V. True effective molecular valency Hamiltonian in a logical semiempricial theory. *Journal of Structural Chem*. **1988**, *29(4)*, 495-501.
13. Glushkov, A.V. Operator Perturbation Theory for Atomic Systems in a Strong DC Electric Field. *In Advances in Quantum Methods and Applications in Chemistry, Physics, and Biology*,; Hotokka, M., Brändas, E., Maruani, J., Delgado-Barrio, G., Eds.; Springer: Cham, **2013**; 27, pp 161–177.
14. Malinovskaya, S.V.; Glushkov, A.V.; Khetselius, O.Yu.; Svinarenko, A.A.; Mischenko, E.V.; Florko, T.A. Optimized perturbation theory scheme for calculating the interatomic potentials and hyperfine lines shift for heavy atoms in the buffer inert gas. *Int. J. Quant. Chem.* **2009,** *109(4)*, 3325-3329.
15. Glushkov A; Khetselius O; Malinovskaya S. Optics and spectroscopy of cooperative laser-electron nuclear processes in atomic and molecular systems – new trend in quantum optics. *Europ. Phys. Journ. ST* **2008,** *160*, 195-204.
16. Glushkov, A.V.; Khetselius, O.Yu.; Malinovskaya, S.V. Spectroscopy of cooperative laser–electron nuclear effects in multiatomic molecules. *Molec. Phys.* **2008,** *106*, 1257-1260.
17. Danilov, V., Kruglyak, Y., Pechenaya, V. Electron density-bond order matrix and the spin density in the restricted CI method. *Theor. Chim Acta*. **1969**, *13*(4), 288-296.
18. Danilov, V., Kruglyak, Y., Kuprievich, V., Ogloblin, V. Electronic aspects of photodimerization of the pyrimidine bases and of their derivatives. *Theor. Chim.Acta*. **1969**, *14*(3), 242-249.
19. Gottwald, G.A. ; Melbourne, I. Testing for chaos in deterministic systems with noise. *Physica D*. **2005**, *212*, 100-110.
20. Abarbanel, H.; Brown, R.; Sidorowich, J; Tsimring, L. The analysis of observed chaotic data in physical systems. *Rev. Mod. Phys*. **1993**, *65*, 1331- 1392.
21. Packard, N.; Crutchfield, J; Farmer, J.; Shaw, R. Geometry from a time series *Phys. Rev. Lett*. **1988**, *45*, 712-716.
22. Kennel, M.; Brown, R.; Abarbanel, H. Determining embedding dimension for phase-space reconstruction using a geometrical construction. *Phys. Rev. A*. **1992**, *45*, 3403-3412.
23. Gallager, R. *Information theory and reliable communication.* N.-Y., **1986**.
24. Grassberger, P. ; Procaccia, I. Measuring the strangeness of strange attractors. *Physica D*. **1983**, *9*, 189-208.
25. Theiler, J.; Eubank, S.; Longtin, A.; Galdrikian, B.; Farmer, J. Testing for nonlinearity in time series: The method of surrogate data. *Phys.D*. **1992**, *58*, 77-94.
26. Sano, M.; Sawada, Y. Measurement of Lyapunov spectrum from chaotic time series. *Phys.Rev.Lett*. **1995**, *55*, 1082.
27. Glushkov, A.V. *Methods of a Chaos Theory*. OSENU: Odessa, **2012**.
28. Glushkov, A.V.; Khetselius, O.Yu.; Brusentseva, S.V.; Zaichko, P.A.; Ternovsky, V.B. Studying interaction dynamics of chaotic systems within a nonlinear prediction method: Application to neurophysiology *In Advances in Neural Networks, Fuzzy Systems and Artificial Intelligence, Series: Recent Advances in Computer Engineering;* Balicki, J., Ed.; WSEAS Press: Gdansk, **2014**; Vol 21, pp 69-75.
29. Glushkov, A.; Prepelitsa, G.; Svinarenko, A.; Zaichko, P. Studying interaction dynamics of the non-linear vibrational systems within non-linear prediction method (application to quantum autogenerators) *In Dynamical Systems Theory;* Awrejcewicz, J., Kazmierczak, M., Olejnik, P., Mrozowski, J., Eds.; Łódz, **2013**; Vol T1, pp 467-477.
30. Khetselius, O. Forecasting evolutionary dynamics of chaotic systems using advanced non-linear prediction method *In Dynamical Systems Applications;* Awrejcewicz, J., Kazmierczak, M., Olejnik, P., Mrozowski, J., Eds.; Łódz, **2013**; Vol T2, pp 145-152.

31. Khetselius, O.; Brusentseva, S.; Tkach, T. Studying interaction dynamics of chaotic systems within non-linear prediction method: Application to neurophysiology *In Dynamical Systems Applications*, Awrejcewicz, J, Kazmierczak, M, Olejnik, P., Mrozowski, J., Eds.; Łódz, **2013**; T2, pp 251-259.
32. Glushkov, A.; Khetselius, O.; Brusentseva, S.; Duborez, A. Modeling chaotic dynamics of complex systems with using chaos theory, geometric attractors, quantum neural networks. *Proc Int. Geom. Center*. **2014**, *7(3)*, 87-94.
33. Glushkov, A.V.; Bunyakova, Yu.Ya.; Zaichko, P.A. Geometry of Chaos: Consistent combined approach to treating chaotic dynamics atmospheric pollutants and its forecasting. *Proc. Intern. Geom. Center*. **2013**, *6(3)*,6-14.
34. Khetselius, O.Yu.; Florko, T.A.; Svinarenko, A.A.; Tkach, T.B. Radiative and collisional spectroscopy of hyperfine lines of the Li-like heavy ions and Tl atom in an atmosphere of inert gas. *Phys. Scripta*. **2013**, *T153*, 014037
35. Khetselius, O.Yu. Relativistic calculating the hyperfine structure parameters for heavy-elements and laser detecting the isotopes and nuclear reaction products. *Phys. Scripta*. **2009,** *T135*, 014023.
36. Svinarenko, A.A. Study of spectra for lanthanides atoms with relativistic many-body perturbation theory: Rydberg resonances. *J. Phys.: Conf. Ser.* **2014,** *548*, 012039
37. Khetselius, O.Yu. Atomic parity non-conservation effect in heavy atoms and observing P and PT violation using NMR shift in a laser beam: To precise theory. *J. Phys.: Conf. Ser.* **2009,** *194*, 022009.
38. Glushkov, A.; Loboda, A.; Gurnitskaya, E.; Svinarenko, A. QED theory of radiation emission and absorption lines for atoms in a strong laser field. *Phys. Scripta.* **2009,** *135*, 014022.
39. Glushkov A.V.; Ivanov, L.N. DC strong-field Stark effect: consistent quantum-mechanical approach. *J. Phys. B: At. Mol. Opt. Phys.* **1993,** *26*, L379-386.
40. Khestelius, O.Yu. *Hyperfine structure of atomic spectra*. Astroprint: Odessa, **2008**.
41. Glushkov A.; Khetselius O.; Svinarenko A. Theoretical spectroscopy of auto ionization resonances in spectra of lanthanide atoms. *Phys. Scr*. **2013**, *T153*, 014029.
42. Glushkov A. Spectroscopy of cooperative muon-gamma-nuclear processes: Energy and spectral parameters *J. Phys.: Conf. Ser.* **2012,** *397*, 012011
43. Khetselius O Spectroscopy of cooperative electron-gamma-nuclear processes in heavy atoms: NEET effect. *J. Phys.: Conf. Ser.* **2012,** *397*, 012012.
44. Ivanova, E., Ivanov, L., Glushkov, A., Kramida, A. High order corrections in the relativistic perturbation theory with the model zeroth approximation, Mg-Like and Ne-Like Ions. *Phys. Scr.* **1985**, *32*, 513-522
45. Glushkov, A.V.; Khetselius,O.Yu.; Svinarenko,A.A.; Buyadzhi, V.V. Spectroscopy of autoionization states of heavy atoms and multiply charged ions (Odessa: TEC) -**2015.**
46. Glushkov, A.V.; Buyadzhi, V.V.; Ponomarenko, E.L. Geometry of Chaos: Advanced approach to treating chaotic dynamics in some nature systems. *Proc. Int. Geom. Center***. 2014** *7(1)*,24-30.
47. Glushkov A., Khetselius O., Kruglyak Yu., Ternovsky V. *Calculational Methods in Quantum Geometry and Chaos theory*. P.3. Odessa , **2014.**
48. Glushkov A., Khetselius O., Svinarenko A, Buyadzhi V. *Methods of computational mathematics and mathematical phys*. P.1.TES, Odessa, **2015.**

PACS 31.15.-p; 33.20.-t

Kirianov S.V., Mashkantsev A.A., Bilan I.I., Ignatenko A.V.

DYNAMICAL AND TOPOLOGICAL INVARIANTS OF NONLINEAR DYNAMICS OF THE CHAOTIC LASER DIODES WITH AN ADDITIONAL OPTICAL INJECTION

Summary. Nonlinear chaotic dynamics of the of the chaotic laser diodes with an additional optical injection is computed within rate equations model, based on the a set of rate equations for the slave laser electric complex amplitude and carrier density. To calculate the system dynamics in a chaotic regime the known chaos theory and non-linear analysis methods such as a correlation integral algorithm, the Lyapunov's exponents and Kolmogorov entropy analysis are used. There are listed the data of computing dynamical and topological invariants such as the correlation, embedding and Kaplan-Yorke dimensions, Lyapunov's exponents, Kolmogorov entropy etc. New data on topological and dynamical invariants are computed and firstly presented.

Key words: Chaotic dynamics, laser diodes, dynamical and topological invariants

PACS 31.15.-p; 33.20.-t

Кирьянов С.В., Машканцев А.А., Билан И.И., Игнатенко А.В.

ДИНАМИЧЕСКИЕ И ТОПОЛОГИЧЕСКИЕ ИНВАРИАНТЫ НЕЛИНЕЙНОЙ ДИНАМИКИ ХАОТИЧЕСКИХ ЛАЗЕРНЫХ ДИОДОВ С ДОПОЛНИТЕЛЬНОЙ ОПТИЧЕСКОЙ ИНЪЕКЦИЕЙ

Резюме. Нелинейная хаотическая динамика хаотических лазерных диодов с дополнительной оптической инжекцией рассчитывается в рамках модели скоростных уравнений, в частности, модели, основанной на системе скоростных уравнений для комплексной электрической амплитуды лазера и плотности. Для моделирования динамики в хаотическом режиме используются известные методы нелинейного анализа и теории хаоса, в т.ч., метод корреляционного интеграла, анализ на основе показателей Ляпунова, энтропии Колмогорова и др. Представлены данные вычисления динамических и топологических инвариантов, в т.ч., размерностей вложения, корреляционной, Каплана-Йорка, показателей Ляпунова, др.

Ключевые слова: хаотическая динамика, лазерные диоды, динамические и топологические инварианты

PACS 31.15.-p; 33.20.-t

Кір'янов С.В., Машканцев О.А., Білан І.І., Ігнатенко Г.В.

ДИНАМІЧНІ І ТОПОЛОГІЧНІ ІНВАРІАНТИ НЕЛІНІЙНОЇ ДИНАМИКИ ХАОТИЧНИХ ЛАЗЕРНИХ ДІОДІВ З ДОДАТКОВОЮ ОПТИЧНОЮ ІНЖЕКЦІЄЮ

Резюме. Нелінійна хаотична динаміка хаотичних лазерних діодів з додатковою оптичної інжекцією розраховується в рамках моделі швидкісних рівнянь, зокрема, моделі, заснованої на системі швидкісних рівнянь для комплексної електричної амплітуди лазера і густини носіїв. Для аналізу динаміки системи в хаотичному режимі використані методи нелінійного аналізу та теорії хаосу, у т.ч., метод кореляційного інтеграла, аналіз на основі показників Ляпунова, ентропії Колмогорова т.і. Надані дані обчислення динамічних і топологічних інваріантів: розмірностей кореляційної, вкладення, Каплана-Йорка, показників Ляпунова, та інших.

Ключові слова: хаотична динаміка, лазерні діоди, динамічні та топологічні інваріанти

PACS 32.30.-r

Cherkasova I. S., Ternovsky V. B., Nesterenko A. A., Mironenko D. A.

Odesa State Environmental University, L'vovskaya str.15, Odesa, 65016
E-mail: ternovskyvb@gmail.com

THEORETICAL STUDYING SPECTRAL CHARACTERISTICS OF ZN-LIKE IONS ON THE BASIS OF RELATIVISTIC MANY-BODY PERTURBATION THEORY

A theoretical study of the spectroscopic characteristics of Zn-like multiply charged ions is carried out within the framework of the relativistic many-body perturbation theory. The optimized Dirac-Kohn-Shem approximation was chosen as the zero approximation of the relativistic perturbation theory. Optimization has been fulfilled by means of introduction of the parameters to the Kohn-Sham exchange and correlation potentials and further minimization of the gauge-non-invariant contributions into radiation width of atomic levels with using relativistic orbital set, generated by the corresponding zeroth approximation Hamiltonian.

1. In recent years, in connection with the unprecedented progress in the development of experimental techniques, an urgent need has arisen to solve the required problems at a fundamentally new level of theoretical consistency and accuracy. First of all, this relates to the determination of such important atomic spectroscopic characteristics as the cross sections of various elementary processes, the probability of radiative transitions, and the strength of oscillators, and if important progress has been made in the study of the most intense allowed (electric dipole) radiative transitions [1–28]). In many papers the standard Hartree-Fock (HF), Dirac-Fock (DF) methods, model potential (MP) approach, quantum defect approximation etc in the different realizations have been used for calculating energies and oscillator strengths. However, it should be stated that for the heavy alkali atoms (such as caesium and francium and corresponding ions) and particularly for their high-excited (Rydberg) states, there is not enough precise information available in literature. The multiconfiguration Dirac-Fock method is the most reliable version of calculation for multielectron systems with a large nuclear charge. However, one should remember about very complicated structure of spectra of the lanthanides atoms and necessity of correct accounting for different correlation effects such as polarization interaction of the valent quasiparticles and their mutual screening, iterations of a mass operator etc.).The known method of the model relativistic many-body perturbation theory (RMBPT) has been earlier effectively applied to computing spectra of low-lying states for some lanthanides atoms [5-11] (see also [12-22]). In this paper theoretical studying spectroscopic characteristics of the Zn--like multicharged ions is carried out within the relativistic many-body perturbation theory. The zeroth approximation of the relativistic perturbation theory is provided by the optimized Dirac-Coulomb one.

2. As the method of computing is earlier presented in detail, here we are limited only by the key topics [5-15]. Generally speaking, the majority of complex atomic systems possess a dense energy spectrum of interacting states with essentially relativistic properties. In the theory of the non-relativistic atom a convenient field procedure is known for calculating the energy shifts ΔE of degenerate states. This procedure is connected with the secular matrix M diagonalization [10-22]. In constructing M, the Gell-Mann and Low adiabatic formula for ΔE is used. In contrast to the non-relativistic case, the secular matrix elements are already complex in the second order of the electrodynamical PT (first order of the interelectron interaction). Their imaginary part of ΔE is connected with the radiation decay (radiation) possibility. In this approach, the whole calculation of the energies and decay probabilities of a non-degenerate excited state is reduced to the calculation and

diagonalization of the complex matrix *M*. The complex secular matrix *M* is represented in the form [6-11]:

$$M = M^{(0)} + M^{(1)} + M^{(2)} + M^{(3)}. \qquad (1)$$

where $M^{(0)}$ is the contribution of the vacuum diagrams of all order of PT, and $M^{(1)}$, $M^{(2)}, M^{(3)}$ those of the one-, two- and three-quasiparticle diagrams respectively. $M^{(0)}$ is a real matrix, proportional to the unit matrix. It determines only the general level shift. The diagonal matrix $M^{(1)}$ can be presented as a sum of the independent one-quasiparticle contributions. For simple systems (such as alkali atoms and ions) the one-quasiparticle energies can be taken from the experiment. Substituting these quantities into (1) one could have summarized all the contributions of the one -quasiparticle diagrams of all orders of the formally exact QED PT. However, the necessary experimental quantities are not often available. The first two order corrections to $\mathrm{Re}M^{(2)}$ have been analyzed previously using Feynman diagrams (look Ref. in [1,2]). The contributions of the first-order diagrams have been completely calculated.

In the second order, there are two kinds of diagrams: polarization and ladder ones. The polarization diagrams take into account the quasiparticle interaction through the polarizable core, and the ladder diagrams take into account the immediate quasiparticle interaction [4-20]. Some of the ladder diagram contributions as well as some of the three-quasiparticle diagram contributions in all PT orders have the same angular symmetry as the two-quasiparticle diagram contributions of the first order. These contributions have been summarized by a modification of the central potential, which must now include the screening (anti-screening) of the core potential of each particle by the two others.

Interelectron interaction operator with accounting for the Breit interaction has been taken as follows:

$$V(r_i r_j) = exp(i\omega r_{ij}) \cdot \frac{(1 - \alpha_i \alpha_j)}{r_{ij}}, \qquad (2)$$

where, as usually, α_i are the Dirac matrices.

The total probability of a λ -pole transition is the sum of the electrical P_λ^E (electric multipole decomposition) and magnetic P_λ^M (corresponding decomposition) parts and is calculated within the relativistic energy formalism [7-20]. In the energy approach with respect to the complex multielectron atomic system the energy shift in the complex form is: δE = Reδ E + i Imδ E, Im δ E = -P/ 2, where P- probability of decay (transition). For a single quasiparticle atomic system Imδ E and, accordingly, P in the 2nd perturbation theory order (the perturbation operator $U_{MF}(r_i \mid b)$ - $J_\mu(x)A^\mu(x)$, where A is the vector of the electromagnetic field potential, J is the current operator, U_{MF} is a mean-field potential) is proportional to the matrix element with Dirac bispinors φ_i^{EFMP} (ab initio RMP наближення):

$$V_{ijkl} = \int\int d^3r_1 d^3r_2 \varphi_i^{EFMP^*}(r_1)\varphi_j^{EFMP^*}(r_2)[(1-\alpha_1\alpha_2)\cdot \cdot \sin|\omega| r_{12}/r_{12}] \cdot \varphi_k^{EFMP}(r_2)\varphi_1^{EFMP}(r_1) \qquad (3)$$

which are decomposed into a series of Bessel functions of the 1st kind (analog of multipole decomposition). In general, the results of all approximate calculations depended on the gauge.

Naturally the correct result must be gauge-invariant. The gauge dependence of the amplitudes of the photo processes in the approximate calculations is a well known fact and is in details investigated by Grant, Armstrong, Aymar and Luc-Koenig, Glushkov-Ivanov et al (see reviews in [5-7] and Refs. therein).

Grant has investigated the gauge connection with the limiting non-relativistic form of the transition operator and has formulated the conditions for approximate functions of the states, in which the amplitudes of the photo processes are gauge invariant [3]. Glushkov-Ivanov [11] have developed a new relativistic gauge-conserved version of the energy approach. In ref. [16-28] it has been developed its further generalization. Here we applied this approach for generating the optimized

relativistic orbitals basis in the zeroth approximation of the many-body PT. Optimization has been fulfilled by means of introduction of the parameter to the Fock and Kohn-Sham exchange potentials and further minimization of the gauge-non-invariant contributions into radiation width of atomic levels with using relativistic orbital bases, generated by the corresponding zeroth approximation Hamiltonians. All calculations are performed with using the PC code Super atom [6-28]. The results of our studying the Zn-like ions are listed in Table 1.

Table 1.

Experimental (exp.) And theoretical energies (in atomic units) and oscillator strengths for the $4s^2(^1S_0)$- 4s4p ($^1P^0_1$) transition in the spectra of various Zn-like ions: HF, DF, DF methods using experimental transition energy and our data (RPT)

Ion	Method	ΔE	f_L	f_V
Ga^+	DF	0.3351	1.89	1.98
	HF	0.2984	2.30	2.01
	DF_{exp}	0.3221	1.97	1.95
	MP	0.3076	1.68	1.73
	RPT	0.3221	1.86	1.86
	Exp.	0.3221	1.85 ± 0.15	1.85 ± 0.15
As^{3+}	DF	0.5247	1.87	1.86
	RPT	0.5140	1.57	1.57
	Exp.	0.5141	1.56 ± 0.23	1.56 ± 0.23
Yb^{40+}	DF	6.2564	1.12	1.10
	RPT	5.1788	0.97	0.96
Pb^{52+}	DF	11.1153	1.21	1.18
	RPT	10.9715	1.13	1.13
U^{62+}	DF	17.8584	1.37	1.36
	HF	17.6087	1.41	1.47
	RPT	17.6285	1.33	1.33
	Exp.	-	1.31 ± 0.05	1.31 ± 0.05

In fact in table 1 for illustration we present the experimental (exp.) and theoretical energies (in atomic units) and oscillator strengths for the $4s^2(^1S_0)$- 4s4p ($^1P^0_1$) transition in the spectra of various Zn-like ions: theory is presented by the Hartree-Fock (HF) Dirac-Fock (DF) methods plus the DF data with experimental transition energy and our data (RPT) (see [1-,5,6] and refs therein). Analysis of the data shows that the computational method used provides a physically reasonable agreement between the theoretical and experimental data. Let us note that the transition probabilities values in the different photon propagator gauges are practically equal. Besides, an account of the inter particle (electron) correlation effects is of a great importance.

.

References

1. Anderson E.K., Anderson E.M., Calculation of the parameters of some E1, E2, E3, M1, M2 transitions in the isoelectronic sequence of Zn. *Opt. Spectr*. **1983**, *54*, 955-960.
2. Weiss A., Hartree-Fock line strengths for lithium, sodium and copper isoelectronic sequences. *J. Quant. Spectr. and Rad. Tr*. **1977**, *18*, 481-491
3. Ivanova, E., Glushkov, A. Theoretical investigation of spectra of multicharged ions of F-like and Ne-like isoelectronic sequences. *J. Quant. Spectr. and Rad. Tr*. **1986**, *36*(2), 127-145.
4. Ivanova, E.P., Ivanov, L.N., Glushkov, A., Kramida, A. High order corrections in the relativistic perturbation theory with the model zeroth approximation, Mg-Like and Ne-Like Ions. *Phys. Scripta* **1985**, *32*, 513-522.
5. Glushkov A., Khetselius O., Svinarenko, A., Buyadzhi V., *Spectroscopy of autoionization states of heavy atoms and multiply charged ions*. TEC: Odessa, **2015**.
6. Glushkov, A.V. *Relativistic Quantum theory. Quantum mechanics of atomic systems*. Astroprint: Odessa, **2008**.
7. Khetselius O. *Quantum structure of electroweak interaction in heavy finite Fermi-systems*. Astroprint: Odessa, **2011**
8. Khetselius, O.Yu. *Hyperfine structure of atomic spectra*. Astroprint: **2008**.
9. Svinarenko, A.A., Ternovsky, V.B., Cherkasova I., Mironenko D. Theoretical studying spectra of ytterbium atom on

the basis of relativistic many-body perturbation theory: doubly excited states. *Photoelectr.* **2018**, 27, 113-120**.**

10. Ivanov, L.N., Ivanova, E.P., Knight, L. Energy approach to consistent QED theory for calculation of electron-collision strengths: Ne-like ions. *Phys. Rev. A.* **1993,** *48,* 4365-4374.
11. Glushkov, A., Ivanov, L. Radiation decay of atomic states: atomic residue polarization and gauge noninvariant contributions. *Phys.Lett.A.***1992,** *170,* 33.
12. Glushkov A.V., Ivanov, L.N. DC strong-field Stark effect: consistent quantum-mechanical approach. *J. Phys. B: At. Mol. Opt. Phys.* **1993,** *26,* L379-386.
13. Glushkov, A.V. *Relativistic and Correlation Effects in Spectra of Atomic Systems*. Astroprint: **2006**.
14. Glushkov, A.V. Relativistic polarization potential of a many-electron atom. *Sov. Phys. Journal.* **1990**, *33(1),* 1-4.
15. Glushkov, A.V. Advanced relativistic energy approach to radiative decay processes in multielectron atoms and multicharged ions. In *Quantum Systems in Chemistry and Physics*: *Progress in Methods and Applications.* Springer: Dordrecht, **2012,** 26, 231–252.
16. Glushkov, A.V. Energy approach to resonance states of compound superheavy nucleus and EPPP in heavy nuclei collisions. In Low Energy Antiproton Physics. AIP: New York, *AIP Conf. Proc*. **2005**, *796,* 206-210.
17. Glushkov, A. Spectroscopy of cooperative muon-gamma-nuclear processes: Energy and spectral parameters *J. Phys.: Conf. Ser.* **2012,** *397,* 012011.
18. Khetselius O. Spectroscopy of cooperative electron-gamma-nuclear processes in heavy atoms: NEET effect *J. Phys.: Conf. Ser.* **2012,** *397,* 012012.
19. Glushkov, A.V. Spectroscopy of atom and nucleus in a strong laser field: Stark effect and multiphoton resonances. *J. Phys.: Conf. Ser*. **2014**, *548,* 012020
20. Glushkov, A., Svinarenko, A., Ternovsky, V., Smirnov, A., Zaichko, P. Spectroscopy of the complex auto ionization resonances in spectrum of helium. *Photoelectr*. **2015**, *24*, 94-102.
21. Glushkov, A. Multiphoton spectroscopy of atoms and nuclei in a laser field: Relativistic energy approach and radiate-on atomic lines moments method. *Adv. in Quantum Chem.* **2019**, *78,* 253-285.
22. Khetselius, O.Yu. Optimized relativistic many-body perturbation theory calculation of wavelengths and oscillator strengths for Li-like multicharged ions. Adv. Quant. Chem. **2019**, *78,* 223-251
23. Svinarenko, A. Study of spectra for lanthanides atoms with relativistic many-body perturbation theory: Rydberg resonances. *J. Phys.: Conf. Ser.* **2014,** *548,* 012039.
24. Khetselius, O.Yu. Relativistic perturbation theory calculation of the hyperfine structure parameters for some heavy-element isotopes. *Int. Journ. Quant. Chem.* **2009,** *109,* 3330-3335.
25. Khetselius, O.Yu. Relativistic calculation of the hyperfine structure parameters for heavy elements and laser detection of the heavy isotopes. *Phys.Scripta.* **2009,** *135,* 014023.
26. Svinarenko, A. A., Glushkov, A. V., Khetselius, O.Yu., Ternovsky, V.B., Dubrovskaya, Yu., Kuznetsova, A., Buyadzhi, V. Theoretical spectroscopy of rare-earth elements: spectra and autoionization resonances. *Rare Earth Element* (InTech). **2017**, pp 83-104.
27. Glushkov A., Khetselius O., Svinarenko A., Buyadzhi V., Ternovsky, V., Kuznetsova A., Bashkarev P. Relativistic perturbation theory formalism to computing spectra and radiation characteristics: application to heavy element. *Recent Studies in Perturbation Theory.* InTech. **2017**, 131.
28. Glushkov A., Svinarenko, A., Ignatenko, A.V. Spectroscopy of autoionization resonances in spectra of the lanthanides atoms. *Photoelectr*. **2011**, *20,* 90-94.

PACS 32.30.-r

Cherkasova I.S., Ternovsky V.B., Nesterenko A.A., Mironenko D.A.

THEORETICAL STUDYING SPECTRAL CHARACTERISTICS OF Ne-LIKE IONS ON THE BASIS OF OPTIMIZED RELATIVISTIC MANY-BODY PERTURBATION THEORY

Summary. A theoretical study of the spectroscopic characteristics of Zn-like multiply charged ions is carried out within the framework of the relativistic many-body perturbation theory. The optimized Dirac-Kohn-Shem approximation was chosen as the zero approximation of the relativistic perturbation theory. Optimization has been fulfilled by means of introduction of the parameters to the Kohn-Sham exchange and correlation potentials and further minimization of the gauge-non-invariant contributions into radiation width of atomic levels with using relativistic orbital set, generated by the corresponding zeroth approximation Hamiltonian.

Keywords: Relativistic perturbation theory, Zn-like multicharged ions

PACS 32.30.-r

Черкасова И.С., Терновский В.Б., Нестеренко А.А., Мироненко Д.А.

ТЕОРЕТИЧЕСКОЕ ИЗУЧЕНИЕ СПЕКТРАЛЬНЫХ ХАРАКТЕРИСТИК Ne-ПОДОБНЫХ ИОНОВ НА ОСНОВЕ ОПТИМИЗИРОВАННОЙ РЕЛЯТИВИСТСКОЙ МНОГОЧАСТИЧНОЙ ТЕОРИИ ВОЗМУЩЕНИЙ

Резюме. Теоретическое изучение спектроскопических характеристик Zn - подобных многозарядных ионов проводится в рамках релятивистской теории возмущений многих тел. В качестве нулевого приближения релятивистской теории возмущений выбрано оптимизированное приближение Дирака- Кона-Шема. Оптимизация выполнена путем введения параметров в обменные потенциалы Фока и Кона-Шэма и дальнейшей минимизацией калибровочно-неинвариантных вкладов в радиационные ширины атомных уровней с использованием релятивистского базиса орбиталей, сгенерированного соответствующим гамильтонианом нулевого приближения.

Ключевые слова: Релятивистская теория возмущений, Zn-подобные ионы

PACS 32.30.-r

Черкасова І.С., Терновський В.Б., Нестеренко А.А., Міроненко Д.А.

ТЕОРЕТИЧНЕ ВИВЧЕННЯ СПЕКТРАЛЬНИХ ХАРАКТЕРИСТИК Ne-ПОДІБНИХ ИОНОВ НА ОСНОВІ ОПТИМІЗОВАНОЇ РЕЛЯТИВІСТСЬКОЇ БАГАТОЧАСТКОВІ ТЕОРІЇ ЗБУРЕНЬ

Резюме. Теоретичне вивчення спектроскопічних характеристик Zn - подібних багатозарядних іонів проводиться в рамках релятивістської теорії збурень багатьох тіл. В якості нульового наближення релятивістської теорії збурень обрано оптимізоване наближення Дірака-Кона-Шема. Оптимізація виконана шляхом введення параметра в обмінний потенціал Кона-Шема і подальшої мінімізації калібрувально-неінваріантних вкладів в радіаційні ширини атомних рівнів з використанням релятивістського базису орбіталей, згенерованого відповідним гамільтоніаном нульового наближення.

Ключові слова: Релятивістська теорія збурень, Zn- подібні іони.

Інформація для авторів наукового збірника «Photoelectronics»

У збірнику "Photoelectronics " друкуються статті, що містять відомості про наукові дослідження і технічні розробки в напрямках:

*** фізика напівпровідників;**
*** гетеро- і низькорозмірні структури;**
*** фізика мікроелектронних приладів;**
*** лінійна і нелінійна оптика твердого тіла;**
*** оптоелектроніка та оптоелектронні прилади;**
*** квантова електроніка;**
*** сенсорика.**

Збірник "Photoelectronics видається англійською мовою. Рукопис подається автором у двох примірниках англійською і російською мовами.

Електронна копія статті повинна відповідати наступним вимогам:
1. Для тексту дозволяються наступні формати – MS Word (rtf, doc).
2. Рисунки приймаються у форматах – EPS. TIFF. BMP, PCX, JPG. GIF, CDR. WMF, MS Word I MS Giaf, Micro Calc Origin (opj).

Рукописи надсилаються за адресою:
Відп. секр. Куталовій М. І., вул. Пастера, 42. фіз. фак. ОНУ, м. Одеса, 65082
E-mail: photoelectronics@onu.du.ua
тел. 0482-726-63-56.

Збірники "Photoelectronics" знаходяться на сайті: http://photoelectronics.onu.edu.ua

До рукопису додаються:
1. Коди PAC і УДК. Допускається використання декількох шифрів, що розділяються комами.
2. Прізвища і ініціали авторів.
3. Установа, повна поштова адреса, номер телефону, номер факсу, адреси електронної пошти для кожного з авторів.
4. Назва статті.
5. Резюме обсягом до 200 слів пишеться англійською, російською і (для авторів з України) – українською мовами.

Текст друкувати шрифтом 14 пунктів через два інтервали на білому папері формату А4. Назва статті, а також заголовки підрозділів друкуються прописними літерами. .
Рівняння необхідно друкувати в редакторі формул MS Equation Editor. Необхідно давати визначення величин, що з'являються в тексті вперше.
Посилання на літературу друкувати через два інтервали, нумеруватися в квадратних дужках послідовно, у порядку їхньої появи в тексті статті. Посилатися необхідно на літературу, що видана пізніше 2000 року.
Підписи до рисунків і таблиць друкуються в тексті рукопису в порядку їхньої ілюстрації.
Резюме обсягом до 200 слів друкується англійською, російською і українською мовами (для авторів з України). Перед текстом резюме відповідною мовою вказуються УДК, прізвища та ініціали всіх авторів, назва статті.

Информация для авторов
Научного сборника «Photoelectronics »

В сборнике "Photoelectronics " печатаются статьи, которые содержат сведения о научных ис-следованиях и технических разработках в направлениях:

*** физика полупроводников;**
*** гетеро- и низкоразмерные структуры;**
*** физика микроэлектронных приборов;**
*** линейная и нелинейная оптика твердого тела;**
*** оптоэлектроника и оптоэлектронные приборы;**
*** квантовая электроника;**
*** сенсорика**

Сборник"Photoelectronics издаётся на английском языке. Рукопись подается автором в двух экземплярах на английском и русском языках.

Электронная копия статьи должна отвечать следующим требованиям:
1. Для текста допустимы следующие форматы - MS Word (rtf, doc).
2. Рисунки принимаются в форматах – EPS. TIFF. BMP, PCX, JPG. GIF, CDR. WMF, MS Word И MS Giaf, Micro Calc Origin (opj).

Рукописи присылаются по адресу:
Отв. секр. Куталовой М. И., ул. Пастера. 42. физ. фак. ОНУ, г. Одесса, 65026
E-mail:photoelectronics@onu.du.ua тел. 0482 - 726 6356 .

Статьи сб."Photoelectronics " находятся на сайте: http://photoelectronics.onu.edu.ua

К рукописи прилагается:
1. Коды PAC и УДК. Допускается использование нескольких шифров, которые разделяются запятой.
2. Фамилии и инициалы авторов.
3. Учреждение, полный почтовый адрес, номер телефона, номер факса, адреса электронной почты для каждого из авторов.
4. Название статьи.
5. Резюме объемом до 200 слов пишется на английском, русском языках и (для авторов из Украины) – на украинском.

Текст должен печататься шрифтом 14 пунктов через два интервала на белой бумаге формата А4. Название статьи, а также заголовки подразделов печатаются прописными буквами и отмечаются полужирным шрифтом.

Уравнения необходимо печатать в редакторе формул MS Equation Editor. Необходимо давать определение величин, которые появляются в тексте впервые.

Ссылки на литературу должны печататься через два интервала, нумероваться в квадратных скобках последовательно, в порядке их появления в тексте статьи. Ссылаться необходимо на литературу, которая издана позднее 2000 года.

Подписи к рисункам и таблицам печатаются в тексте рукописи в порядке их иллюстрации.

Резюме объемом до 200 слов печатается на английском, русском языках и на украинском (для авторов из Украины). Перед текстом резюме соответствующим языком указываются УДК, фамилии и инициалы всех авторов, название статьи.

Information for contributors of «Photoelectronics» articles

"Photoelectronics" Articles publishes the papers which contain information about scientific research and technical designs in the following areas:

- Physics of semiconductors;
- Physics of microelectronic devices;
- Linear and non-linear optics of solids;
- Optoelectronics and optoelectronic devices;
- Quantum electronics;
- Sensorics.

"Photoelectronics" Articles is defined by the decision of the Highest Certifying Commission as the specialized edition for physical-mathematical and technical sciences and published and printed at the expense of budget items of Odessa I.I. Mechnikov National University.

«Photoelectronics» Articles is published in English. Authors send two copies of papers in English. The texts are accompanied by 3.5» diskette with text file, tables and figures. Electronic copy of a material can be sent by e-mail to the Editorial Board and should meet the following requirements:

1.The following formats are applicable for texts – MS Word (rtf, doc).

2. Figures should be made in formats – EPS, TIFF, BMP, PCX, JPG, GIF, WMF, MS Word I MS Giaf, Micro Calc Origin (opj). Figures made by packets of mathematical and statistic processing should be converted into the foregoing graphic formats.

The papers should be sent to the address:

Kutalova M.I., Physical Faculty of Odessa I. I. Mechnikov National University, 42 Pastera str, 65026 Odessa, Ukraine, e-mail: wadz@mail.ru, tel. +38-0482-7266356. Information is on the site:

http://www.photoelectronics.onu.edu.ua

The title page should contain:

1. Codes of PACS
2. Surnames and initials of authors
3. TITLE OF PAPER
4. Name of institution, full postal address, number of telephone and fax, electronic address

An abstract of paper should be not more than 200 words. Before a text of summary a title of paper, surnames and initials of authors should be placed.

Equations are printed in MS Equation Editor.

References should be printed in double space and should be numbered in square brackets consecutively throughout the text. References for literature published in 2000-2009 years are preferential.

Illustrations will be scanned for digital reproduction. Only high-quality illustrations will be taken for publication. Legends and symbols should be printed inside. Neither negatives, nor slides will be taken for publication. All figures (illustrations) should be numbered in the sequence of their record in text.

For additional information please contact with the Editorial Board.

Підп.до друку 24.12.2020 р.
Формат 60×84/8. Ум.-друк.арк. 19,07.
Тираж 300 прим. Замов. № 2197.

Видавець і виготовлювач
«Одеський національний університет імені І. І. Мечникова»
Свідоцтво ДК № 4215 від 22.11.2011 р.

65082, м. Одеса, вул. Єлісаветинська, 12, Україна
Тел.: (048) 723 28 39, e-mail: druk@onu.edu.ua